

**INVESTIGATIONS ON SMALL SCALE
STANDALONE HYBRID SYSTEM FOR RURAL
ELECTRIFICATION**

Submitted
in fulfillment of the requirements
of the degree of
DOCTOR OF PHILOSOPHY

by
BHARAT BHUSHAN JAIN

(2009REE101)

Under the supervision of

Prof. BHIM SINGH

Prof. R. A. GUPTA

to the



**DEPARTMENT OF ELECTRICAL ENGINEERING
MALAVIYA NATIONAL INSTITUTE OF TECHNOLOGY JAIPUR
JAIPUR (INDIA)
AUGUST, 2016**

© MALAVIYA NATIONAL INSTITUTE OF TECHNOLOGY JAIPUR 2016

ALL RIGHTS RESERVED



Department of Electrical Engineering
MALAVIYA NATIONAL INSTITUTE OF TECHNOLOGY
JAIPUR

CERTIFICATE

This is to certify that the thesis entitled “**Investigations on Small Scale Standalone Hybrid System for Rural Electrification**” submitted by **Mr. Bharat Bhushan Jain** (ID. No. 2009REE101) to Malaviya National Institute of Technology Jaipur for the award of the degree of **Doctor of Philosophy** in Electrical Engineering is a bonafide record of original research work carried out by him under our supervision.

It is further certified that:

1. The results contained in this thesis have not been submitted in part or in full, to any other university or institute for the award of any degree or diploma.
2. Mr. Bharat Bhushan Jain has fulfilled the requirement for the submission of this thesis.

(Prof. Bhim Singh)
Supervisor
Department of Electrical Engineering
IIT Delhi
New Delhi - 110 016, India

(Prof. R. A. Gupta)
Supervisor
Department of Electrical Engineering
MNIT Jaipur
Jaipur - 302 017, India

Date: **13/08/2016**



Department of Electrical Engineering
MALAVIYA NATIONAL INSTITUTE OF TECHNOLOGY
JAIPUR

CANDIDATE'S DECLARATION

I hereby declare that the thesis entitled “**Investigations on Small Scale Standalone Hybrid System for Rural Electrification**” is my own work conducted under the supervision of Prof. R. A. Gupta, Department of Electrical Engineering, Malaviya National Institute of Technology, Jaipur (Rajasthan), India and Prof. Bhim Singh, Department of Electrical Engineering, Indian Institute of Technology Delhi, New Delhi, India.

I firmly declare that the presented work does not contain any part of any work that has been submitted for the award of any degree either in this University or in any other University/Deemed University without proper citation.

Date: **13/08/2016**
MNIT, Jaipur

(Bharat Bhushan Jain)
2009REE101

ACKNOWLEDGEMENT

I take this opportunity to express my sincere gratitude towards my supervisors, **Prof. R. A. Gupta**, Professor, Department of Electrical Engineering, Malaviya National Institute of Technology (MNIT) Jaipur and **Prof. Bhim Singh**, Professor, Department of Electrical Engineering, Indian Institute of Technology (IIT) Delhi, for their invaluable guidance, advice and continuous encouraging support for the completion of this research work. I humbly acknowledge my life time's gratitude to them for managing to find time to have stimulated technical discussions and for providing the decisive constructive expert criticism. I look forward to even greater level of support and guidance for my future endeavors.

I express my deep sense of gratitude to Prof. A. B. Gupta, Director MNIT, Jaipur and Prof. I. K. Bhat, Ex- Director MNIT, Jaipur, for strengthening the research environment of institute by providing all the necessary facilities to research scholars.

I express my deep sense of gratitude to Dr. H. P. Tiwari, Dr. Rajive Tiwari and Dr. Nikhil Gupta, DREC members, for evaluating my progress from time to time and their invaluable suggestions during the course of my work.

I express my thanks to Dr. Rajesh Kumar, DPGC Convener, Prof. K. R. Niazi, Ex-DPGC Convener and Dr. Vikas Gupta, Head, Department of Electrical Engineering, MNIT Jaipur for providing me all necessary facilities and extended support for carrying out this work till its completion.

The sponsorship and support provided by the Arya Institute of Engineering and Technology (AIET), Jaipur is thankfully acknowledged. I am also thankful to Dr. Arvind Agarwal (Chairman, ARYA Main Campus), Dr. Puja Agarwal (MD, ARYA Main Campus) for their inspiration and encouragement given to me during my research. I am also thankful to all my colleagues of Arya Institute of Engineering and Technology, Jaipur especially to Dr. Surendra Sharma, Dr. Ishwar Chand Sharma, Prof. M. L. Gupta, and Dr. R. C. Bansal for their moral supports.

I have no words to express my thanks to my research group members Dr. Manoj Gupta, Dr. Ajay Kumar Bansal, Dr. Virendra Swaroop Sangtani,

Mr. Nand Kishore Gupta and Mr. Tushar Srivastava for helping me in my work and encouraging to complete the assignment.

I sincerely expressed my special thanks and gratitude to my father Shri Ramvatar Jain, my mother Smt. Saroj Jain, my younger brother Mr. Kirti Gopal Jain, my brother in law Mr. Gopal Krishan Agarwal and all my family members for their affection, encouragement and support during all these years of my education. There are no words to good enough to express my gratitude towards them.

I owe my special thanks to my supervisor's family members particularly Mrs. Madhu Gupta and Mrs. Sushila Singh, always been on my side morally and for their continuous encouragements during this work. They deserve my special thanks for sparing the family time of my supervisors during this work.

I would like to record high appreciation for my wife **Anshu Jain** for her constant encouragement and tremendous patience during the completion of this work. My lovely children **Laksh** and **Poorab** are to be credited for their love, patience, and pleasant company in the entire period of this work.

Date: 13.08.2016

(Bharat Bhushan Jain)

MNIT, Jaipur

2009REE101

ABSTRACT

Renewable energy sources like solar energy, wind energy etc. are seen as clean and green options to meet deficit energy and have vast potential to reduce dependence on fossil fuels based energy systems and take the edge off green house gas emissions. Although they are widely integrated into the electric sector, certain issues remain such as the variability and uncertainty in the availability of the renewable energy resources. This makes these sources less reliable and dependable than the conventional sources used for the majority of electricity generation.

In addition, the deployment of an energy system using a single renewable resource becomes less reliable in many cases. This calls for a hybrid energy system (HES) where a number of renewable energy sources along with electrical energy storage components are integrated, to work as a reliable power source and fulfill the electrical energy requirement. They can be either grid-connected or stand-alone installations depending on the application and geography of the site.

The cost of commercially electricity supply system is very high, as it is highly dependent on the centralized grid energy systems which operate mostly on thermal and nuclear power plants and require big investments for establishing transmission and distribution networks. It would be even more uneconomical if the grid facilities are to penetrate remote regions making rural electrification, as it becomes more costly compared to electrification of urban areas. Therefore, to overcome above said problems, alternative systems of electricity generation and distribution are highly required. Unlike the centralized power systems, decentralized power systems are generally based on renewable energy sources like solar and wind. These sources work at lower scales (of the order of few kW) both in the absence and presence of grid. They are easily available at remote or isolated locations due to the ability to function independently and generate power in the closeness of demand site. Hence, the use of renewable energy based decentralized power systems are more effective for the rural electrification, by providing reliable, sustainable and environmentally friendly energy supply.

A grid interfaced hybrid energy system is connected to the centralized grid system and feeds the generated power to the grid. Any local load connected to the system may

derive power from the integrated system directly or through the grid. Such a system eliminates the requirement of a storage system since the loads may be supplied from the grid when the integrated energy system is not operational and does not produce any power. Here, the grid works like a storage unit with unrestricted capacity, which takes care of seasonal load demand variations and accommodates all fluctuations in the energy generation from the HES side. However, a grid connected system may not be feasible in remote locations where the grid cannot penetrate and there may be no other sources of energy. In such cases, a standalone system may be employed giving priority to the needs and usage pattern of the local region with ample storage facilities.

A stand-alone hybrid renewable energy system is a hybrid system includes two or more renewable energy sources like solar-thermal, solar photovoltaic, wind, biomass and hydropower etc. to supply electrical energy to the load demand. The most commonly used hybrid energy system is to supply electrical energy, with the combinations of solar photovoltaic (PV) modules and wind turbines.

Because the intermittent supply pattern of different available renewable energy sources at different locations, combination of two or more renewable energy sources gives a better overall supply pattern. Sometimes, as per the need of the demand, an energy storage system is also included to make the energy supply system more effective, less intermittent, or more firm.

A combination of storage system like batteries with renewable hybrid energy system, not only increases the duration of energy independence but it also ensures best possible use of the available renewable energy resources, which yields high reliability. The cost of said system is high, as a large capacity of storage system is needed to deal with varying weather conditions at different locations and to ensure the energy supplies to the load demand at the worst weather conditions. There is better and cheaper solution to supply energy demand, during poor wind days or cloudy weather days or peak loads, with a diesel generator working as secondary back up supply, although the percentage of renewable energy used is also reduced. However, one can maximize fuel savings by minimize the diesel generator running time, by selecting appropriate size of the storage system.

There are many possible topologies or configurations of hybrid energy systems. One way to classify hybrid energy systems architectures is to discriminate between DC and

AC bus systems. In DC bus system, renewable energy source components and the backup source like the diesel generator feed power to a DC bus, after that the power is converted in to AC supply through an inverter, which is connected between DC bus and the loads. This system is suitable for small hybrid energy systems. In large hybrid energy systems, AC bus configuration is used where large solar system, wind energy system, diesel generators etc. are connected to the AC distribution bus and can serve the loads directly or may feed power to the grid system.

The topology or configuration used to be evaluated in this thesis has solar PV and wind as renewable sources, with a battery and a diesel generator as backup sources.

This thesis “Investigations on Small Scale Standalone Hybrid System for Rural Electrification” is to design and the analyses of a small scale stand-alone hybrid system for rural electrification, in order to cater the demand of electricity in remote areas by using renewable sources such as solar and wind as major sources, a battery as storage device and the diesel generator as backup source.

The purpose of the study is to model, simulate and develop a hardware prototype of HES suitable for a small utility of a village. The small utility selected for the study is Kukas village near Jaipur (India). The load profile of the small utility is estimated for each season (i.e. summer, rainy and winter), considering domestic and street lighting load. Based on the estimated load profile, solar irradiation profile and wind speed profile, solar, wind and battery based HES with a diesel generator backup is found suitable and has been proposed for the village. The components of the system consist of solar PV system, wind energy conversion system (WECS), battery bank, DC-DC boost and buck converters, the inverter with a filter and a step-up transformer, a diesel generator, a auxiliary charger and a hybrid smart controller (HSC).

Initially, the mathematical model of each component of the HES is developed for clear understanding of their characteristics. The seasonal load profile (i.e. summer, rainy and winter seasons) of the selected area has been investigated. The solar irradiation data, wind speed data and other associated data required for system analysis have been recorded for all the months considering seasonal variations in the year 2014. The initial investment required in HES for a rural setup with a low energy demand may be

higher comparatively, especially when components like diesel generator and battery banks are involved.

To examine the behavior of the system under varying load demand, simulation model of various HES such as solar-wind-battery hybrid system, solar-battery-diesel generator hybrid system, wind-battery-diesel generator hybrid system and solar-wind-battery-diesel generator hybrid system and their components have been developed in MATLAB/Simulink platform. Performance of each HES, is investigated for a typical day of each season, for the given load profile, solar irradiation data, wind speed data and other relevant input data to the model. The power shared by each source and the battery with respect to time has also been investigated.

From the discussions of the performance analysis, it is concluded that the proposed stand-alone solar-wind-battery-diesel generator hybrid system is successful in meeting the load requirements of the village throughout the year and handle the variations in load profile as well as transient load conditions effectively.

CONTENTS

Certificate	i
Candidate's Declaration	ii
Acknowledgement	iii
Abstract	v
Contents	ix
List of Figures	xiii
List of Tables	xix
List of Symbols and Abbreviations	xxi
Chapter 1 INTRODUCTION	1-16
1.1 General	1
1.2 Energy Scenario of India and Rajasthan	2
1.2.1 Energy Scenario of India	2
1.2.2 Energy Scenario of Rajasthan	4
1.3 Energy Systems	5
1.4 Hybrid Energy Systems	6
1.4.1 Benefits of Hybrid Energy Systems	7
1.4.2 Stand-alone and Grid-Interfaced Hybrid Energy Systems	8
1.4.3 Topologies of Stand-Alone Hybrid Energy Systems	10
1.4.3.1 AC-Coupled Hybrid Energy Systems	10
1.4.3.2 DC-Coupled Hybrid Energy Systems	12
1.4.3.3 Mixed-Coupled Hybrid Energy Systems	12
1.5 Scope of Work and Objectives	13
1.6 Organization of Thesis	15
1.7 Conclusions	16
Chapter 2 LITERATURE REVIEW	17-30
2.1 General	17
2.2 Literature Review	17
2.2.1 PV Hybrid Energy Systems	17
2.2.2 Wind Hybrid Energy Systems	18
2.2.3 Solar PV-Wind Hybrid Energy Systems	19

2.3 The Configuration of Proposed Systems	21
2.3.1 Load Profile of a Small Utility at Kukas, Jaipur, India	21
2.3.2 Solar Irradiation Profile of Kukas, Jaipur, India	26
2.3.3 Wind Speed Profile of Kukas, Jaipur, India	28
2.4 Conclusions	30
Chapter 3 MODELING OF STAND-ALONE SOLAR PV, WECS AND DG SYSTEMS	31-88
3.1 General	31
3.2 Modeling of Solar PV System	31
3.2.1 Introduction to Solar PV Generation System	32
3.2.2 Design and Simulation of 1 kW Stand-alone Solar PV System	36
3.2.3 Modeling of MPPT Techniques for Solar PV System	38
3.2.3.1 Perturbation and Observation (P&O) Algorithm	38
3.2.3.2 Design of DC-DC Boost Converter	40
3.2.3.3 Proportional Integral (PI) Voltage Controller	41
3.2.3.4 Simulation Results of DC-DC Boost Converter	42
3.2.4 Storage Battery	45
3.2.4.1 Lead Acid Battery Construction and Performance	45
3.2.4.2 Lead Acid Battery Rating and Model	46
3.2.4.3 Battery Bank Sizing	46
3.2.5 Single Phase Inverter	47
3.2.5.1 Hysteresis Current Controller & PI Voltage Controller	48
3.2.5.2 Design of Voltage Source Inverter	49
3.2.5.3 Design of PI Controller	49
3.2.5.4 Design of Low Pass Filter (LPF)	50
3.2.5.5 Simulation Results of Inverter Circuit	51
3.2.6 Simulation Results & Discussion	54
3.3 Design and Simulation of 1kW Wind Energy Conversion System (WECS) with Battery Storage	60
3.3.1 Introduction to Wind Energy Conversion System (WECS)	61
3.3.2 Parameters and Modeling of WECS	62
3.3.2.1 Model of a Small Wind Turbine	63
3.3.2.2 Permanent Magnet Synchronous Generator Model	65

3.3.2.3 DC-DC Buck Converter	73
3.3.3 Simulation Results and Discussion	76
3.4 Design and Simulation of 1.2 kVA Diesel Generator System	83
3.4.1 Parameters and Modeling of System	83
3.4.2 Simulation Results and Discussion	85
3.5 Conclusions	87
Chapter 4 MODELING OF STAND-ALONE HYBRID SYSTEMS	89-128
4.1 General	89
4.2 Design and Simulation of Stand-alone Solar-Wind-Battery Hybrid System	90
4.3 Design and Simulation of Stand-alone Solar-Battery-Diesel Generator Hybrid System	98
4.4 Design and Simulation of Stand-alone Wind-Battery- Diesel Generator Hybrid System	106
4.5 Design and Simulation of Stand-alone Solar-Wind-Battery-Diesel Generator Hybrid System	116
4.6 Comparative Analysis of Hybrid Systems	126
4.7 Conclusions	127
Chapter 5 HARDWARE IMPLEMENTATION OF PROPOSED STAND-ALONE HYBRID SYSTEM	129- 144
5.1 General	129
5.2 Hardware Components for Stand-alone Solar-Wind-Battery-Diesel Generator Hybrid System	129
5.2.1 Hardware Configuration of 1.0 kW Solar PV Array	130
5.2.2 Solar MPPT Controller	130
5.2.3 Hardware Configuration of 1.0 kW Wind Energy Conversion System	131
5.2.4 Hardware Configuration of 1.2 KVA Diesel Generator	131
5.2.5 Battery Bank	132
5.2.6 Hardware Configuration of Hybrid Smart Controller	132
5.2.7 Hardware Configuration of Data Logger and Sensor Circuit	133
5.3 Results and Discussion	135

5.4 Conclusions	144
Chapter 6 MAIN CONCLUSIONS AND SUGGESTIONS FOR FURTHER WORK	145-148
6.1 General	145
6.2 Main Conclusions	145
6.3 Suggestion for Further Work	147
References	149-162
Appendixes	163-164
List of Publications	165

LIST OF FIGURES

Figure	Page No.
Figure 1.1 Source-wise installed capacity in India (MW) as on 30.06.2015	03
Figure 1.2 Region-wise installed capacity in India (MW), as on 30.06.2015	04
Figure 1.3 Source-wise installed capacity in Rajasthan (MW) as on 30.06.2015	05
Figure 1.4 Block diagram of centralized AC-coupled hybrid energy systems	11
Figure 1.5 Block diagram of decentralized AC-coupled hybrid energy systems	11
Figure 1.6 Block diagram of centralized DC-coupled hybrid energy systems	12
Figure 1.7 Block diagram of mixed-coupled hybrid energy systems	13
Figure 1.8 Block diagram of proposed stand-alone hybrid energy system	14
Figure 2.1 Load profile for summer season of small utility	22
Figure 2.2 Load profile for rainy season of small utility	23
Figure 2.3 Load profile for winter season of small utility	23
Figure 2.4 Energy requirement of small utility in Kukas, Jaipur, India	23
Figure 2.5 Matlab/Simulink model of single phase load	
(a) Matlab/Simulink model of single phase load	24
(b) Connection diagram of single phase load profile for 24-hours	24
Figure 2.6 Simulation result of a 24 hour - load variation of summer, rainy and winter seasons	25
Figure 2.7 Solar irradiation (watt/m ²) of a year (hourly basis) for village Kukas, Jaipur, India	26
Figure 2.8 Solar irradiation (watt/m ²) of a month (hourly basis) for village Kukas, Jaipur, India	27
Figure 2.9 Wind speed (m/sec) of a year (hourly basis) for village Kukas, Jaipur, India	28
Figure 2.10 Wind speed (m/sec) of a month (hourly basis) for village Kukas, Jaipur, India	29
Figure 3.1 Block diagram of proposed system configuration	31
Figure 3.2 Ideal PV cell with R-load	32
Figure 3.3 An accurate model of PV cell	33
Figure 3.4 Final equivalent circuit of PV cell	33
Figure 3.5 MATLAB/Simulink model of solar PV panel	35

Figure 3.6 Characteristics of 125W-1-36-REIL solar panel at different solar irradianations and reference temperature	36
Figure 3.7 Schematic diagram of proposed stand-alone solar PV- battery system	37
Figure 3.8 Connection diagram of solar PV panels for PV array	37
Figure 3.9 Operating flowchart of P&O algorithm	39
Figure 3.10 Boost DC-DC converter topology used as PV power interface	40
Figure 3.11 Switching control generation for boost converter	42
Figure 3.12 Matlab/Simulink model of boost converter with PV	43
Figure 3.13 Matlab/Simulink model of MPPT scheme with PV	43
Figure 3.14 Simulated results of MPPT & boost converter with PV array	44
Figure 3.15 Battery characteristics of 48 V, 80Ah battery bank	47
Figure 3.16 VSI and hysteresis current controller	48
Figure 3.17 Switching diagram of hysteresis current controller	49
Figure 3.18 Matlab/Simulink model of inverter system	51
Figure 3.19 Simulation results of inverter system with 500 watt linear load	52
Figure 3.20 Simulation results of inverter system with 375VA (P=400 w, Q=150 var) non-linear load	53
Figure 3.21 Matlab/Simulink model of proposed stand-alone solar PV-battery system	54
Figure 3.22 Solar profile of stand-alone solar PV-battery system	55
Figure 3.23 Load profile of stand-alone solar PV-battery system	56
Figure 3.24 Inverter output of stand-alone solar PV-battery system	57
Figure 3.25 Battery voltage and current for stand-alone solar PV-battery system	57
Figure 3.26 Solar irradiation profiles for a typical day of three seasons	58
Figure 3.27 Power sharing curve for a summer day for solar PV-battery system	58
Figure 3.28 Power sharing curve for a rainy day for solar PV-battery system	59
Figure 3.29 Power sharing curve for a winter day for solar PV-battery system	59
Figure 3.30 Functional structure of a typical wind energy conversion system (WECS)	61
Figure 3.31 Basic block diagram of PMSG based WECS with battery storage	62
Figure 3.32 Schematic diagram of proposed WECS system	63

Figure 3.33 Matlab/Simulink model of the wind turbine	64
Figure 3.34 Turbine output power v/s rotor rpm at different wind speeds	65
Figure 3.35 Simplified $d-q$ -axis model of PMSG in synchronous reference frame	66
Figure 3.36 Matlab/Simulink model of PMSG	68
Figure 3.37 Matlab/Simulink model of PMSG with wind turbine	69
Figure 3.38 Wind speed variations of a typical day of three Seasons	70
Figure 3.39 Wind turbine speed variations of a typical day of three Seasons	70
Figure 3.40 Wind turbine torque variations of a typical day of three Seasons	71
Figure 3.41 Wind turbine power variations of a typical day of three Seasons	71
Figure 3.42 Wind generator voltage variations of a typical day of three seasons ($t=0.06$ sec)	72
Figure 3.43 Wind generator current variations of a typical day of three seasons ($t=0.06$ sec)	72
Figure 3.44 Buck DC-DC converter topology used as wind power interface	73
Figure 3.45 Matlab/Simulink model of buck converter with PMSG	75
Figure 3.46 Buck converter output voltage	76
Figure 3.47 Matlab/Simulink model of proposed WECS	76
Figure 3.48 Wind profile input of wind-battery system	77
Figure 3.49 Load profile of wind-battery system	78
Figure 3.50 Wind generator power, voltage and current for wind – battery system	79
Figure 3.51 DC link input and output voltage	79
Figure 3.52 Inverter output of wind-battery system	80
Figure 3.53 Battery voltage and current for wind-battery system	80
Figure 3.54 Power sharing curve for a summer day for wind-battery system	81
Figure 3.55 Power sharing curve for a rainy day for wind-battery system	81
Figure 3.56 Power sharing curve for a winter day for wind-battery system	82
Figure 3.57 Block diagram of working principle of DG set	84
Figure 3.58 Matlab/Simulink model of diesel engine & generator system	84
Figure 3.59 Matlab/Simulink model of diesel engine speed & voltage control	85
Figure 3.60 Matlab/Simulink model of diesel generator with load	85
Figure 3.61 Simulated result of diesel engine speed & voltage control	86

Figure 3.62 Simulated result of DG output voltage, current and power	86
Figure 3.63 Simulated result of DG output load voltage	87
Figure 3.64 Simulated result of DG output load current	87
Figure 4.1 Block diagram of stand-alone solar-wind-battery hybrid system	90
Figure 4.2 Schematic diagram of proposed stand-alone solar-wind-battery hybrid system	90
Figure 4.3 Matlab/Simulink model of proposed stand-alone solar-wind-battery hybrid system	91
Figure 4.4 (a) Solar irradiation profile, (b) Wind speed profile	92
Figure 4.5 Load profile of stand-alone solar-wind-battery hybrid system	94
Figure 4.6 Battery output of stand-alone solar-wind-battery hybrid system	95
Figure 4.7 Inverter output of stand-alone solar-wind-battery hybrid system	96
Figure 4.8 Power sharing curve for a summer day for stand-alone solar-wind-battery hybrid system	96
Figure 4.9 Power sharing curve for a rainy day for stand-alone solar-wind-battery hybrid system	97
Figure 4.10 Power sharing curve for a winter day for stand-alone solar-wind-battery hybrid system	97
Figure 4.11 Block diagram of proposed stand-alone solar-battery-diesel generator hybrid system	98
Figure 4.12 Schematic diagram of proposed stand-alone solar-battery-diesel generator hybrid system	99
Figure 4.13 Algorithm of the HSC for stand-alone solar-battery-diesel generator hybrid system	100
Figure 4.14 Matlab/Simulink model of proposed stand-alone solar-battery-diesel generator hybrid system	101
Figure 4.15 Solar irradiation profile	102
Figure 4.16 Load profile of stand-alone solar-battery-diesel generator hybrid system	103
Figure 4.17 Inverter output of stand-alone solar-battery-diesel generator hybrid system	103
Figure 4.18 Battery output of stand-alone solar-battery-diesel generator hybrid system	104
Figure 4.19 DG output of stand-alone solar-battery-diesel generator hybrid system	105
Figure 4.20 Block diagram of stand-alone wind-battery-diesel generator hybrid system	107

Figure 4.21 Schematic diagram of proposed stand-alone wind-battery-diesel generator hybrid system	107
Figure 4.22 Algorithm of the HSC for stand-alone wind-battery-diesel generator hybrid system	109
Figure 4.23 Matlab/Simulink model of proposed stand-alone wind-battery-diesel generator hybrid system	110
Figure 4.24 Wind speed profile	110
Figure 4.25 Load profile of stand-alone wind-battery-diesel generator hybrid system	111
Figure 4.26 Inverter output of stand-alone wind-battery-diesel generator hybrid system	112
Figure 4.27 Battery output of stand-alone wind-battery-diesel generator hybrid system	113
Figure 4.28 DG output of stand-alone wind-battery-diesel generator hybrid system	114
Figure 4.29 Block diagram of proposed stand-alone solar-wind-battery-diesel generator hybrid system	116
Figure 4.30 Schematic diagram of proposed stand-alone solar-wind-battery-diesel generator hybrid system	117
Figure 4.31 Algorithm of the HSC for stand-alone solar-wind-battery-diesel generator hybrid system	118
Figure 4.32 Matlab/Simulink model of proposed stand-alone solar-wind-battery-diesel generator hybrid system	119
Figure 4.33 (a) Solar irradiation profile, (b) Wind speed profile	120
Figure 4.34 Load profile of stand-alone solar-wind-battery-diesel generator hybrid system	121
Figure 4.35 Inverter output of stand-alone solar-wind-battery-diesel generator hybrid system	123
Figure 4.36 Battery output of stand-alone solar-wind-battery-diesel generator hybrid system	123
Figure 4.37 DG output of stand-alone solar-wind-battery-diesel generator hybrid system	125
Figure 5.1 Actual installation setup of 1.0 kW solar PV array, at Kukas, Jaipur	130
Figure 5.2 Hardware configuration of solar MPPT controller	130
Figure 5.3 (a) Actual installation setup of 1.0 kW wind generator at 11 m height (b) Real prototype model of 1.0 kW wind energy conversion	131

system (WECS) at Kukas, Jaipur

Figure 5.4 Real installation of 1.2 kVA diesel generator at Kukas, Jaipur	132
Figure 5.5 Real installation of battery bank at Kukas, Jaipur	132
Figure 5.6 Hardware configuration of hybrid smart controller (HSC)	133
Figure 5.7 Installation of Data Logger	133
Figure 5.8 Installation of sensor circuits	134
Figure 5.9 Overall view of stand-alone solar-wind-battery-diesel generator hybrid system	134
Figure 5.10 DC Link Voltages	135
Figure 5.11 Load voltage and current with solar PV system of proposed hybrid system	136
Figure 5.12 Load voltage and load current for PMSG of proposed hybrid system	137

LIST OF TABLES

Table	Page No.
Table 2.1 Details of the proposed electrical appliances	22
Table 3.1 Different parameters of 125 watt solar panel (Make: REIL, India)	35
Table 3.2 Different parameters of 1000 watt solar PV array	38
Table 3.3 Parameters of 1kW Wind Turbine	65
Table 3.4 Parameters of 1kW PMSG	68
Table 3.5 Parameters of DC-DC buck converter	75
Table 4.1 Comparative analysis of stand-alone hybrid systems	126
Table 5.1 Diesel power requirement (in watt-hr) with average solar and wind power contribution in the Month of March	138
Table 5.2 Diesel power requirement (in watt-hr) with average solar and wind power contribution in the Month of April	138
Table 5.3 Diesel power requirement (in watt-hr) with average solar and wind power contribution in the Month of May	139
Table 5.4 Diesel power requirement (in watt-hr) with average solar and wind power contribution in the Month of June	139
Table 5.5 Diesel power requirement (in watt-hr) with average solar and wind power contribution in the Month of July	140
Table 5.6 Diesel power requirement (in watt-hr) with average solar and wind power contribution in the Month of August	140
Table 5.7 Diesel power requirement (in watt-hr) with average solar and wind power contribution in the Month of September	141
Table 5.8 Diesel power requirement (in watt-hr) with average solar and wind power contribution in the Month of October	141
Table 5.9 Diesel power requirement (in watt-hr) with average solar and wind power contribution in the Month of November	142
Table 5.10 Diesel power requirement (in watt-hr) with average solar and wind power contribution in the Month of December	142
Table 5.11 Diesel power requirement (in watt-hr) with average solar and wind power contribution in the Month of January	143
Table 5.12 Diesel power requirement (in watt-hr) with average solar and wind power contribution in the Month of February	143

LIST OF SYMBOLS AND ABBREVIATIONS

ABBREVIATIONS:

LPG	:	Liquefied Petroleum Gas
NSSO	:	National Sample Survey Office
HES	:	Hybrid Energy system
IES	:	Integrated Energy System
PV	:	Photovoltaic
RES	:	Renewable Energy Source
PMSM	:	Permanent Magnet Synchronous Machine
PMSG	:	Permanent Magnet Synchronous Generator
WECS	:	Wind Energy Conversion System
DG	:	Diesel Generator
CFL	:	Compact Fluorescent Lamp
LED	:	Light Emitting Diode
TV	:	Television
MPPT	:	Maximum Power Point Tracking
P&O	:	Perturbation and Observation
PI	:	Proportional Integral
PWM	:	Pulse Width Modulation
SOD	:	Self of Discharge of Battery
DOD	:	Depth of Discharge of Battery
DA	:	Daily Autonomy
VSI	:	Voltage Source Inverter
HCC	:	Hysteresis Current Controller
LPF	:	Low-Pass Filter
THD	:	Total Harmonics Distortion
SCIG	:	Squirrel Cage Induction Generator
DFIG	:	Doubly Fed Induction Generator
BESS	:	Battery Energy Storage System
RL	:	Relay
HSC	:	Hybrid Smart Controller
IGBT	:	Insulated Gate Bipolar Transistors

SYMBOLS:

I_{PV}	:	Photovoltaic Current
I_d	:	Diode Current
I_{d1}, I_{d2}	:	Diode Current
T_{ref}	:	Reference Temperature (=25°C)
K	:	Boltzmann's Constant
V_{PV}	:	Voltage across the PV cell
P_{PV}	:	PV Array Power
I_G	:	Wind Generator DC Current
V_G	:	Wind Generator DC Voltage
P_{WG}	:	Wind Generator Power
I_0	:	Load Current
V_0	:	Load Voltage
V_{ref}	:	Reference Voltage
P_{load}	:	Load Power
L_{1S}	:	Inductor in Boost Converter
C_{1S}	:	Capacitor in Boost Converter
L_{1W}	:	Inductor in Buck Converter
C_{1W}	:	Capacitor in Buck Converter
V_C	:	DC Link Voltage
L_0	:	Inductor in DC Link
C_0	:	Capacitor in DC Link
L_f	:	Inductor in Low-Pass Filter
C_f	:	Capacitor in Low-Pass Filter
V_B	:	Battery Bank Voltage
C_{Wh}	:	Watt-Hour Capacity of Battery
C_{ah}	:	Amp-Hour Capacity of Battery
ΔI_0	:	Ripple of output current
F_{sw}	:	Switching Frequency
D	:	Duty Cycle
ΔV	:	Ripple in Output Voltage
$S_2 - S_5$:	IGBT

Chapter 1

Introduction

T HIS chapter explains the background, context, and motivation for this work. It also explains main contributions of this research and then organization of the thesis chapters.

CHAPTER 1

INTRODUCTION

1.1 GENERAL

Electricity is a driving force to most of the activities performed by human beings and has become a basic necessity for one and all. However, large numbers of people in the world especially in India, living in remote or rural areas do not have any access to electricity. They have dependence on local resources like firewood or animal dung for their daily energy requirement and usually have a low quality of life as compared to people living in urban areas. For improving the living standards in such areas, the first and foremost action is to provide electricity. This would impart an economic impetus to such communities and also contribute to the overall growth of the society and the nation [1-2].

Currently, the fossil fuel such as coal, oil and natural gas are having great impact on electrical power production. However, they are causing great damage to the environment in the form of pollution and climate change. Moreover, it is estimated that these fossil fuels are expected to be eventually exhausted in near future, which motivates the search for alternate energy resources to fulfill the energy demand [3-5].

If, present trend continues, the world in next two decades is expected to be more crowded than today. The conventional sources of energy are limited and due to rapid uses may be exhausted in near future. However, renewable energy sources like bio gas, wind, solar etc. are the sources for future and non-depleting in nature [6].

Since, only renewable options are not sufficient to cater the demand of energy in the country. Hence it is recommended to use the renewable options in combination with conventional energy sources to fulfill the energy demand [7]. The advantages of renewable energy options are as follows [8]:

- Renewable energy sources are local energy resource easily available to all developing countries and capable in having a significant regional and national economic impact.
- In remote locations, these available renewable energy options are economically competitive with conventional energy options.

- In near future the economic range of renewable energy applications may be expanded due to rapid technological developments.

1.2 ENERGY SCENARIO OF INDIA AND RAJASTHAN

In this section, energy scenario of India and Rajasthan is discussed, which shows the dependency of both India's and Rajasthan's energy sector on conventional fuels and renewable energy sources.

1.2.1 Energy Scenario of India

The economic growth of the Indian economy has experienced unprecedented over the last decade. India's GDP growth in last five years is 8.7% (more than 7.5 % in last ten years) makes it ninth largest economy in world. [9] Available energy resources face high pressure to fulfill the required energy demand due to this high order of sustained economic growth. The Government of India needs to take very serious efforts against imbalance in demand and supply of electrical energy, to augment the energy supplies; otherwise India may possibly face a severe energy crisis. In India, mostly installed electricity generation is from coal based power plants, in fact it has 60% share in total electricity generation installation and the dependence on coal in the energy mix seems to continue in the near future [10,11].

Although the energy sector is largely driven by coal and India's energy sector has a mix of all the available resources including non-conventional energy resources. Over 60% of the installed power capacity in India comes from coal based thermal power. Hydroelectricity has 15% share, natural gas has 9% share, nuclear power holds a 2% share whereas the renewable energy including solar, wind, biomass, small hydro power *etc.* has 13% share, as of June 2015 [12].

India faces a considerable challenge to facilitate a large section of the rural population with affordable, adequate and clean electricity and cooking fuel. As per 2011 census, cooking energy requirements of almost 85% of rural households have been habitually dependent on biomass fuels. Though a considerable rise in the use of liquefied petroleum gas (LPG) has been generally observed in rural areas, however the usage of fuels such as firewood, dung cake, kerosene *etc.* is still popular. Further, as per the national sample survey office (NSSO) reports (55th, 61st and 66th rounds), in rural households, the uses of biomass fuel have increased over the past decade [11].

However, burning of biomass fuel is highly hazardous for human beings health. This poses a barrier for achieving developmental goals, *i.e.* ensuring minimum living standards and provisioning of basic minimum needs in such areas. Thus, to access the electricity in cleaner forms of energy is quite essential and would have implications regarding, energy security and enabling greater development and social progress of society as well as nation.

As the installed capacity is a key indicator to show the state of awareness of the nation for generation of required electricity, Figure 1.1 shows the installed capacity of 278733.62 Megawatts (MW) of Indian power sector as of June 2015 [12]. The thermal power plants contribute to the major chunk of the installed capacity *i.e.* about 194199.56 MW, large hydroelectric plants about 42283.42 MW, nuclear energy plants about 5780 MW and the rest 36470.64 MW being a mix of solar, wind, biomass, waste-to-electricity plants and small hydro-plants, *etc.* As shown in Figure 1.2, India has five major grid regions and one island region with their installed capacity.

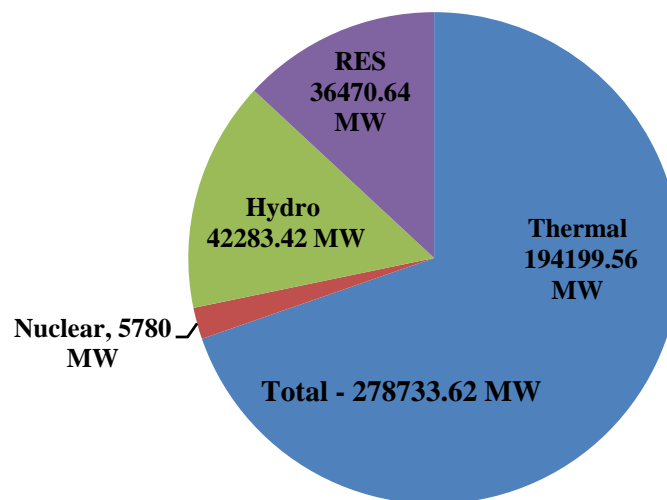


Figure 1.1 Source-wise installed capacity in India (MW) as on 30.06.2015 [12]

In renewable energy utilization, India's power sector plays an important role in the world. Nearly 55,000 MW of new generation capacity including renewable energy has been created during the 11th Five Year Plan. However there is an overall energy deficit of 8.7% and peak shortage of 9% is continued [10]. Therefore, the available installed capacity is not sufficient to fulfill this energy gap. Only 55.3% of the rural population

in India has access to electricity, as per 2011 census. National sample survey (NSS) results show that in rural India 62% households depend on kerosene as primary source of energy for lighting in 1993-94. However, in 2009-10, around 66% rural households have been using electricity as primary energy source [11]. Hence, it is evident that during the last decade, kerosene has been replaced by electricity for lighting in rural households.

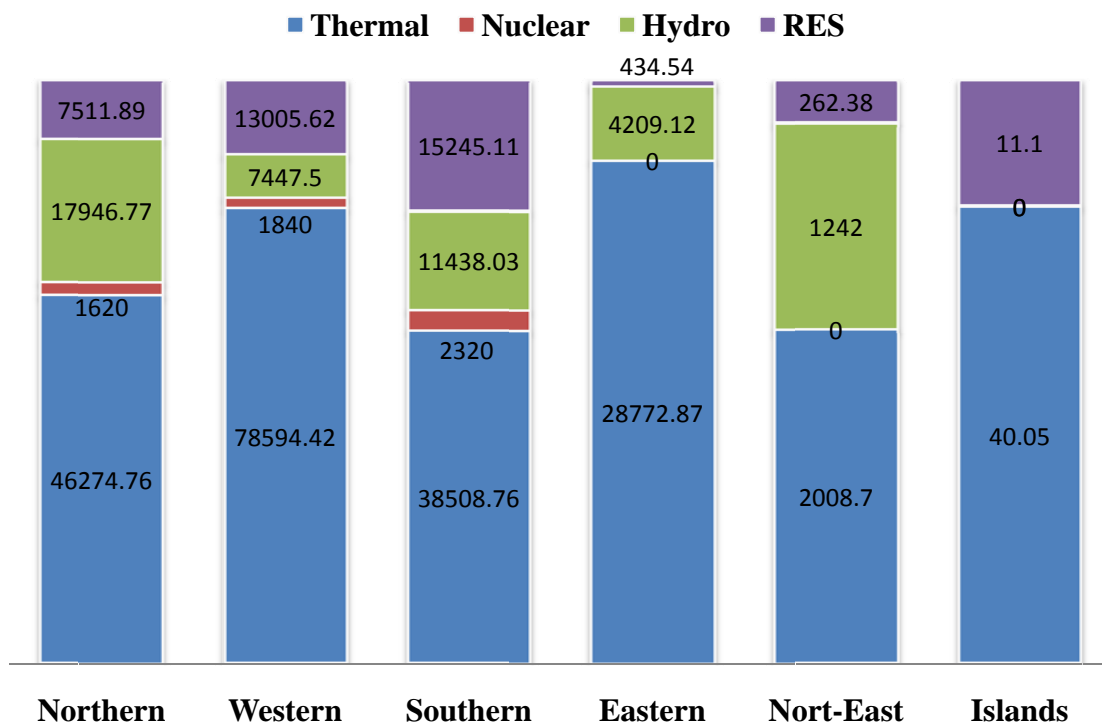


Figure 1.2 Region-wise installed capacity in India (MW), as on 30.06.2015[12]

Therefore, by providing more electricity in clean form to rural households/remote locations as well as urban areas, India may resolve the key challenges in achieving the projected growth outcomes. This is possible by incorporating renewable energy options along with conventional options in form of stand-alone for remote locations whereas grid connected for other users.

1.2.2 Energy Scenario of Rajasthan

As the economy of Rajasthan, is primarily dependent on the agriculture. About 73% of its population lives in the rural areas, where agriculture is most prominent. The current energy requirement of Rajasthan is heavily dependent on conventional energy sources.

Rajasthan has an electricity generation capacity of 17228.55 MW, 59.35% of which is coal and gas based, hydroelectricity has 9.98% share, nuclear holds a 3.33% share and renewable energy such as solar, wind, biomass *etc.* represents a 27.34% share of the Rajasthan fuel mix [12]. The installed capacity of the various conventional and renewable sources of energy in the state, in terms of MW is shown in Figure 1.3.

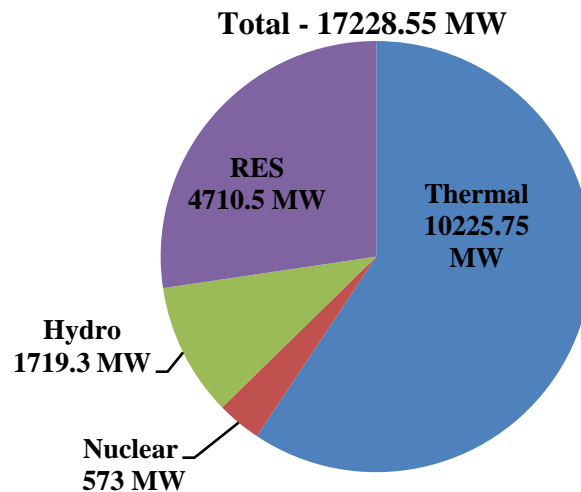


Figure 1.3 Source-wise installed capacity in Rajasthan (MW) as on 30.06.2015 [12]

As discussed, the conventional fuels like coal and oil have been the primary sources for current energy requirement of Rajasthan. However, the Government of Rajasthan acknowledges the increasing concern related to the long term availability of such fuels and their environmental impacts like climate change, global warming *etc.* [13].

The promotion of renewable energy is one of the key measures taken by the state government in this direction. Presently, electricity generation from renewable sources has been increased in a significant manner and becomes an integral part of energy security initiative in the state. The state of Rajasthan is endowed with diverse forms of renewable energy sources including wind, biomass and specially solar *etc.*

1.3 ENERGY SYSTEMS

An energy system can be referred to an electric power system for generation, transmission and consumption of electric power. On the basis of generation of electrical power, the energy systems can be divided as conventional, non-conventional and hybrid energy systems. As name implies conventional energy systems are having

conventional energy sources and non-conventional energy systems are having renewable energy sources, and hybrid energy system (HES) is the energy system which consists of both conventional and non-conventional energy systems.

Renewable resources like solar and wind are unpredictable as far as their availability round the clock. Owing to their intermittent nature, the reliability and consistency of an energy system involving a single renewable energy source is very less. Moreover, this would be called for elaboration of energy storage to ensure uninterrupted supply of power, especially when a stand-alone installation is considered. To utilize the various renewable resources efficiently, two or more individual renewable energy sources can be combined together to function as an energy generation system. Such type of system is called hybrid energy systems (HESs) and can be deployed to meet the energy demand of rural areas, off-grid communities and remote applications. A mix of various sources like solar PV panels, wind generators, micro hydro turbines, biomass, ocean wave, geothermal, tides, fuel cell and others sources of electrical energy can be utilized as required to meet energy demand in a way that is appropriate to the local geography and other specifics [14].

1.4 HYBRID ENERGY SYSTEMS

When conventional sources incorporated along with the renewable sources the system is termed as Hybrid Energy Systems (HESs). Complete HES may have the various units other than the energy generating units, such as power conditioning units, energy storage units, controller units, backup power supply units etc.

HESs increase the reliability of supply and reduce the energy storage requirements. It also reduces the overall cost and per-unit cost of electricity, since many smaller units are to be designed to function in parallel with high efficiency. Moreover, the incorporation and utilization of renewable energy sources present environmental advantages. Before developing HES for a specific site, it is essential to know the particular energy demand and the resources available at that site. Therefore, energy planners must study the availability of solar, wind, and other potential resources of energy at the site, in addition to the energy demand. This allows them to design the suitable kind of HES that would be able to harvest the available energy effectively and meet the demand of the location at the best [15].

1.4.1 Benefits of Hybrid Energy Systems [HESs]

Hybrid energy systems possess following benefits over conventional energy systems:

(a) Improved Reliability – By using HES, a robust power supply may be achieved with less downtime during power failure by virtue of varying power energy sources [16]. Failure of electrical system and diesel supply interruption are the leading factors for utilizing another generation system which consists of renewable energy and diesel hybrid system to support reliable and uninterruptible power supply. In renewable energy system less downtime is required during maintenance due to less mechanical parts involved as compared to other system.

(b) Improved Energy Services - A conventional system using a diesel engine with generating set is less viable due to high operating cost and poor running condition, but non-conventional energy system working in combination with a diesel generator, contributes to dynamic and high quality electricity services for long duration [17-19]. The main cost of wind and solar PV power generation is direct capital expenditures whereas the operational and maintenance costs are considerably very low.

(c) Reduced Emissions and Noise Pollution - Renewable energy system does not cause air, water and noise pollution [20]. Thus, HES with renewable energy sources produces less emission and noise compared to a conventional diesel generator energy system.

(d) Continuous Power with Efficient Use of Energy - Hybrid energy system not only provides continuous power but it also gives the technology for efficient use of energy. For this solar/wind system deals with base load demand and a diesel generator deals with peak load demand, diesel generator also gives electrical energy in bad weather conditions [21-25].

(e) Increased Operational Life - Life of overall HES is enhanced due to the alternate operation of renewable energy sources and a diesel generator at regular time periods and its use is also reduced due to availability of renewable energy [21-25]. Furthermore, the discharging level of the batteries is optimized hence; operational life of batteries is increased.

(f) Reduced Cost - This type of hybrid system is most cost-effective due to less consumption of diesel as operation of a diesel generator is for less period of time also leads to less maintenance cost [21-25]. For a conventional diesel system at isolated areas, the fuel cost, transportation cost and maintenance cost are very high, which are not viable to rural community.

Recent research, improvement and development of alternative energy sources have shown outstanding potential as a part of power generation systems. To provide continuous and high quality power supply to remote locations, there is an enormous potential of utilizing renewable energy resources.

1.4.2 Stand-Alone and Grid-Interfaced Hybrid Energy Systems

An electrification of rural areas and other sites which are situated at a very long distance from general load centers, using electricity from the grid would be an extremely costly affair. This is where autonomous energy systems like stand-alone hybrid energy system come into prominence and serve as the key to the energy problems faced by such off-grid communities [26].

In addition, the deployment of an energy system using a single renewable resource becomes less economical in many cases. This calls for HES where a number of renewable energy sources along with electrical energy storage components are integrated, to work as a reliable power source and fulfill the electrical energy requirement. They can be either grid-connected or stand-alone installations depending on the application and geography of the site [26].

The cost of commercial electricity supply system is very high, as it is highly dependent on the centralized grid energy systems which operate mostly on thermal and nuclear power plants require big investments for establishing transmission and distribution networks. It would be even more uneconomical if the grid facilities are to penetrate remote regions making rural electrification, as it becomes more costly compared to electrification of urban areas. So to overcome above said problems, alternative systems of electricity generation and distribution are highly required. Unlike the centralized power systems, decentralized power systems are generally based on renewable energy sources such as solar and wind, work at lower scales (of

the order of few kW) both in the absence and presence of grid [27-32]. They are easily available at remote or isolated locations because of the ability to function independently and generate power in the proximity of demand site. Hence, the use of renewable energy based decentralized power systems are more effective for the rural electrification, by providing reliable, sustainable and environmentally friendly energy supply.

A grid interfaced hybrid energy system is connected to the centralized grid system and feeds the generated power to the grid. Any local load connected to the system may derive power from the hybrid system directly or through the grid. Such a system eliminates the requirement of a storage system since the load may be supplied from the grid when the hybrid energy system is not operational and does not produce any power. Here, the grid works like a storage unit with unrestricted capacity, which takes care of seasonal load demand variations and accommodates all fluctuations in the energy generation from the HES side [33]. However, a grid connected system may not be feasible in remote areas where the grid cannot be connected and there may be no other sources of energy. In such cases, a stand-alone system may be employed giving priority to the needs and usage pattern of the local region with ample storage facilities.

A stand-alone hybrid renewable energy system is a hybrid system includes two or more renewable energy sources like solar-thermal, solar photovoltaic, wind, biomass and hydropower *etc.* and is incorporated to supply electrical energy or heat energy or both, to the same demand. The most commonly used hybrid energy system is to supply electrical energy, with the combinations of solar photovoltaic (PV) modules and wind turbines [34].

Because of the intermittent supply pattern of different available renewable energy sources at different locations, a combination of two or more renewable energy sources gives a better overall supply pattern [35]. Sometimes, as per the need of the demand, an energy storage system is also included to make the energy supply system more effective, less intermittent, or more firm.

A combination of storage system like batteries with renewable hybrid energy system, not only increases the duration of energy independence but also ensures best possible use of the available renewable energy resources, which yields high reliability [36].

The cost of said system is high, as to deal with varying weather conditions at different locations and to ensure the energy supplies to the load demand at the worst weather conditions, the capacity of storage system needed is large. There is better and cheaper solution to supply energy demand during poor wind days or cloudy weather days or peak loads, with a diesel generator working as secondary back up supply, although the percentage of renewable energy used is also reduced [21-24]. However, one can maximize fuel savings by minimizing the diesel generator running time, by selecting appropriate size of the storage system.

1.4.3 Topologies of Stand- Alone Hybrid Energy Systems

For understanding the various topologies, a hybrid system of renewable sources as solar, wind with a diesel generator and battery bank is taken. In these topologies, AC and DC power generating units are connected at some point in the system and somewhere before the loads are supplied.

Generally, three types of hybrid energy system topologies are used in the literature [3, 15, 37-39], which are as follows:

- (a) AC-coupled hybrid energy systems
- (b) DC-coupled hybrid energy systems
- (c) Mixed-coupled hybrid energy systems

1.4.3.1 AC-Coupled Hybrid Energy Systems

In AC coupled HES configuration, all the different energy conversion system are supplying AC loads. It can be further classified as follows:

- i. Centralized AC-Coupled HES
- ii. Decentralized AC-Coupled HES

i. Centralized AC-coupled Hybrid Energy Systems

In centralized AC-coupled HES, a main AC-bus comprises all the energy generating systems before being supplying to the load [14-15]. This configuration can be depicted by the Figure 1.4.

The wind generator and a diesel generator produce AC power, thus they can be directly coupled onto the main AC-bus or with AC-AC converters. The PV-array

produces DC power and an inverter must be used before it is coupled with the main AC-bus [14-15, 38]. A bidirectional inverter must be used for the charging and discharging of the battery bank as shown in Figure 1.4.

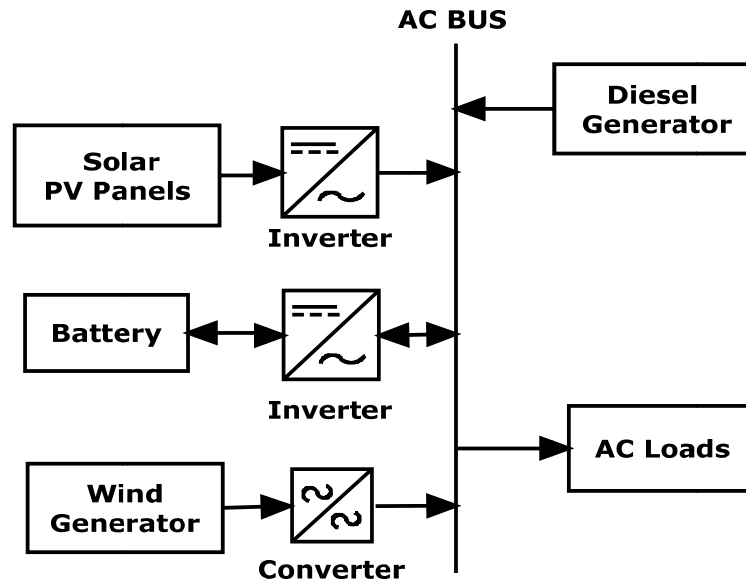


Figure 1.4 Block diagram of centralized AC-coupled hybrid energy systems

ii. Decentralized AC-coupled Hybrid Energy Systems

AC-coupled HES, as shown in Figure 1.5, is said to be distributed or decentralized when all the energy conversion systems are not connected on a common AC-bus; whereas the load is supplied by the individual unit or all of these units.

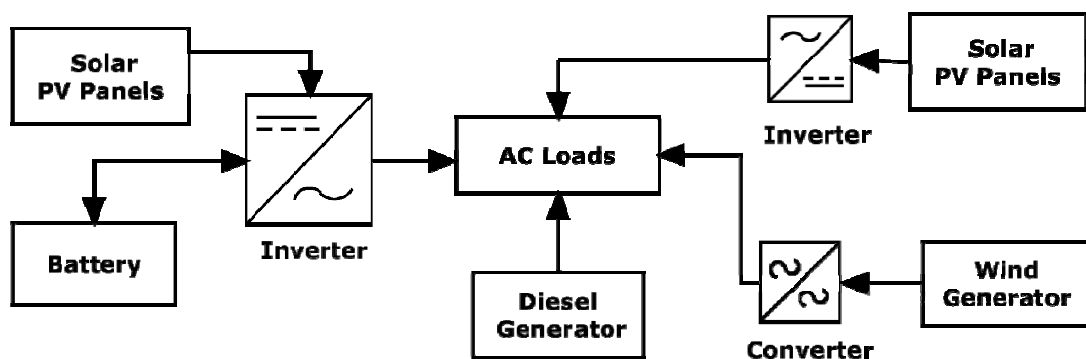


Figure 1.5 Block diagram of decentralized AC-coupled hybrid energy systems

In this topology, the energy sources are not connected to one common bus as in the previous cases. Moreover, these sources may not be installed close to each other i.e. the generation sources are scattered in different appropriate locations and each source

is supplying load separately [14-15, 38]. The DC power obtained from the PV-system and the battery need to be converted to AC before feeding the AC loads, thus appropriate inverters are required. The main advantage of this topology is that the different energy conversion systems are installed geographically and appropriately located in such a way that the solar PV systems are installed in places where there is more solar irradiation and the wind generators in locations where there is more wind. However, the topology contains difficult controlling due to installation of each unit at far distances.

1.4.3.2 DC-Coupled Hybrid Energy Systems

In DC-coupled HES configuration as shown in Figure 1.6, all the energy conversion systems, unlike AC-coupled HES, are connected to a DC main bus. AC loads are connected to DC bus through a main inverter [14-15, 38].

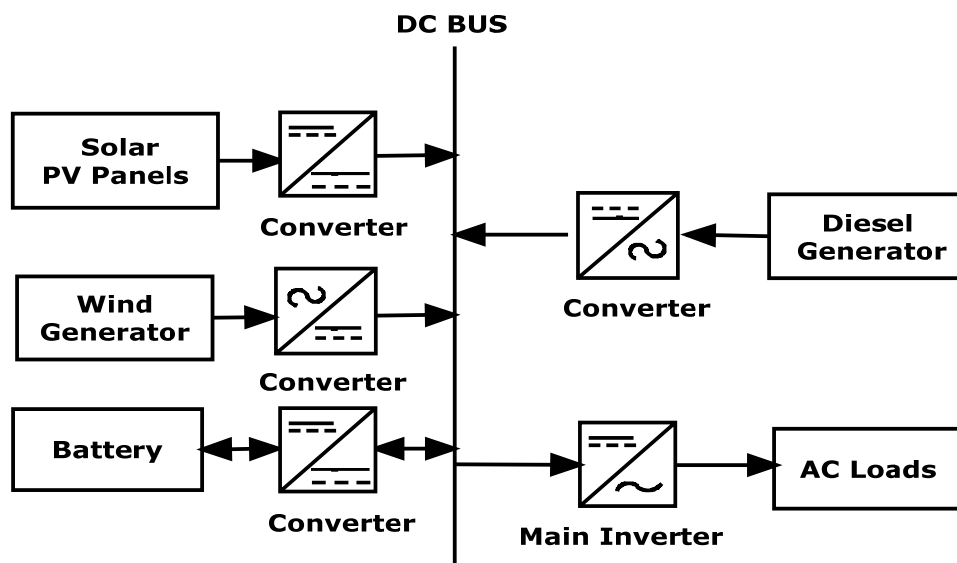


Figure 1.6 Block diagram of centralized DC-coupled hybrid energy systems

1.4.3.3 Mixed-Coupled Hybrid Energy Systems

It is also possible to combine AC-coupled and DC-coupled hybrid energy systems and to form mixed HES [14-15, 38]. With this type of configuration as shown in Figure 1.7, some of the renewable energy sources (RESs), PV-array, in this case are

connected with the battery bank at the DC-bus and other RESs (wind generator, in this case) are connected with the diesel generator at the AC-bus.

A comparison of mixed, AC- coupled and DC-coupled hybrid systems show that AC-coupled hybrid systems have many advantages [15] such as simplified design, standardized coupling of various components, common available grid components can be used and operation of island grids, compatibility with existing grids, reduced system cost, good reliability and expandability of electrical power supply.

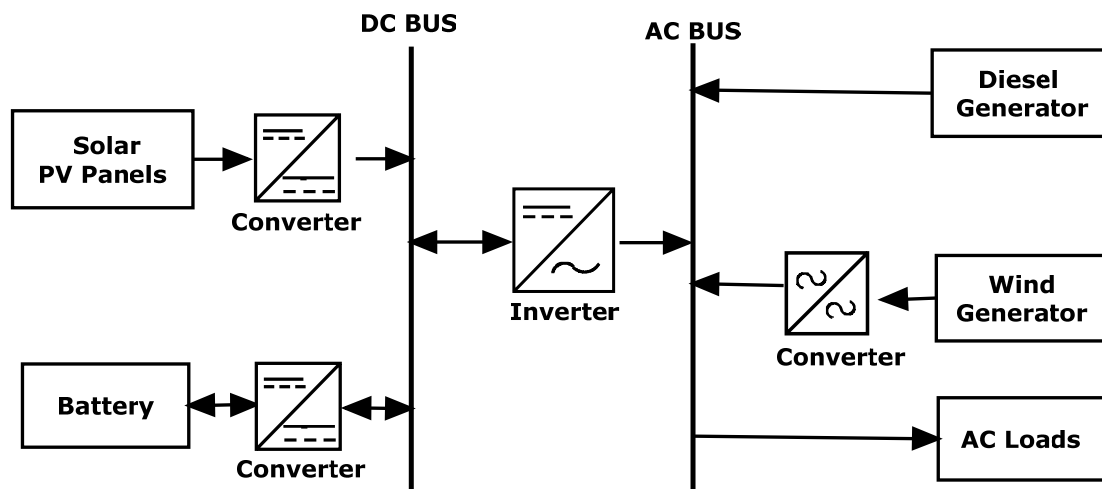


Figure 1.7 Block diagram of mixed-coupled hybrid energy systems

1.5 SCOPE OF WORK AND OBJECTIVES

There are many possible topologies or configurations of hybrid energy systems. One way to classify hybrid energy system architectures is to discriminate between DC and AC bus systems. In DC bus system, renewable energy source components and the backup source like a diesel generator feeds power to a DC bus, after that the power is converted in to AC supply through an inverter, which is connected between DC bus and the AC loads. This system is suitable for small hybrid energy system. In large hybrid energy system, AC bus configuration is used where large solar PV system, wind energy system, diesel generators etc. are connected to the AC distribution bus and can serve the loads directly or may feed power to grid system.

The topology or configuration used in this thesis has solar PV array and wind turbine as renewable sources, with a battery bank as energy storage and a diesel generator as

backup sources. Figure 1.8 illustrates the block diagram of proposed hybrid system configuration with DC and AC buses.

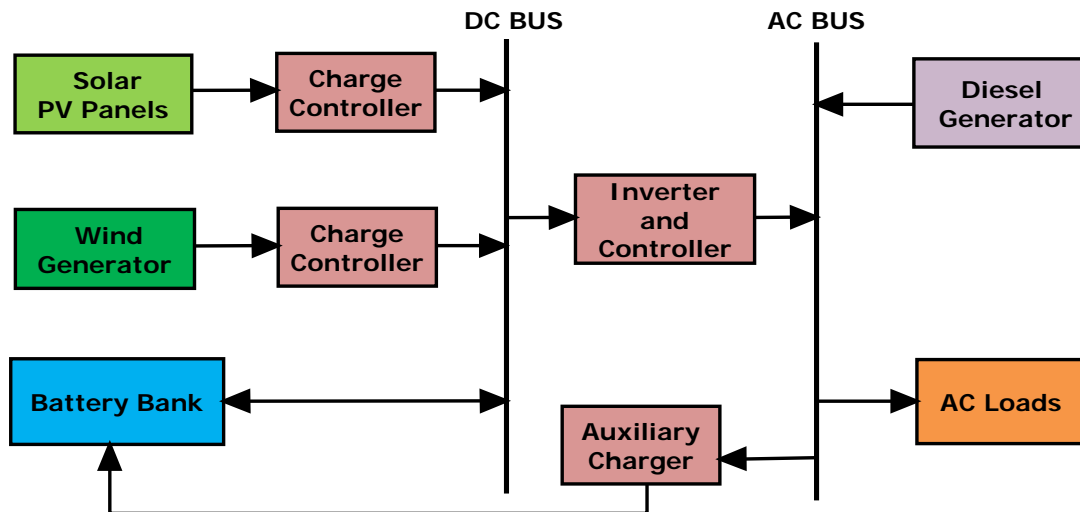


Figure 1.8 Block diagram of proposed stand-alone hybrid energy system

The main objective of this research work on “**Investigations on Small Scale Standalone Hybrid System for Rural Electrification**” is to design and analyses of a small scale stand-alone hybrid system for rural electrification, in order to cater the demand of electricity in remote areas by using renewable energy sources with a battery storage and a diesel generator.

To achieve these objectives, this work addresses following specific tasks:

- Review the state of the art in the hybrid energy system by updating the literature survey.
- To develop a Simulink model of 1.0 kW solar PV system in Matlab/Simulink.
- To design, modeling and implementation of maximum power point tracking on solar PV system.
- To develop a Simulink model of 1.0 kW permanent magnet synchronous generator (PMSG) based wind energy conversion system (WECS) in Matlab/Simulink.
- To develop the model of a 1.2 kVA Diesel Generator (DG) in Matlab/Simulink.

- To estimate the load profile of un-electrified small utility at Kukas, Jaipur, India.
- To estimate the solar irradiation profile of Kukas, Jaipur, India.
- To estimate the wind speed profile of Kukas, Jaipur, India.
- To develop a Matlab/Simulink model of stand-alone solar-wind-battery hybrid system.
- To develop a Matlab/Simulink model of stand-alone solar-battery-diesel generator hybrid system.
- To develop a Matlab/Simulink model of stand-alone wind-battery-diesel generator hybrid system.
- To develop a Matlab/Simulink model of stand-alone solar-wind-battery-diesel generator hybrid system.
- To compare above 4 cases of stand-alone hybrid systems.
- To develop hardware implementation of stand-alone solar-wind-battery-diesel generator hybrid system.
- To analyze, validate and compare the simulation and test results of stand-alone solar-wind-battery-diesel generator hybrid systems.

1.6 ORGANIZATION OF THESIS

The thesis is organized into six chapters. An overview of each chapter is presented as follows:

Chapter 1 presents, an introduction to the subject, the details of various renewable and non-renewable energy resources, the present energy scenario in India and Rajasthan in particular, grid connected and stand-alone systems and hybrid energy systems and their topologies. The research objectives and the methodology adopted have also been included.

Chapter 2 includes a comprehensive literature review and details of load profile, solar irradiation profile and wind speed profile for configuration of proposed system at Kukas, Jaipur, India location.

Chapter 3 includes the design and mathematical modeling of solar PV system with MPPT and wind energy conversion system using PMSG, power electronics

converters, a battery storage and a diesel generator system to supply single phase AC loads.

Chapter 4 includes dynamic modeling of the stand-alone hybrid energy system with four cases- (i) Solar-wind-battery hybrid system, (ii) Solar-battery-diesel generator hybrid system, (iii) Wind-battery-diesel generator hybrid system, (iv) Solar-wind-battery-diesel generator hybrid system and comparison among these cases is made to select a proper HES for a selected location.

Chapter 5 deals with the hardware implementation of solar-wind-battery-diesel generator hybrid system to supply a small rural utility and validation of various simulation results.

Chapter 6 exhibits overall conclusions of the research and proposes directions for future work.

A detailed bibliography of the literature related to this work is appended at the end. The technical specifications and parameters of various components are given in Appendixes.

1.7 CONCLUSIONS

Extensive brief review has been presented for the energy requirement. Study on the scenario of India and Rajasthan has been carried out. Benefits of hybrid energy systems using renewable sources such as solar and wind energy have been discussed. Further many topologies for supplying AC loads have been discussed, as power generation of solar PV source and battery source is DC, while the power in the wind power generator and a diesel generator are in AC. At last section of the chapter, the scope of work and objectives of the thesis have been discussed and organization of thesis is also included.

Chapter 2

Literature Review

T HIS chapter begins with fundamental thought of an insight into various aspects of hybrid energy systems. Load profile, solar profile and wind profile are also presented for a small utility at Kukas Village, Jaipur Rajasthan, India. All the profiles are classified in three season's summer, rainy and winter and are to be used in next chapters for study of various stand-alone hybrid energy systems.

CHAPTER 2

LITERATURE REVIEW

2.1 GENERAL

This chapter provides an overview of the literature pertaining to the proposed research work. The first section focuses on a review of the literature concerning the solar PV generation and hybrid energy system. In the second section, wind hybrid energy systems are reviewed. The third section focuses on a review of the literature concerning the solar PV–wind hybrid energy systems. Load profile, solar profile and wind profile are also presented for a small utility at village Kukas, Jaipur, Rajasthan, India.

2.2 LITERATURE REVIEW

Recently the use of non-conventional sources to generate electricity is gaining ground due to its pollution free nature and availability of resources. In this research work, the objective is to concentrate on the development of an isolated solar power generation system for low power applications.

Hybrid energy system consists of two or more than two energy systems interconnected. Following stand-alone hybrid energy system configurations are available in the literature and commercially viable:

- (i) PV-battery hybrid energy system
- (ii) PV-diesel hybrid energy system
- (iii) Wind-battery hybrid energy system
- (iv) Wind-diesel hybrid energy system
- (v) PV- wind-battery hybrid energy system
- (vi) PV-wind-diesel hybrid energy system

2.2.1. PV Hybrid Energy Systems

Solar PV energy system uses solar irradiation to produce energy. PV-HES can be best suited technology to reduce the dependence on conventional fuels [40-42]. In PV HES

PV panels and controllers, battery bank or diesel generator, are major components. With help of battery storage in PV HES, the flexibility of system control can be assured [43, 44]. These PV HES can be used as a better economic and cheaper solution to meet energy requirement in remote/rural as well as urban areas [32, 45-48].

PV HES performance can be assessed by different available models based on probabilistic or deterministic approaches for getting optimal mix of PV with a diesel generator. PV HES configuration can work in both modes either with a battery storage or without a battery storage. Modeling of the battery storage in respect to state of charge with optimal size of HES is studied in recent literature [49-53]. A mathematical technique to find minimum battery storage days and PV array area is demonstrated in [22]. Further, optimal combination of a battery and a PV sizing is being determined by Shrestha and Goel [41] by using statistical approaches.

An iterative optimization technique is used to model PV HES [21], where optimal mix of a PV and a diesel is calculated with respect to cost of electricity generation. PV HES system with battery storage is optimized by Bhuiyan and Asgar [52] for Dhaka, Bangladesh, where power output for different tilt and azimuth angle has been considered for optimum performance of PV HES.

PV HES performance is evaluated in [54] where reliability of PV system has been considered in respect to widely varying conditions in terms of loss of power supply probability (LOLP) [54]. Further, computing capacity of a battery storage and a PV array has been reviewed by Egido and Lorenzo [55] and on the basis of review an analytical model based on LOLP has been presented. While an effective methodology is developed by Marwali et al. [56], in which production cost of PV HES is calculated on the basis of PV size.

PV-diesel hybrid system practices have been reviewed by Wichert [17] and many researchers [21,23,57-60] where maintenance free energy storage system is used along with fully automatic energy management system.

2.2.2. Wind Hybrid Energy Systems

Wind hybrid energy system effectively and economically uses good potential of wind energy [61]. In recent studies, the economic viability and technical feasibility of wind

hybrid energy system are analyzed to meet the demand capacity [62, 63]. In recent researches [64-68], different forecasting models using regression analysis, Monte-Carlo simulation has been reported in order to predict the wind performance. In wind HES, the capacity factor of wind turbine also affects the wind generation, while planning for wind power production optimal site selection and wind turbine installation are also important [69,70]. Various control methods for wind HES are also reviewed in the literature [71-73].

In [74], an easy method was developed by Celik to estimate the monthly wind energy system performance. Where, Weibull distribution is used for estimation of wind speed parameters on monthly basis. The used algorithm finds better solution in case of hourly wind data is missing for wind power estimation on monthly basis.

Wind HES with battery storage increases to get optimal solution to meet load demand. In [75], a battery storage optimum size has been determined by Elhadidy [75] by calculating the impact of variation of battery storage on HES. In [76], LOLP based wind hybrid energy system operation has been reported where constant trade-off between battery storage size and diesel power has been assumed and for a given LOLP, an optimal mix for wind HES is obtained. In [34, 77], network basis wind potential penetration has been reported.

2.2.3. Solar PV - Wind Hybrid Energy Systems

Stand-alone wind or solar PV power generation is not recommended commercially due to unavailability of useful energy throughout the year. Combination of wind and solar PV power is popular as HES due to its feasibility and less requirement of the battery storage system and a diesel generator. Solar PV generation is available if only solar irradiations are present. Similarly incase of wind power generation, wind power is available only when the wind is present. In recent literature, the various feasibility and performance issues have been reported in [20, 28, 30, 75, 78-79,144-147]. In [80], Nehrir et al. discussed the general performance of solar PV-wind HES with reference to computer-modeling approach. While in [81] Celik has used synthetically generated weather data for calculating performance of solar PV-wind HES.

In [29, 82], solar PV-wind HES's optimal size is calculated by using hourly basis data of daily average power per month. Further, the performance of solar PV-wind HES is compared by wind generators capacity fixing method and LOLP based capacity of PV array with a battery bank storage capacity.

In recent literature, various optimization techniques are used to design solar PV-wind HES. Mainly used optimization techniques are as probabilistic approach [61], linear programming based approach [18, 83], dynamic programming based approach [84] and multi-objective based optimization approach [85]. Further, Karki and Billinton [77] have used Monte-Carlo simulation approach in small isolated power system to calculate reliability/cost implications. However, in [86], results of two different optimization techniques for optimal operation of solar PV-wind HES are analyzed.

An optimal proportion of a wind generator capacity and a solar PV generator capacity by using LOLP is calculated by Al-Ashwal and Moghram [65]. Here combination of optimal design of solar PV and wind power systems is chosen on the basis of annual autonomy level and capital cost. However, annual autonomy of the system is based on LOLP and it is used to find better system configuration [16, 35]. Considering different design factors like annual autonomy, a general methodology is developed by Protogeropoulos et al. [66] for sizing and optimization of solar PV and wind power. Here a battery storage sizing is also calculated by using system performance model to achieve desired autonomy level, where backup diesel generator is used to achieve high annual autonomy in order to reduce the battery storage capacity.

Techno-economic analysis is presented for autonomous solar PV-wind HES on the basis of wind and solar monthly bias by Celik [27, 81]. The monthly combinations of wind and solar resources are known as wind and solar monthly bias respectively. In [87], it is observed that optimal combination of wind and solar PV power would provide higher performance in comparison to only single wind or single solar PV system.

Further controller design is presented by Chedid and Rahman [88] that is used to monitor the operation of HES in isolated or grid connected mode. The controller is used to determine each component's energy availability and system environmental

credit. This model is able to calculate the battery charging and discharging losses, unmet and spilled energies and production cost.

The decision support models based on economical, technical, political and social, issues have been discussed in [19, 24,147]. Here to plan optimal operation of solar PV-wind HES using analytical approach, various divergences of opinions, events and practices have been carried out in order to meet out different confusion and uncertainties. Finally, the trade-off risk method is used for generating multiple plans, and on the basis of these trade-off curves conditional decision set is made to carry out risk analysis.

From the critical review, it is revealed that solar PV-wind HES are very economical to use with a battery storage and a diesel generator system in remote areas as well as urban areas.

2.3 THE CONFIGURATION OF PROPOSED SYSTEMS

In this section, load profile of a small utility at Kukas, Jaipur is estimated on hourly basis. A Matlab/Simulink model of single phase load is developed and simulation results are presented for summer, rainy and winter seasons. Solar irradiation and wind speed data are also estimated, at Kukas, Jaipur, for the year 2014.

2.3.1 Load Profile of a Small Utility at Kukas, Jaipur, India

For the identified un-electrified small utility, HES based on solar PV, wind and diesel generator has been proposed for reliable power supply. Based on the energy requirement of the small utility, the load profile is estimated.

The energy requirement in such areas can be classified as domestic, commercial and street lighting. For domestic purposes, electricity is required for appliances like tube light, compact fluorescent lamp (CFL), LED, fan, radio, TV etc. Commercial applications include CFL, fans, water pump etc. The street light load is considered to be CFL based.

The energy requirements in the small utility vary from season to season. Therefore, in this study, yearly data has been divided into three seasons, depending on the demand and energy consumption pattern: winter season (November to February), summer season (March to June), rainy season (July to October). The numbers of electrical

appliances proposed for the electrification of the small utility of village Kukas, Jaipur are shown in Table 2.1.

Table 2.1 Details of the proposed electrical appliances

Sr. No.	Type of Electrical Appliance	Power Rating (watt)	Total Nos.
1	Lighting Load(CFL/LED)	15/8	4/4
2	Fan(Ceiling/Table)	55	3
3	Misalliance Load (Radio/ T.V.)	30/140	1/1
4	Water Pump(Induction Motor)	0.5HP(373W)	1
5	Street Light	36	2

Based on the data given in Table 2.1 and the pattern of the usage and duration depending upon the seasonal variations, the load profile for summer, rainy and winter seasons have been calculated and shown in Figures 2.1, 2.2 and 2.3 respectively. From the load profile, it can be depicted that the load demand in the morning and late night hours is relatively less. The load demand is relatively high during the day time due to the operation of water pump and domestic load.

However, in the winter season the demand is less than the summer season as shown in Figures 2.1 and 2.3. Considering component-wise use, it is found that in the winter season, the use of ceiling fan is not considered, but in summer almost all the appliances are put to maximum use and hence display the highest load demand. The peak requirement of the load dictates the system size and hence the operation of both the water pump and TV/Radio are staggered so that the connected load of the system is 927 W and peak load is 402 W.

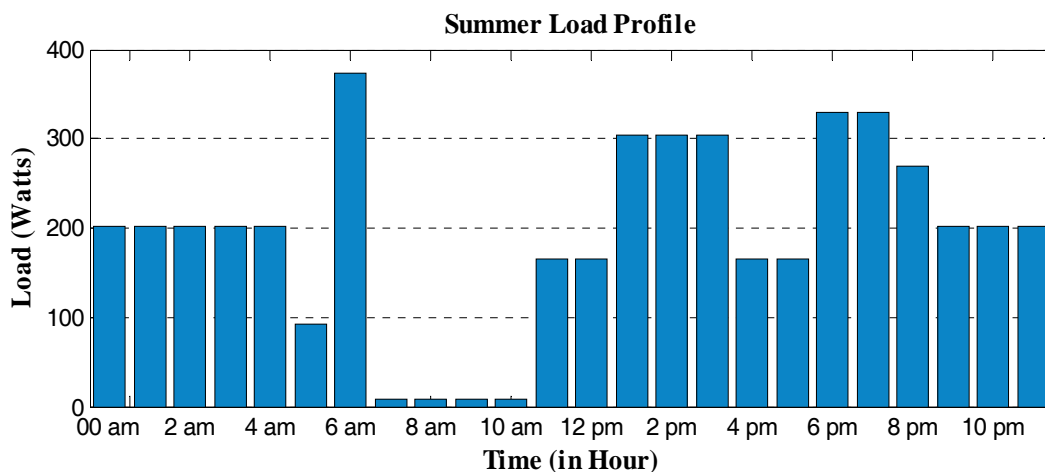


Figure 2.1 Load profile for summer season of small utility

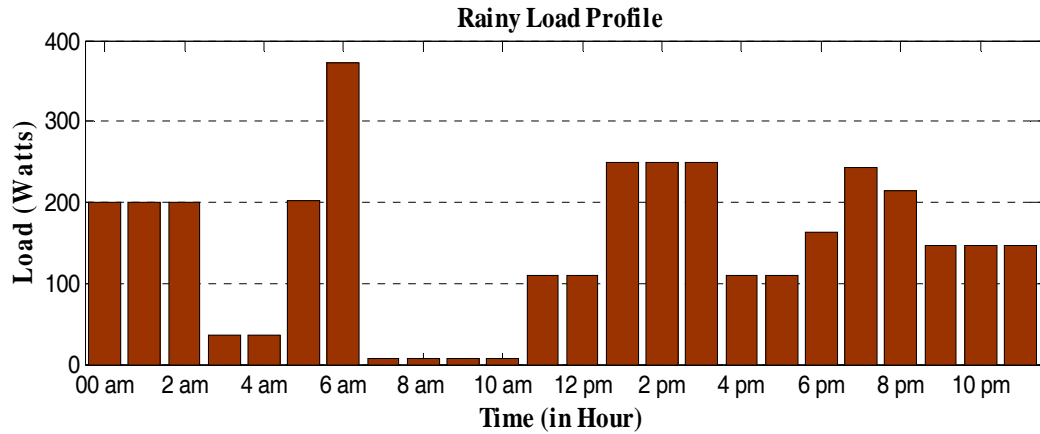


Figure 2.2 Load profile for rainy season of small utility

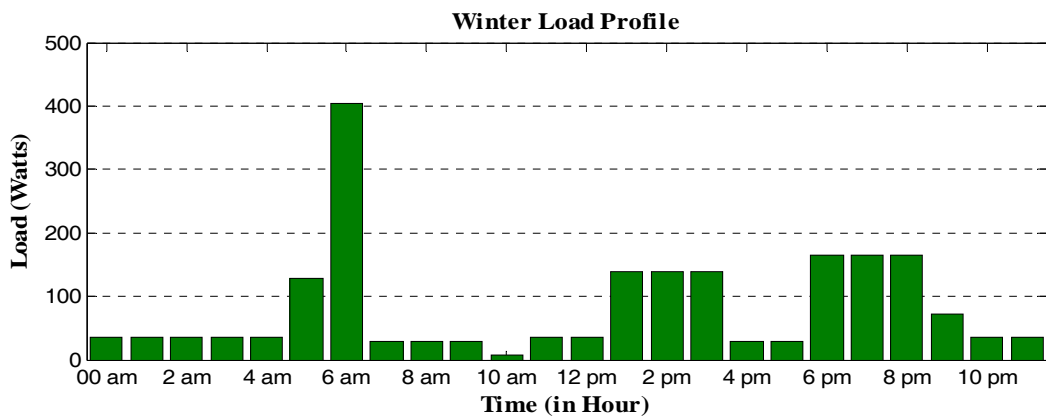


Figure 2.3 Load profile for winter season of small utility

On the basis of load profile, available energy requirements of small utility on monthly basis for a year is calculated and shown in Figure 2.4.

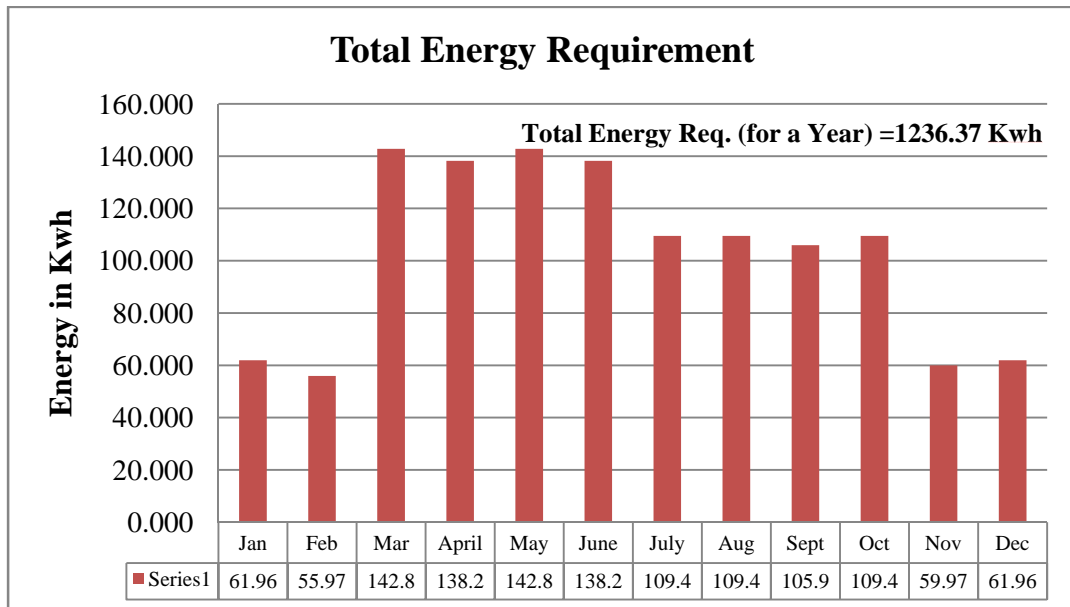
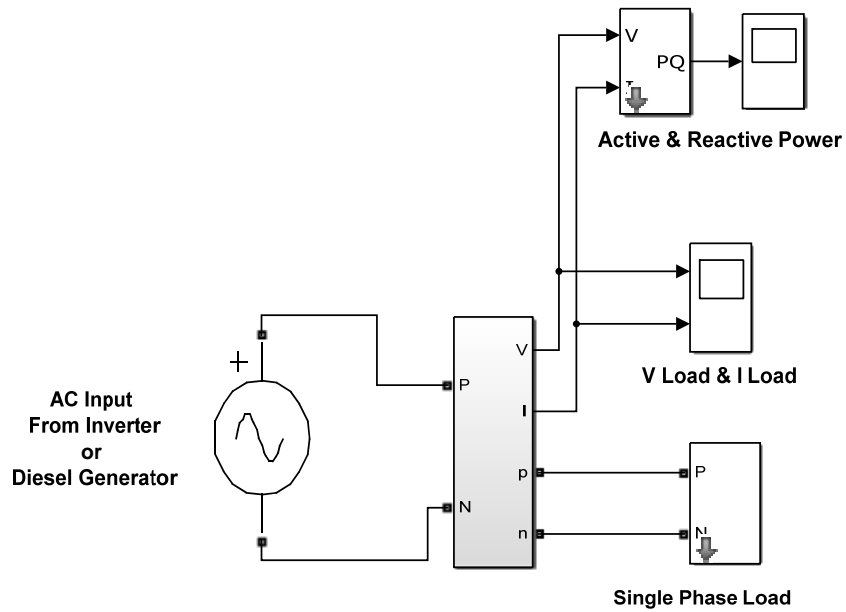
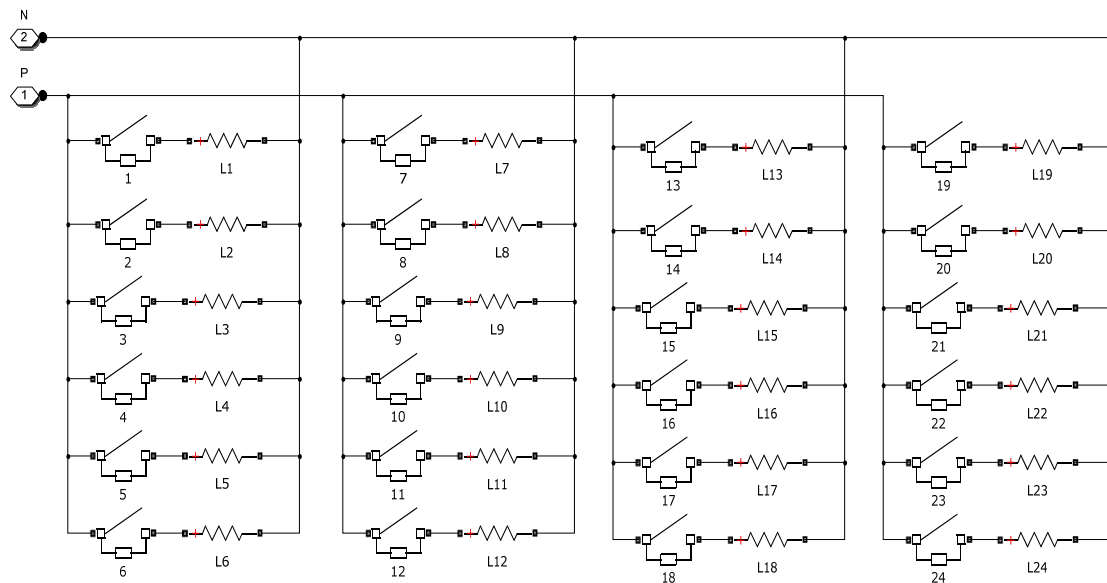


Figure 2.4 Energy requirement of small utility in Kukas, Jaipur, India



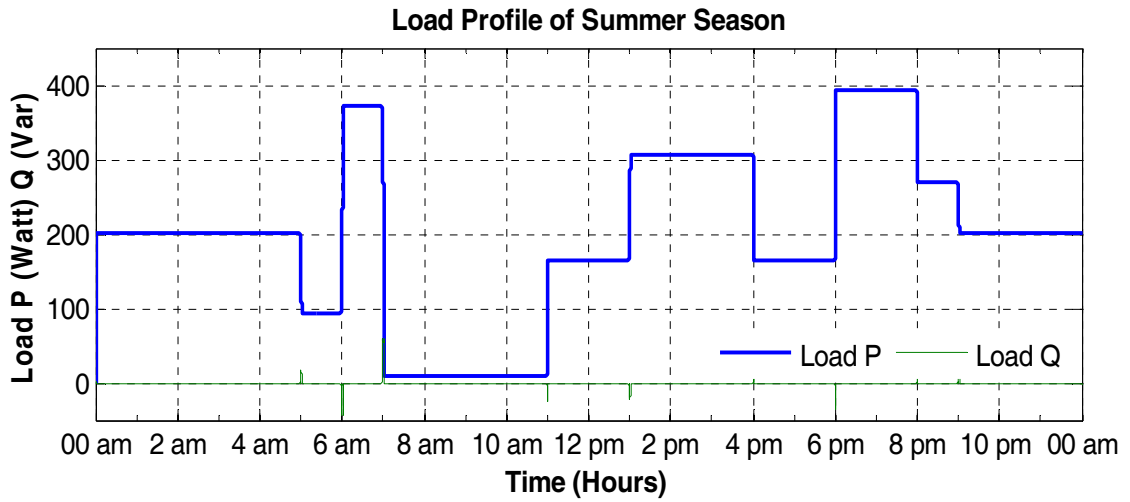
(a) Matlab/Simulink model of single phase load



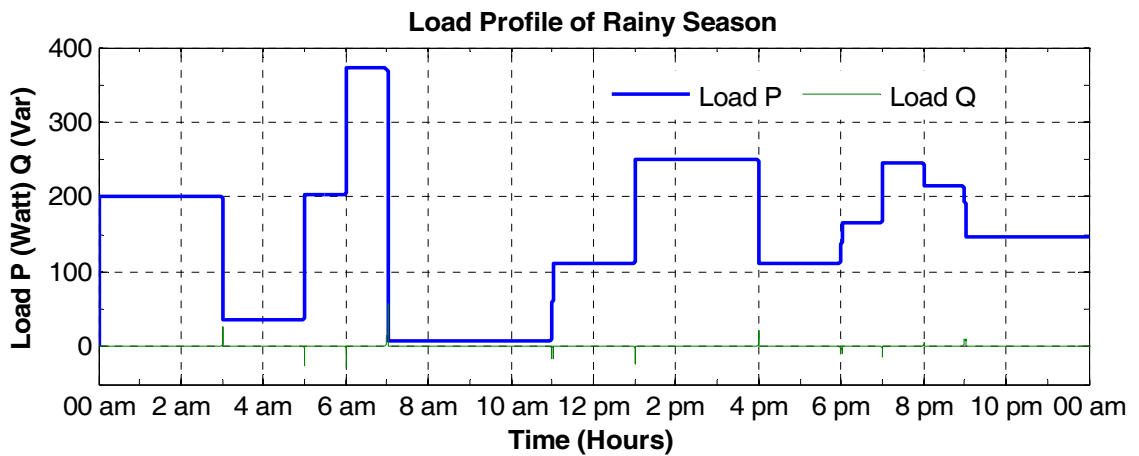
(b) Connection diagram of single phase load profile for 24 hours

Figure 2.5 Matlab/Simulink model of single phase load

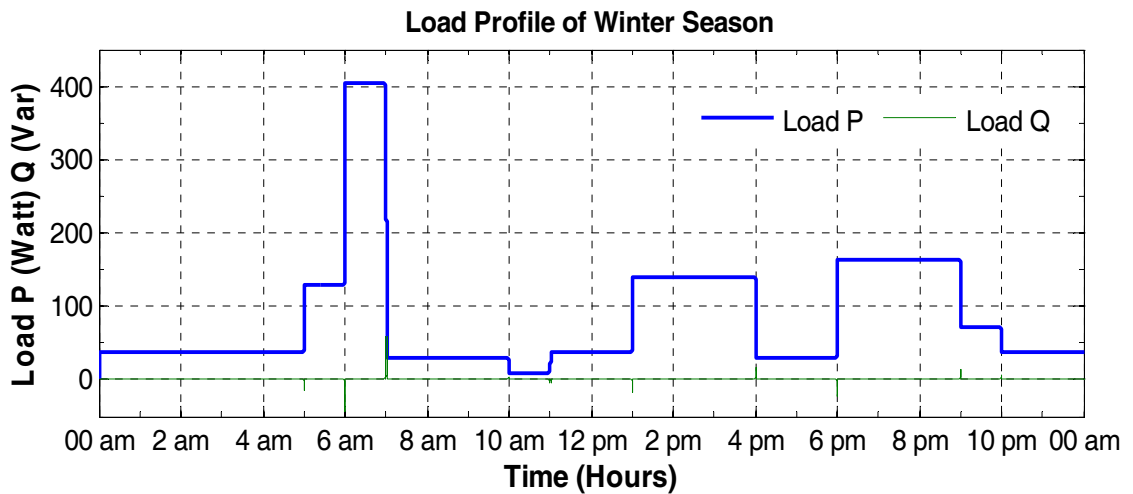
A Matlab/Simulink model is developed to show the 24 hour load variation as per previous discussion for small utility at Kukas, Jaipur which is shown in Figure 2.5. Simulations results are shown in Figure 2.6 for summer, rainy and winter seasons load variations.



(a) Summer season



(b) Rainy season



(c) Winter season

Figure 2.6 Simulation result of a 24 Hour - load variation in summer, rainy and winter seasons

2.3.2 SOLAR IRRADIATION PROFILE OF KUKAS, JAIPUR, INDIA

For estimating the exact solar generation of solar panels installed at Kukas, India solar irradiation data on hourly basis is recorded for a year in 2014 as shown in Figure 2.7.

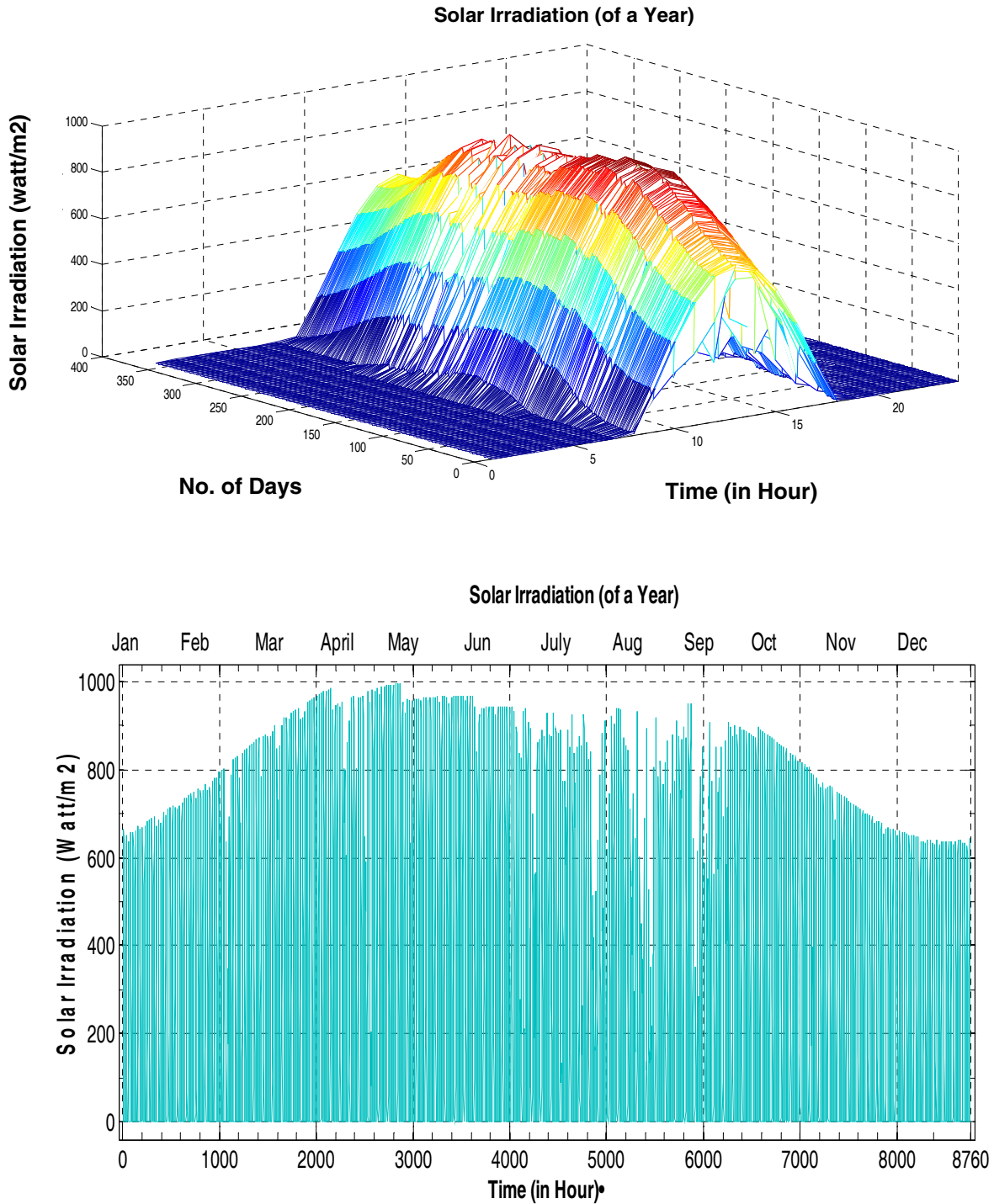
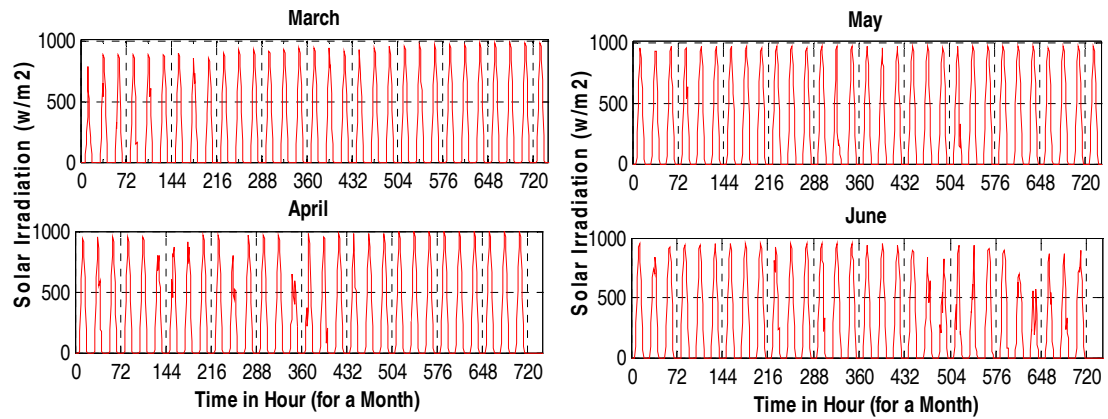
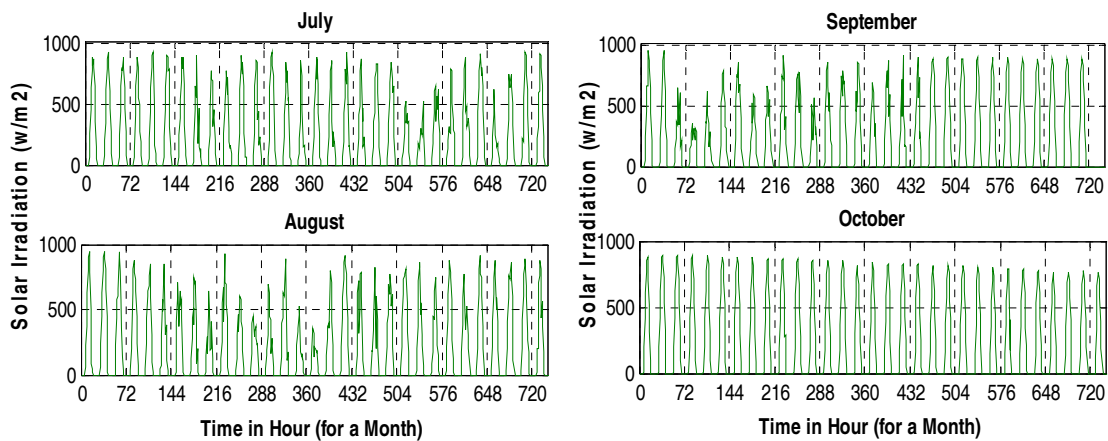


Figure 2.7 Solar irradiation (Watt/m²) of a year (hourly basis), for village Kukas, Jaipur, India

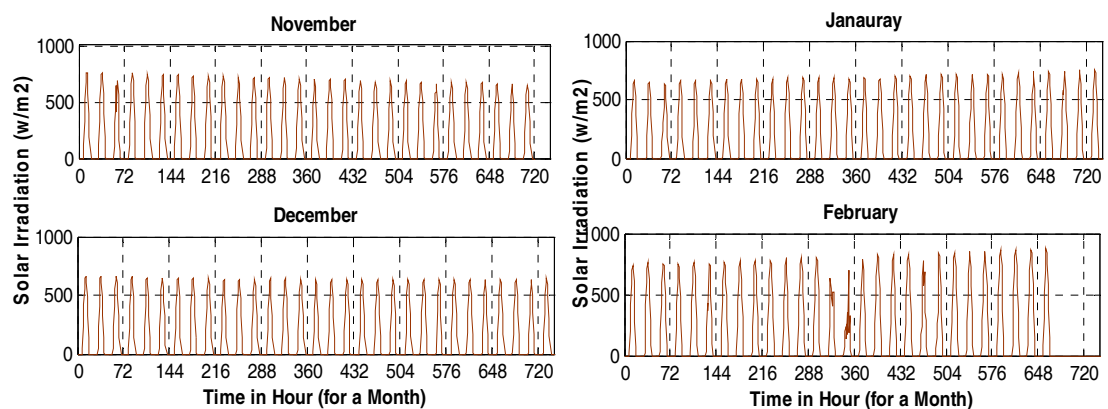
As discussed earlier that total load is distributed mainly in three seasons as summer, rainy and winter, so solar irradiation profile is also segregated as per these three seasons as shown in Figure 2.8, where 0 indicates the first day of the month.



(a) Summer season



(b) Rainy season



(c) Winter season

Figure 2.8 Solar irradiation (watt/m²) of a month (hourly basis), for village Kukas, Jaipur, India

2.3.3 WIND SPEED PROFILE OF KUKAS, JAIPUR, INDIA

Similarly, for estimating the exact wind energy generation from wind generator installed at Kukas, Jaipur, India wind speed data on hourly basis is recorded for a year in 2014, as shown in Figure 2.9.

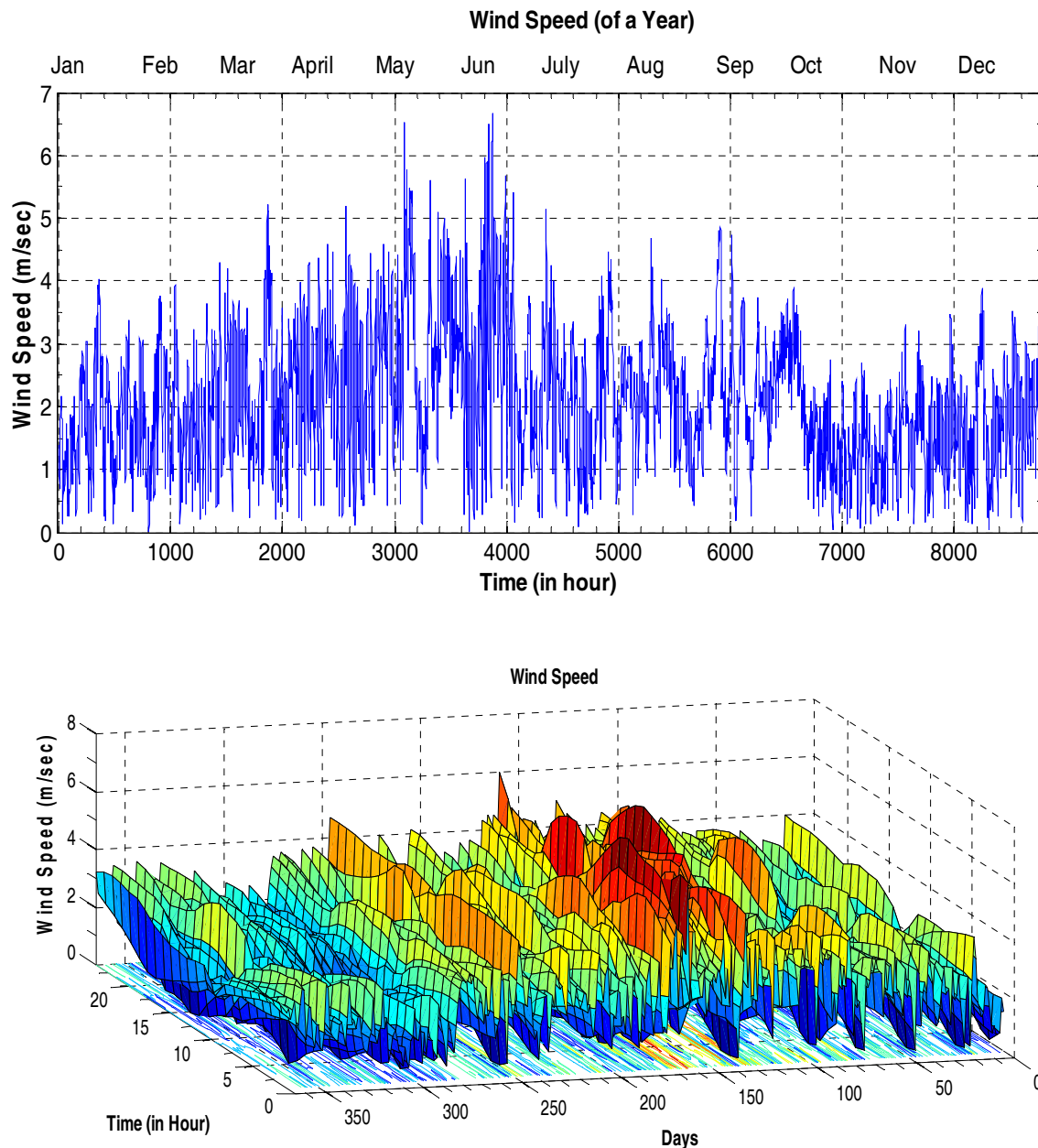
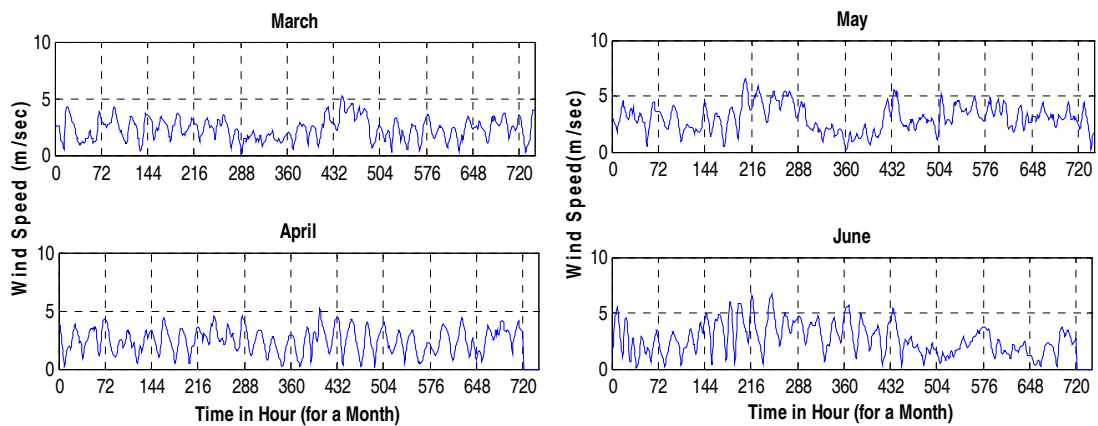


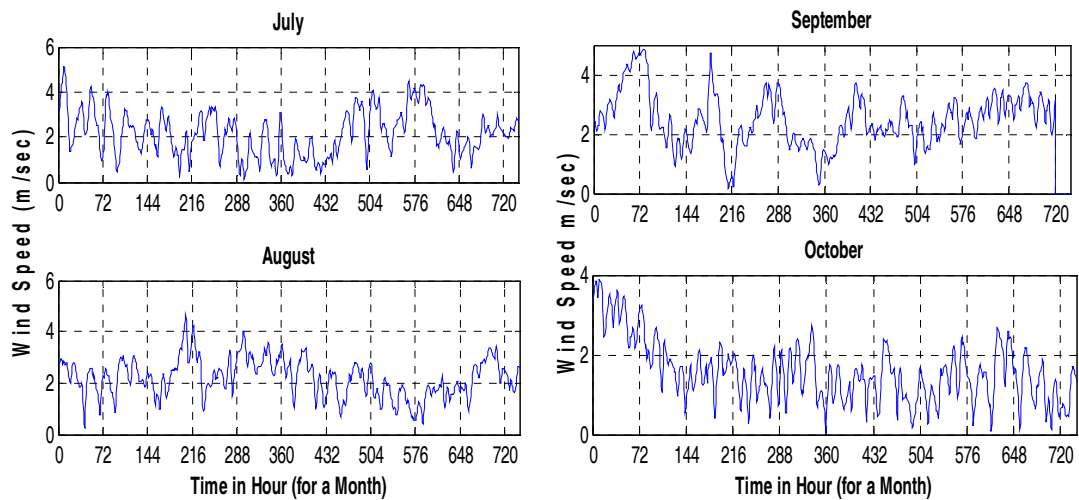
Figure 2.9 Wind speed (m/sec) of a year (hourly basis) for village Kukas, Jaipur, India

As discussed in previous section that total load is distributed mainly in three seasons as summer, rainy and winter, so as per solar irradiation profile, wind speed profile is

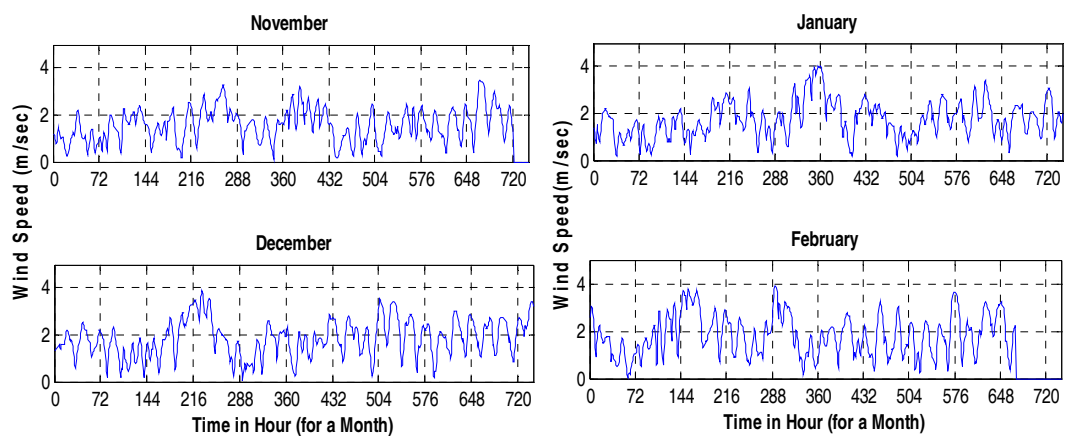
also segregated as per these three seasons as shown in Figure 2.10, where 0 indicates the first day of the month.



(a) Summer season



(b) Rainy season



(c) Winter season

Figure 2.10 Wind speed (m/sec) of a month (hourly basis) for village Kukas, Jaipur, India

2.4 CONCLUSIONS

An insight into various aspects of hybrid energy systems has been visualized through the extensive literature survey. About 136 research publications are reviewed to understand the extend of work carried out in this area. It is felt that ample scope is left for the analysis, modeling, design, and testing of small scale stand-alone hybrid system for rural electrification.

Load profile, solar profile and wind profile are also presented for a small utility at Kukas Village, Jaipur Rajasthan, India. All the profiles are classified in three season's summer, rainy and winter and are to be used in next chapters for study of various stand-alone hybrid energy systems.

Chapter 3

Modeling of Stand-alone Solar PV, WECS, And DG Systems

THIS chapter presents the basics of design and modeling of different components of stand-alone hybrid system. The controlling of solar PV and WECS system, which consists of MPPT with buck or boost converter, inverter, filter and load circuit has been designed. The load is designed for small rural utility of a day with seasonal variations. Solar PV and WECS system are validated through simulation results by giving solar and wind profile. Further power sharing curve for a typical day of summer, rainy and winter seasons have been obtained for both solar PV and WECS system. A DG system is also designed for back up sources.

CHAPTER 3

MODELING OF STAND-ALONE SOLAR PV, WECS AND DG SYSTEMS

3.1 GENERAL

In this thesis, a stand-alone hybrid energy system is designed for a small rural utility where light and fan load are considered for load study. Here, a mixed AC-DC coupled configuration is considered as shown in Figure 3.1 to supply AC loads through an inverter or a diesel generator. To ensure the less consumption of diesel, it is necessary to run the diesel generator for minimum period for which the load is fed through solar PV and wind as renewable sources. A battery bank is also considered for energy storage if surplus renewable power is available after supplying the load. It is also taken into account that if a diesel generator is in running condition, the battery bank would be charged through an auxiliary charger via the remaining power of the diesel generator after supplying the load.

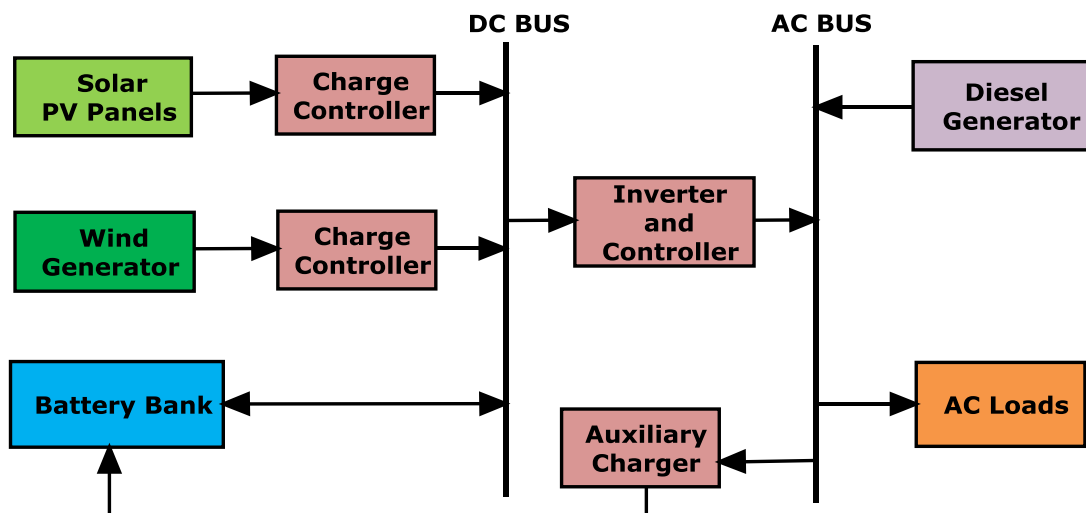


Figure 3.1 Block diagram of proposed system configuration

3.2 MODELING OF SOLAR PV SYSTEM

This section describes the Matlab/Simulink modeling and simulation results related to stand-alone solar PV system which consists of solar PV array, DC-DC converter, MPPT, storage battery, inverter *etc.*

3.2.1 Introduction to Solar PV Generation System

The concept of photovoltaic has firstly been observed by Becquerel in 1839 [89] which converts solar irradiation into electrical energy. In this process, the junction of two dissimilar materials illuminated with photons for creation of electrical potential. In modern photovoltaic (PV) cells, semiconductor p-n junction is used in which the density of charge carriers is more after absorbing the photons as per band-gap potential [37].

A typical PV cell is basically fabricated consisting of a 0.2 mm thick silicon wafer of two different doping level layers of polycrystalline or monocrystalline or amorphous with different electrical potentials at junctions [89]. When the solar irradiation impacts on the PV cell, the free charges are produced due to photon energy, separated by the electrical field. Hence, a potential (V_{PV}) followed by a photovoltaic current (I_{PV}) is developed if the load is connected between terminals. The amount of energy highly depends upon the material of the cell and the incidence of solar irradiation. Figure 3.2 shows a simple model of a PV cell having an ideal current source (I_{PV}) in parallel with an ideal diode (D_1) [53].

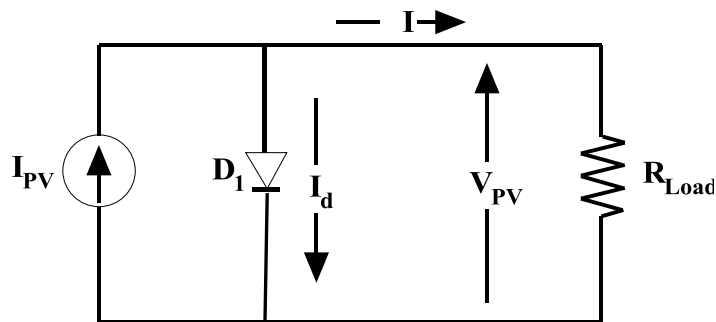


Figure 3.2 Ideal PV cell with R-Load

Equation (3.1) shows the PV cell output current as,

$$I = I_{PV} - I_d \quad (3.1)$$

Where I_{PV} represents short circuit current and I_d represents diode current as given by equation (3.2),

$$I_d = I_0 * \left(e^{\frac{q*V_d}{k*T}} - 1 \right) \quad (3.2)$$

Where I_0 represents reverse saturation current of the diode, q represents electron charge (1.602×10^{-19} C), V_d represents diode's voltage, k is Boltzmann's constant (1.381×10^{-23} J/K) and T is the junction temperature in Kelvin.

From equations (3.1) & (3.2), PV cell output current is obtained as:

$$I = I_{PV} - I_0 * \left(e^{\frac{q \cdot V_{PV}}{k \cdot T}} - 1 \right) \quad (3.3)$$

Where V_{PV} is the voltage across the PV cell.

As solar PV cell produces voltage nearly 0.5 V, therefore numbers of PV cells are necessarily to connect in series/parallel to get required voltage/current in a PV module. In a PV panel, a number of PV modules are connected electrically and physically to form a PV Array. Figure 3.3 shows an accurate model of PV cell [90-93].

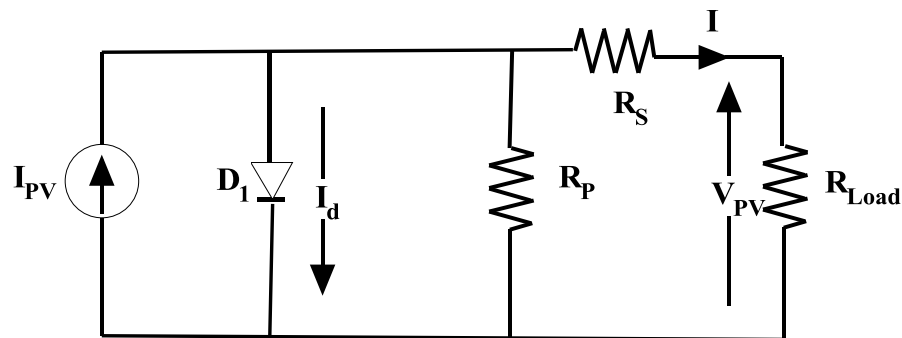


Figure 3.3 An accurate model of PV cell

In the above circuit, R_s is the resistance appearing in the current path of semiconductor material, contacts, metal grid, and currents controlling the system. The shunt resistance (R_p) indicates the loss occurring due to slight leakage current in parallel resistive path of device [94]. However, it can also be neglected in most cases as it has not considerable effect unless a large numbers of cells are connected in parallel. Recombination factor (n) as shown in equation (3.4) is associated with the depletion region of semiconductor in PV cells and to the numbers of cells connected in series. Value of n lies between 1 & 2 and generally it is taken as 1.3 [37-38]. Generally, it is characterized by adding another diode (D_2) in the equivalent circuit of PV cell as shown in Figure 3.4 [95-96].

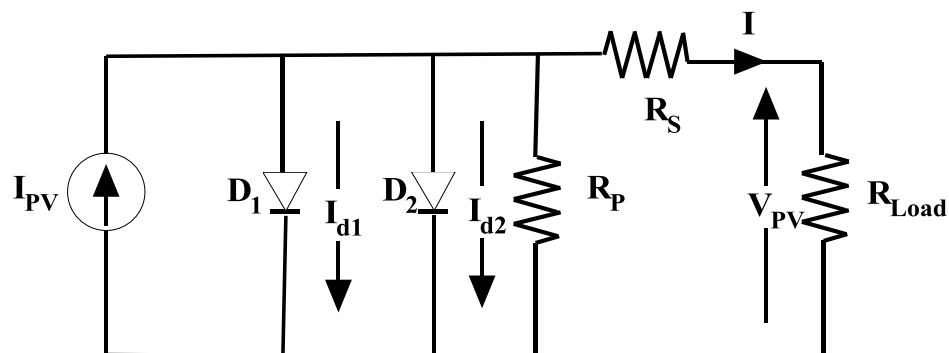


Figure 3.4 Final equivalent circuit of PV cell

Thus, equation (3.3) can be rewritten including R_s , R_p and n as follows:

$$I = I_{PV} - I_0 * \left(e^{\frac{q*(V_{PV}+I*R_s)}{n*k*T}} - 1 \right) - \frac{(V_{PV}+I*R_s)}{R_p} \quad (3.4)$$

Similarly, the characteristic equation for double diode model as shown in Figure 3.4 for a PV cell including R_s , R_p and n can be written as follows [97]:

$$\begin{aligned} I &= I_{PV} - I_{d1} - I_{d2} - \frac{(V_{PV}+I*R_s)}{R_p} \\ &= I_{PV} - I_{01} * \left(e^{\frac{q*(V_{PV}+I*R_s)}{n*k*T}} - 1 \right) - I_{02} * \left(e^{\frac{q*(V_{PV}+I*R_s)}{n*k*T}} - 1 \right) - \frac{(V_{PV}+I*R_s)}{R_p} \end{aligned} \quad (3.5)$$

Where I_{01} and I_{02} represent reverse saturation currents of diode D_1 and D_2 respectively.

A simplified equation of PV cell current as a function of temperature and solar irradiance can be written as [93]:

$$I_{PV} = (I_{PV_ref} + K_i \Delta T) \frac{G}{G_{ref}} \quad (3.6)$$

Where I_{PV_ref} represents PV cell current at reference solar irradiation ($G_{ref} = 1000$ watt/m²), K_i represents short-circuit temperature coefficient, $\Delta T = T - T_{ref}$ (in Kelvin, $T_{ref} = 25^{\circ}\text{C}$) and G is the surface solar irradiation of the PV cell.

Table 3.1 shows the various parameters of 125 W solar panel (REIL, India make), which is used for simulation as well as installation purposes.

Figure 3.5 shows the Matlab/Simulink model of solar PV panel and Figure 3.6 shows the I-V and P-V characteristics at different solar irradiance and reference temperature of 25°C .

Table 3.1 Different parameters of 125 W solar panel (Make: REIL, India)

Parameter	Value
Short Circuit Current (I_{sc})	7.759 A
Open Circuit Voltage (V_{oc})	22.73 V
Number of Parallel Cells (N_p)	1
Number of series Cells (N_s)	36
Reference Temperature (T_{ref})	298 Kelvin
Boltzmann's Constant (K)	1.381×10^{-23} J/K
Ideality Factor (n)	1.3
Electron Charge (q)	1.602×10^{-19} C
Short Circuit Temperature Coefficient (K_i)	0.003
Maximum Power (P_{max})	128.53 W
Voltage at P_{max}	18.32 V
Current at P_{max}	7.016 A

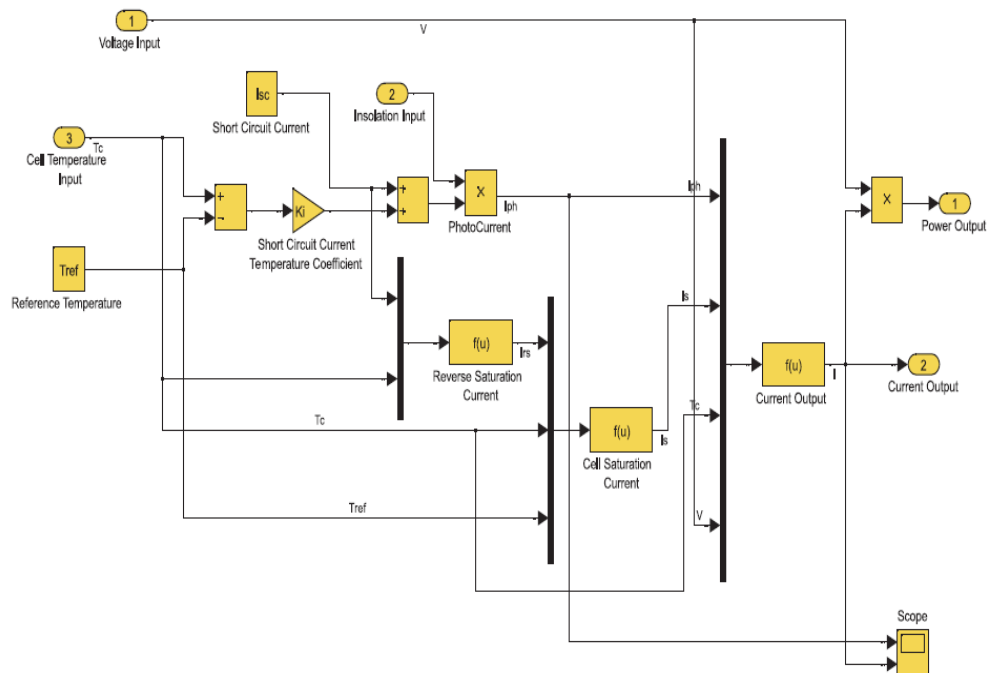
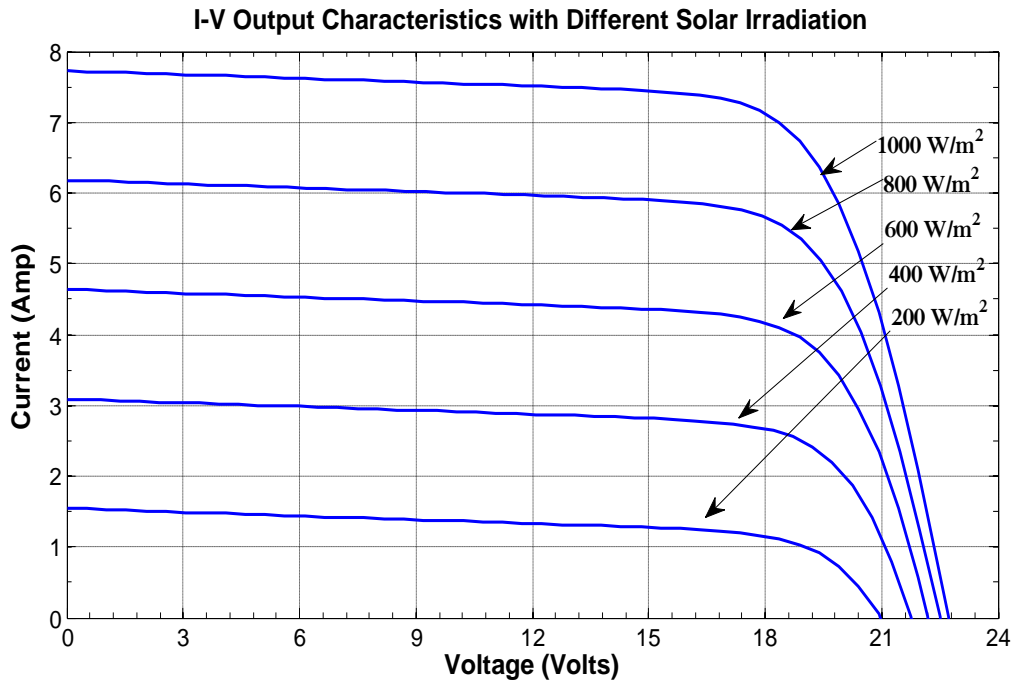
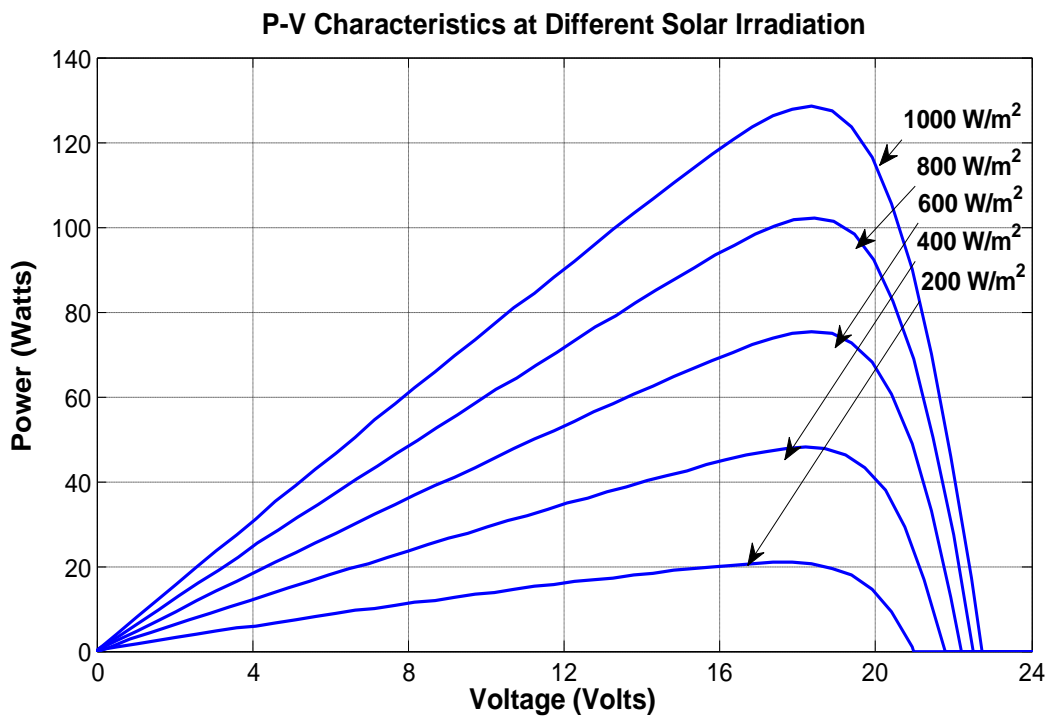


Figure 3.5 Matlab/Simulink model of solar PV panel



(a) I-V characteristics



(b) P-V characteristics

Figure 3.6 Characteristics of 125W-1-36-REIL solar panel at different solar irradiancations and reference temperature

3.2.2 Design and Simulation of 1 kW Stand-alone Solar PV System

Figure 3.7 shows the schematic diagram of proposed stand-alone solar PV-battery system to supply the AC loads.

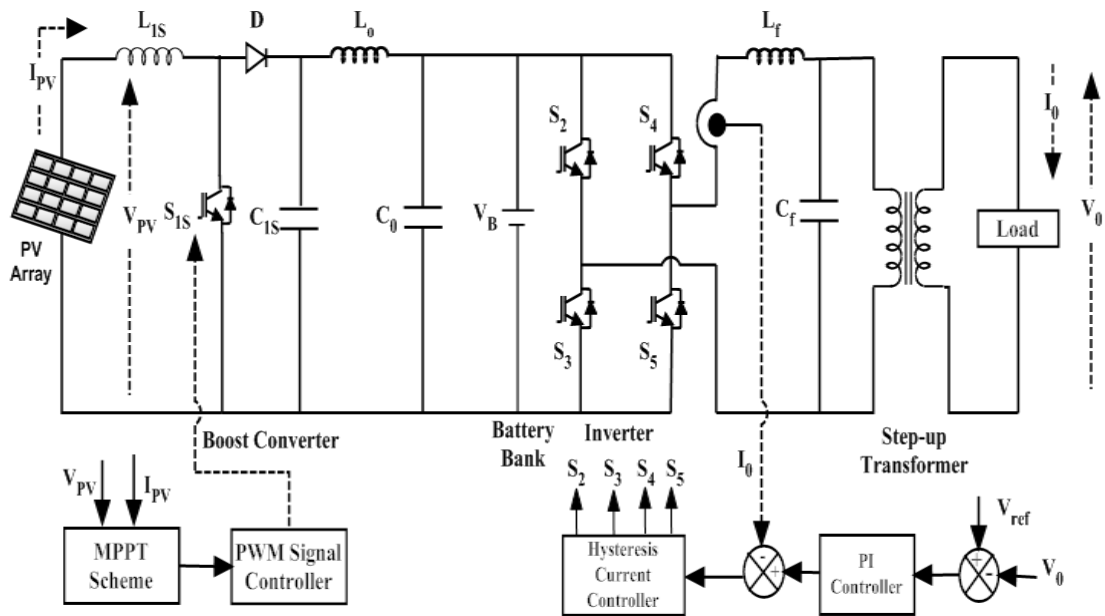


Figure 3.7 Schematic diagram of proposed stand-alone solar PV- battery system

In this scheme of stand-alone solar PV system, two solar panels of 125 W each is connected in series and four such combination of solar panels are connected in parallel to generate 1000 W (1.0 kW) solar power as shown in Figure 3.8. Table 3.2 shows the different parameters of the 1000 W solar PV array.

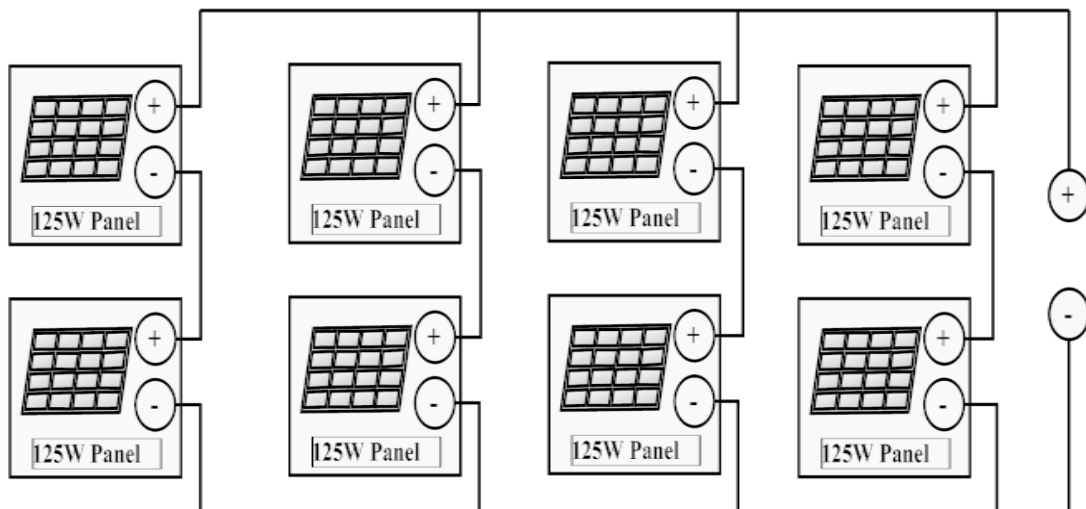


Figure 3.8 Connection diagram of solar PV panels for PV array

Table 3.2 Different parameters of 1000 W solar PV array

Parameter	Value
Short Circuit Current (I_{sc})	31.036 A
Open Circuit Voltage (V_{oc})	45.46 V
Number of Parallel Panels (N_p)	4
Number of series Panels (N_s)	2
Maximum Power (P_{max})	128.53 W
Voltage at P_{max}	36.64 V
Current at P_{max}	28.064 A

The open circuit voltage V_{oc} across the solar PV array as shown in Table 3.2 is 45.46 V, and solar PV array voltage at P_{max} is about 36.64 V. An intermediate DC-DC boost converter with MPPT technique is used to extract maximum energy from the solar panels [98-99]. A 48 V battery bank is also used to store the surplus solar energy and to supply the load in the absence of solar energy. A single phase voltage source inverter with hysteresis current controller is used to convert the DC supply into AC supply. An LC filter is also used before supplying the load through a step-up transformer for harmonics reduction.

3.2.3 Modeling of MPPT Technique for Solar PV System

The efficiency of solar PV system is highly affected by amount of solar irradiation and weather conditions but it can be improved by using an appropriate maximum power point tracking (MPPT) technique. The MPPT controller with DC-DC converter aims to regulate the operating point of the PV system while weather conditions are improper [100-108]. There are many MPPT algorithms available to track the maximum power from solar PV system [109-116]. Perturbation and observation (P&O) algorithm is mostly used algorithm to track the maximum power.

3.2.3.1 Perturbation and Observation (P&O) Algorithm

Perturbation and observation (P&O) algorithm is used in solar PV energy conversion system to track maximum power point. In P&O algorithm, maximum power point is obtained through an iterative method on operating curve of PV array. In an iterative method, PV array terminal voltage and current are periodically measured for finding

increment or decrement in output power [105,117]. The complete P&O algorithm is shown in Figure 3.9 [117]. The MPP can be obtained at $dP/dV = 0$, where P represents the output power and V represents the output voltage of PV array, for any value of solar radiation and temperature.

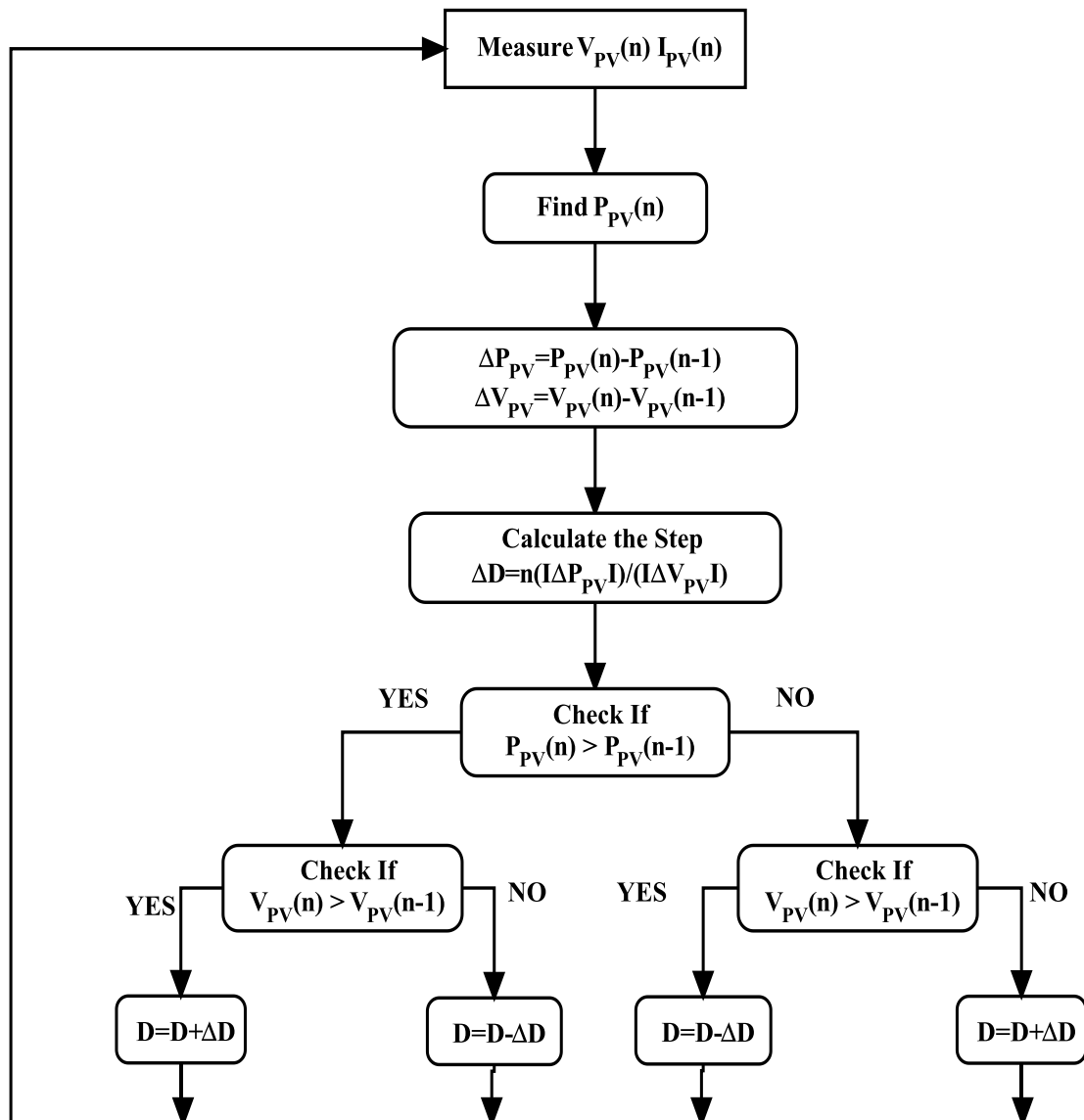


Figure 3.9 Operating flowchart of P&O algorithm

In P&O algorithm, first PV array operating voltage is perturbed with finite increment corresponding to this voltage; accordingly change in output power is observed. If positive change in output power is obtained then operating point is moving closure to MPP else it is moving away. According to this change in output power, the subsequent perturbation is generated in the same direction. When MPP is obtained the system may oscillate, to overcome this problem the perturbation step size is decreased.

3.2.3.2 Design of DC-DC Boost Converter

Figure 3.10 shows the diagram of a boost converter used in the PV system, which gives higher output voltage as compared to input (PV) voltage. A diode (D), a MOSFET (S_{1S}) with proper gating scheme, an inductor (L_{1S}) and a capacitor (C_{1S}) as shown in Figure 3.10 are used to design the boost converter [37]. In the boost converter, the average inductor current ($I_L=I_{PV}$) is more than the average output current (I_0) and a high rms output current (I_{Cf}) in filter capacitor, which yields a large value of filter capacitor (C_0) and inductor (L_0) as compared to buck converter [37].

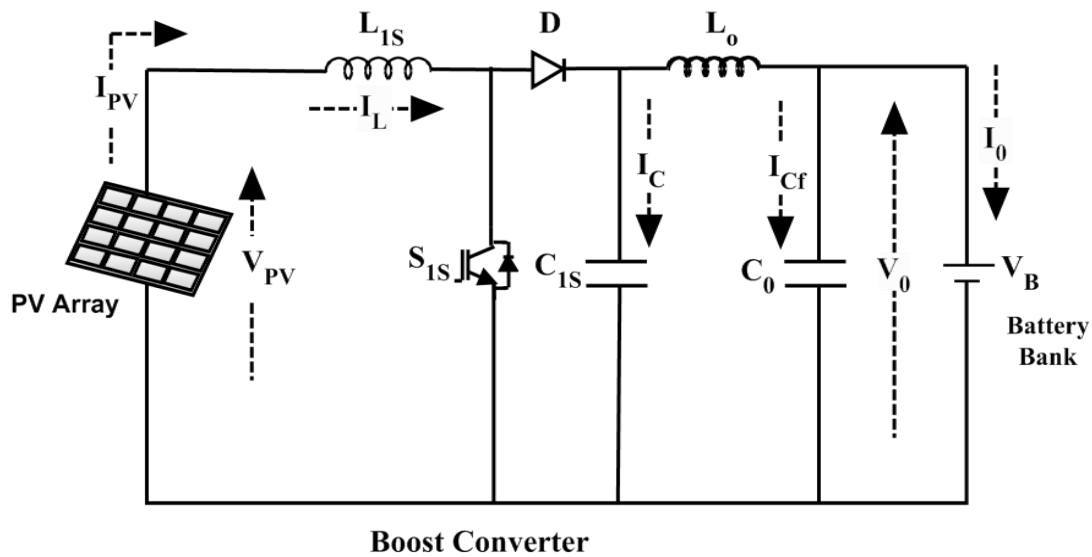


Figure 3.10 Boost DC-DC converter topology used as PV power interface

The design parameter of proposed boost converter is discussed as follows [37]:

$$\text{Duty Cycle (D)} = 1 - \frac{V_{in}}{V_o} \quad (3.7)$$

Where V_{in} represents boost converter input voltage which equals to the PV array output voltage (V_{PV}) and V_o represents the boost converter output voltage.

The voltage (V_{PV}) is taken in the range of 16-36 V, while V_o is taken 53 V for proposed system. Hence, the value of D is obtained from equation (3.7) in the range of 0.32-0.698.

An inductor value for this boost converter can be obtained as [37]:

$$\text{Inductance } L_{1S} = \frac{V_{in}D}{2\Delta I_0 F_{sw}} \quad (3.8)$$

Where ΔI_0 and F_{sw} represent ripple of output current and switching frequency respectively.

For $\Delta i_0 = 5\%$ and $F_{sw} = 50$ kHz, the value of inductance (L_{1S}) is obtained 2.24 mH from equation (3.8) as:

$$\text{Inductance } L_{1S} = \frac{V_{in}D}{2\Delta I_0 F_{sw}} = \frac{16 * 0.698}{2 * 0.05 * 50 * 10^3} = 2.24 \text{ mH}$$

The value of output capacitor can be determined by using equation (3.9) as [37]:

$$\text{Capacitance } C_{1S} = \frac{I_0 D}{\Delta V F_{sw}} \quad (3.9)$$

Where I_0 represents the output current and ΔV represents the ripple in output voltage.

For $I_0 = 28$ A and $\Delta V = 10\%$, the value of output capacitor (C_{1S}) is obtained 1792 μF from equation (3.9) as:

$$\text{Capacitance } C_{1S} = \frac{I_0 D}{\Delta V F_{sw}} = \frac{28 * 0.32}{0.1 * 50 * 10^3} = 1792 \mu\text{F}$$

However, the value of inductor (L_{1S}) and capacitor (C_{1S}) has been considered as 2.5mH and 2200 μF respectively in simulation as well as hardware due to easily available standard specifications.

3.2.3.3 Proportional Integral (PI) Voltage Controller

The gating circuit of MOSFET (S_{1S}) as shown in Figure 3.7 can be expressed by using a PI voltage controller with a PWM scheme [37, 118-121]. The proportional and integral voltage controller gives an output signal ($u(t)$) which is proportional to voltage error signal ($e(t)$) and integral of voltage error signal as given in equation (3.10):

$$u(t) \propto \{e(t) + \int e(t)dt\} \quad (3.10)$$

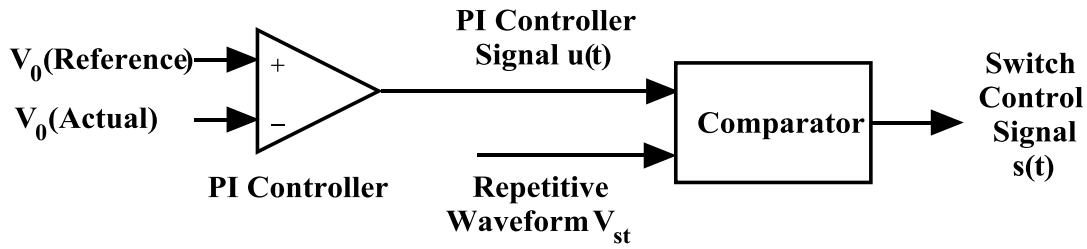
With a proportional gain constant (K_P) and integral time constant (K_i), equation (3.10) can be rewritten as :

$$u(t) = K_P e(t) + \frac{K_P}{K_i} \int e(t)dt \quad (3.11)$$

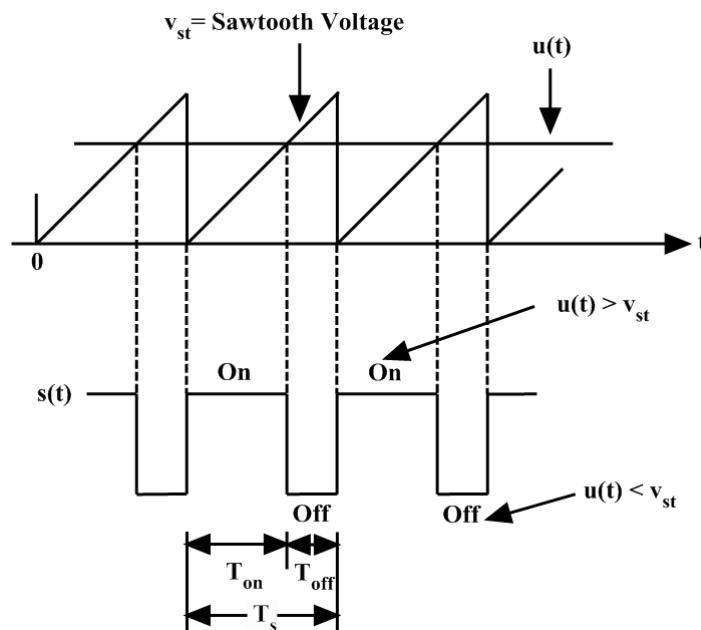
Steady state error is reduced or eliminated by integral action and loop gain is increased by proportional action, which reduces system sensitivity against variation of system parameters.

The output of boost converter (V_0 (actual)) is compared with the reference voltage (V_0 (reference)) and a voltage error signal $e(t)$ is generated as shown in Figure 3.11 (a).

Further, the output of PI controller ($e(t)$) is compared with a reference waveform (V_{st}), as shown in Figure 3.11 (b) [122-126].



(a) PI controller scheme



(b) Switch control signal generation with PWM [37]

Figure 3.11 Switching control signal generation for boost converter

After this comparison, a switch control signal or gating pulse ($s(t)$) is generated in order to control the output of DC-DC boost converter. If there is any change in the input voltage of the DC-DC boost converter, corresponding change in output of the converter observed, but this control regulates the output of the converter irrespective of the variations in the input of the DC-DC converter and gives a constant output voltage.

3.2.3.4 Simulation Results of DC-DC Boost Converter

Figures 3.12 and 3.13 show the developed Matlab/Simulink model of proposed boost converter with its control scheme and MPPT scheme respectively. The input supply to the boost converter is the output of the photovoltaic model which is incorporated with

maximum power point tracking to track the maximum power irrespective of the variations in solar irradiations. The switching frequency of this DC-DC converter is 50 kHz. The output of the converter is used to charge the storage battery bank of 48V and to supply the load.

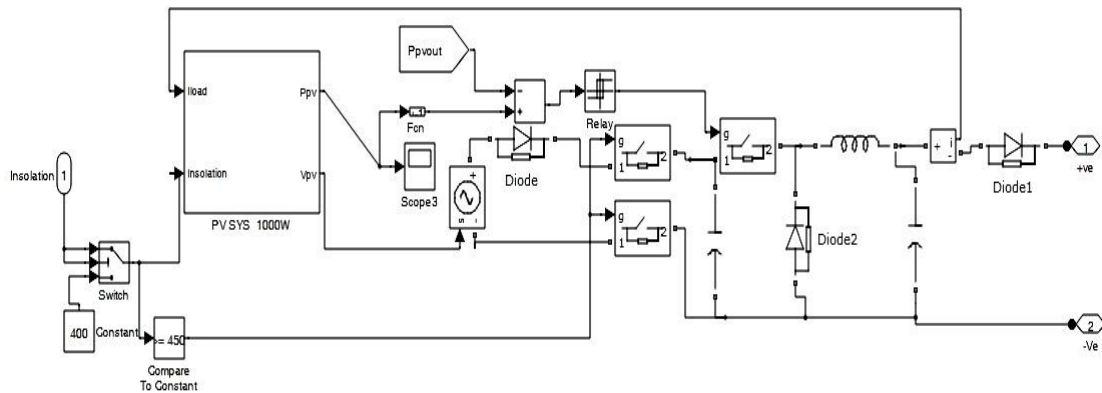


Figure 3.12 Matlab/Simulink model of boost converter with PV

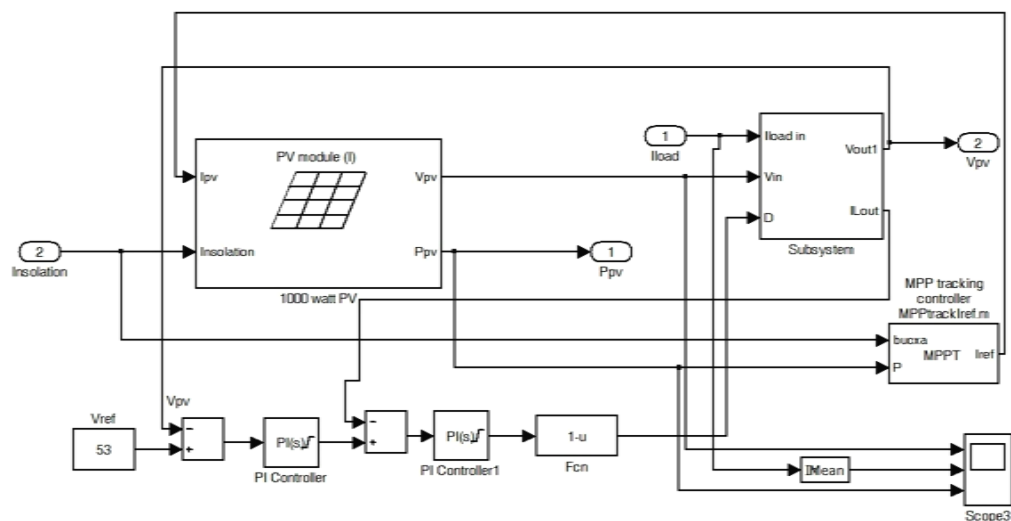
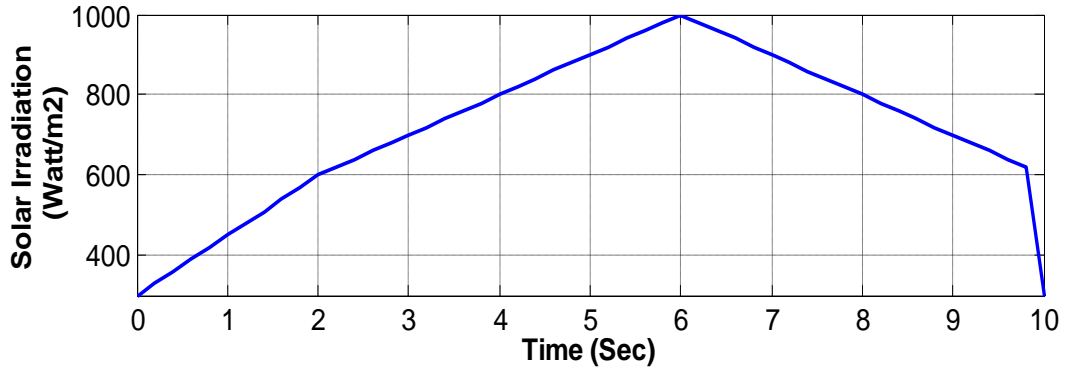
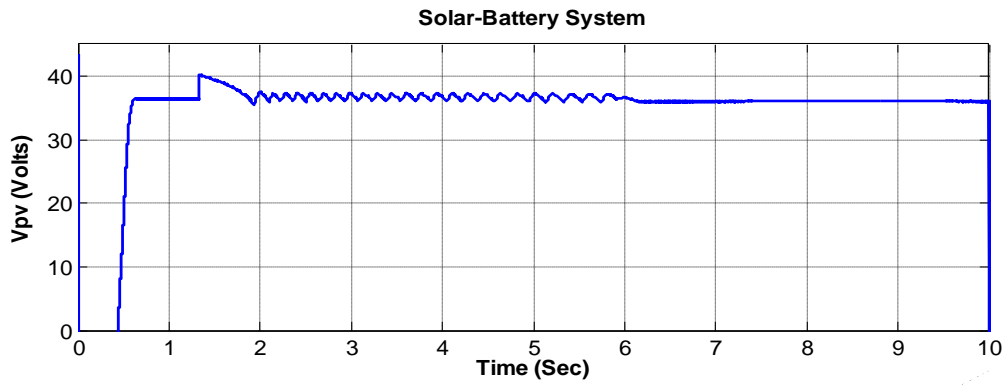


Figure 3.13 Matlab/Simulink model of MPPT scheme with PV

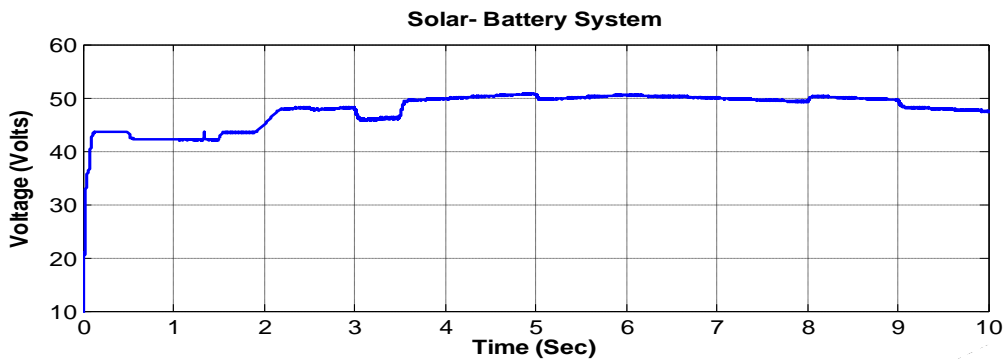
Figures 3.14 (a), (b) and (c) show the solar irradiation input profile, output of solar-PV and boost converter respectively. The DC-DC boost converter increases the voltage of PV array in the range of 45 V to 50 V as shown in Figure 3.14 (c). The output of boost converter is fed to a DC link having an inductor L_o and a capacitor C_o which smoothen the output to a voltage of 60 V as shown in Figure 3.14 (d). Further, this voltage is fed to an inverter circuit to supply the AC loads.



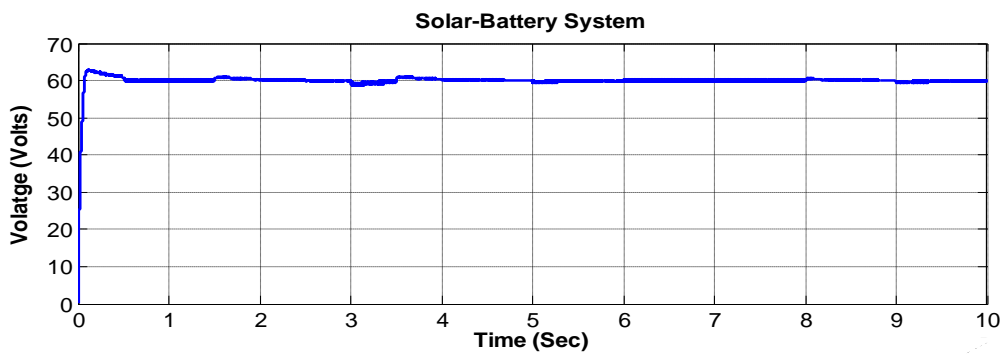
(a) Solar irradiation input profile



(b) Solar PV output voltage



(c) Boost converter output voltage



(d) DC link output voltage

Figure 3.14 Simulated results of MPPT & boost converter with PV array

3.2.4 Storage Battery

As the power from wind generator varies with variations in wind speeds throughout the day. Similarly the PV panel output power varies according to solar irradiation and temperature variations. So the use of PV and wind generators alone is not to be suggested for fulfilling the load demands at all the times. Therefore, a storage battery between the DC bus and the load of the hybrid system is required as a backup supply. If wind and PV generator powers exceed the load requirement then it is stored in the battery bank to supply the load in the absence of PV and wind generator power.

3.2.4.1 Lead Acid Battery Construction and Performance

For small scale applications, there are four types of battery storage technologies available such as lithium-ion, lead-acid, nickel metal hydride and nickel cadmium [15, 36].

The dominant use of battery in urban renewable energy system is limited by its low energy density, relatively limited life and non-environment friendly electrolyte. However, lead-acid batteries offer a better and cheap solution for energy storage requirements with relatively low self discharge rate and less maintenance [127-129].

Generally, a 12 V battery has six 2 V lead-acid cells and its maximum and minimum charging and discharging open circuit voltages at 25°C are 14.4 V and 10.5 V respectively [128].

A linear relation is obtained between the battery voltage and its depth of discharge (DOD), until a cut-off-voltage point is reached. The internal resistance of the battery increases when operation of the battery is above this cut-off point and this causes the damage in the battery. The operation of a battery is controlled with a charge controller within its design limits, also not to exceed overcharge limit.

In lead acid battery, some of its capacity is lost due to internal chemical reaction, which is known as self of discharge (SOD), which depends on the battery temperature [127-128]. For considering a battery for hybrid system applications, its life time, capability of standing very deep discharge and cycling stability rate are main design parameters.

3.2.4.2 Lead Acid Battery Rating and Model

A battery is rated in specified terms as Ampere-hours (Ahs) and Watt-hours (Wh) capacity. The quantity of discharge current available for a specified length of time at a certain temperature and discharge rate is known as ampere-hour capacity of a battery. The battery capacity is reduced due to high discharge current.

Minimum storage level of a battery can be expressed from equation (3.12) as [15]:

$$E_{\min} = E_{BN} * (1 - DOD) \quad (3.12)$$

Where E_{\min} and E_{BN} represent the battery bank's minimum allowable capacity and nominal capacity, respectively.

Equations (3.13) and (3.14) give the energy balance equations of a battery in charging and discharging mode respectively as [15]:

$$E_b(t) = E_b(t-1) * (1 - \sigma) + (E_w(t) + E_{PV}(t) + E_{DG}(t) - E_L(t) / \eta_v) * \eta_{wh} \quad (3.13)$$

$$E_b(t) = E_b(t-1) * (1 - \sigma) - (E_L(t) / \eta_v - (E_w(t) + E_{PV}(t) + E_{DG}(t))) \quad (3.14)$$

Where $E_b(t)$ and $E_b(t-1)$ represent energy stored in the battery at times (t) and (t-1) respectively. σ represents hourly self discharge rate, $E_w(t)$, $E_{PV}(t)$, $E_{DG}(t)$ and $E_L(t)$ represent wind generator energy, PV generator energy, diesel generator energy and load energy requirements respectively in the time duration, and η_v and η_{wh} represent the efficiencies of the inverter and the battery bank respectively.

3.2.4.3 Battery Bank Sizing

Equations (3.15) and (3.16) show the watt-hour capacity (C_{Wh}) and Amp-hour capacity (C_{Ah}) of a battery bank respectively, essential to supply a load demand for a certain time period when no energy available from renewable resources as:

$$C_{Wh} = \frac{E_L * DA}{\eta_v * \eta_{wh} * DOD} \quad (3.15)$$

$$C_{Ah} = \frac{C_{Wh}}{\text{Battery Volatge}} \quad (3.16)$$

Where DA is known as daily autonomy and E_L is the load energy in watt-hour.

In this thesis, it is considered that the load energy ($E_L=2000$ watt-hours) is to be supplied for at least one day autonomy in the absence of solar or wind energy, with

90% η_v and η_{wh} and 70% DOD. Hence, from equations (3.15) and (3.16), the watt-hour capacity (C_{Wh}) and Ampere-hour capacity (C_{Ah}) are obtained as:

$$C_{Wh} = \frac{2000 * 1}{0.9 * 0.9 * 0.7} = 3527 \text{ Watt - Hour}$$

$$C_{Ah} = \frac{3527}{48} = 73.48 \text{ Amp - Hour}$$

Hence, to supply the load energy ($E_L=2000$ watt-hours) throughout a day, four 12 V, 80Ah batteries are connected in series for obtain a battery bank of 48 V, 80Ah capacity. Figure 3.15 shows the battery characteristics of 48 V, 80Ah battery. It is observed from Figure 3.15 that the battery discharge time for large load current of 32.5 A is only 2.2 hours whereas for load current of 6.5 A it is up to 11.5 hours as shown in Figure 3.15. Hence, a battery bank can supply the load for more time if load is less.

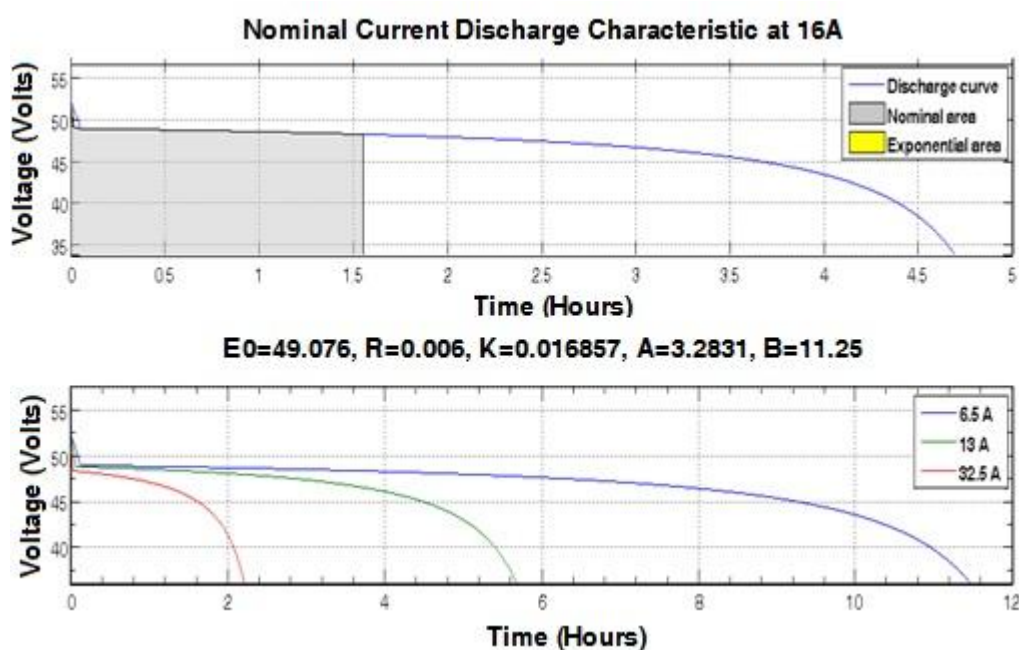


Figure 3.15 Battery characteristics of 48 V, 80Ah battery bank

3.2.5 Single Phase Inverter

A voltage source inverter (VSI) with full bridge configuration is used to supply the AC loads [117]. VSI is fed by a DC-link with a DC voltage of 60 V which is converted into 220 V (rms), 50 Hz AC supply. A VSI topology with its control schematic is shown in Figure 3.16.

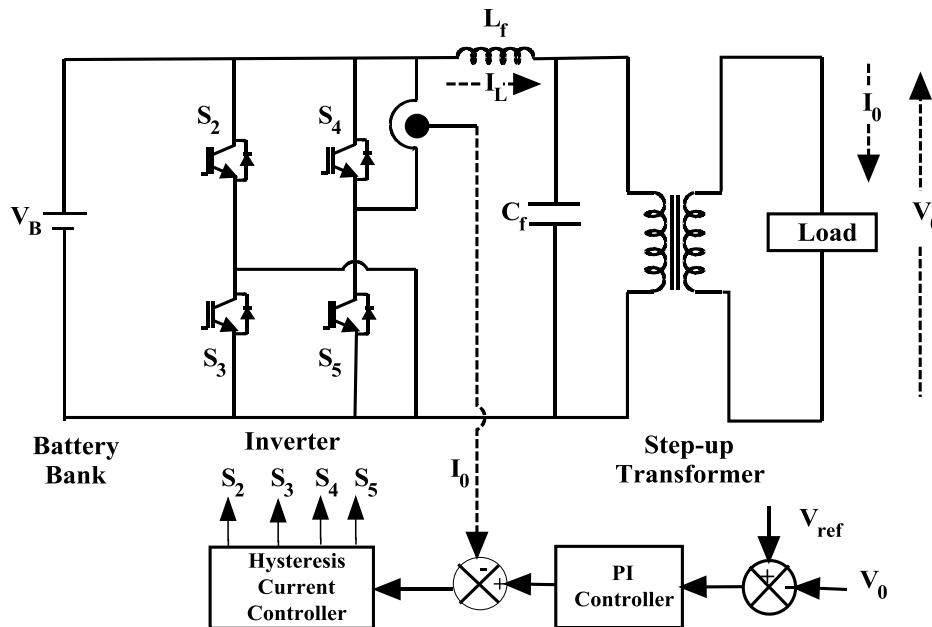


Figure 3.16 VSI and hysteresis current controller

In sinusoidal PWM, pulses are generated by dividing the period of the desired output sine wave into a number of intervals. Each interval consists of on-time and off-time control signals. At any instant, the ratio of the “on time” to “off time” is known as duty cycle [125,135]. This duty cycle is given to four IGBTs (Insulated Gate Bipolar Transistors) of the VSI.

The full-bridge VSI’s output signal is a pulse waveform along with high frequency components. A low-pass filter (LPF) is also used to extract the fundamental frequency output voltage by separating it from the switching frequency. Further, the output voltage of the inverter is fed to a step-up transformer (50 V/220 V) to supply the ac loads.

3.2.5.1 Hysteresis Current Controller & PI Voltage Controller

To get better quality VSI output voltage, a reasonably smooth DC voltage is required at input side. However, it cannot be guaranteed always so a hysteresis control technique at VSI side is used to overcome this problem [131-133]. The block diagram of the hysteresis current controller (HCC) and PI controller is shown in Figure 3.16. In proportional integral (PI) controller the instantaneous voltage error is fed, which improves the tracking through integral component by reducing the instantaneous voltage error. The resulting signal (I_{ref}) is compared with output load current *i.e.* inverter output current (I_o) and the error signal is created. This error signal is fed to

HCC, which generates gating pulses to the IGBTs in the VSI. The HCC forces the inverter to track the reference current that is derived from the output voltage and hence the load power factor is made to unity.

The hysteresis band of the controller is fixed to operate at an average switching frequency of 20 kHz. At this switching frequency, the switching harmonics are around half frequency, which provides clean 50 Hz fundamental frequency [134]. Whenever, the error reaches $(I_{ref} + I_{th})$ or $(I_{ref} - I_{th})$ as shown in Figure 3.17, the inverter is switched so that the current begins to move in other direction. The threshold value of current (I_{th}) is given in equation (3.17) as:

$$I_{th} = I_{ref} \frac{R_2}{(R_1 + R_2)} \quad (3.17)$$

Where R_1 and R_2 are the resistors deciding the hysteresis band of HCC.

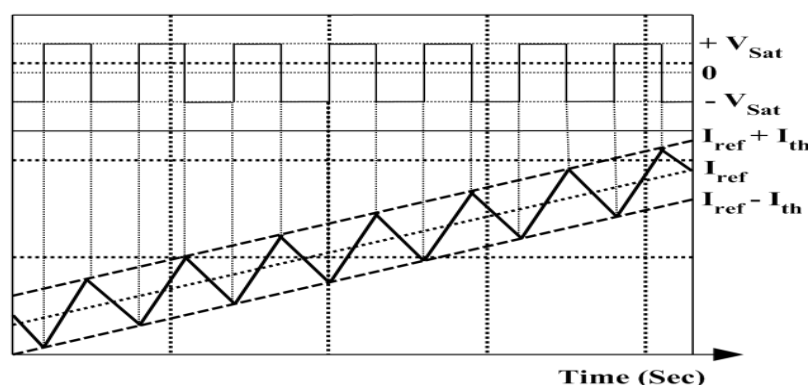


Figure 3.17 Switching diagram of hysteresis current controller

3.2.5.2 Design of Voltage Source Inverter

The first step of designing a VSI is the selection of topology, after that selection of proper rating of devices. Here, a full bridge VSI is used and the rating of VSI is determined on the basis of load. An average load of 500 W is considered, to handle out this load VSI power output must be 625 VA at 0.8 p.f. and 220 V voltage with 4.02 A peak current. However, considering the worst case of full load (920 W, 7.39 A peak current) or a nonlinear load e.g. computer loads (SMPS), the device rating of the switches in VSI are taken as 600V, 15A. For controlling duty cycle, a closed loop control is used which maintains system output voltage under varying load conditions.

3.2.5.3 Design of PI Controller

For load balancing, a PI controller can be used. During transients and steady state operation, the PI controller performs satisfactorily. Since P & I gains are constant and

for a specific operating condition they are fine tuned. For tuning of PI controller, Ziegler and Nichols have suggested that proportional gain (K_p) and integral gain (K_i) can be obtained by setting the controller in the proportional mode and increasing the gain until an oscillation takes place [117,136]. At this point, the value of oscillation frequency is obtained. At quite small oscillation amplitude, the period of oscillations (P_c) is measured and with Nyquist and root locus criteria the crossover frequency (ω_c) and critical gain (G_c) are obtained.

The characteristic equation of PI controller can be shown as equation (3.18). The parameter K_p and K_i can be set according to equations (3.19) and (3.20) as [136]:

$$G_{PI}(S) = \frac{K_p K_i S + K_p}{K_i S} \quad (3.18)$$

$$K_p = 0.5 G_c \quad (3.19)$$

$$K_i = 0.5 P_c \quad (3.20)$$

Where G_{PI} represents the PI controller gain, and G_c and P_c represents the system critical gain and oscillation period respectively.

An optimum performance of the controller is obtained by setting K_p to unity and K_i equal to the frequency of the triangular waveform.

3.2.5.4 Design of Low Pass Filter (LPF)

A low pass filter (LPF), has an inductor (L_f) and a capacitor (C_f) as shown in Figure 3.16, is used to get the fundamental frequency voltage from the switching frequency voltage. The cut off frequency of the LPF can be obtained by equation (3.21) as [37, 117]:

$$f_c = \frac{1}{2\pi\sqrt{L_f C_f}} \quad (3.21)$$

The design of an LC filter for the VSI, considering $V_d = 60V$, $V_o = 50 V(\text{peak})$, $F_{si} = 20$ kHz, $\Delta V = 1.5 V$ (3%) and $R_{L\min} = 5 \Omega$ for a load of 500W is carried out as follows:

Peak inductor current, can be expressed as [37, 117]:

$$I_L = \frac{2V_m}{R_{L\min}} = \frac{2*50}{5} = 20 A \quad (3.22)$$

Where $R_{L\min}$ represents the minimum load resistance and V_m represents the peak magnitude of the output voltage.

For specific switching frequency (F_{si}), filter capacitor (C_f) is determined as [37, 117]:

$$C = \frac{V_m}{2R_{Lmin}F_{si}\Delta V} = \frac{50}{2*5*20*10^3*1.5} = 166.67 \mu F \quad (3.23)$$

Where ΔV represents the ripple in output voltage.

The duty cycle for VSI can be calculated using equation (3.24) [37, 117] as:

$$\frac{T_{on}}{T_{off}} = \frac{V_d+V_o}{V_d-V_o} = \frac{60+50}{60-50} = 1.1 \quad (3.24)$$

Where V_d and V_o represent the DC link voltage and the VSI output voltage respectively.

Using minimum switching frequency, the ratio of on time and off time can be set as shown in equation (3.25) as:

$$T_{on} + T_{off} = \frac{1}{F_{si}} = \frac{1}{20*10^3} = 0.05 \text{ msec} \quad (3.25)$$

From equations (3.24) and (3.25), T_{on} is calculated as $T_{on} = 0.0262 \text{ msec}$.

Inductor (L_f) value can be obtained from equation (3.26) as [37, 117]:

$$L_f = \frac{V_d-V_o}{I_L} T_{on} = \frac{60-50}{20} * 0.0262 * 10^{-3} = 0.0131 \text{ mH} \quad (3.26)$$

The parameters of LC low pass filter used in the system as shown in Figure 3.16 are: $L_f = 0.0131 \text{ mH}$ and $C_f = 166.67 \mu F$. However, the values of inductor (L_f) and capacitor (C_f) has been considered as 0.02 mH and $200 \mu F$ respectively in simulation as well as in hardware due to easily available standard specifications.

3.2.5.5 Simulation Results of Inverter Circuit

The Matlab/Simulink model of the proposed inverter system is given in Figure 3.18.

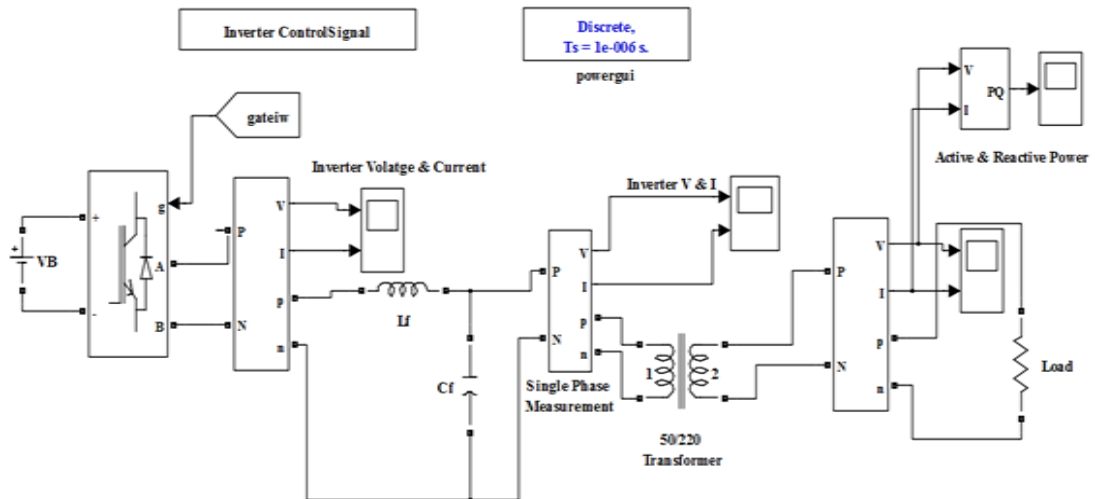


Figure 3.18 Matlab/Simulink model of inverter system

The system is simulated for 1 sec considering linear load of 500 W and nonlinear load of 375 VA. Figure 3.19 (a) and Figure 3.19 (b) show the inverter voltage and current and load voltage and current for linear load respectively. Figure 3.19 (c) and Figure 3.19 (d) show the harmonic analysis of load voltage and current for linear load respectively, which give Total Harmonics Distortion (THD) of the order of 0.04 % in both voltage and current as the load is linear.

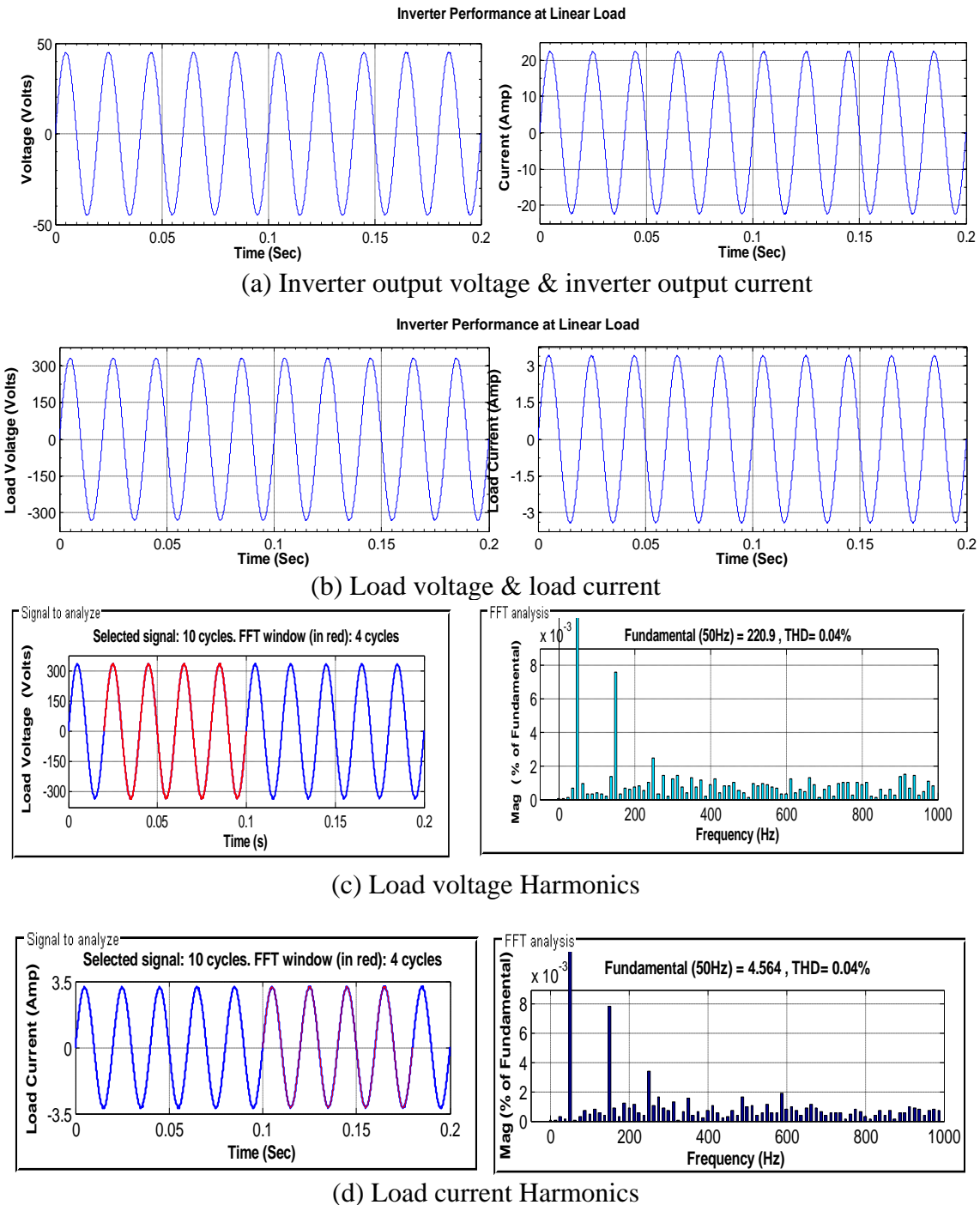


Figure 3.19 Simulation results of inverter system with 500 watt linear load

Similarly, Figure 3.20 (a) and Figure 3.20 (b) show the inverter voltage and current and load voltage and current for non-linear load respectively. Figure 3.20 (c) and Figure 3.20 (d) show the harmonic analysis of load voltage and current for non-linear load respectively, which give Total Harmonics Distortion (THD) 10.35 % and 3.74% for voltage and current respectively.

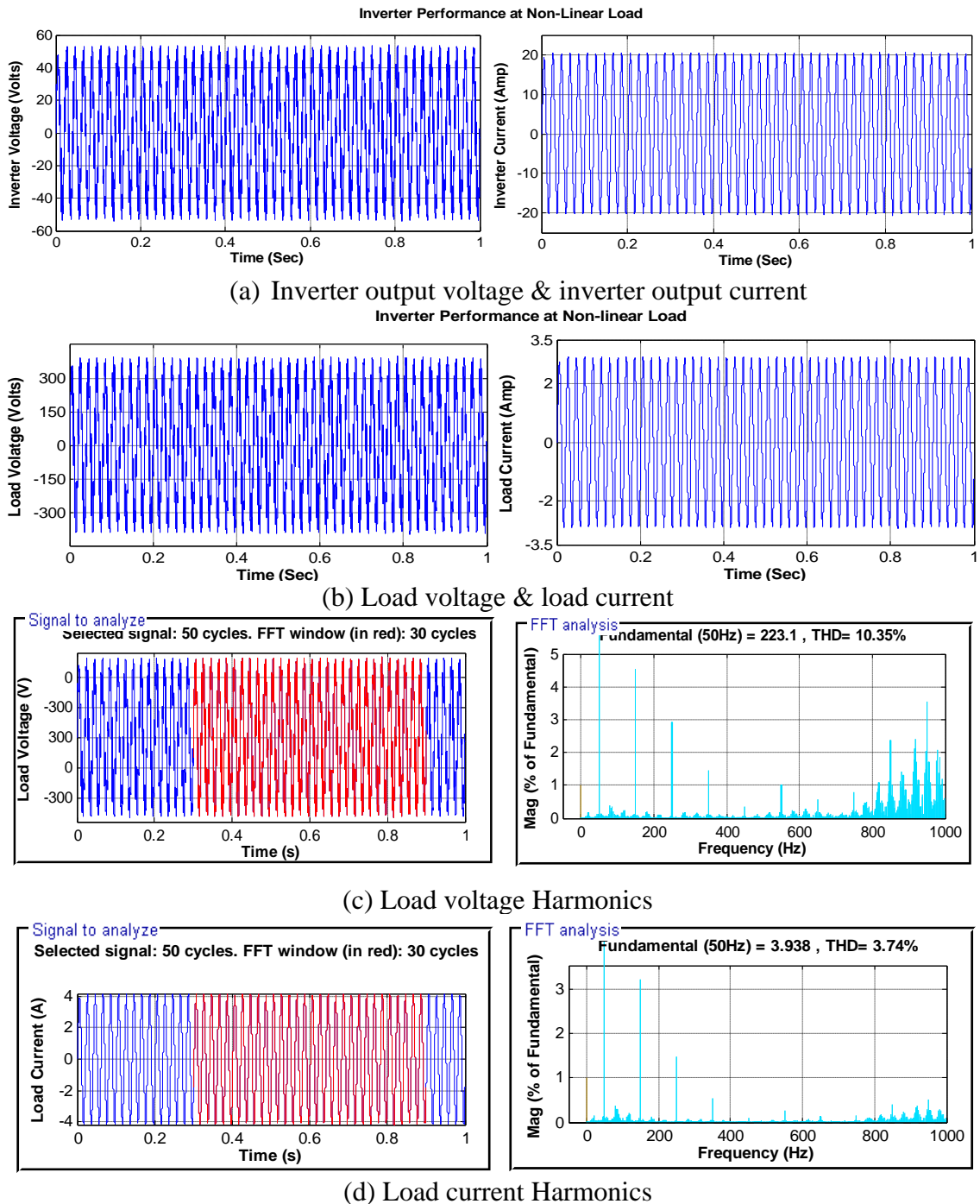


Figure 3.20 Simulation results of inverter system with 375VA ($P=400$ W, $Q= 150$ var) non-linear load

It is clear from harmonic spectra of voltage and current for linear and non-linear loads, as shown in Figures 3.19 and 3.20 respectively, voltage % magnitude at higher order of harmonics are larger in a case of non-linear load. However, this higher magnitude is compensated by current harmonics of same order.

3.2.6 Simulation Results and Discussion

The Matlab/Simulink model of proposed stand-alone solar PV-battery system is shown in Figure 3.21 and it consists of all the components as discussed in previous section. MPPT technique is also incorporated which is discussed earlier.

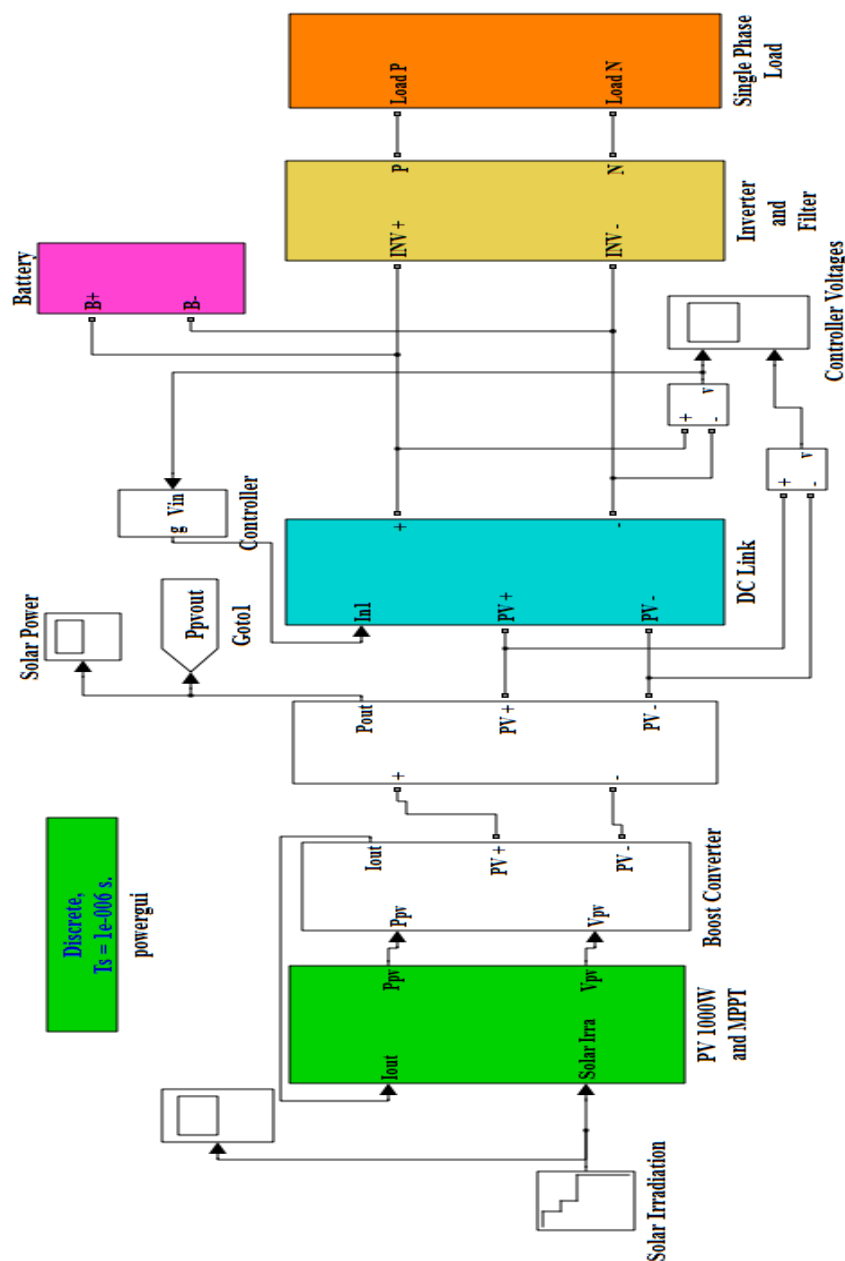


Figure 3.21 Matlab/Simulink model of proposed stand-alone solar PV-battery system

A typical solar irradiation profile is fed to the system as shown in Figure 3.22 to test the system for 4.8 sec.

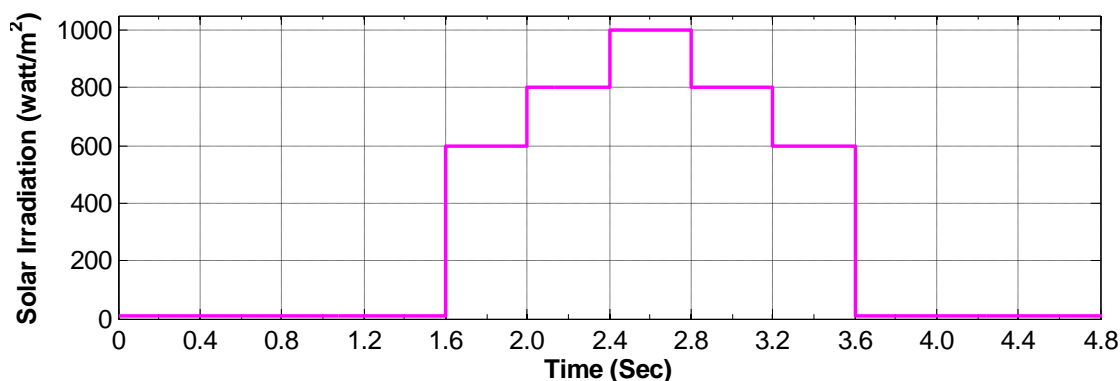
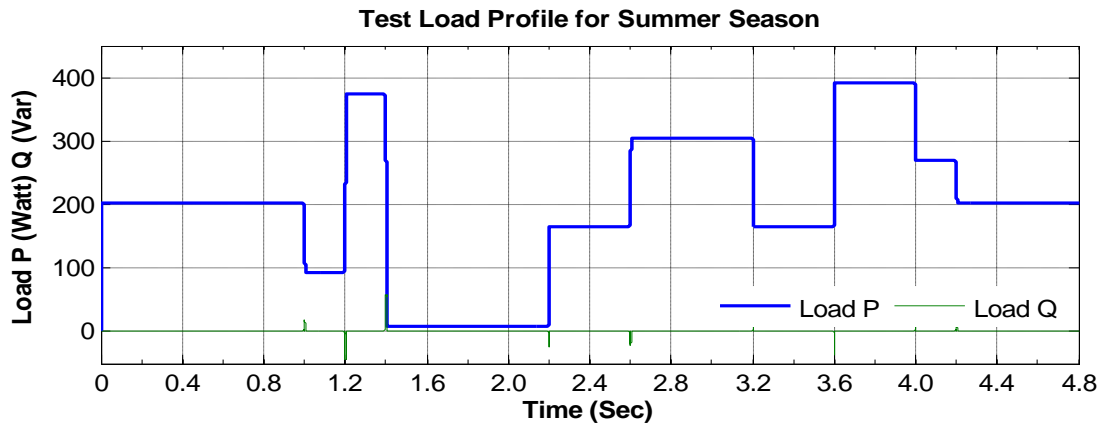


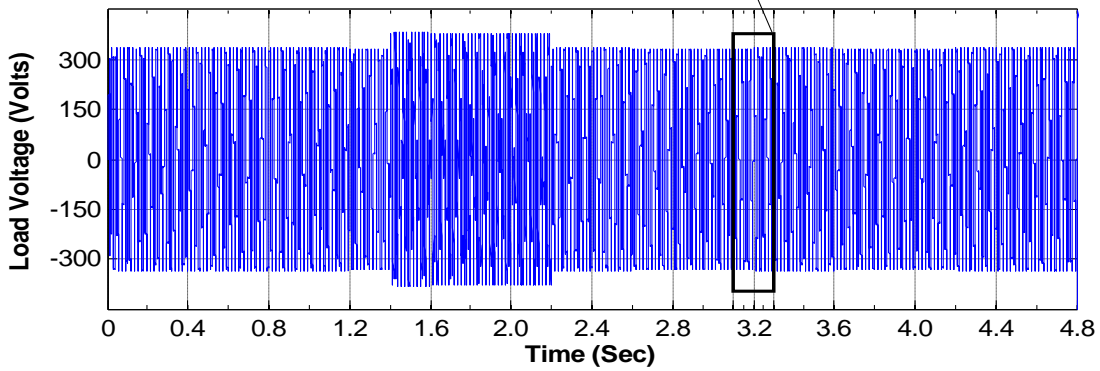
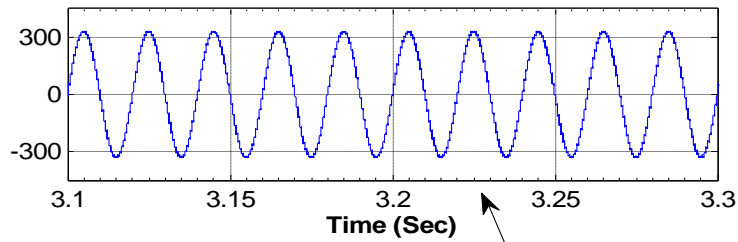
Figure 3.22 Solar profile input of stand-alone solar PV-battery system

Figure 3.23 (a) shows the test load profile, similar to the 24 hours load profile as shown in Figure 2.6 (a), for analyses purposes (*i.e.* simulation of load voltage, current *etc.*). Figures 3.23 (b) and (c) show the corresponding variations in load voltages and current. At time 1.4 sec to 2.2 sec load is very less around *i.e.* 8 W, thus corresponding large changes are observed in load voltage and current. Figures 3.24 (a) and (b) show the inverter output voltage and current respectively. As inverter output voltage is less than the output load voltage, it is increased by using a step-up transformer as shown in Figure 3.7. Figures 3.25 (a) and (b) show the battery voltage and current. From Figure 3.25 (b) it is clear that battery charges (negative battery current) in the duration of 2.45 sec to 3.2 sec, as solar energy availability at this time duration is high as compared to the load energy requirement, however it discharges (positive battery current) through the load as solar PV input is not available in the duration 0 sec to 1.6 sec and 3.2 sec to 4.8 sec.

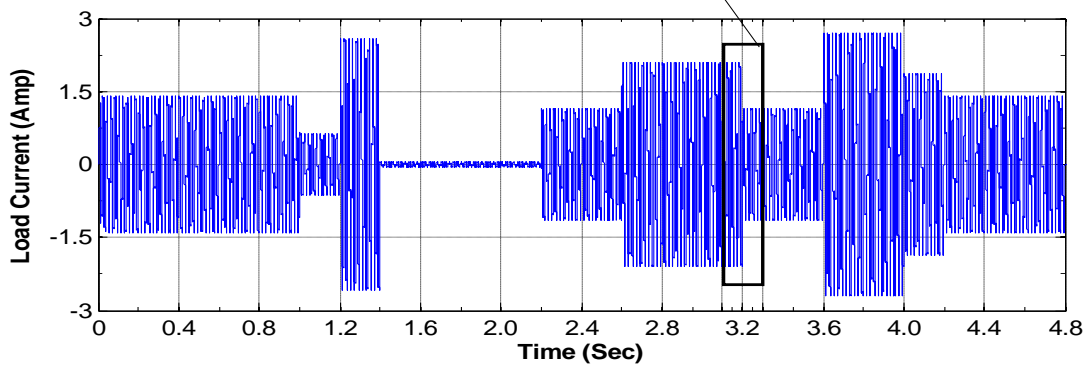
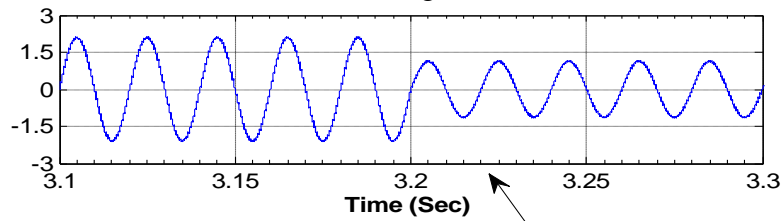
Further, the system is tested with 24-hour load profiles and solar irradiation profiles for a typical day of summer, rainy and winter seasons respectively as shown in Figure 3.26. Typical day of a season is selected in such a manner that the solar irradiation available on that day is optimum as compared to other days of the season as shown in Figure 2.8. On the basis of simulation results power sharing curves are plotted between solar PV power, battery power and load power as shown in Figure 3.27, Figure 3.28 and Figure 3.29 for summer, rainy and winter seasons respectively.



(a) Typical load variation

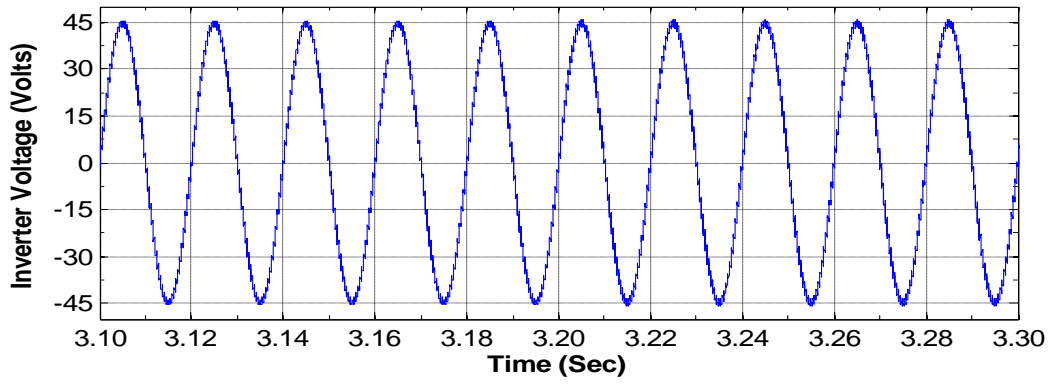


(b) Load voltage

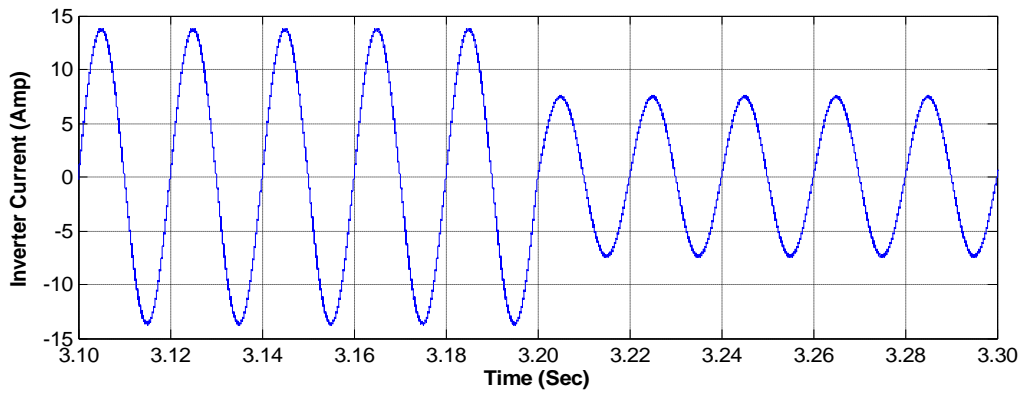


(c) Load current

Figure 3.23 Load profile of stand-alone solar PV-battery system

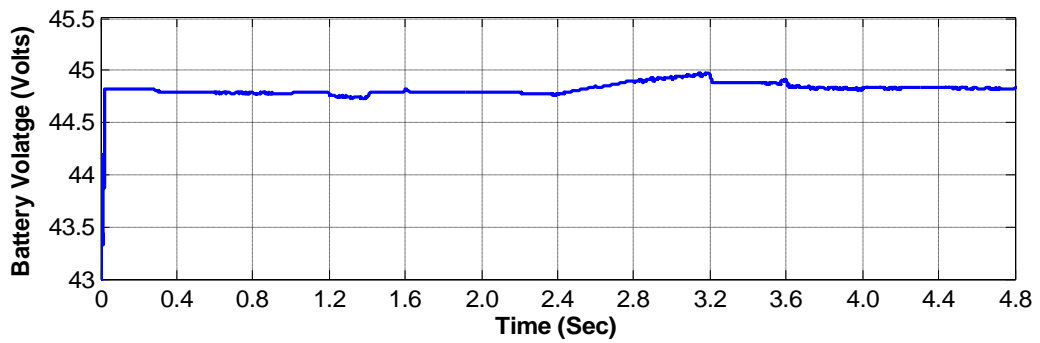


(a) Inverter voltage

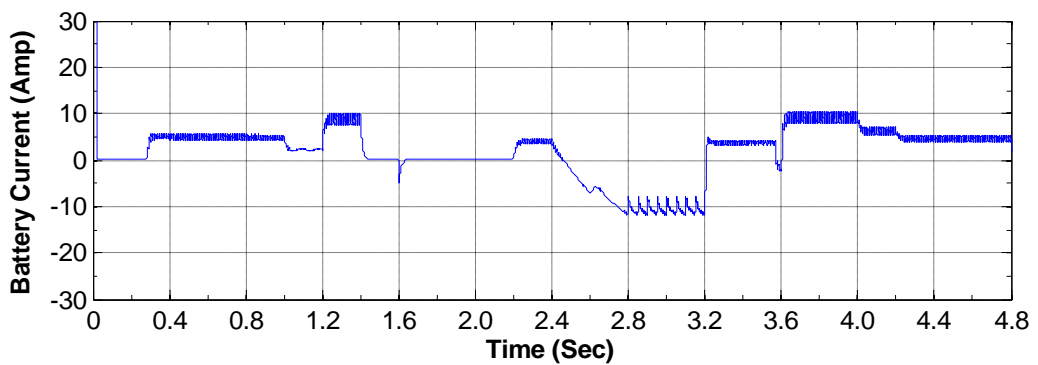


(b) Inverter current

Figure 3.24 Inverter output of stand-alone solar PV-battery system

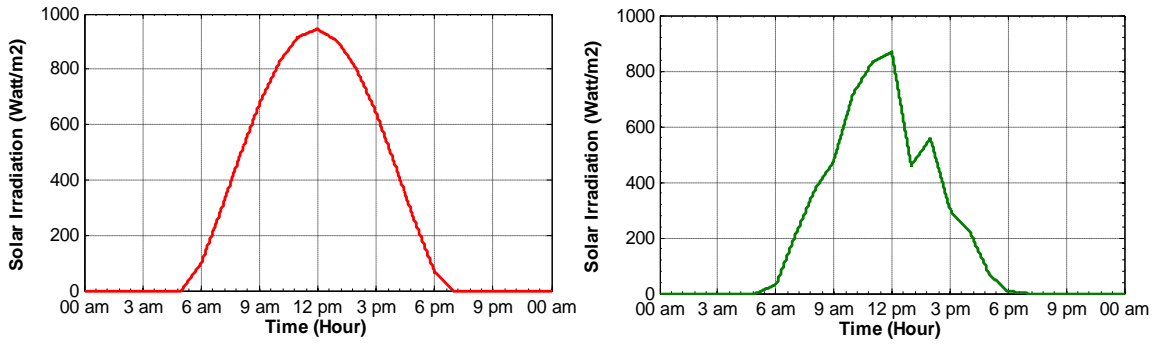


(a) Battery voltage



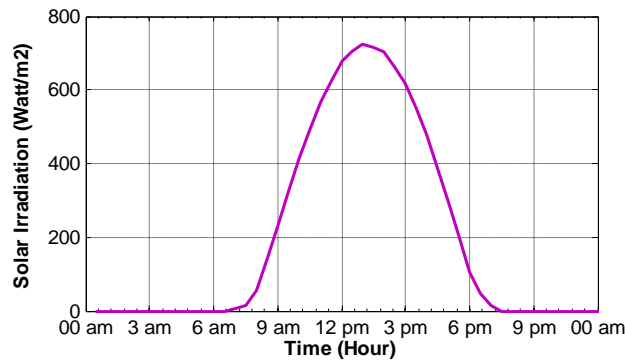
(b) Battery current

Figure 3.25 Battery voltage and current for stand-alone solar PV-battery system



(a) On a summer day

(b) On a rainy day



(c) On a winter day

Figure 3.26 Solar irradiation profiles for a typical day of three seasons

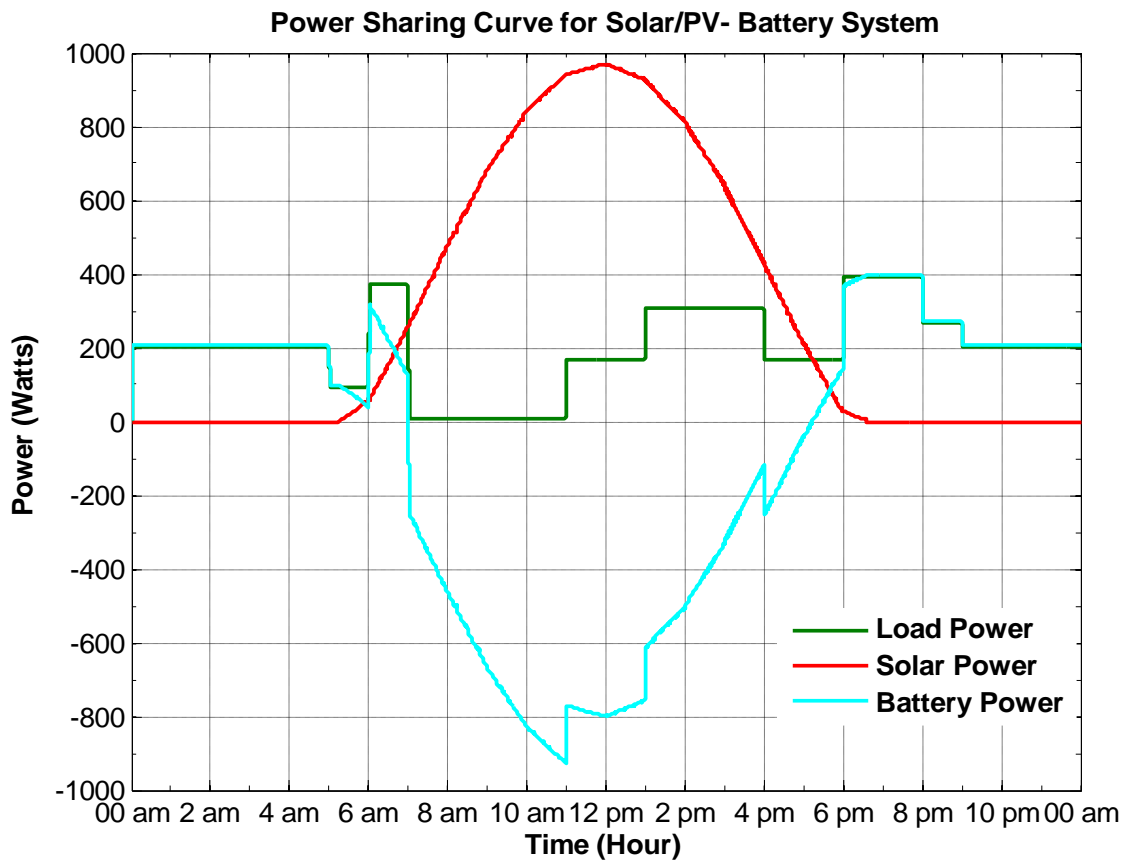


Figure 3.27 Power sharing curve for a summer day for solar PV-battery system

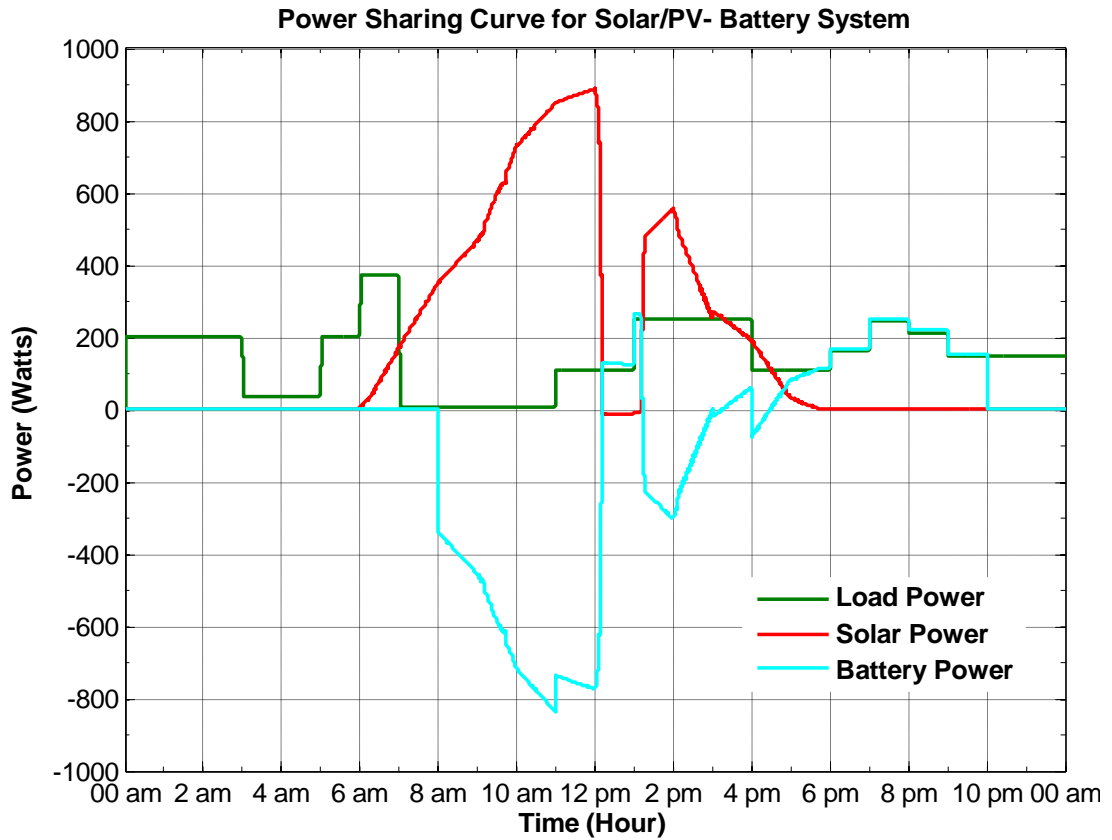


Figure 3.28 Power sharing curve for a rainy day for solar PV-battery system

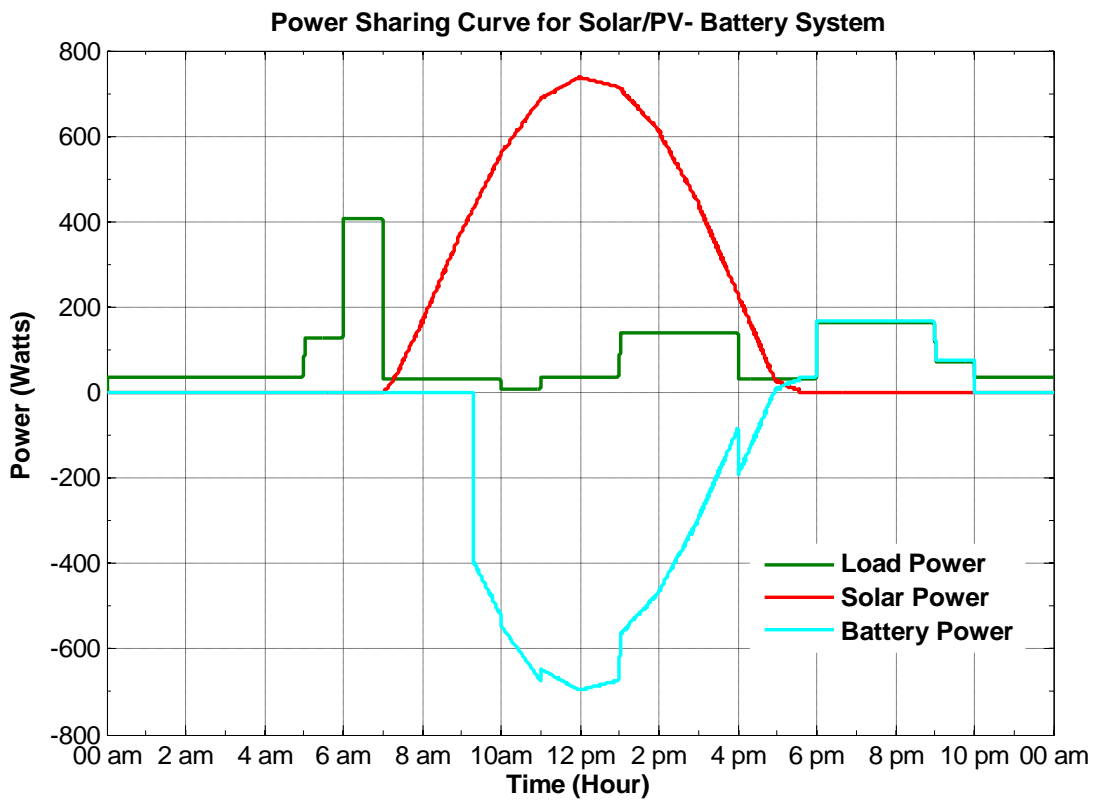


Figure 3.29 Power sharing curve for a winter day for solar PV-battery system

From Figure 3.27, it is observed that in summer season, solar energy is available only for 6 am-6:30 pm and in rest of the time solar power is unavailable as solar irradiation is not present. As shown in Figure 2.6 (a), domestic load requirement is comparably low during 7 am-5 pm, so surplus solar power in this duration is used to charge the battery. During 5 pm-6:30 pm and 6 am-7 am, the load is supplied by solar and battery power and from 6:30 pm to 6 am load is supplied by battery power only. Thus, it is cleared that 1 kW solar PV system is sufficient to supply the load in typical summer days in which good solar power available. However, many days with poor solar irradiation profile are observed in summer season as shown in Figure 2.8 (a), in comparison of selected typical summer day solar irradiation profile, hence stand-alone solar PV-battery system is not capable to supply the load of summer season for all summer days.

From Figure 3.28 and Figure 3.29, it is observed that the load is not supplied efficiently in rainy season as well as in winter seasons, although the load profile of these seasons are less as compared to summer load profile as shown in Figure 2.6. Further, it is observed that if there is any increase in the load, it may also not be supplied by the stand-alone solar PV-battery system in summer, rainy and winter seasons. Hence, to supply the load for 24 hours in all 12 months, larger size of the battery bank and solar panels are required, which increases the rating and size of the system components, which increases the capital cost of the system.

3.3 DESIGN AND SIMULATION OF 1kW WIND ENERGY CONVERSION SYSTEM (WECS) WITH BATTERY STORAGE

The cost of utility-scale wind systems can be minimized by incorporating new technologies. In fact in last two decades, the cost of electricity from wind as well as solar drops more than 80 %. So the electricity generation from wind power plants is also very attractive from economic point of view.

In this thesis, as discussed earlier hybrid energy system is designed with the wind energy as a secondary renewable energy source with solar PV energy to supply a small rural utility load. For this purpose, a stand-alone 1kW wind energy conversion system

(WECS) using PMSG with battery storage is designed and simulated. Basic theory, simulation model and results are presented in this section.

3.3.1 Introduction to Wind Energy Conversion System (WECS)

Figure 3.30 shows the functional structure of a typical wind energy conversion system [7].

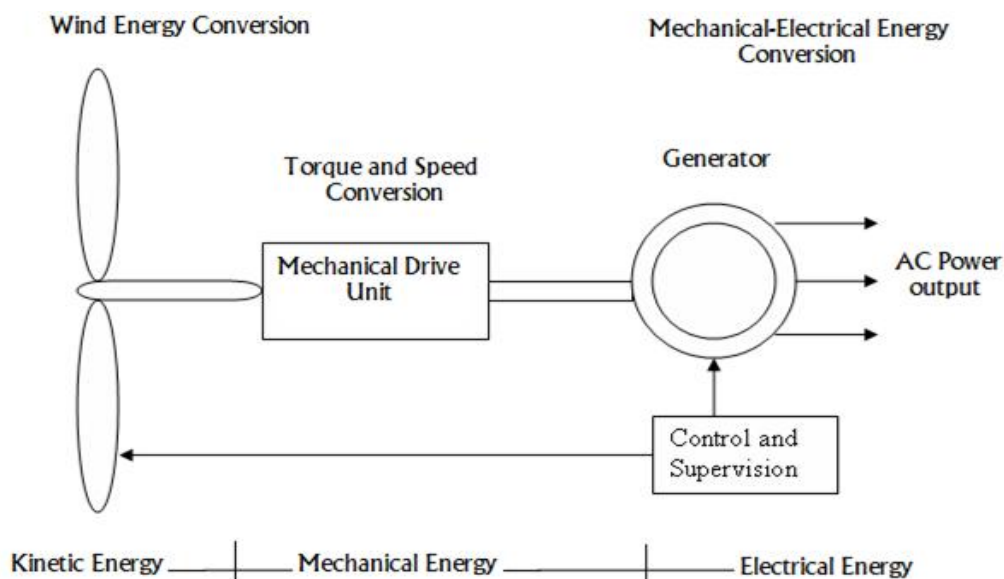


Figure 3.30 Functional structure of a typical wind energy conversion system (WECS)

Wind's kinetic energy is captured by the wind turbine. The rotor of wind turbine consists of two or more blades mechanically coupled to an electrical generator as shown in Figure 3.30. In mechanical assembly, the gearbox is used to transform the slower rotational speeds of the wind turbine into higher rotational speeds on the electrical generator side. An electrical generator output is maintained by employing suitable control techniques, however the output of wind turbine is affected by several factors like wind velocity, size and shape of the turbine *etc* [139].

The most common concepts in wind energy conversion system are [39,140]:

- (a) Fixed Speed Wind Turbine with Squirrel Cage Induction Generator (SCIG)
- (b) Variable Speed Wind Turbine with Doubly Fed Induction Generator (DFIG)
- (c) Variable Speed Wind Turbine with Synchronous Generator (Electrically Excited and Permanent Magnet Excited)

3.3.2 Parameters and Modeling of WECS

The wind power is one of the prominent energy sources in renewable energy sources. In stand-alone applications, the wind power is used with different types of generators such as synchronous generator, asynchronous generator, and reluctance generator [38] *etc.* The permanent magnet synchronous generators are widely used for stand-alone small scale wind power generation due to its simplicity. Figure 3.31 shows a typical block diagram of PMSG based WECS with battery storage [38,73, 140].

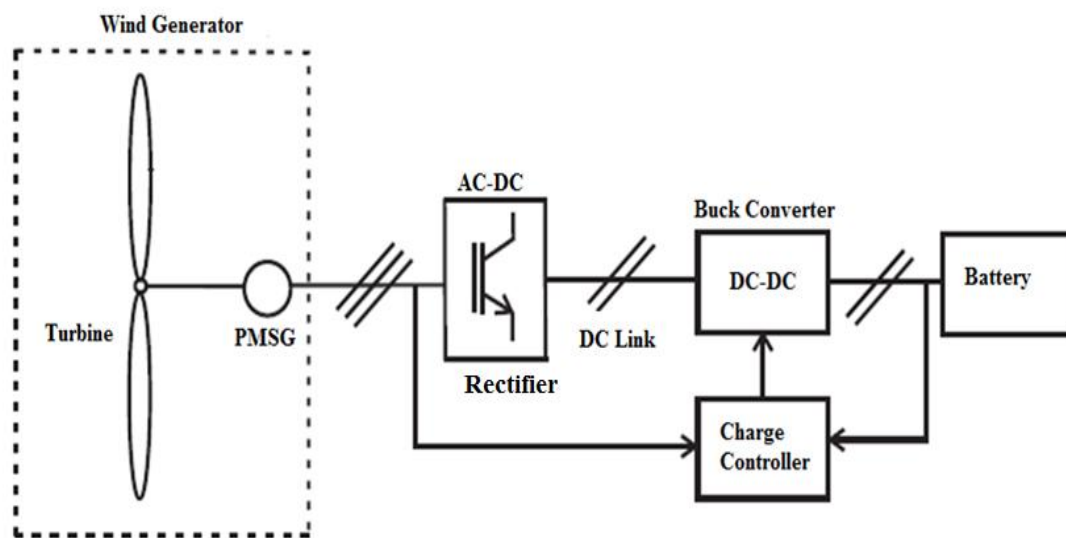


Figure 3.31 Basic block diagram of PMSG based WECS with battery storage

Due to variable speed operation of PMSG based WECS, an intermediate diode bridge rectifier is used to convert AC in to DC output. Further, to achieve maximum power at all available wind speeds, a buck or boost converter (according to desired voltage level) is used. At DC link, a battery energy storage system (BESS) is interfaced to absorb wind power fluctuations under varying wind conditions.

Figure 3.32 shows the system configuration of proposed WECS. It includes a variable speed wind turbine, a PMSG generator, an AC-DC diode rectifier with capacitor filter (C_{1f}), an DC-DC buck converter, DC link, an single-phase VSI with low pass filter and output controller. The detailed design of the system, selection of parameters and modeling are discussed as follows:

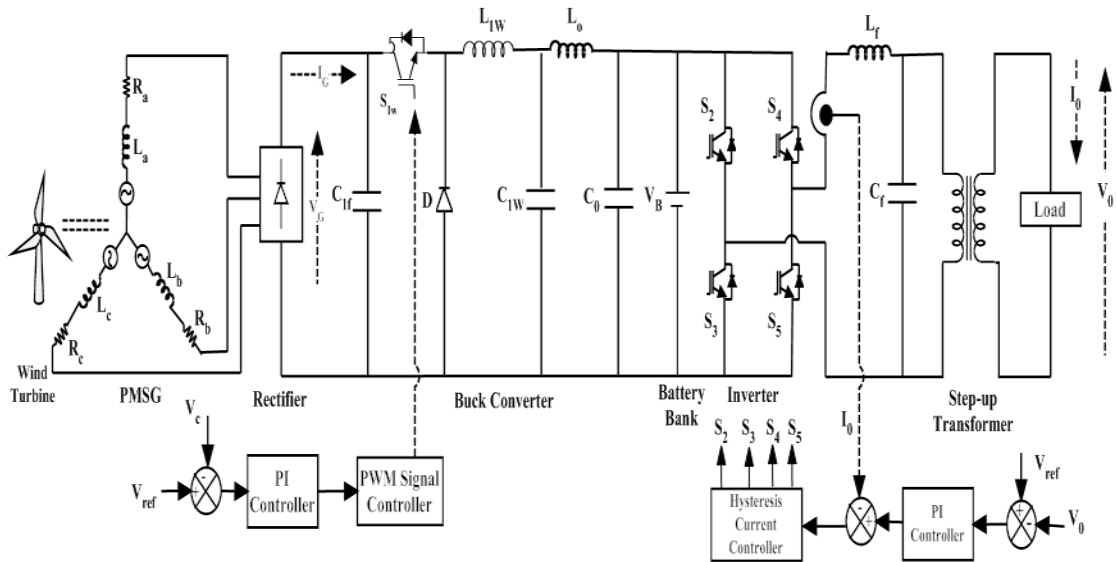


Figure 3.32 Schematic diagram of proposed WECS system

3.3.2.1 Model of a Small Wind Turbine

The power output from a wind turbine depends upon the rotor swept area, velocity of the wind and density of air. The general power equation for a wind turbine is given as [7]:

$$P = 0.5C_p(\lambda, \beta)\rho_a\pi R^2V_\omega^3 \quad (3.27)$$

Where C_p and R represent power coefficient and rotor radius of wind turbine respectively, and ρ_a and V_ω represent the density of air and wind velocity respectively.

The power coefficient (C_p) is defined as the power that could be extracted out from the total available wind power, which is a function of a blade tip speed ratio (λ) and blade pitch angle (β) (angle between the chord of the blade and the reference line on the rotor hub). Theoretically, a wind turbine can only be, at maximum, 59.3 % efficient (which is also known as Betz's limit) [7].

This could be regarded as an efficient factor considering different aerodynamic constraints such as constantly changing wind speed and direction as well as the frictional losses due to blade surface roughness [7].

For most small wind turbines, (β) is kept constant (normally zero). Hence for a constant β , C_p is only a function of (λ). Tip speed ratio (λ) can be given as [7]:

$$\lambda = \frac{V_{tip}}{V_\omega} = \frac{\omega_r R}{V_\omega} \quad (3.28)$$

Where ω_r represents the turbine angular speed.

The dynamic equation of the wind turbine is given by equation (3.29), as:

$$\frac{d\omega_r}{dt} = \frac{T_m - T_L - F\omega_r}{J} \quad (3.29)$$

Where J represents the system inertia, F represents the viscous friction coefficient, T_m and T_L represents the torque developed by the turbine, and the Load torque respectively.

Equation (3.30) is used to model $C_p(\lambda, \beta)$ of the wind turbine [39] as:

$$C_p(\lambda, \beta) = C_1 \left(\frac{C_2}{\lambda_i} - C_3\beta - C_4 \right) e^{\frac{-C_5}{\lambda_i}} + C_6\lambda \quad (3.30)$$

Where, λ_i is a variable which is a function of λ and β is defined as shown in equation (3.31) and the coefficients C_1 to C_6 are assumed as [39]:

$C_1 = 0.5176$, $C_2 = 116$, $C_3 = 0.4$, $C_4 = 5$, $C_5 = 21$ and $C_6 = 0.0068$.

$$\frac{1}{\lambda_i} = \frac{1}{\lambda + 0.08\beta} - \frac{0.035}{\beta^3 + 1} \quad (3.31)$$

Using equations (3.27) to (3.31), a wind turbine model is developed in Matlab/Simulink which as shown in Figure 3.33. The inputs to the model are blade pitch angle (in degrees), wind speed (in m/s) and rotor speed (in rad/s). The blade pitch angle is normally kept at zero as pitch angle control is not standard for small wind turbines but it can be assigned to certain value within the model if desired. Different parameters used for the wind turbine model development are shown in Table 3.3. Figure 3.34 shows the turbine output power v/s turbine speed curve for different wind velocity.

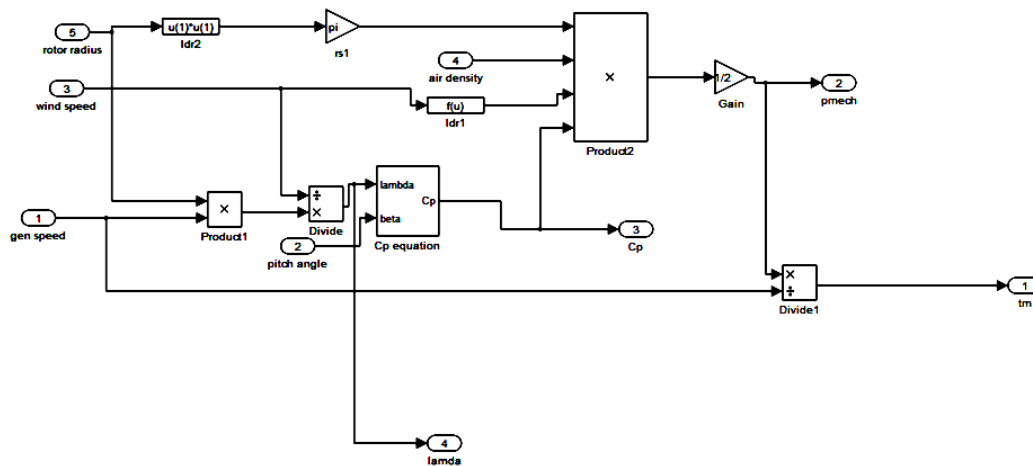


Figure 3.33 MATLAB/ Simulink model of the wind turbine

Table 3.3 Parameters of 1kW Wind Turbine

Parameter	Value
Rated Mechanical power (P_m)	1000 W
Wind Speed for the rated power (V_w)	10 m/s
Density of air (ρ_a)	1.2 kg/m ³
Radius of the blade for the rated power (R)	1.15 m
Area swept by the rotor blades (A_w), πR^2	4.16 m ²

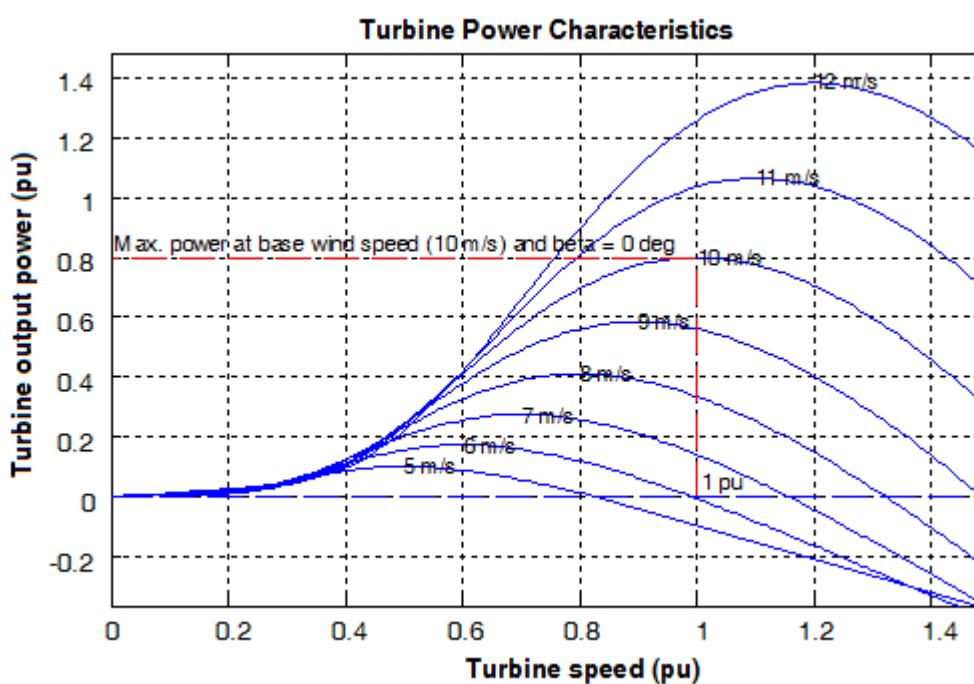


Figure 3.34 Turbine output power v/s Turbine speed at different wind speeds

3.3.2.2 Permanent Magnet Synchronous Generator (PMSG) Model

In the mathematical modeling of PMSG model following assumptions are considered [138]:

1. The stator windings along the air-gap are positioned sinusoidal as far as the mutual effect with the rotor is concerned.
2. No appreciable variations in the rotor inductance with rotor position due to the stator slots.
3. Negligible magnetic hysteresis and saturation effects.
4. Symmetrical stator windings.

5. Damping windings are not considered while the capacitance of all the windings is neglected and resistances of the coils are assumed to be constant.

The dynamic model of a PMSG is derived from a two-phase synchronous reference, namely direct (d) and quadrature (q) axis frame in which the q-axis is 90° ahead of the d-axis with respect to the direction of rotation. In the case of a balanced three phase system, application of d-q transformation reduces the three AC quantities into two DC quantities as [138]:

$$\begin{bmatrix} F_d \\ F_q \end{bmatrix} = \frac{2}{3} \begin{bmatrix} \sin \omega t & \sin\left(\omega t - \frac{2\pi}{3}\right) & \sin\left(\omega t + \frac{2\pi}{3}\right) \\ \cos \omega t & \cos\left(\omega t - \frac{2\pi}{3}\right) & \cos\left(\omega t + \frac{2\pi}{3}\right) \end{bmatrix} \begin{bmatrix} F_a \\ F_b \\ F_c \end{bmatrix} \quad (3.32)$$

Simplified calculations can be performed within these imaginary DC quantities before performing the inverse transform to recover actual three phase quantities. The d-q transform applied to the three phase system is as shown by equation (3.32) [138]. The inverse transform is given in equation (3.33) as:

$$\begin{bmatrix} F_a \\ F_b \\ F_c \end{bmatrix} = \begin{bmatrix} \sin \omega t & \cos \omega t \\ \sin\left(\omega t - \frac{2\pi}{3}\right) & \cos\left(\omega t - \frac{2\pi}{3}\right) \\ \sin\left(\omega t + \frac{2\pi}{3}\right) & \cos\left(\omega t + \frac{2\pi}{3}\right) \end{bmatrix} \begin{bmatrix} F_d \\ F_q \end{bmatrix} \quad (3.33)$$

The simplified d-q axis model in the rotor-field synchronous frame is shown in Figure 3.35 [138].

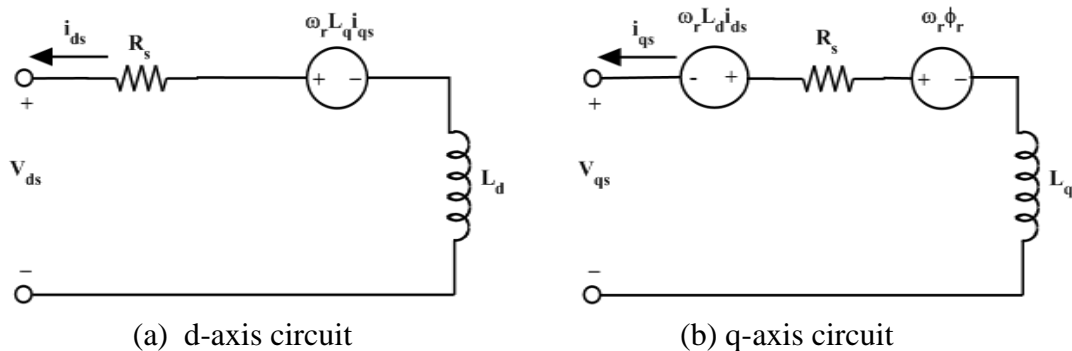


Figure 3.35 Simplified d-q axis model of PMSG in synchronous reference frame

The d-axis and q-axis stator currents in the frequency domain are represented by equations (3.34) & (3.35) [38,138] respectively as:

$$i_{ds} = \frac{(-V_{ds} - R_s i_{ds} - \omega_r L_q i_{qs})}{sL_d} \quad (3.34)$$

$$i_{qs} = \frac{(-V_{qs} - R_s i_{qs} - \omega_r (L_{ds} + L_{qs}) i_{ds} + \omega_r \phi_r)}{s(L_{ds} + L_{qs})} \quad (3.35)$$

Where V_{ds} and V_{qs} represent the stator d and q axis voltages respectively, i_{ds} and i_{qs} represent the stator d-axis and q-axis currents respectively, R_s represents the stator resistance, ϕ_r represents the rotor flux and ω_r represents the angular speed of the generator.

L_d and L_q are the stator d-axis and q-axis self inductances respectively and expressed as [38]:

$$L_d = L_{ls} + L_{dm} \quad \& \quad L_q = L_{ls} + L_{qm} \quad (3.36)$$

Where L_{dm} and L_{qm} are the magnetizing inductances in the d and q axis respectively, and L_{ls} is the leakage inductance. For a non-salient pole PMSG, d-axis and q-axis magnetizing inductances are equal (i.e. $L_{dm} = L_{qm}$), whereas for a salient pole PMSG d-axis magnetizing inductance is normally lower than the q-axis magnetizing inductance (i.e. $L_{dm} < L_{qm}$) [38].

The electromagnetic torque (T_e) and the rotor speed (ω_r) of the PMSG are expressed as given in equations (3.37) & (3.38) respectively [38].

$$T_e = \frac{3N_{pp}}{2} (\phi_r i_{qs} - (L_d - L_q) i_{ds} i_{qs}) \quad (3.37)$$

$$\omega_r = \frac{N_{pp}}{J_s} (T_e - T_m) \quad (3.38)$$

Where N_{pp} is the number of pole pairs of the rotor, J is the rotational inertia of the generator and T_m is the mechanical torque for the generator (in the case of the PMSG connected to a wind turbine, T_m is the torque from the turbine).

Using above equations (3.32) to (3.38) Matlab/Simulink model of PMSG has been developed as shown in Figure 3.36.

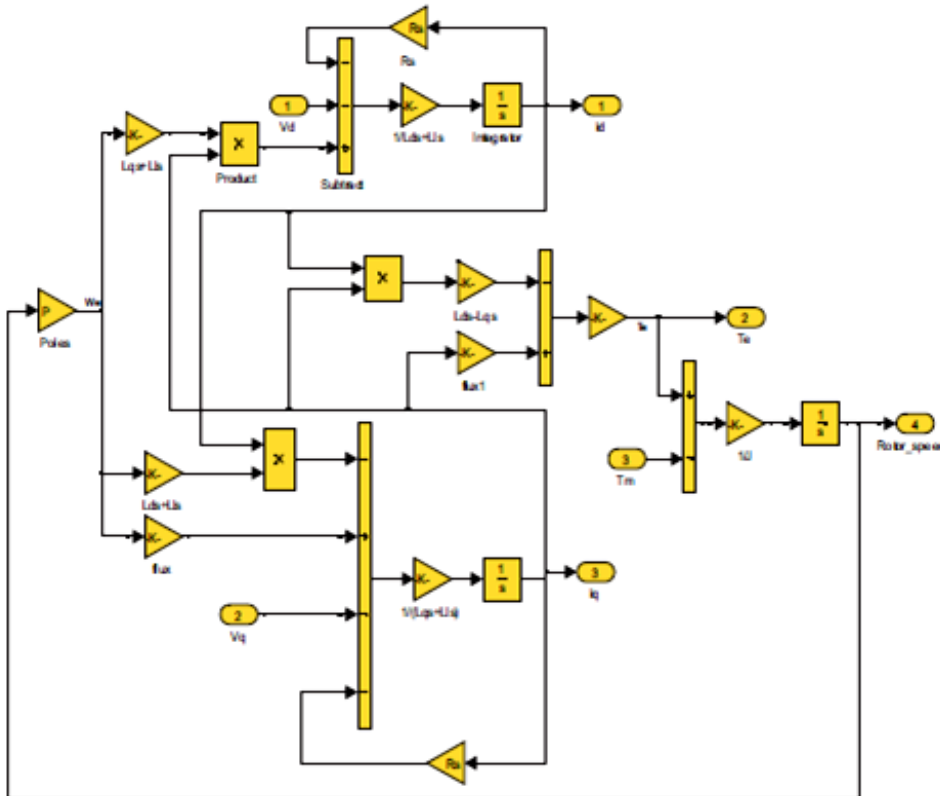


Figure 3.36 Matlab/Simulink model of PMSG

Rotor speed (ω_r) as calculated through equation (3.38) is a feedback to the system. Number of pole pairs, d-axis and q-axis inductances, leakage inductance, magnetic flux of the rotor magnets, stator resistance and moment of inertia of rotor and load can be initially set for a particular size of the generator. Different parameters used for the 1 kW PMSG model development are shown in Table 3.4.

Table 3.4 Parameters of 1kW PMSG

Parameter	Value
Stator Resistance (R_s)	2.875 Ω
d-axis Inductance (L_d)	0.0085H
q-axis Inductance (L_q)	0.0085H
Permanent Magnet Flux Density (λ_0)	0.175Weber
Pole Pairs (N_{pp})	4
Moment of Inertia (J)	0.0008Kgm ²

Wind speed variation for a typical day of summer, rainy and winter seasons is fed to the wind turbine and PMSG system as shown in Figure 3.37 and corresponding

variation of three seasons are shown in results. Wind profile of the day shows considerable change in wind speed during 4.8 sec simulation period.

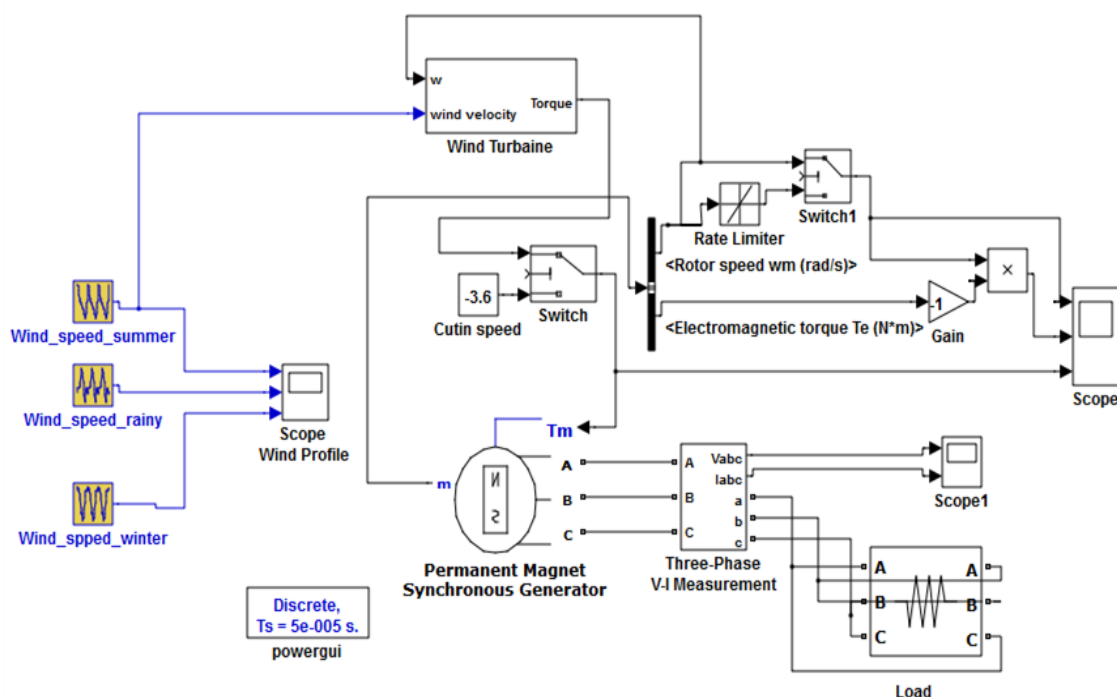


Figure 3.37 Matlab/Simulink model of PMSG with wind turbine

Figure 3.38 shows the wind speed variations of a typical day in various seasons. Corresponding to these wind speed variations, Figure 3.39 shows the wind turbine speed variations of these typical days. Similarly, Figure 3.40 shows the wind turbine torque variations of a typical day and Figure 3.41 shows the wind power variations of a typical day of various seasons. Here, cut-in speed for wind power generation is considered as 3.6 m/sec.

Wind generator voltage and current are also obtained for 4.8 sec duration, but Figure 3.42 and Figure 3.43 show the variations of wind generator voltage and current only for time duration of 0.06 sec respectively for more clarification. It is observed from Figures 3.42 (a), (b) and (c) that voltage output from the wind generator is three phase sinusoidal. It is also observed that magnitude and frequency of these output voltage in three seasons day profile are not equal, as output is varying according to the variations in wind speed as shown in Figure 3.38. Corresponding variations in load current can be observed in Figures 3.43 (a), (b) and (c) for three season's day profile.

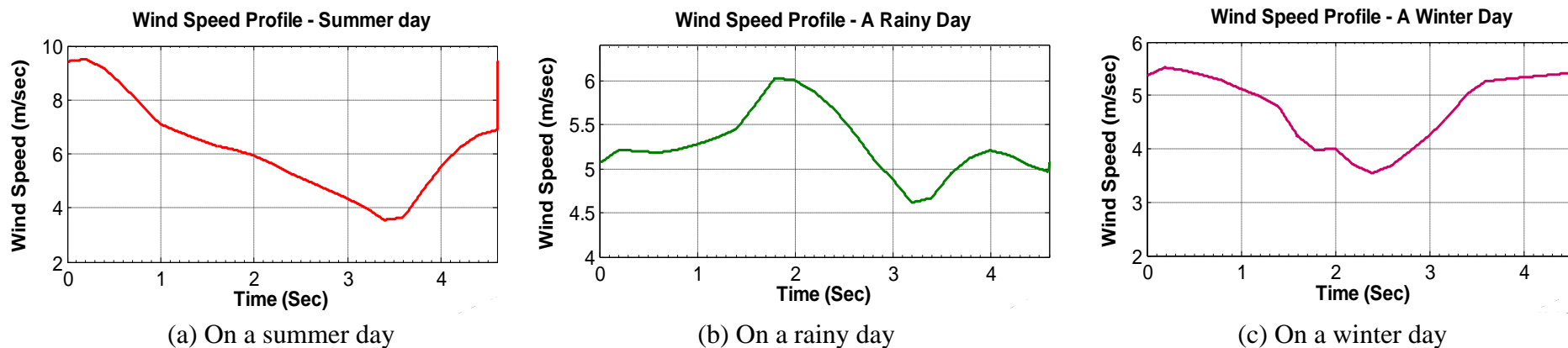


Figure 3.38 Wind Speed variations of a typical day of three seasons

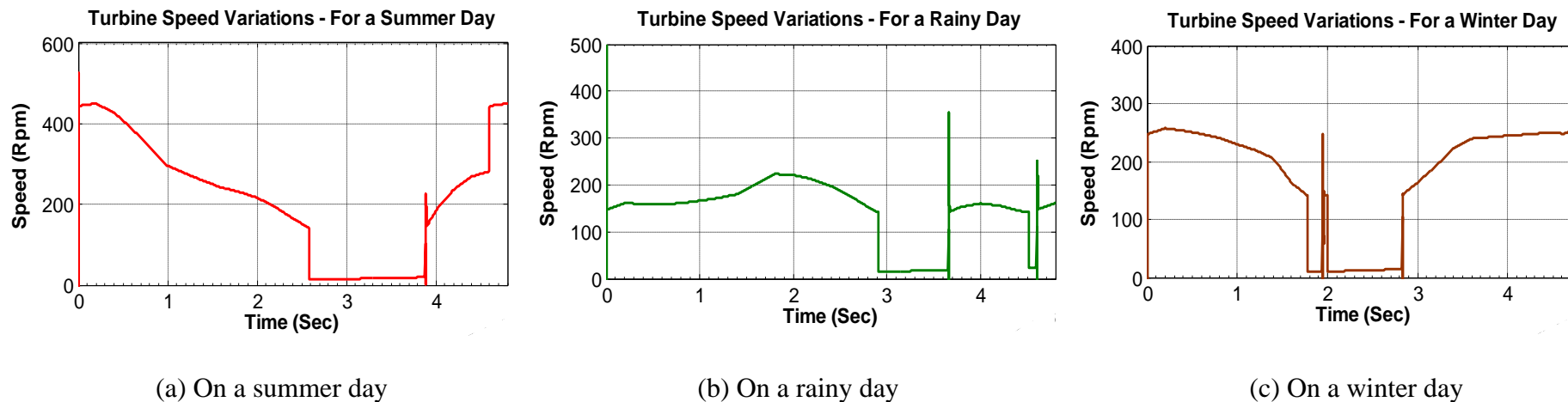


Figure 3.39 Wind turbine speed variations of a typical day of three seasons

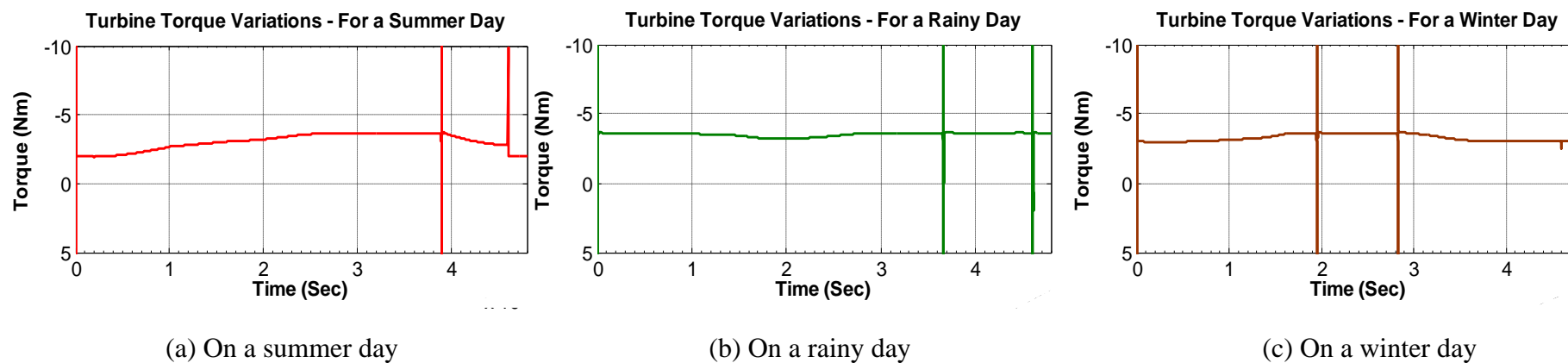


Figure 3.40 Wind turbine torque variations of a typical day of three seasons

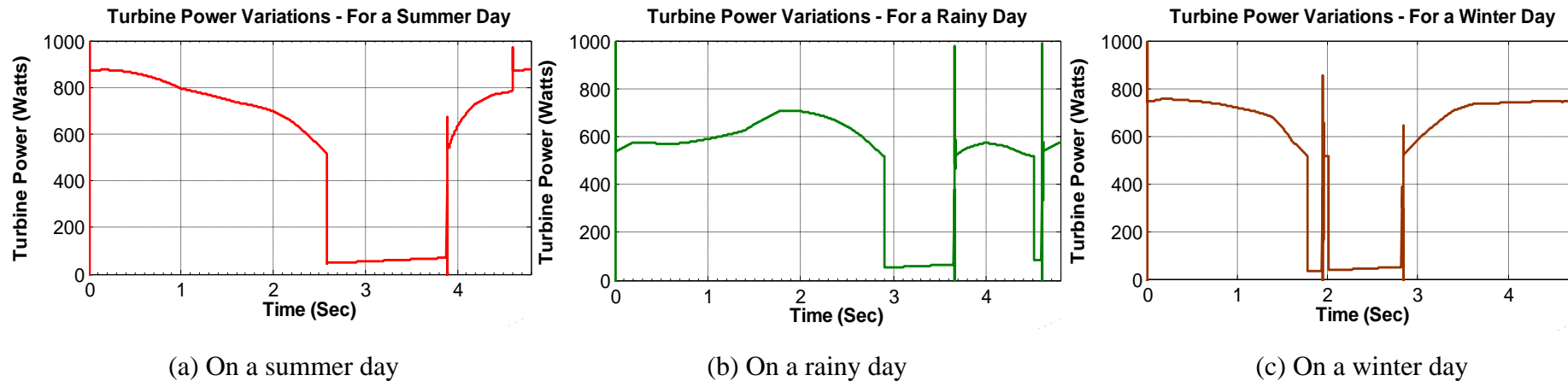


Figure 3.41 Wind turbine power variations of a typical day of three seasons

3.3.2.3 DC-DC Buck Converter

From Figures 3.42 and 3.43 it is clear that output voltage and current are of variable frequency. So an intermediate three phase rectifier and a filter with a buck converter is proposed for conversion of AC into DC to connect the system to DC bus or charge battery bank.

A buck converter proposed for maintain the output voltage of rectifier within limit, as shown in Figure 3.44 which is a DC voltage to DC voltage buck in which the output voltage has a same polarity as input.

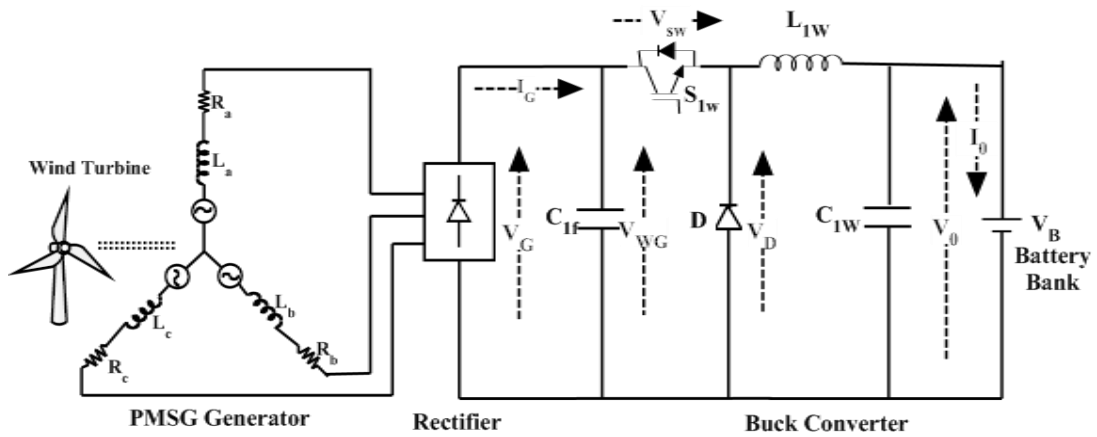


Figure 3.44 Buck DC-DC converter topology used as wind power interface

In the buck configuration as shown in Figure 3.44, when the switch is ‘ON’, energy is delivered to the inductor (L_{1w}) through switch (S_{1w}). When S_{1w} is ‘OFF’, energy stored in the inductor passes to the output via freewheeling diode (D) and none of it comes from the input source [37,136]. Since the average current from the capacitor is zero, the average inductor current from buck converter is equal to the load current.

From Figure 3.44 the voltage across the inductor during ‘ON’ and ‘OFF’ time is given as:

$$V_{ON} = V_{WG} - V_{SW} - V_o \approx V_{WG} - V_o \quad (3.39)$$

$$V_{OFF} = V_o + V_D \approx V_o \quad (3.40)$$

Where V_{ON} and V_{OFF} are voltage drops across the inductor during ‘ON’ and ‘OFF’ time, respectively. Similarly V_{WG} , V_{SW} , V_o , V_D are input voltage, voltage drop across the switch, output voltage and voltage drop across the diode respectively.

The duty cycle (D) for buck converter is given as [37,136]:

$$D = \frac{V_0}{V_{WG}} \quad (3.41)$$

The change in inductor current (ΔI) can be given as [37,136]:

$$\Delta I = \frac{V\Delta t}{L_{1w}} \quad (3.42)$$

From volt-second law, $V_{ON}T_{ON} = V_{OFF}T_{OFF}$, equation (3.42) can be rewritten as:

$$\Delta I = \frac{V_{ON}T_{ON}}{L_{1w}} - \frac{V_{OFF}T_{OFF}}{L_{1w}} \quad (3.43)$$

Using equations (3.39), (3.40) and (3.43), the value of the inductance in terms of peak inductor current (ΔI), switching frequency (F_{si}), duty cycle (D) and output voltage (V_0) can be expressed as [37,136]:

$$L_{1w} = \frac{V_0(1-D)}{F_{si}\Delta I} = \frac{V_{ON}*D}{F_S*r*I_0} \quad (3.44)$$

Where (r) represents current ripple factor and I_0 represents load current.

Components Selection for the Buck Converter Design

Different parameters used for selecting the components for the DC-DC buck converter are shown in Table 3.5. A nominal 48 V DC bus system (i.e. 48 V battery bank system) and 53 V output from the buck converter are considered.

A variable voltage up to 80 V is assumed to be the input for the buck converter due to variable wind speed for typical circumstances, beyond this system is to be in cut-off mode. The controller is designed to operate in the range of 50 W to 1000 W system. Hence there is a wide variation in the peak current values which determines the required inductance. A specific ripple current is initially chosen for the design. The load current is equal to the inductor current in case of the buck converter assuming that the average capacitor current is zero for steady state condition.

The size of the inductor is obtained from the minimum load current (for 50 W load) and the current rating is obtained from maximum current (for 1000 W system) [32]. Assuming ripple factor (r) of 0.4, minimum load current of 0.9 A, duty cycle ($D=0.6875$) and switching frequency ($F_{si}=30$ kHz), the size of inductor is calculated as:

$$L_{1w} = \frac{V_{ON}*D}{F_S*r*I_{Load}} = \frac{27*0.6875}{30*10^3*0.4*0.9} = 1.72\text{mH} \quad (3.45)$$

Table 3.5 Parameters of DC-DC buck converter

Parameter	Value
Input Voltage (V_{WG})	80 V
Output Voltage (V_{out})	53 V
On Voltage (V_{on})	27 V
Current Ripple Factor (r)	0.4
Minimum & Maximum Power	50 W & 1000W
Minimum & Maximum Load Current (I_0)	0.9 A & 18.1 A
Minimum & Maximum Peak Current (ΔI)	0.36 A & 7.24 A
Duty Cycle (D)	0.6875
Switching frequency (F_{si})	30 kHz
Inductance (L_{1W})	1.72 mH
Capacitance (C_{1W})	151 μ F

With this value of inductance, current ripple (r) is reduced at the higher power values. Hence, peak current of 18.1 A is obtained for 1000 W wind system.

In order to calculate the value of capacitance (C_{1W}) for a buck converter, peak to peak ripple voltage ($\Delta V=0.2$ V) is specified. Equation (3.46) is used to calculate the value of output capacitor [37,136].

$$C_{1W} = \frac{\Delta I}{8 * F_{si} * \Delta V} = \frac{0.4 * 18.1}{8 * 30 * 10^3 * 0.2} = 151 \mu F \quad (3.46)$$

Figure 3.45 shows the developed Matlab/Simulink model of buck converter with PMSG and Figure 3.46 shows the output of buck converter.

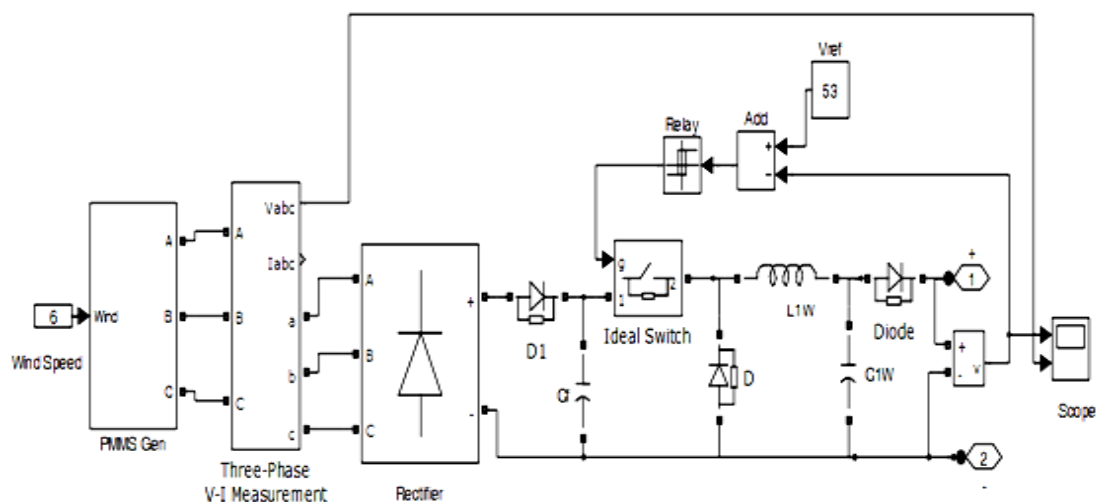


Figure 3.45 Matlab/Simulink model of buck converter with PMSG

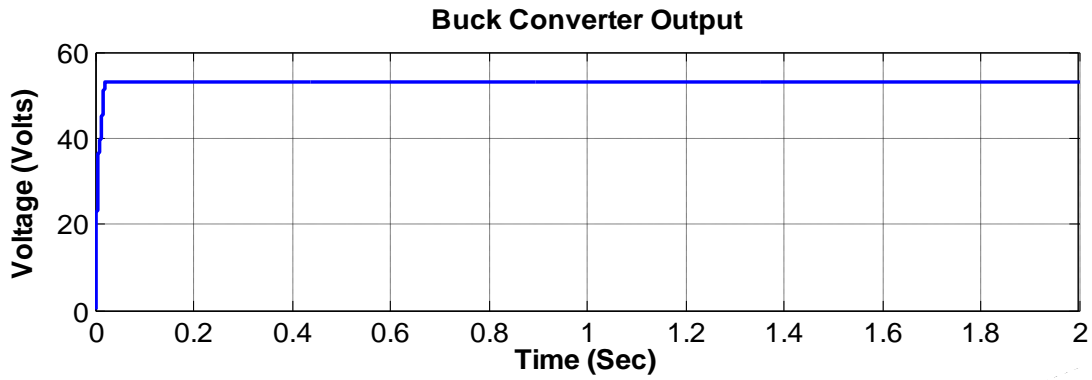


Figure 3.46 Buck converter output voltage

3.3.3 Simulation Results and Discussion

Matlab/Simulink model of proposed WECS is shown in Figure 3.47.

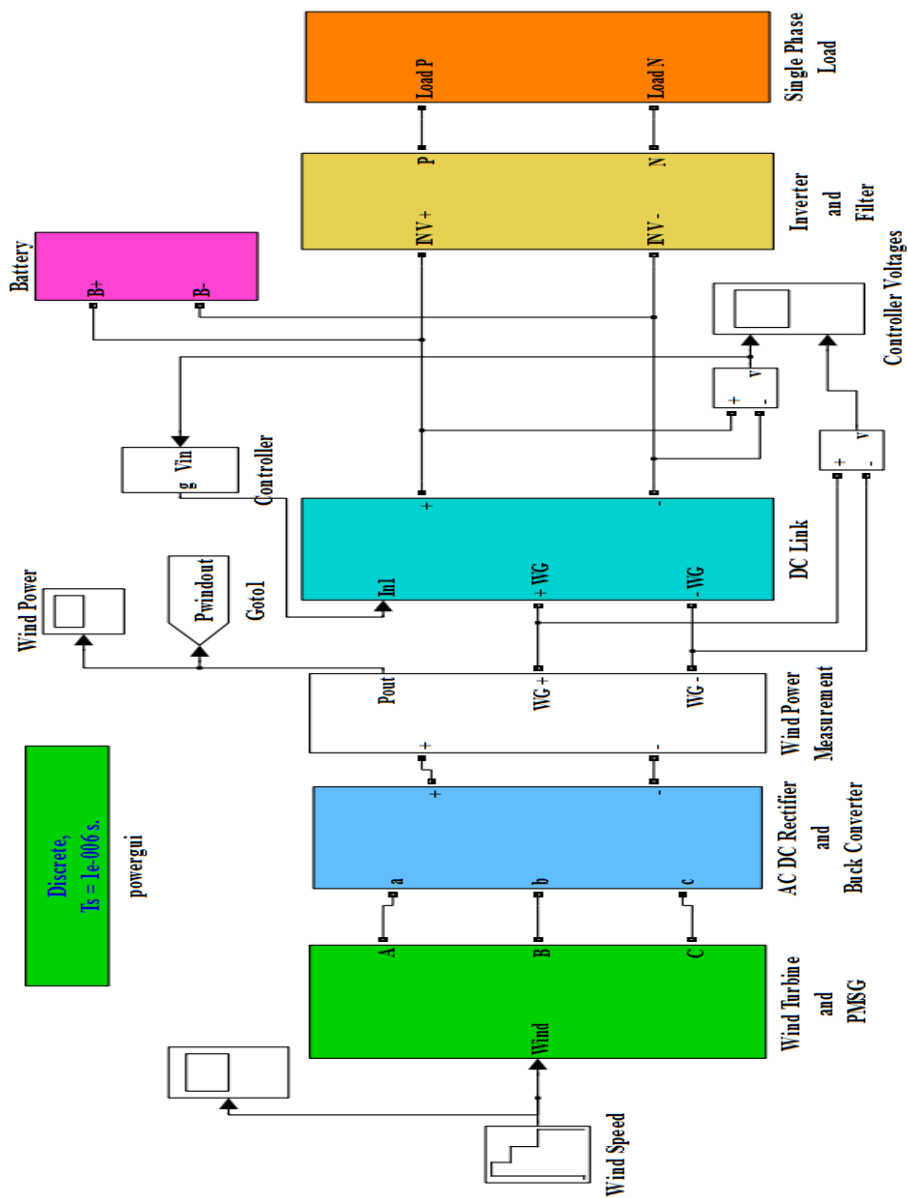


Figure 3.47 Matlab/Simulink model of proposed WECS

The design of load circuit, inverter circuit and its controller and filter are already discussed in solar-battery system and they are also used in the wind-battery system as shown in Figure 3.32.

For system performance analyses, a special wind profile as shown in Figure 3.48 is fed to the system for total 4.8 sec of simulation time.

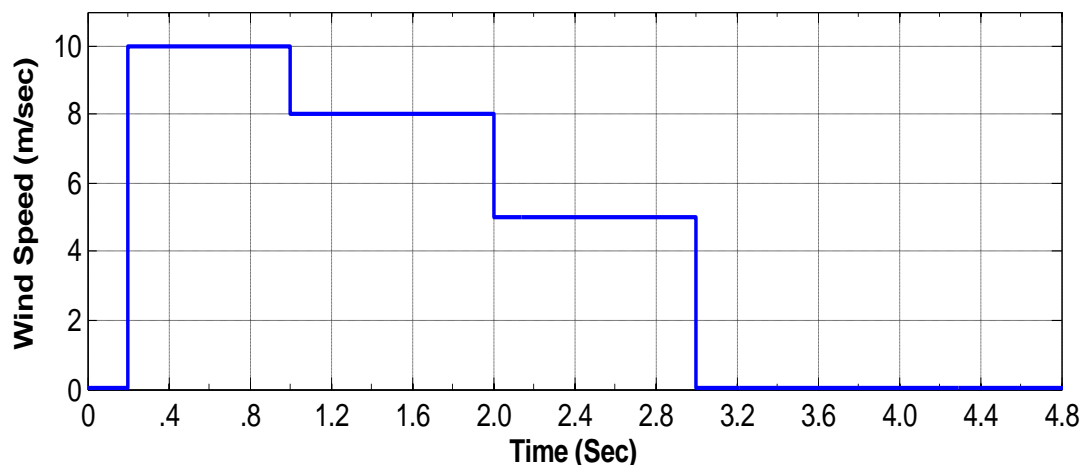
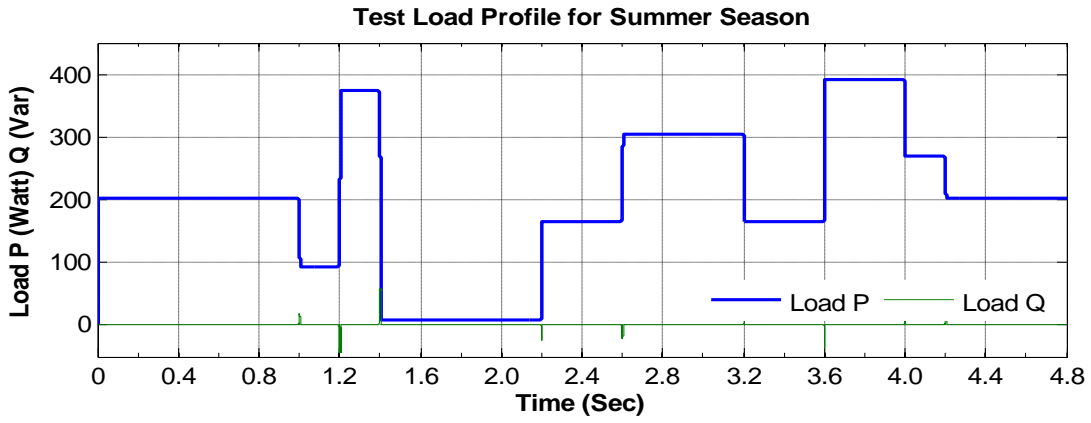


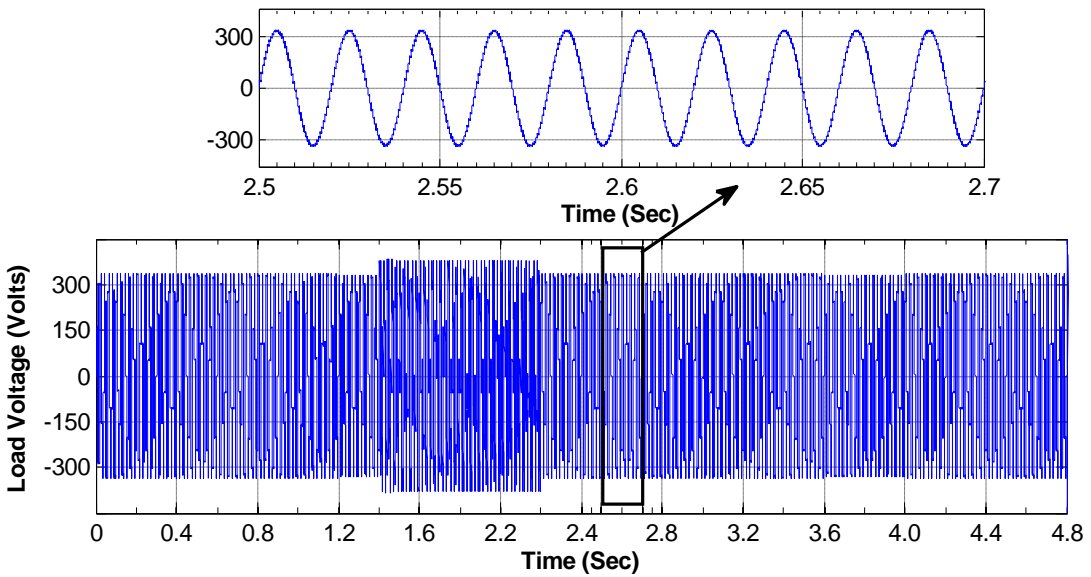
Figure 3.48 Wind profile input of wind-battery system

A typical load profile for a day of summer season is considered as shown in Figure 3.49 (a). Figures 3.49 (b) and (c) show the corresponding variations in load voltage and current. At time 2.6 sec, load changes from 165 W to 305 W as shown in Figure 3.49 (a). Corresponding changes in current are also observed and shown in Figure 3.49 (c) in expanded view of load current. No change in the load voltage is observed during this period. Figure 3.50 (a) shows the power generation from wind system for given wind input. Figures 3.50 (b) & (c) show the wind generator voltage, current at the filter point after AC-DC rectification.

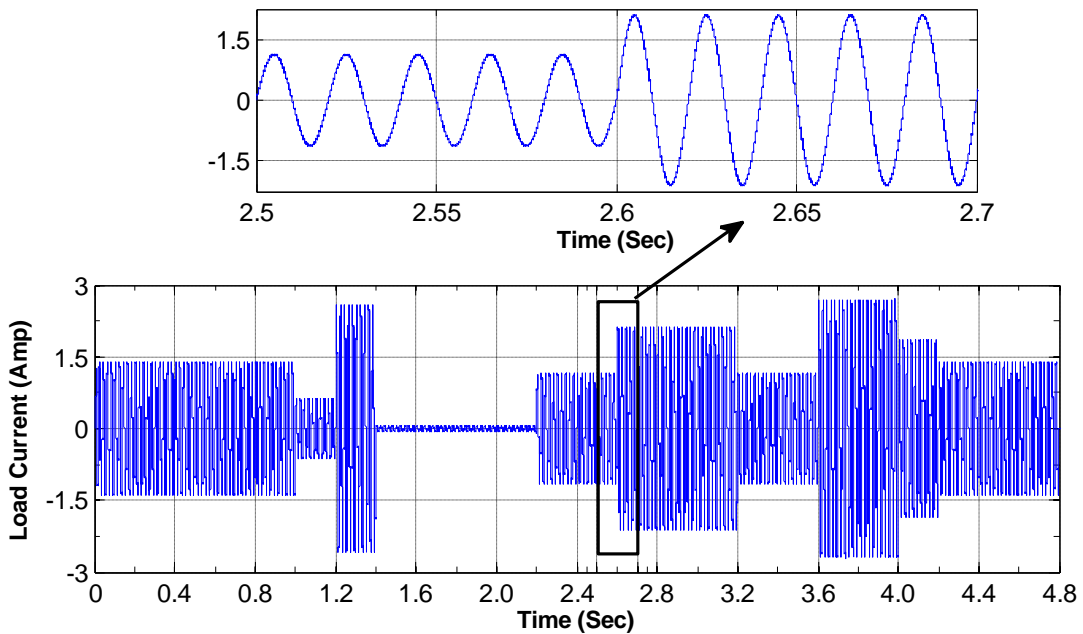
The output of buck converter is almost constant to 53 V by using the control algorithm and output of DC link is kept around 60 V as shown in Figure 3.51 which is fed to inverter and inverter output is shown in Figure 3.52 which is almost sinusoidal in nature. The battery voltage and current are shown in Figures 3.53 (a) & (b) respectively. It is cleared from Figure 3.53 (b) that battery charges between 0.2 sec-3.0 sec by the surplus power available after supplying to load and after 3.0 sec, as wind power is not available, the battery supplies power to load, and hence it has started to discharge through load. Variations in battery current are as per connected load.



(a) Typical load variation

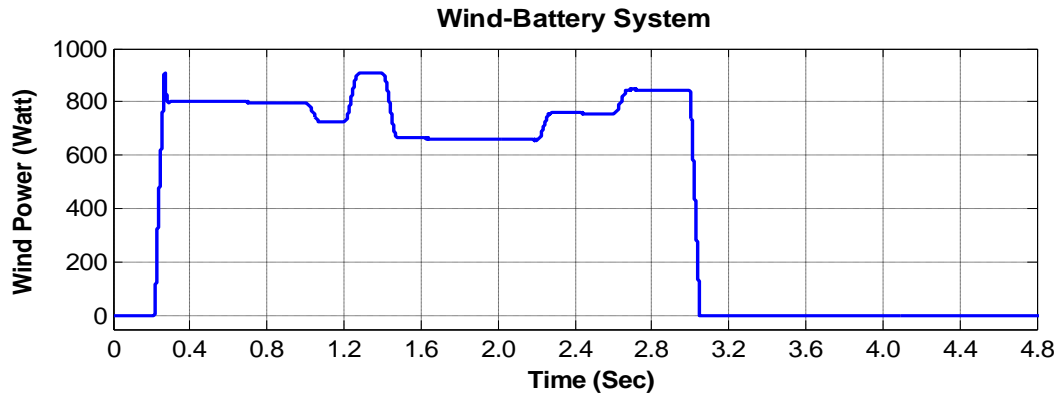


(b) Load voltage

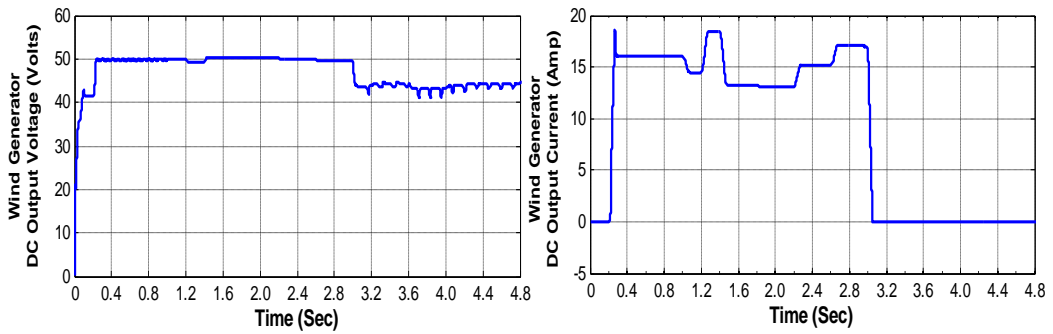


(c) Load current

Figure 3.49 Load profile of wind-battery system



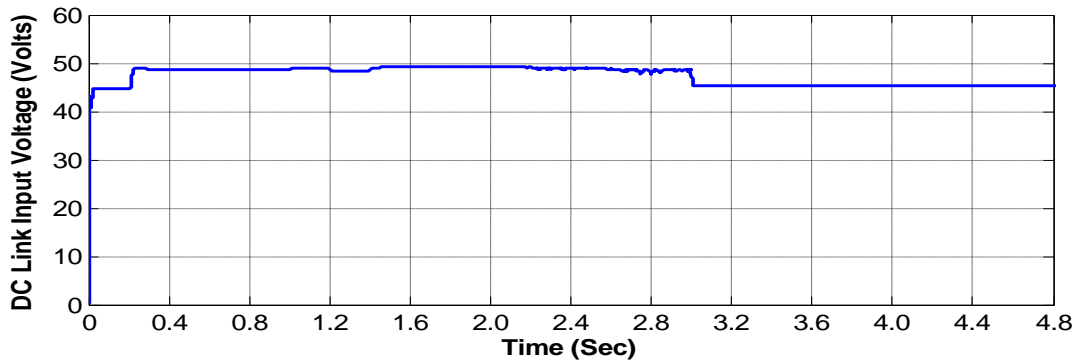
(a) Wind generator power



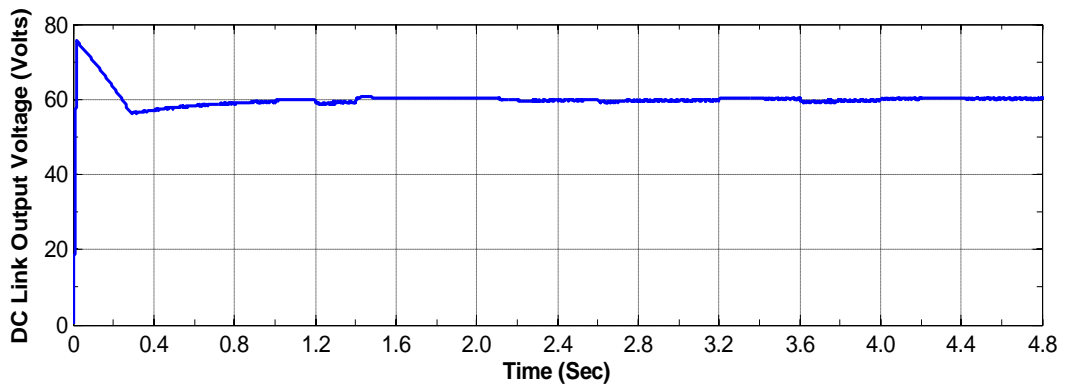
(b) Wind generator DC voltage

(c) Wind generator DC current

Figure 3.50 Wind generator power, voltage and current for wind-battery system

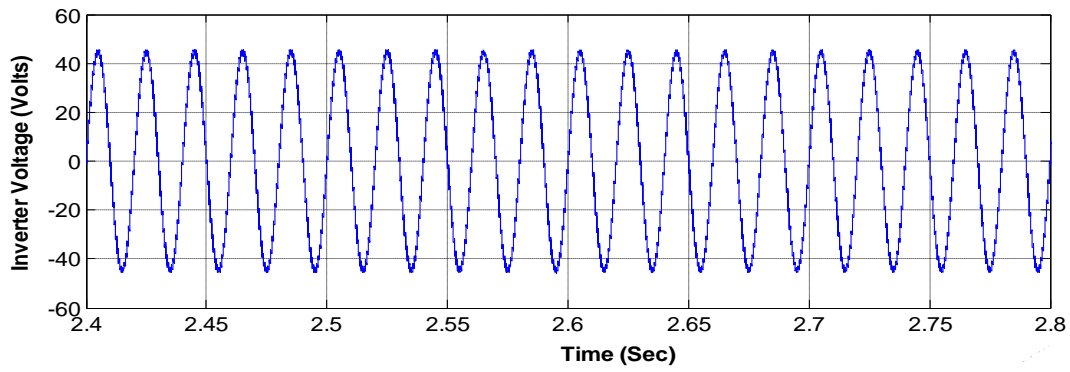


(a) Input voltage

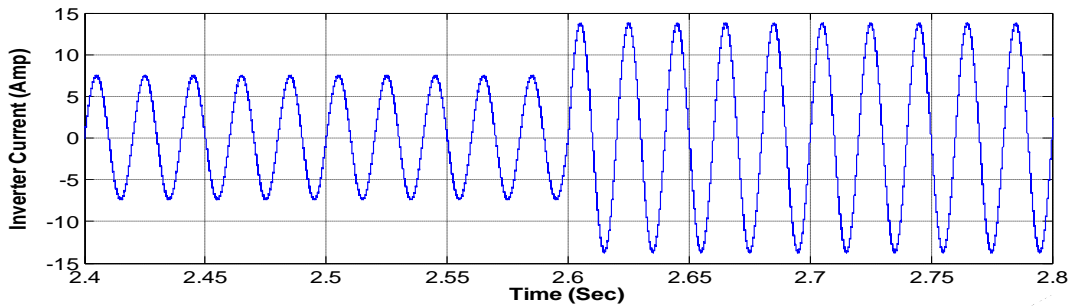


(b) Output voltage

Figure 3.51 DC link input and output voltage

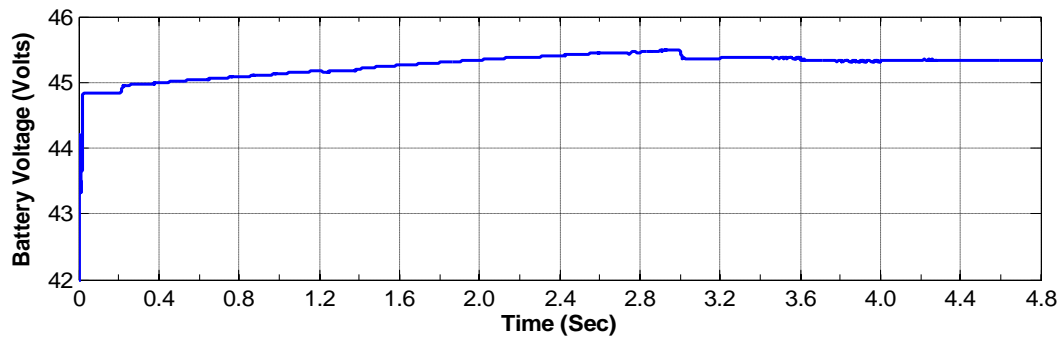


(a) Inverter voltage

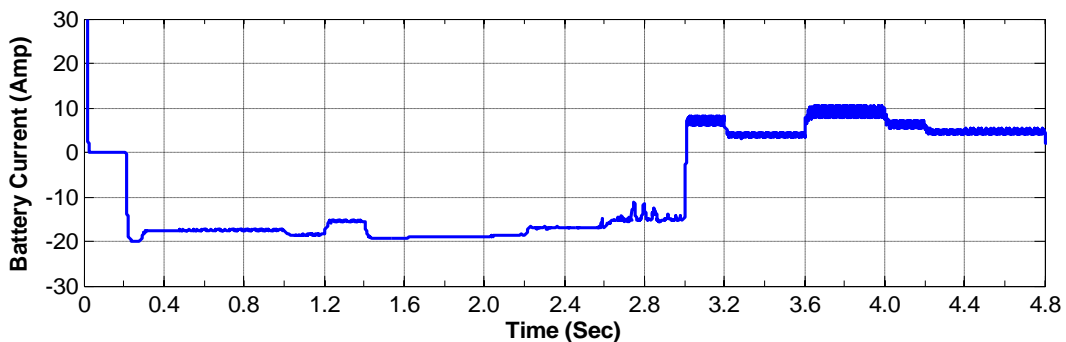


(b) Inverter current

Figure 3.52 Inverter output of wind-battery system



(a) Battery voltage



(b) Battery current

Figure 3.53 Battery voltage and current for wind-battery system

Power sharing curves for wind power with battery power and load power are shown in Figure 3.54 to Figure 3.56 for a typical day of summer, rainy and winter seasons respectively.

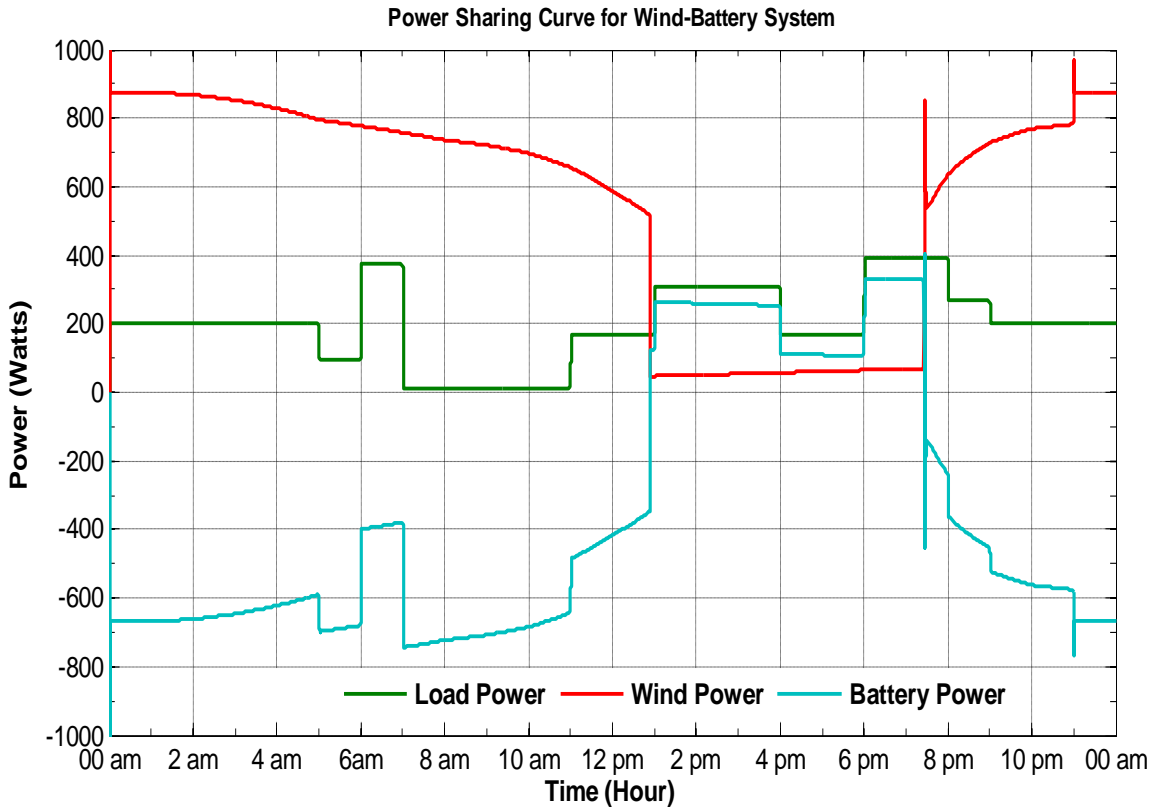


Figure 3.54 Power sharing curve for a summer day for wind-battery system

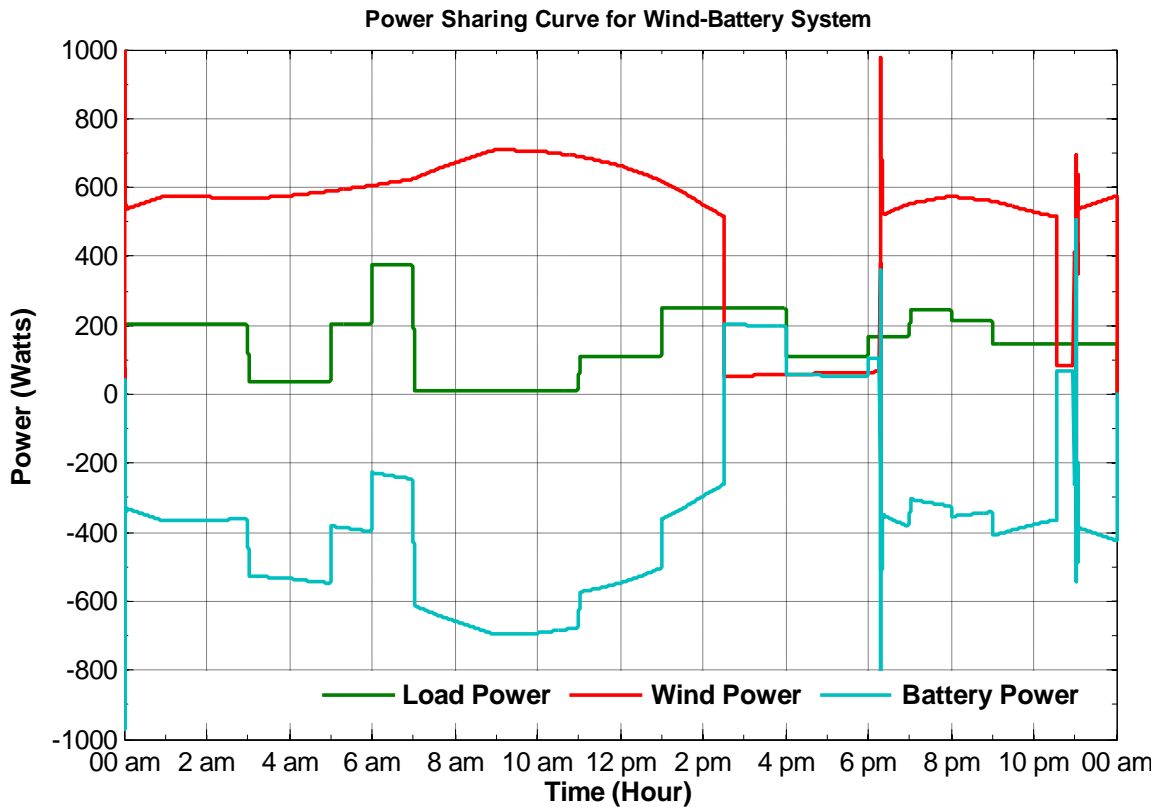


Figure 3.55 Power sharing curve for a rainy day for wind-battery system

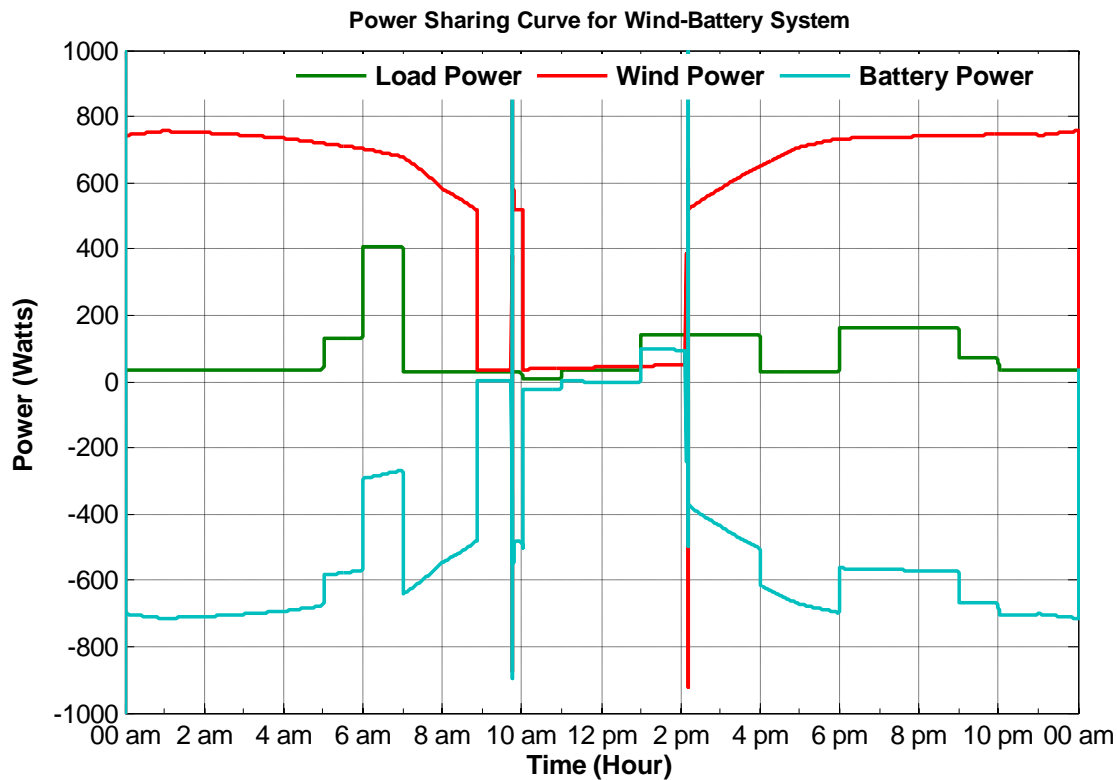


Figure 3.56 Power sharing curve for a winter day for wind-battery System

It is observed that wind power is sufficient to supply the load and charge battery during these typical days for summer, rainy and winter seasons. Further, it is also observed from Figures 3.55 & 3.56 that, in the case of rainy and winter seasons, as load demand is less as compared to summer season, the wind power is sufficient to supply the load for some days except some duration, *i.e.* battery is also not providing the power to the load during this duration.

It is clear that, since typical day is chosen in a particular season, as the best wind power output days, however, wind variations in whole seasons are not same as the typical days as shown in Figures 2.10 (a), (b), (c). So, it is not possible to supply the load demand and to charge battery for emergency need in whole season by WECS only. If there is any change in typical load profile pre assumed on hourly basis, than the system is also not capable to supply the load demand.

So to supply the load for 24 hour in all months, larger size of the battery bank and wind generator is required, which increases the size of the system components, hence capital cost of the system is also increased.

3.4 DESIGN AND SIMULATION OF 1.2 kVA DIESEL GENERATOR SYSTEM

As discussed earlier, stand-alone solar PV-battery system and stand-alone wind-battery system both are incapable to supply the load demand either due to change in load or change in the input *i.e.* solar and wind profile which are uncertain in nature. Moreover the system is not able to charge battery for emergency need. So for fulfill the load demand, either system capacity is to be increased or another supply system is to be used. Although, capital cost also increases with an increase in capacity of the system and efficiency of overall system is also decreased.

A diesel generator (DG) may be a choice to supply the load, although at present people are using DG in urban and rural areas with grid connected mode as back supply source *i.e.* DG is running if only if grid supply is not available [23,24]. However, the use of DG time increases as power cut time increases and the diesel consumption increases which causes more CO₂ production. In the case of DG stand-alone system, *i.e.* no grid connection, the problem of maintenance and life time of DG also considerable. So, it is not advised to use DG stand-alone system as concern for environment.

Although, if DG is used in combination with renewable sources such as solar and wind *etc.* as a hybrid energy system, DG running time may be reduced which causes less consumption of fuel and less pollution. The detail of such hybrid energy systems is to be discussed in chapter 4. Here, discussion only about the DG system and its working is presented.

3.4.1 Parameters and Modeling of System

The diesel generator set (diesel engine driven generating set) is a compact and robust machine in which mechanical energy is converted into electrical energy. It uses high speed diesel oil and works on diesel cycle. In this system, the air is drawn into the cylinder and compressed in to a high ratio (14:1 to 25:1) at a temperature of 700⁰C-900⁰C. At this point, a metered quantity of diesel fuel is injected into the cylinder, which ignites spontaneously because of the high temperature of compressed air. The diesel is injected through injector in the chamber. Hence, the diesel engine is also known as compression ignition (CI) engine.

An alternator is coupled with the diesel engine and the kinetic energy of engine is transmitted to an alternator and converted into electrical energy as shown in Figure 3.57. This electrical energy is then fed to the load and also used to charge battery bank [142].

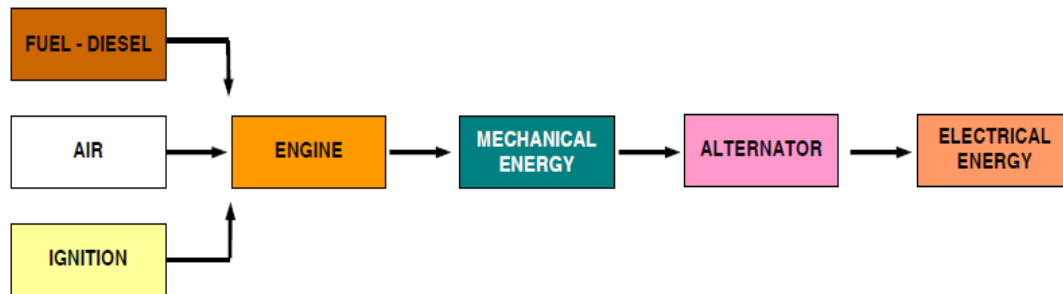


Figure 3.57 Block diagram of working principle of DG set

For a typical 1kW hybrid energy system, a 1.2 kVA, 220 V, single phase diesel generator is selected for supplying an average load of 500 W, 0.8 p.f. and charging of a 48 V, 80Ah battery bank. The total connected load to the system is 972 W and the DG is capable to supply the load up to 1000 W. Figures 3.58 and 3.59 show the Matlab/Simulink model of diesel engine & generator system and diesel engine speed & voltage control respectively [141-143].

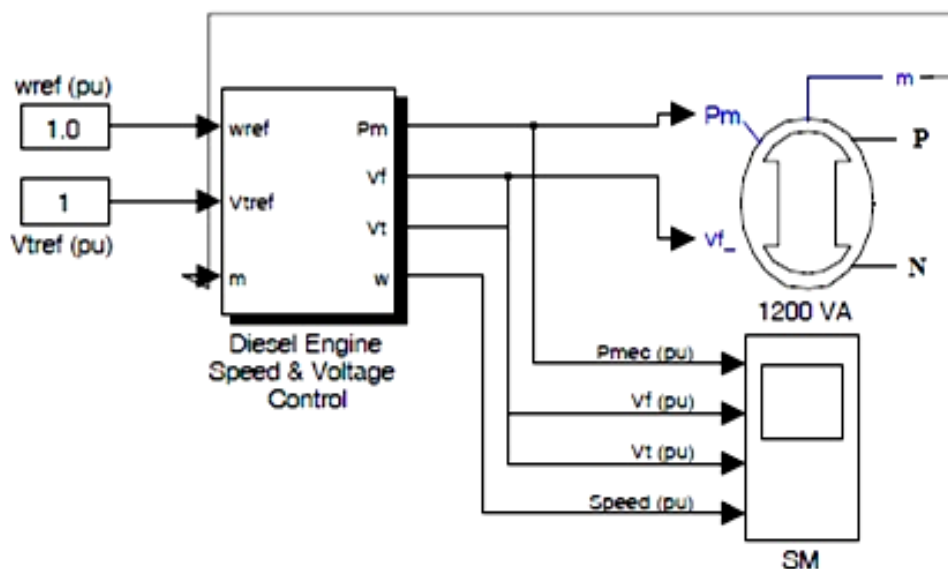


Figure 3.58 Matlab/Simulink model of diesel engine & generator system

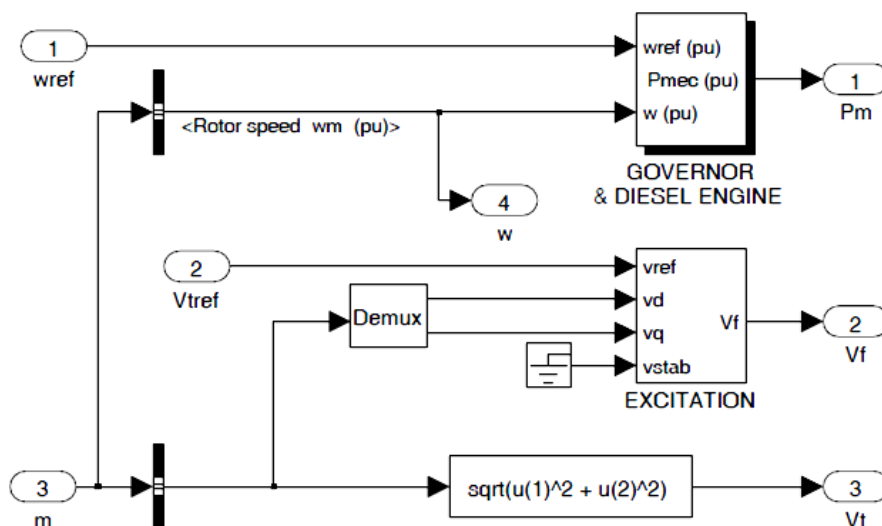


Figure 3.59 Matlab/Simulink model of diesel engine speed & voltage control

3.4.2 Simulation Results and Discussion

For simulation study of diesel generator system, DG is connected with a 500 W resistive load as shown in Figure 3.60 and system is simulated for a time period of 1 sec.

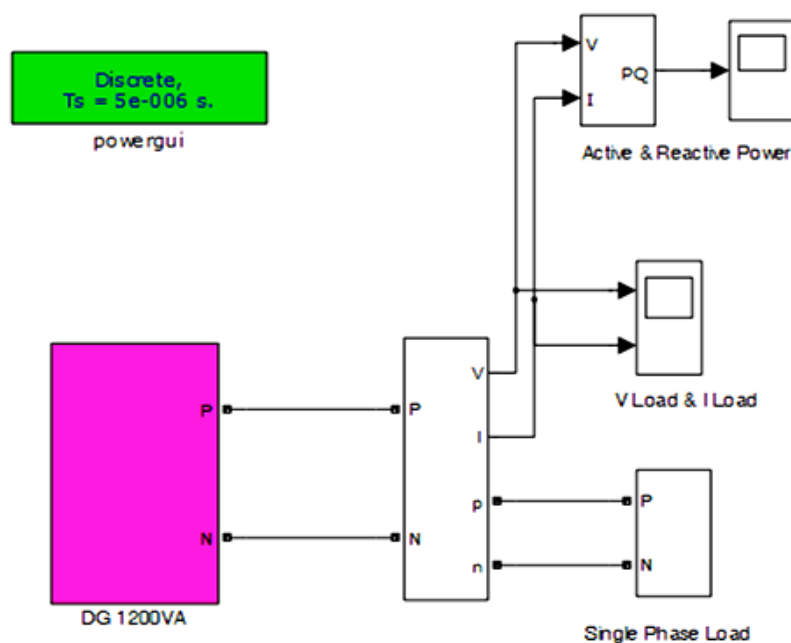


Figure 3.60 Matlab/Simulink model of diesel generator with load

The DG system takes 0.08 sec time to give steady state output as shown in Figure 3.62. Various simulation results are presented in Figure 3.61 for diesel engine speed & voltage control and Figure 3.62 shows the results of DG output voltage, current and

power. Figures 3.63 and 3.64 show the result of load voltage and current respectively. From Figures 3.63 to 3.64, it is clear that output is pure sinusoidal in nature and have a frequency of 50Hz.

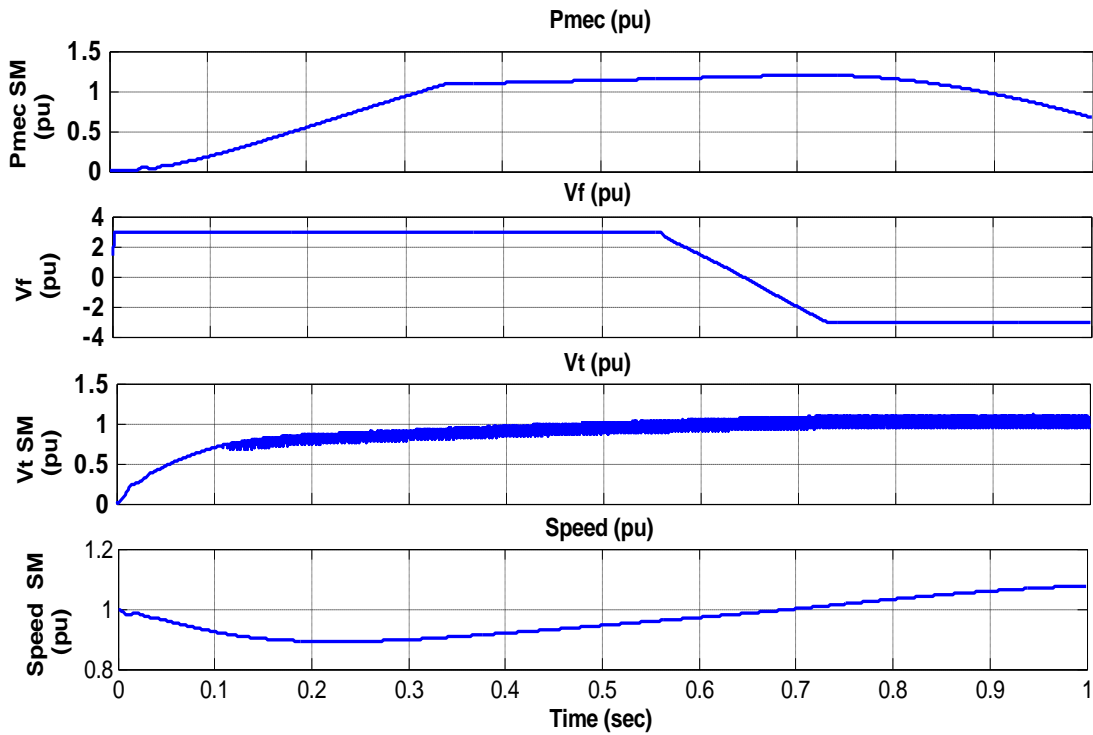


Figure 3.61 Simulated result of diesel engine speed & voltage control

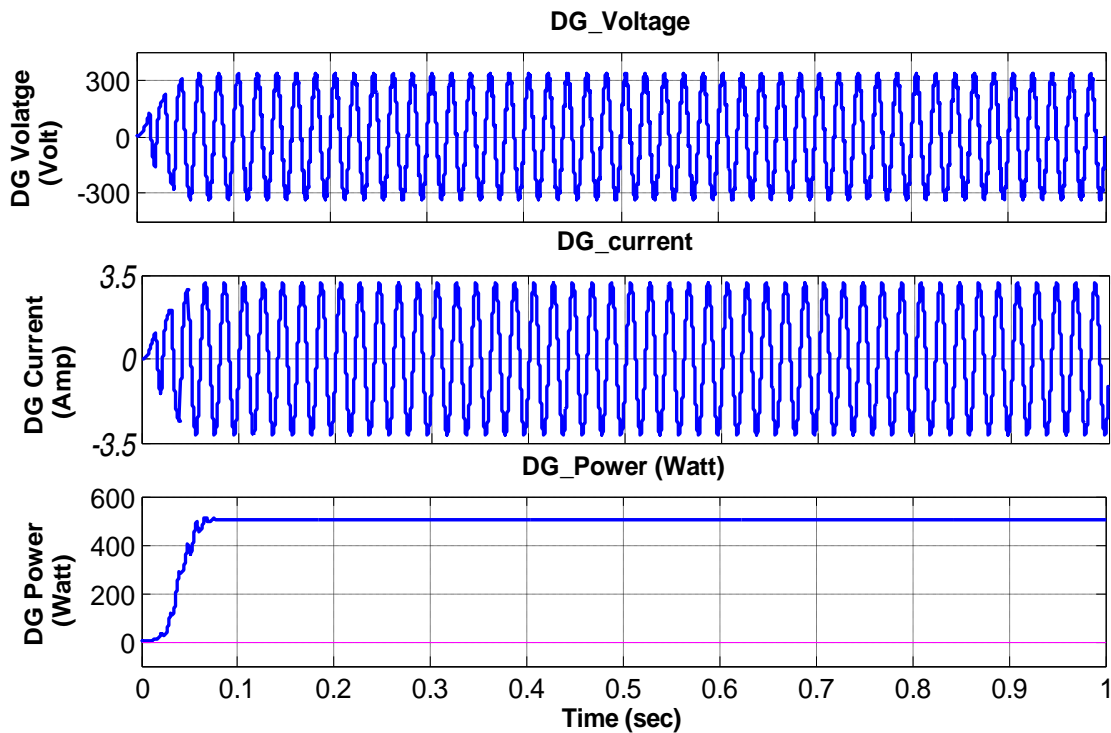


Figure 3.62 Simulated result of DG output voltage, current and power

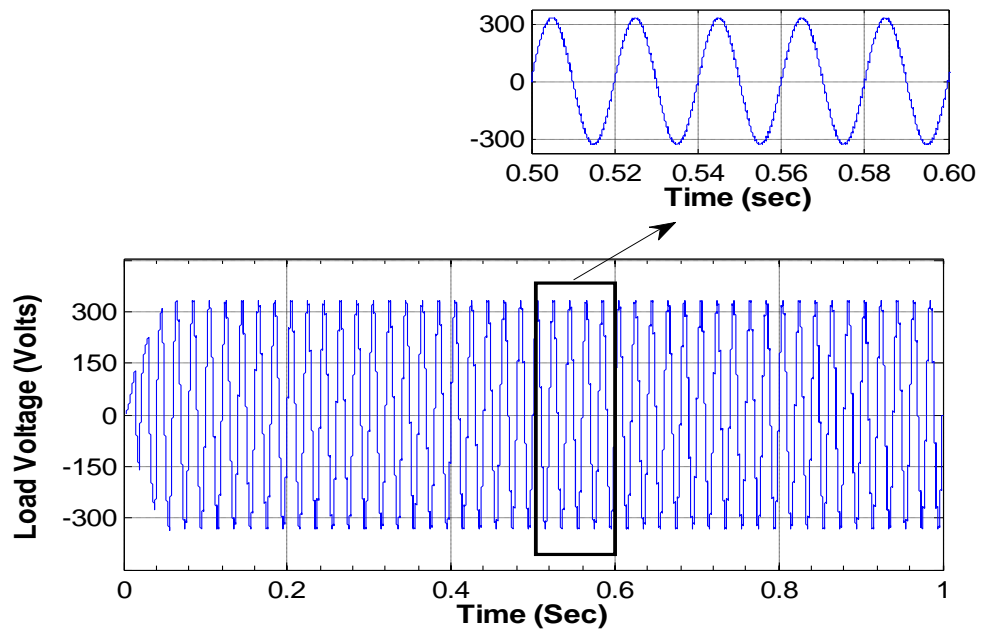


Figure 3.63 Simulated result of DG output load voltage

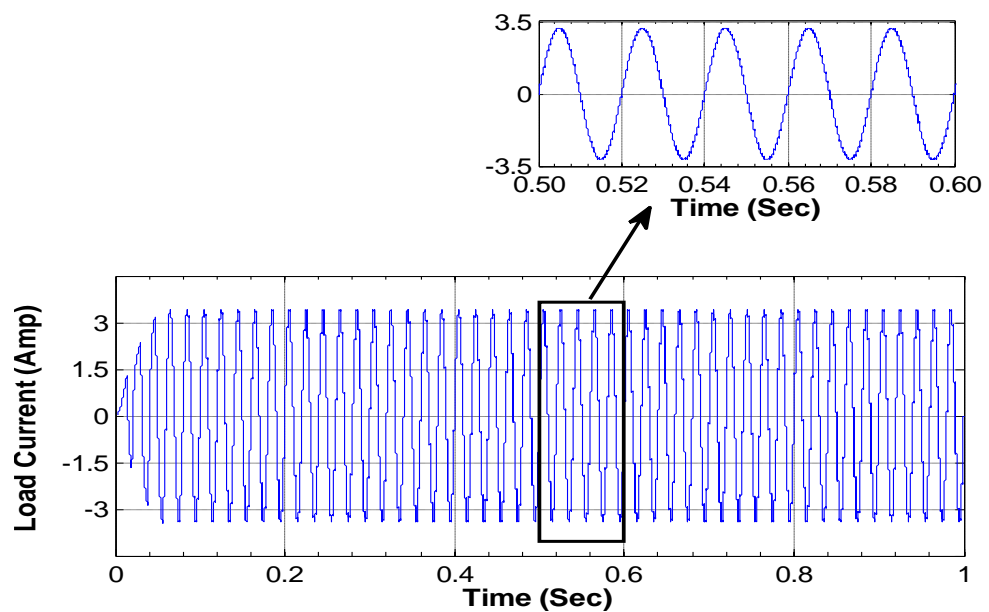


Figure 3.64 Simulated result of DG output load current

3.5 CONCLUSIONS

In this chapter, design and modeling of different components of stand-alone hybrid system have been studied. For 1 kW solar PV array, eight solar panels of 125 W each has been considered. The controlling of solar PV system, which consists of MPPT with boost converter, inverter, filter and load circuit has been designed. The load is

designed for small rural utility of a day with seasonal variations. Similarly, for wind energy conversion system, 1 kW of wind turbine and PMSG have been considered and their design and modeling is presented. The wind turbine and PMSG characteristics have been discussed for a typical day in all seasonal variations. Further the design of buck converter has been discussed and sizing of battery bank is determined to supply a typical day load. The design and modeling of 1.2 kVA diesel generator are also discussed.

Solar PV and WECS system are validated through simulation results by giving solar and wind profile. Further power sharing curve for a typical day of summer, rainy and winter seasons have been obtained for both solar PV and WECS system. From power sharing curves, it is observed that stand-alone solar PV and stand-alone WECS system both are not capable to supply the typical load demand for 24 hours in all seasons and also not able to supply increased load demand. Stand-alone DG system is also not suggested as concern of consumption of fossils fuels and environmental issues.

Hence, to supply the load demand for 24 hours in all seasons, it is required to increase the capacity of stand-alone solar PV or stand-alone WECS energy system. However, it is not viable as the capital cost increases and efficiency of overall system decreases. Higher efficiency and less consumption of fossil fuel can be achieved by a hybrid energy system with the combination of solar PV, wind, battery and DG for supplying the load demand for 24 hours in all seasons.

Modeling of Stand-alone Hybrid Systems

T HIS chapter presents Matlab/Simulink model and result of various stand-alone hybrid systems configuration like solar-wind-battery hybrid system, solar – battery - diesel generator hybrid system, wind – battery - diesel generator hybrid system and solar-wind-battery-diesel generator hybrid system.

CHAPTER 4

MODELING OF STAND-ALONE HYBRID SYSTEMS

4.1 GENERAL

As discussed in previous chapter, stand-alone solar PV-battery system and stand-alone wind-battery system are not able to fulfill the load demand of a small utility for all seasons. Further, it is also observed that if load demand changes beyond the load profile assumed than it is not able to be supplied from the stand-alone solar PV system and stand-alone wind system. So, to supply the load demand continuously, it is necessary to increase the size of the system which yields higher capital cost and lower efficiency.

Another way for finding uninterruptable power supply is a hybrid system, in which two or more than two energy sources are used, to supply the load of remote or rural area in stand-alone power generation mode, where grid connection is almost impossible in terms of cost and geography.

Stand-alone hybrid system can be categorized in the following hybrid systems having combination of solar, wind, battery and the diesel generator:

- (a) Solar-wind-battery hybrid system
- (b) Solar-battery-diesel generator hybrid system
- (c) Wind-battery-diesel generator hybrid system
- (d) Solar-wind-battery-diesel generator hybrid system

Here, all the four cases are simulated using Matlab/Simulink models. Simulated results are discussed in this chapter. A comparative study is also presented for four cases to show the use of renewable sources for a given load profile, solar irradiation and wind speed profile for a small utility at village Kukas, Jaipur, India.

In this chapter, a stand-alone hybrid system for rural or remote area is designed for electrification. In this system solar PV and wind are connected as primary renewable energy sources while a lead-acid battery bank and a diesel generator are connected as storage device and backup source respectively.

4.2 DESIGN AND SIMULATION OF STAND-ALONE SOLAR-WIND-BATTERY HYBRID SYSTEM

A typical block diagram of proposed stand-alone solar-wind-battery hybrid system is shown in Figure 4.1. Figure 4.2 shows the schematic diagram of proposed stand-alone solar-wind-battery hybrid system with proper connection of various components such as solar PV with boost converter and MPPT, wind generator with buck converter, DC link, battery bank, VSI inverter with filter and a step-up transformer and the load sub system. Each part has also been discussed in chapter 3. Figure 4.3 shows the developed Matlab/Simulink model of proposed system.

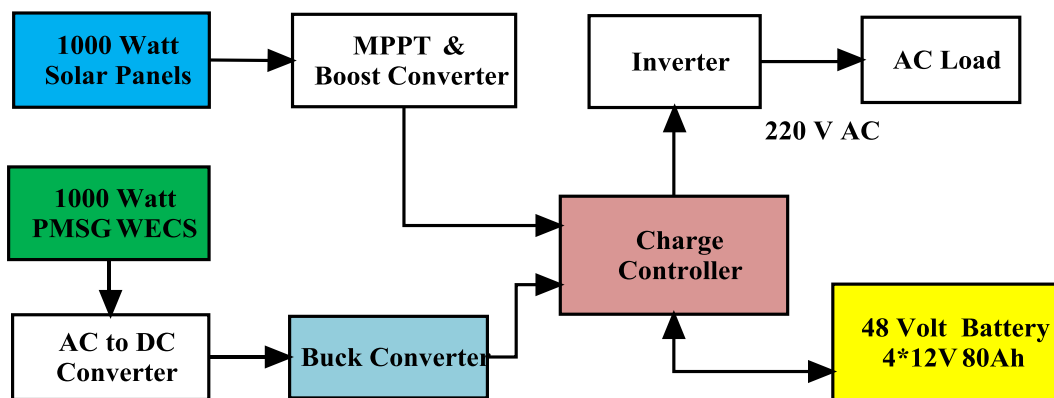


Figure 4.1 Block diagram of stand-alone solar-wind-battery hybrid system

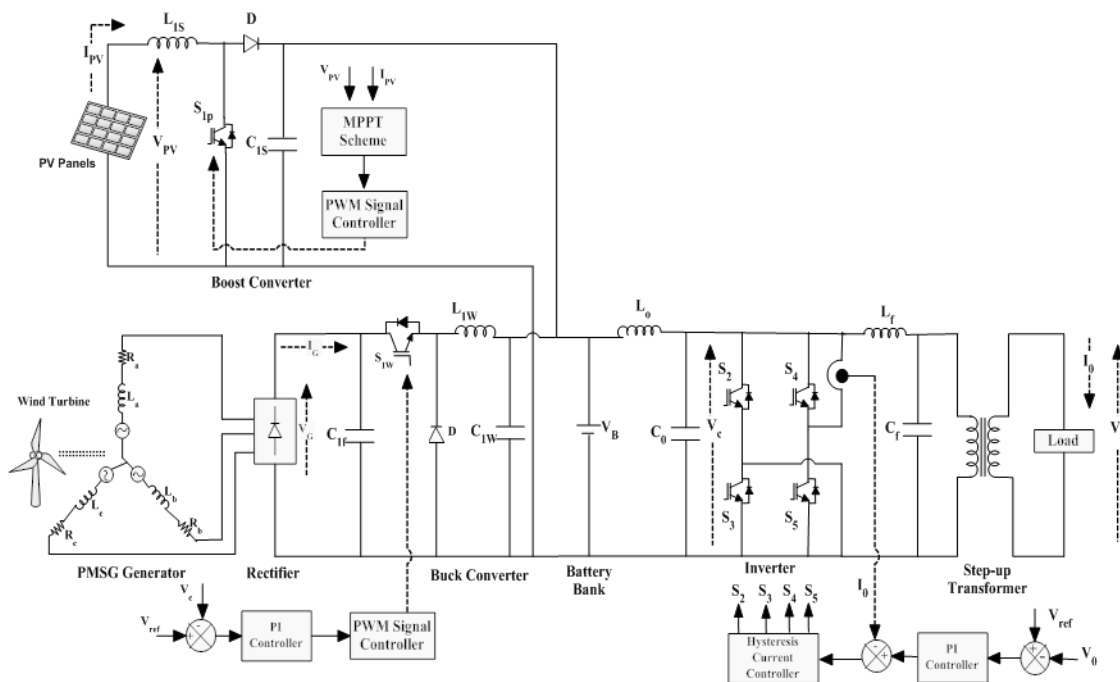


Figure 4.2 Schematic diagram of proposed stand-alone solar-wind-battery hybrid system

In this hybrid system, solar PV is generating electrical energy at a voltage ranging from 16 V-36 V according to the solar irradiation; this voltage is fed to the inverter circuit through a DC link as shown in Figure 4.2. After that, this energy is fed to the load through step-up transformer. Since, the wind generator generates variable frequency output; therefore it is first converted into filtered DC, than it is step down to 53 V before feeding to same DC link where solar system is also connected as shown in Figure 4.2. A battery bank is also connected before DC link, as shown in Figure 4.2, which absorbs the power variation of the load and solar PV power, *i.e.* surplus power is to be stored in the battery during low load and this is supplied to the load in the absence of solar PV power.

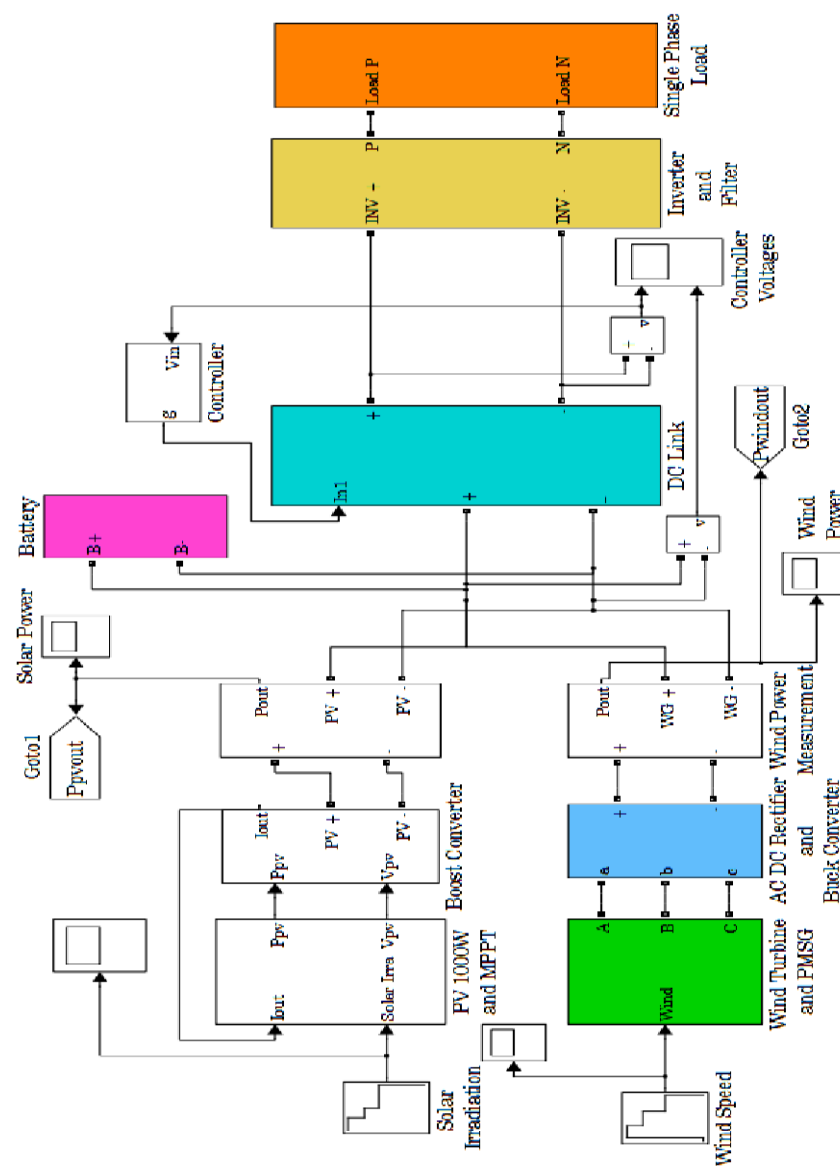
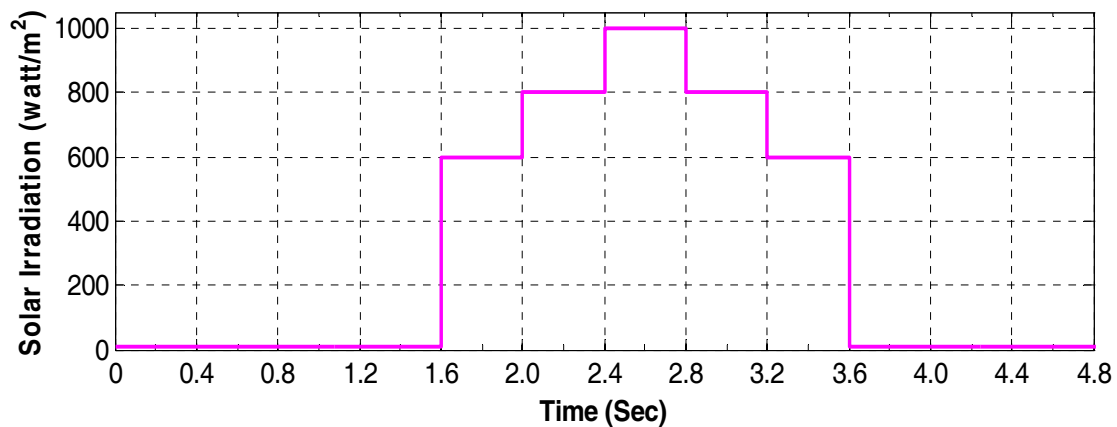


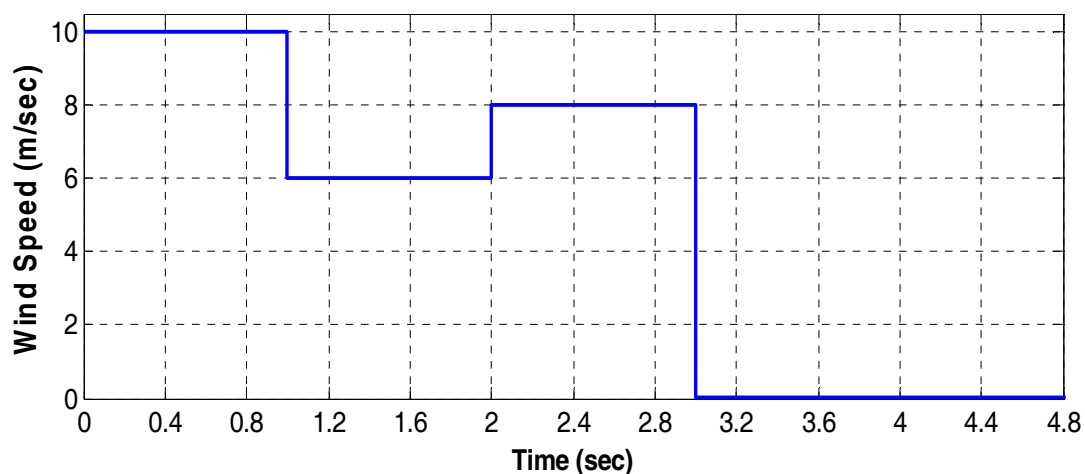
Figure 4.3 Matlab/Simulink model of proposed stand-alone solar-wind-battery hybrid system

In the above hybrid system, if solar not available than wind supplies the load and vice versa, and if both are not available than battery bank is used to supply the load. So, the system as discussed above is more capable to supply the load as compared to stand-alone solar PV-battery system or stand-alone wind-battery system. However, in this type of system, supply of the load depends on the amount of energy stored in the battery in the absence of primary renewable energy. So, it is clear that if the battery bank is not having sufficient stored energy, than load will not be supplied in such cases. Hence, this hybrid system is viable in such areas where wind is available in sufficient duration where as solar is available only for day time *i.e.* 8-10 hours.

For the system testing, solar input profile and wind speed profile are created as shown in Figure 4.4 (a) and (b) respectively.



(a)



(b)

Figure 4.4 (a) Solar irradiation profile, (b) Wind speed profile

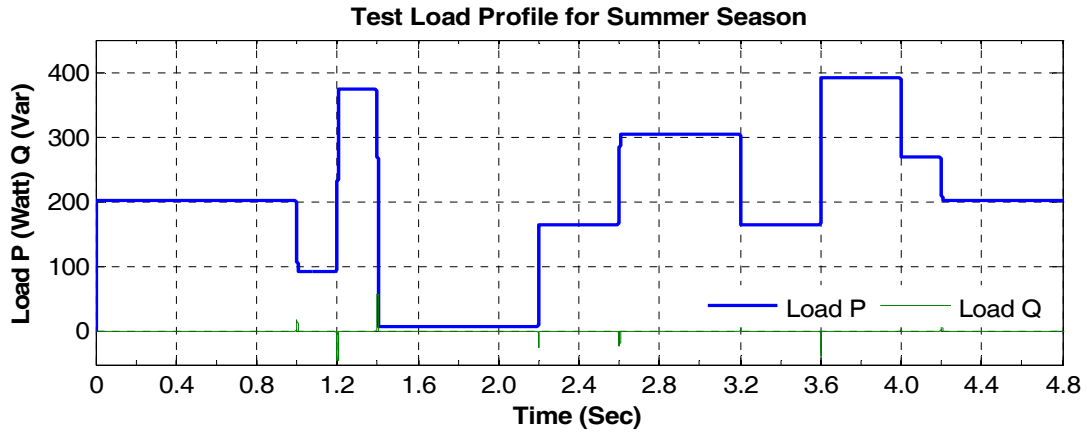
At time duration 0 sec - 1.6 sec and 3.6 sec - 4.8 sec the solar irradiation are 0 watt/m², however during 1.6 sec - 2.0 sec the solar irradiation is 600 watt/m² as shown in Figure 4.4(a). During 2.0 sec - 2.4 sec, the solar irradiation is 800 watt/m² after that it increases up to 1000 watt/m² till 2.8 sec and after that it reduces in sub sequential manner to 0 watt/m² at 3.6 sec.

In the wind speed profile, wind speed variations are taken as 10 m/sec in the duration of 0 sec - 1 sec, 6 m/sec in the duration of 1 sec - 2 sec, 8 m/sec till 3 sec and then it reduces to zero from 3 sec - 5 sec *i.e.* no wind condition is created as shown in Figure 4.4 (b).

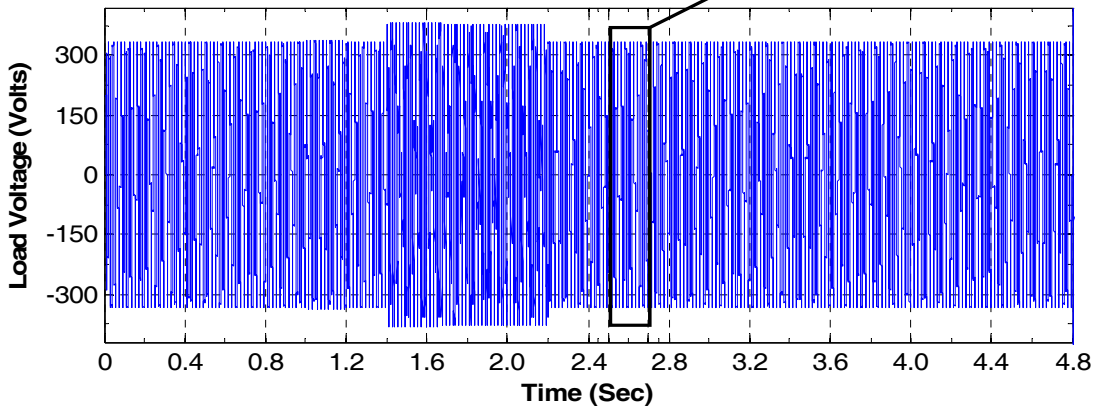
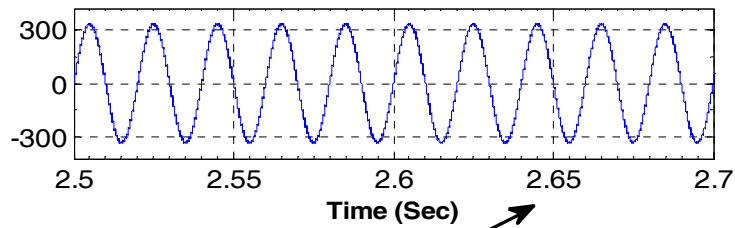
A test summer load profile as shown in Figure 4.5 (a) is considered for simulation purpose. Here, system is simulated for a time period of 4.8 sec. Figures 4.5 (b) and (c) show the variation of load voltage and load current respectively according to the load variations. After 3.0 sec, as shown in Figure 4.4, the wind power is not available and less solar power is available as compared to load requirement. The load is supplied by the battery and it is to be continued till the battery stored energy as shown in Figure 4.5.

Figure 4.6 shows the battery voltage and current variation during simulation period (*i.e.* 0 sec - 4.8 sec time duration), where negative current shows the battery charging condition and positive current shows the battery discharging condition through the load.

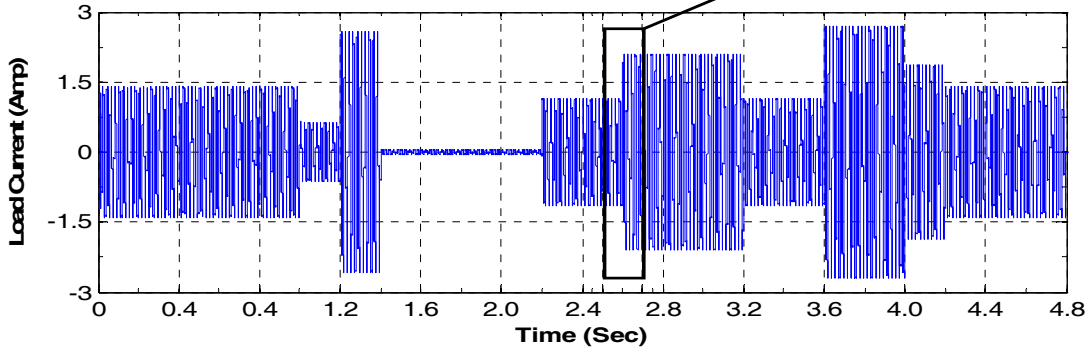
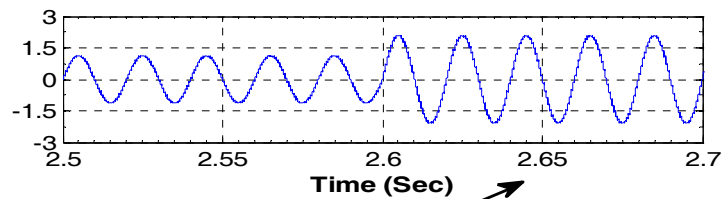
Figures 4.7(a) and (b) show the output voltage and current of the inverter respectively. At 3.6 sec, as shown in Figure 4.4, as solar and wind power are zero, but the inverter current is not zero, as the load is supplied by the battery. From Figure 4.7, it is observed that at time 2.6 sec, when the load is suddenly increased the corresponding inverter current is also increased. From Figure 4.7, the variation in the load voltage is also observed during 1.4 sec - 2.2 sec time duration, as the load is very low (8 W) during this time period as shown in Figure 4.5 (a).



(a) Typical - load variation

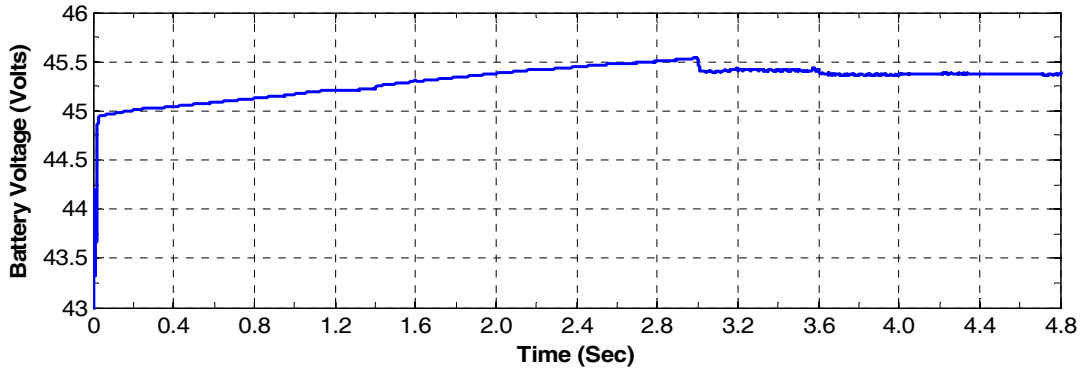


(b) Variation of load voltage

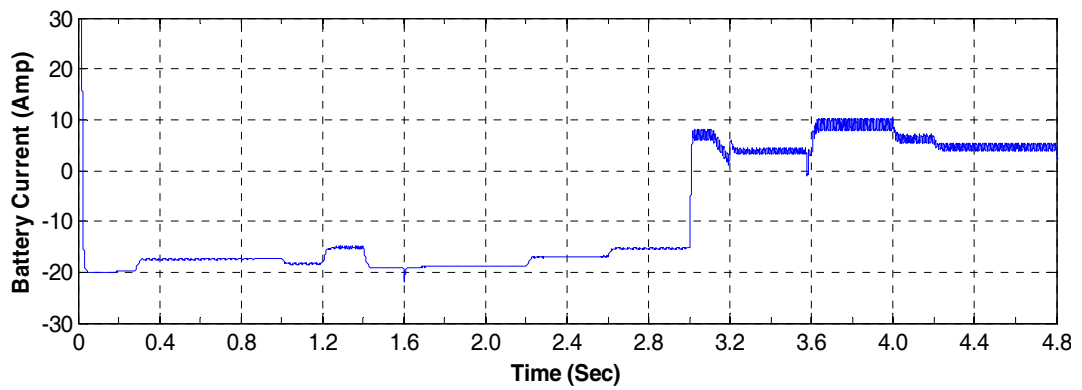


(c) Variation of load current

Figure 4.5 Load profile of stand-alone solar-wind-battery hybrid system

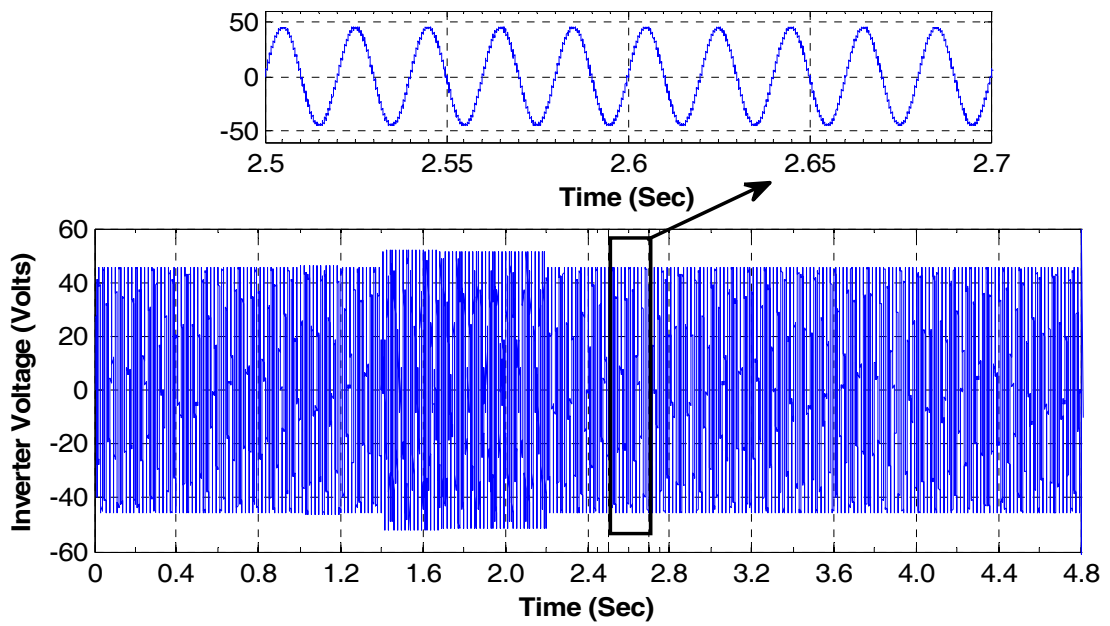


(a) Battery voltage



(b) Battery current

Figure 4.6 Battery output of stand-alone solar-wind-battery hybrid system



(a) Inverter voltage

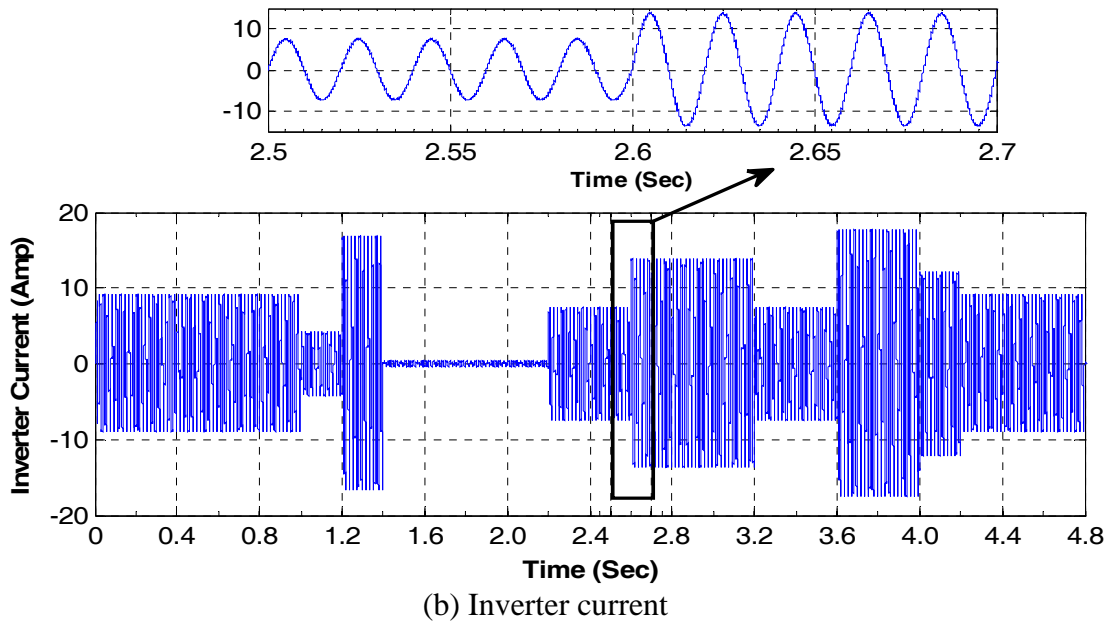


Figure 4.7 Inverter output of stand-alone solar-wind-battery hybrid system

Figures 4.8 to 4.10 show the power sharing curve of solar, wind, battery and load power for a typical summer, rainy and winter days as per the solar and wind profile as shown in Figure 3.26 and Figure 3.38 respectively.

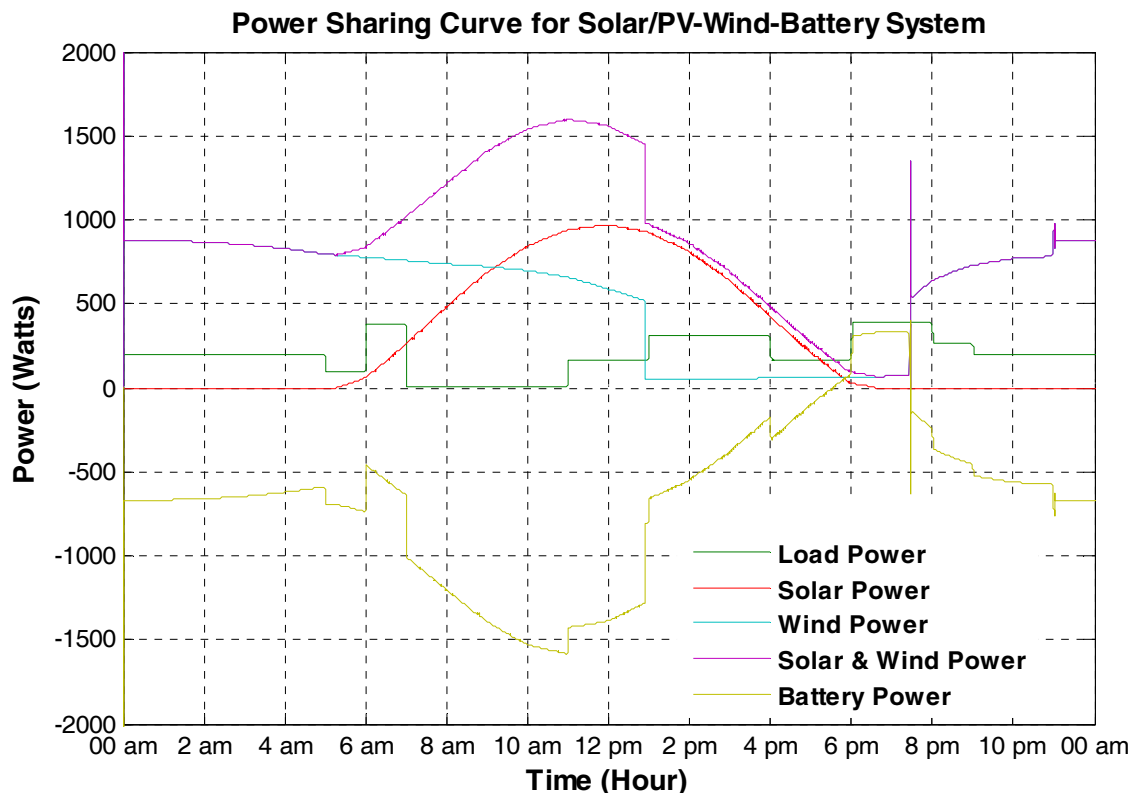


Figure 4.8 Power sharing curve for a summer day for stand-alone solar-wind-battery system

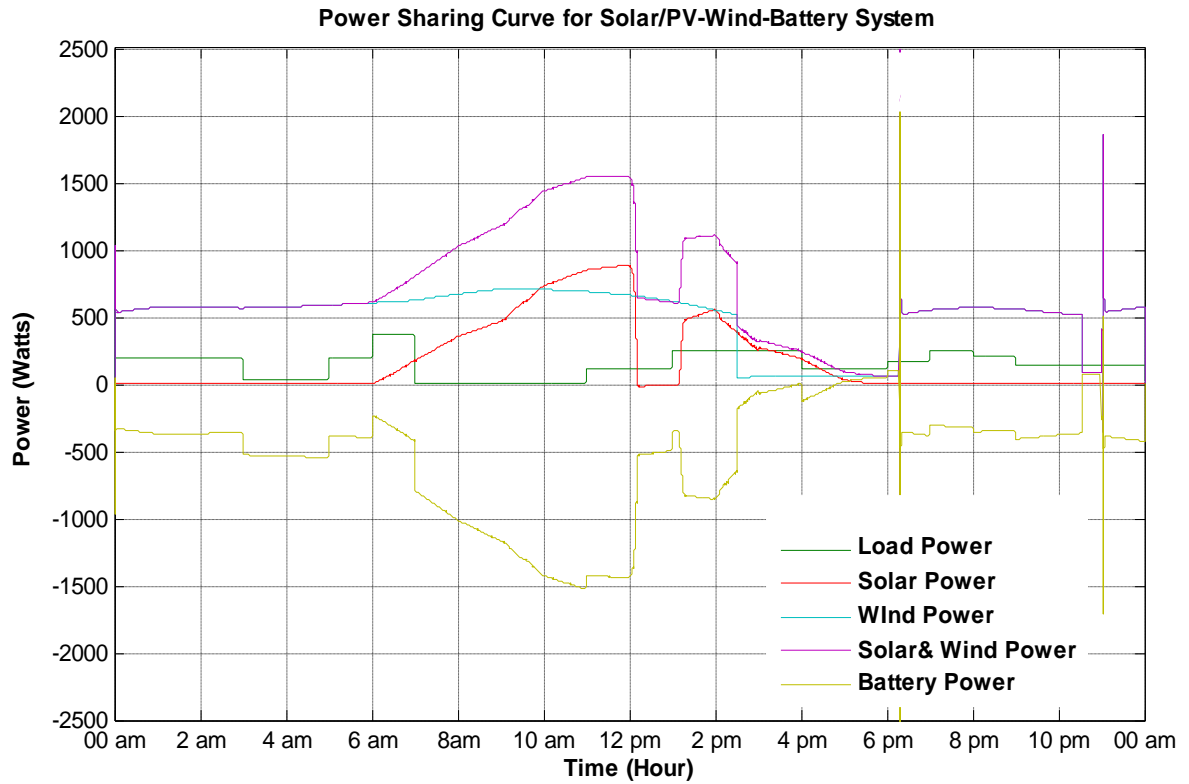


Figure 4.9 Power sharing curve for a rainy day for stand-alone solar-wind-battery system

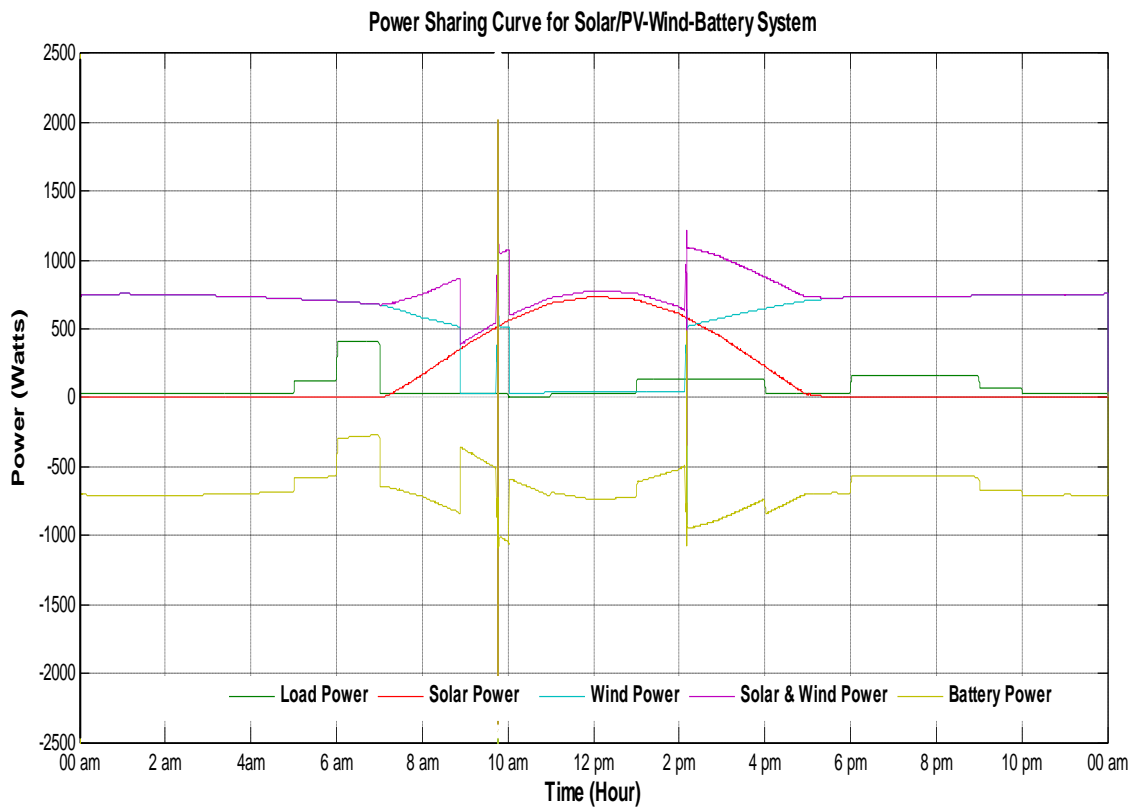


Figure 4.10 Power sharing curve for a winter day for stand-alone solar-wind-battery system

Thus, from these results, it can be observed easily that the given solar-wind-battery hybrid system is capable to supply load power if continuous wind power is available. In previous chapter, the performance of the stand-alone solar-battery system and the stand-alone wind-battery system has been analyzed and both are incapable to supply the load demand especially in rainy and winter seasons. Moreover, the stand-alone solar-wind-battery hybrid system is not capable to supply the increased load *i.e.* if demand is increased from the typical load profile.

4.3 DESIGN AND SIMULATION OF STAND-ALONE SOLAR-BATTERY-DIESEL GENERATOR HYBRID SYSTEM

As discussed in previous section, the stand-alone solar-wind-battery hybrid system is capable to supply the load power if and only if continuous wind power is available in rainy and winter season, whereas in summer season, due to sufficient solar irradiation, it might be capable to supply the load, even if the wind is not available if there is no occurrence of any significant change in the load demand. So, to supply the varying load demand, another configuration of hybrid system as shown in Figure 4.11 is designed, which uses solar PV power, a battery bank and a diesel generator as renewable source, storage device and backup source respectively.

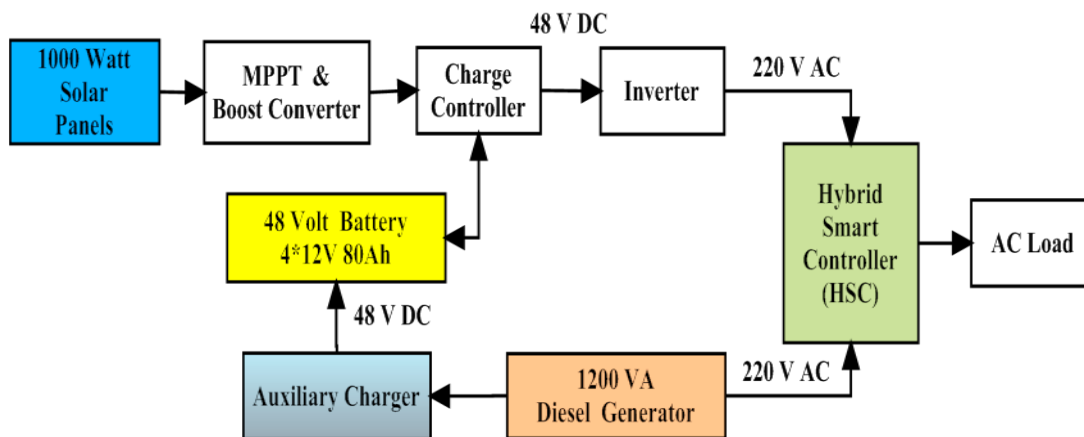


Figure 4.11 Block diagram of proposed stand-alone solar-battery-diesel generator hybrid system

Figure 4.12 shows the schematic diagram with proper connection of all the components such as solar PV with MPPT technique and DC-DC boost converter, DC link, a battery bank, a VSI inverter with the filter and the step-up transformer, a diesel generator, auxiliary charger circuit for battery and the load sub system. A hybrid smart

controller (HSC) and auxiliary charger are also introduced to control the diesel generator operation with solar PV system to supply the load without interruption and to charge the battery bank with excess DG power.

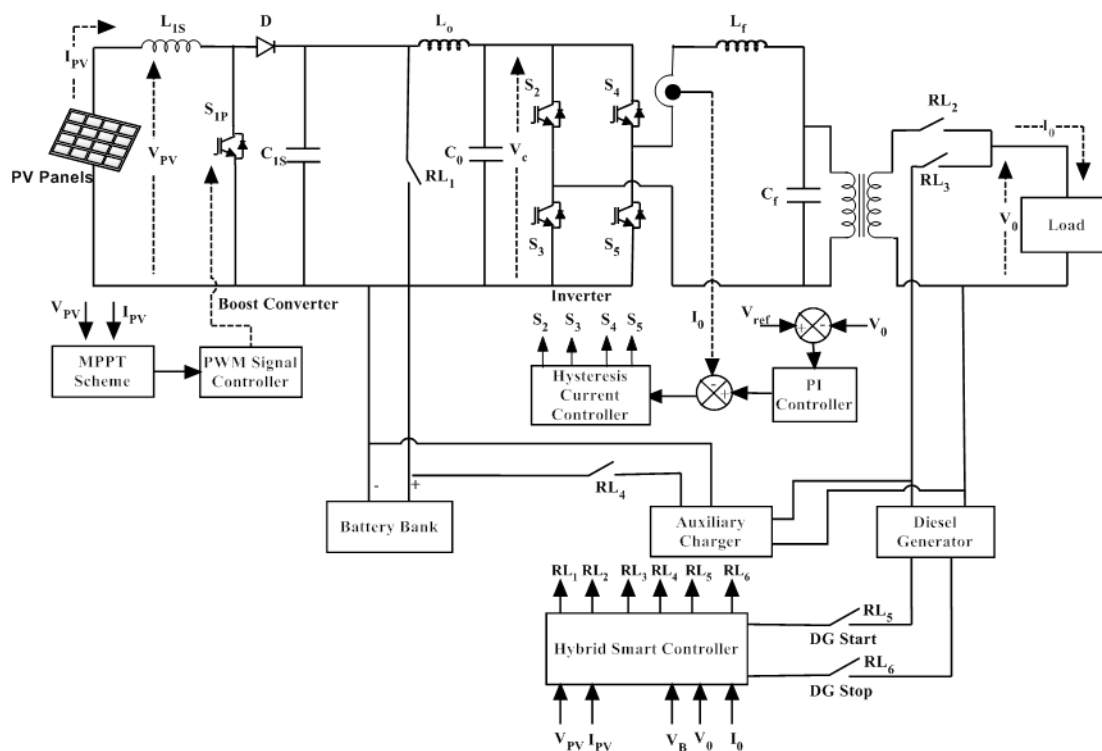


Figure 4.12 Schematic diagram of proposed stand-alone solar-battery-diesel generator hybrid system

The working of solar PV system is already explained in chapter 3, although some modifications have been made at load side and battery side, such as four relays are introduced in the main circuit, RL_1 and RL_4 are put in battery side, and similarly RL_2 and RL_3 are put at load side for smooth operation of the proposed system as shown in Figure 4.12. Two more relays RL_5 and RL_6 are also introduced for DG start and stop circuit, to start and stop the diesel generator.

An auxiliary charger, which consists of an AC-DC rectifier and a filter, is designed to charge the battery bank at a voltage level of 53 V. It charges the battery bank also, when DG is required to be ON while load demand is less. At this condition, the excess power of DG is utilized to charge the battery bank to improve the efficiency of DG operation in the proposed system. The algorithm of the HSC working is shown in Figure 4.13. Initially, RL_1 and RL_2 are kept in ON condition *i.e.* load is connected to solar- battery system through inverter and transformer.

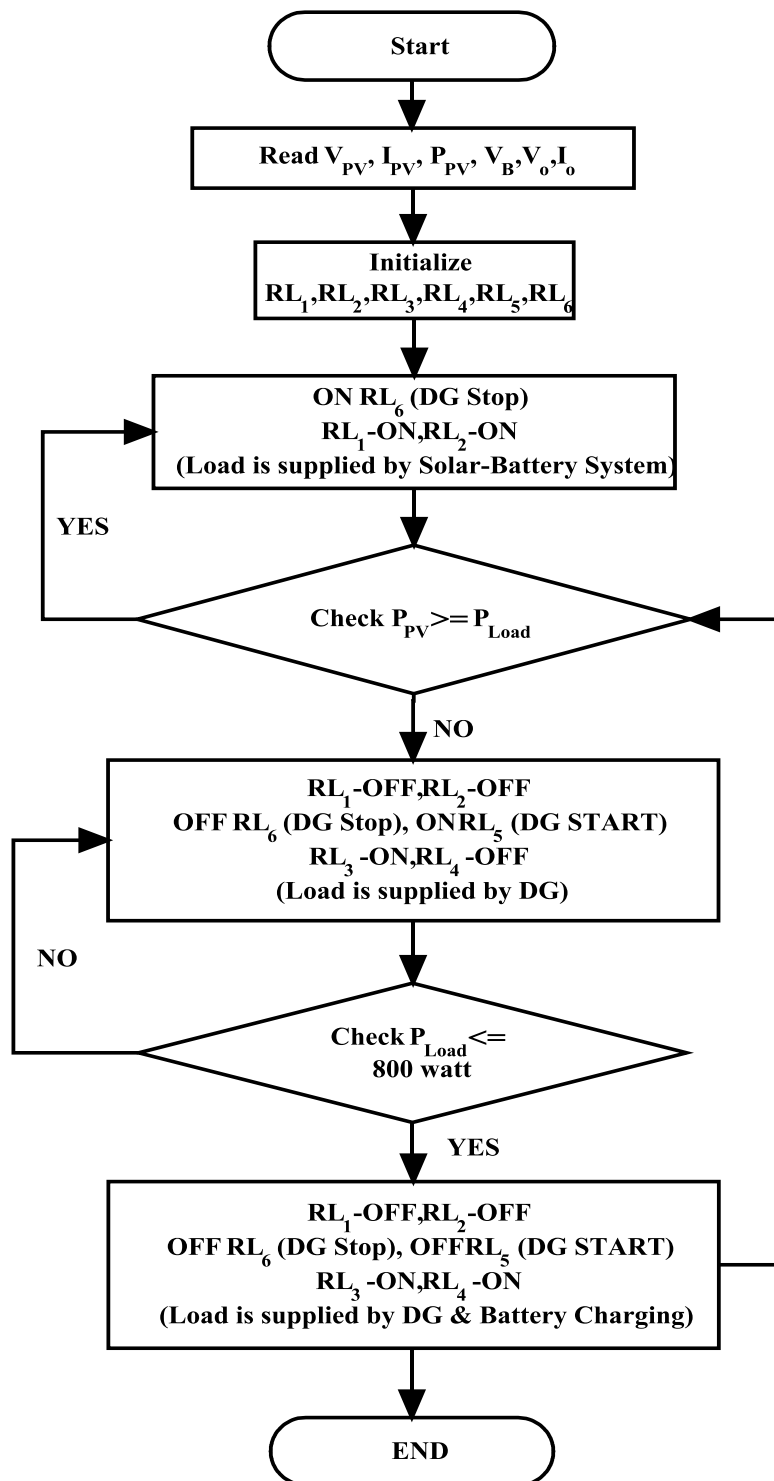


Figure 4.13 Algorithm of the HSC for stand-alone solar-battery-diesel generator hybrid system

At the same time, HSC is measuring the available power from solar and battery and comparing it with power requirement from load side. Firstly, load will be supplied by solar power plus battery power and if both powers are not sufficient than it will take a decision to start DG. Before starting the DG, RL_1 and RL_2 will be OFF and RL_3 and

RL_4 is to be in ON condition, after that RL_5 is made ON and DG starts circuit that is powered by a 12 V battery starts the DG. At the same time, an auxiliary charger circuit starts to charge the battery with the excess power available with DG after supplying the load. Figure 4.14 shows the developed Matlab/Simulink model of proposed stand-alone solar-battery-diesel generator hybrid system.

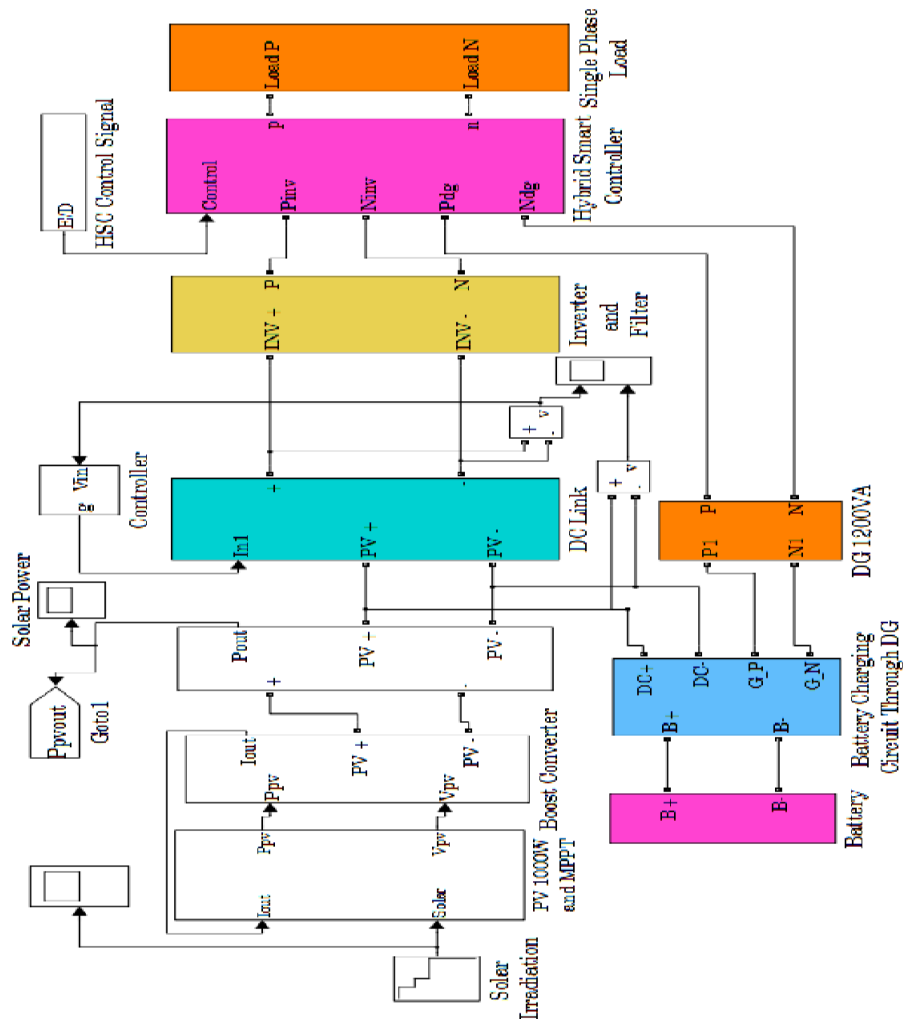


Figure 4.14 Matlab/Simulink model of proposed stand-alone solar-battery-diesel generator hybrid system

Figure 4.15 shows the solar irradiation profile, which is taken as input to the solar PV system for simulation purpose. At time duration 0 sec - 1.6 sec and 3.6 sec - 4.8 sec the solar irradiation are 0 watt/m², however during 1.6 sec - 2.0 sec the solar irradiation is 600 watt/m² as shown in Figure 4.4 (a). During 2.0 sec - 2.4 sec the solar irradiation is 800 watt/m² after that it increases up to 1000 watt/m² till 2.8 sec and after that it reduces in sub sequential manner to 0 watt/m² at 3.6 sec.

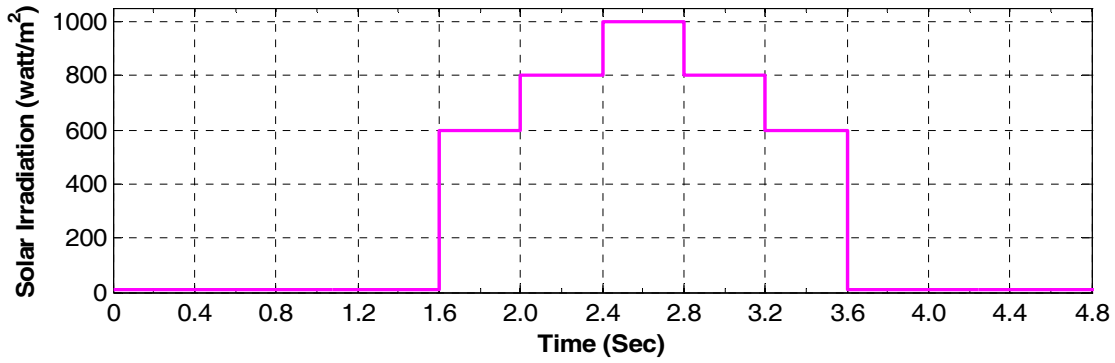
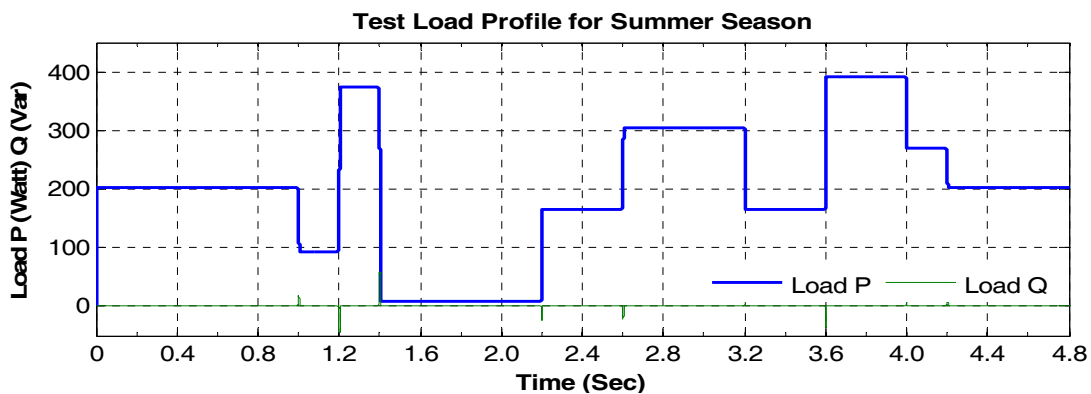
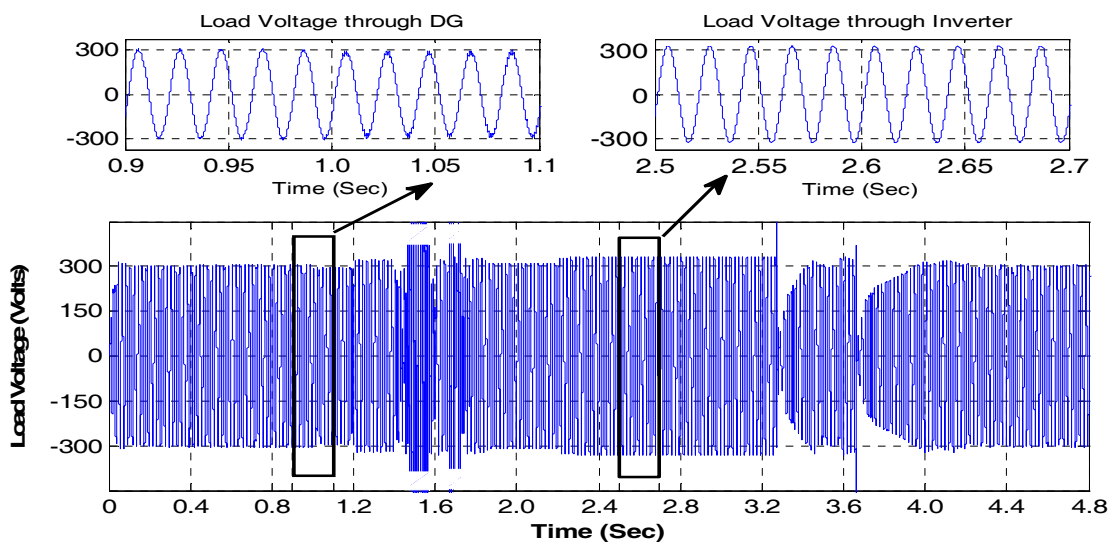


Figure 4.15 Solar irradiation profile

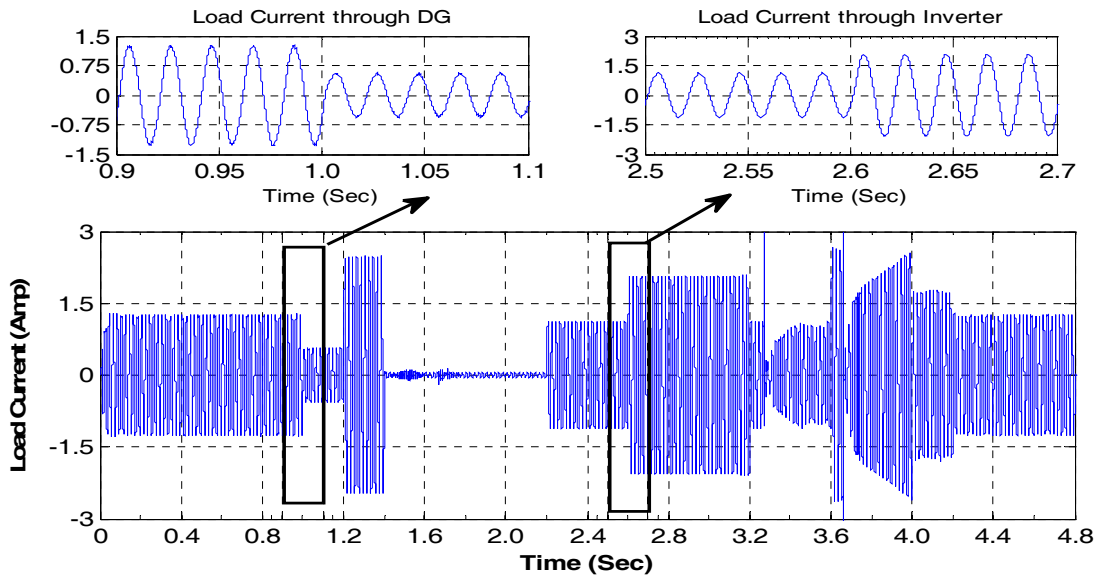
Further the summer load profile considered for the solar-battery-diesel hybrid system with variation in load voltage and load current is shown in Figure 4.16. Figure 4.16(a) shows the test load profile pattern for a summer day for analyses purpose, which follows the similar pattern as shown in Figure 2.6., Figure 4.16(b) represents the variation in load voltage and Figure 4.16(c) represents the variation in load current of the considered hybrid system.



(a) Typical load variation

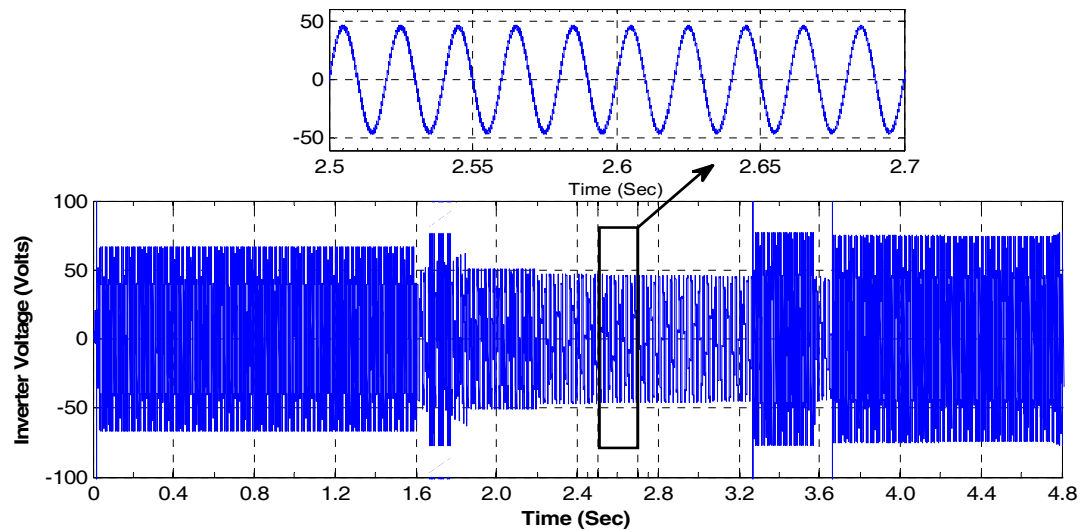


(b) Variation of load voltage

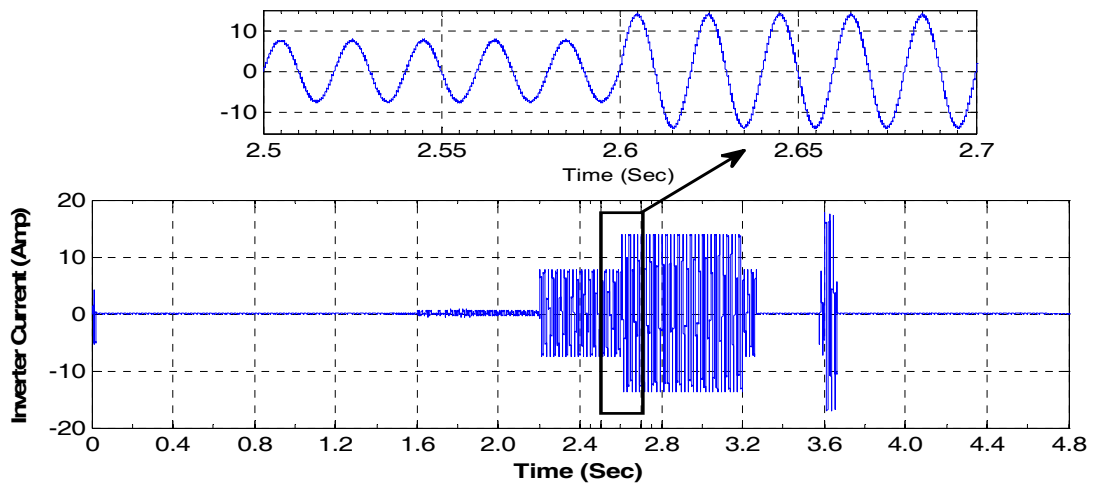


(c) Variation of load current

Figure 4.16 Load profile of stand-alone solar-battery-diesel generator hybrid system



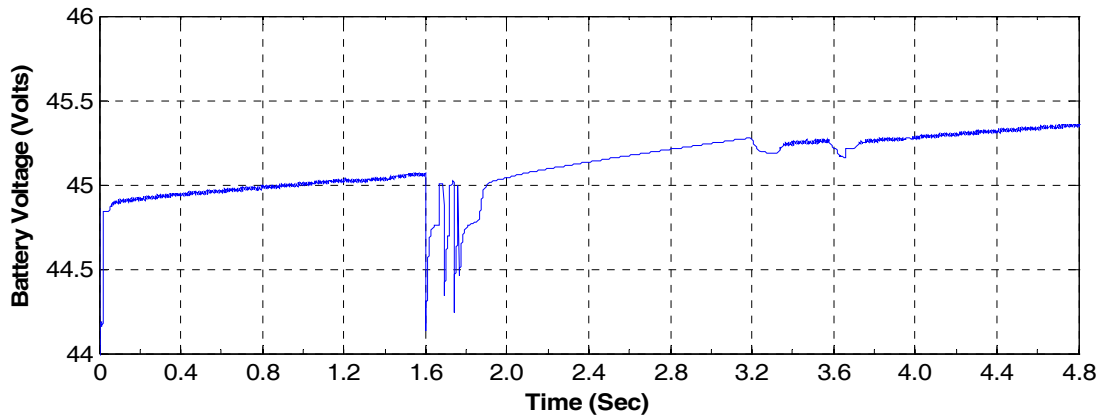
(a) Inverter voltage



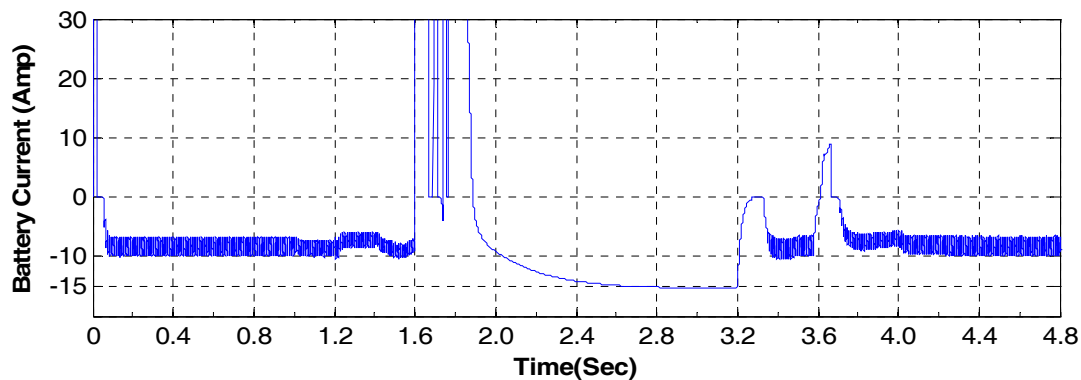
(b) Inverter current

Figure 4.17 Inverter output of stand-alone solar-battery-diesel generator hybrid system

Similarly, Figure 4.17(a) and Figure 4.17(b) represent the inverter output voltage and current of solar-battery-diesel generator hybrid system respectively. The battery output voltage and current of solar-battery-diesel generator hybrid system are shown in Figure 4.18 (a) and Figure 4.18 (b) respectively.



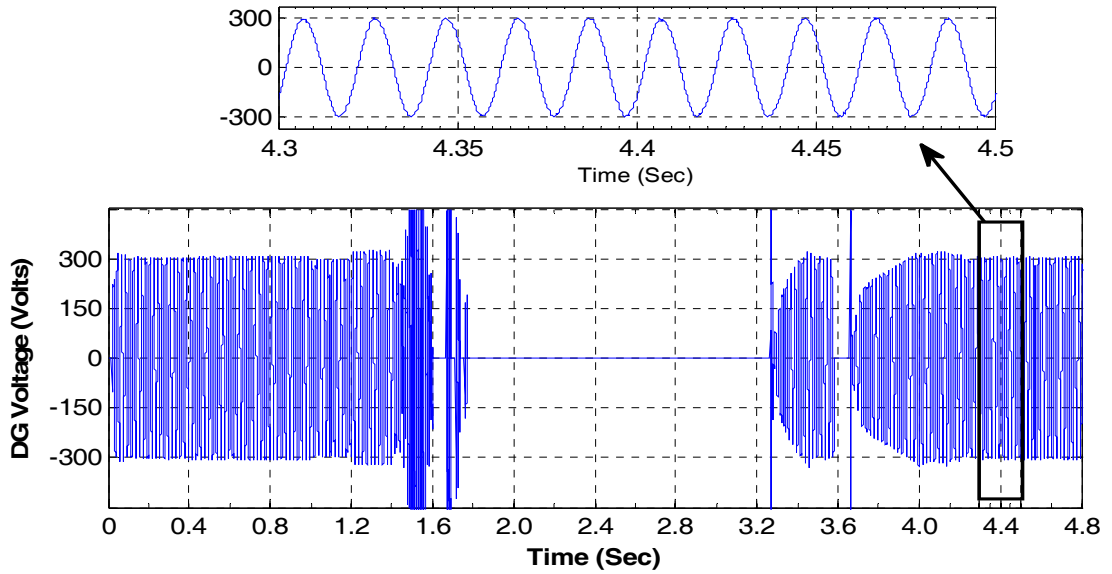
(a) Battery voltage



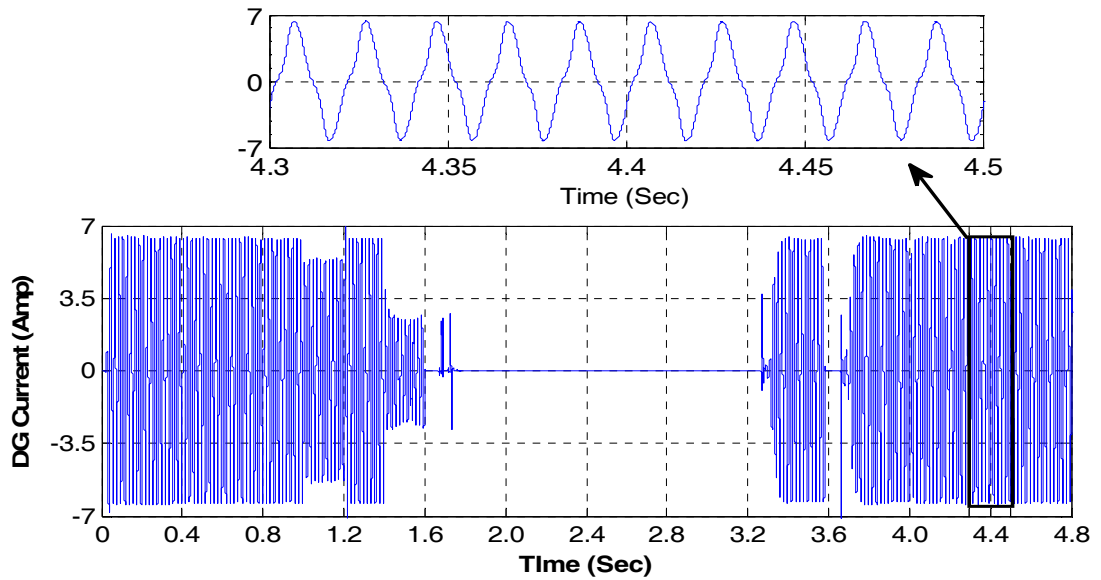
(b) Battery current

Figure 4.18 Battery output of stand-alone solar-battery-diesel generator hybrid system

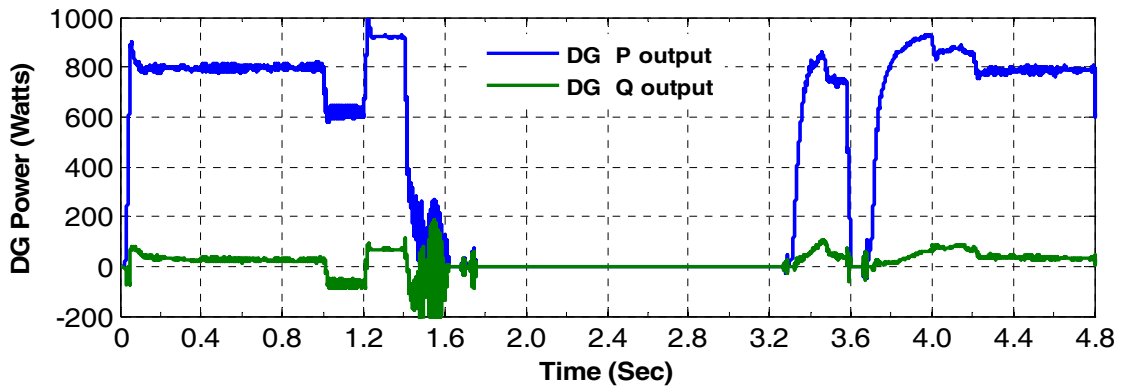
The inverter supplies the power to the load during 1.8 sec to 3.2 sec only as shown in Figure 4.17, due to availability of solar power in the duration of 1.6 sec to 3.6 sec as shown in Figure 4.15. The rest demand of the load during 0 sec to 1.6 sec and 3.2 sec to 4.8 sec is supplied by the DG as shown in Figure 4.19. At 1.6 sec as shown in Figure 4.15, HSC has observed the solar power availability. Now HSC gives a signal to relay RL_6 to stop DG. It takes around 0.2 sec to stop DG and switches the system on an inverter circuit. The variation of DG voltage and current is shown in Figure 4.19 (a) and (b) respectively. Similarly, after 3.2 sec due to less solar power availability and higher load demand, HSC gives a signal to relay RL_5 to start DG and it takes around 0.4 sec to reach steady state condition. Corresponding variation in DG voltage and current are shown in Figure 4.19 (a) and (b) respectively.



(a) DG voltage



(b) DG current



(c) DG power

Figure 4.19 DG output of stand-alone solar-battery-diesel generator hybrid system

From Figure 4.19 (c), it is observed that DG power that consists both active and reactive power is utilized when the solar power is not available to supply the load and to charge the battery bank during its running period through an auxiliary charger. The charging current of a battery bank through DG is limited to maximum of 10 A as the maximum load demand is 400 W and DG power is 1200 VA. Corresponding charging of battery bank is shown in Figure 4.18 (b). However, at 1.6 sec, abnormal variations in battery voltage and current are observed as shown in Figure 4.18. This variation is due to the switching operation of relays and DG (*i.e.* ON to OFF) and it takes around 0.2 - 0.3 sec in this process.

In this simulation, initial battery charging condition is considered as 25% to show the charging of the battery bank. It is able to supply the load after charging of 80% either through solar or DG. When the battery bank is supplying the load in the absence of solar, DG is not able to start till the battery discharges at the level of 30% charge, this leads to the increased life cycle of the battery bank.

As the ON time of DG power in the solar-battery-diesel generator hybrid system is more which is not economical. However the load demand is completely fulfilled by this system. Hence, this hybrid system can't be suggested for economical and environmental point of view for stand-alone operation.

4.4 DESIGN AND SIMULATION OF STAND-ALONE WIND-BATTERY-DIESEL GENERATOR HYBRID SYSTEM

As discussed in previous sections, a stand-alone solar-wind-battery hybrid system is capable to supply the load if continuous solar and wind power are available in rainy and winter season, whereas in summer season the same system may be capable to supply the load if load profile is as per Figure 2.6(a). Likewise, in stand-alone solar-battery-diesel hybrid system, as solar profile is not available for whole day, the load demand is to be supplied by the DG in absence of solar power. This results in overall increased operating cost of system. Hence, for supplying the varying load demand, another configuration of hybrid system is designed which includes wind power as renewable source, a battery as storage device and a diesel generator as backup source.

A typical block diagram of stand-alone wind-battery-diesel generator hybrid system is shown in Figure 4.20. Figure 4.21 shows the schematic connection diagram of the above system with proper connection of components such as wind power source with buck converter, DC link, a battery bank, VSI inverter with the filter and step-up transformer, a diesel generator, an auxiliary charger circuit for battery and load sub system etc.

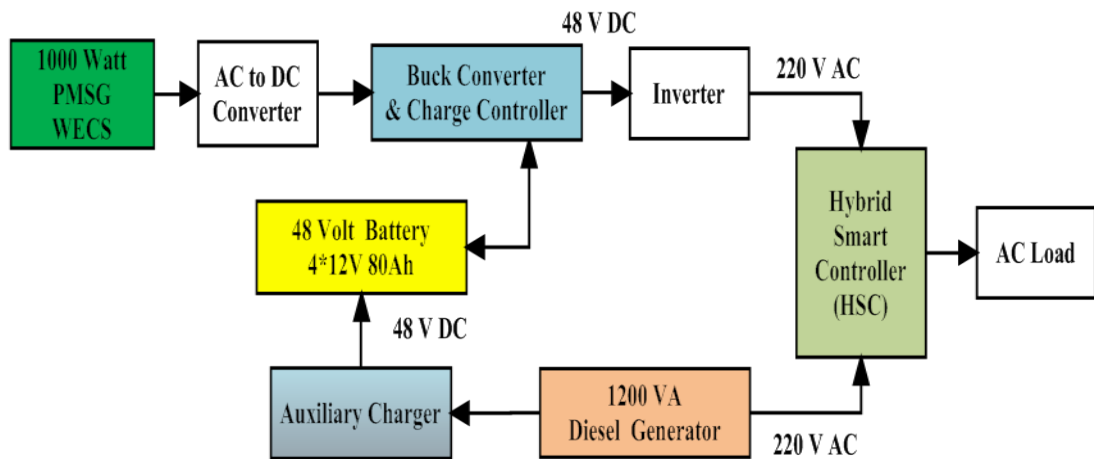


Figure 4.20 Block diagram of stand-alone wind-battery-diesel generator hybrid system

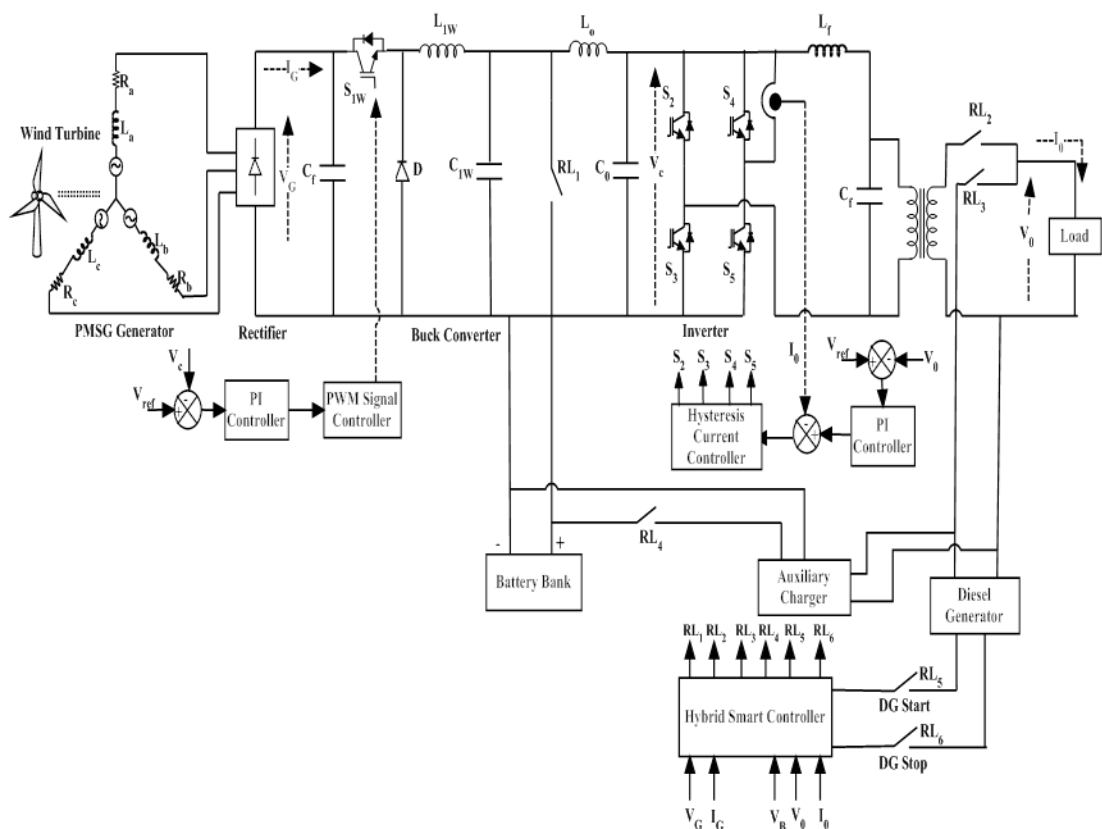


Figure 4.21 Schematic diagram of proposed stand-alone wind-battery-diesel generator hybrid system

A hybrid smart controller (HSC) and auxiliary charger are also introduced to control the diesel generator operation with wind energy system, to supply the load without interruption and to charge the battery bank with excess DG power.

The working of wind energy conversion system (WECS) as explained in chapter 3, has introduced some more modifications at load side and battery side, such as four relays *i.e.* RL_1 and RL_4 in battery side, and RL_2 and RL_3 at load side as shown in Figure 4.21 for optimum utility of battery and DG. Two more relays RL_5 and RL_6 are also introduced for DG start and stop circuit, to start and stop the diesel generator.

As discussed in previous section, an auxiliary charging circuit with an AC-DC rectifier and a filter is designed to charge battery at a voltage level of 53 V. The battery bank is to be charged, while DG in operation and supplying the load less than full load. Hence, DG power is utilized optimally. For coordination of all relays and proper working of the system a hybrid smart controller (HSC) has been introduced.

Initially, RL_1 and RL_2 are kept in ON condition *i.e.* load is connected to wind-battery system through a step-up transformer and inverter. At the same time, HSC is measuring the available power from wind and battery and compare it with power requirement from load side. The HSC algorithm is shown in Figure 4.22 for stand-alone wind-battery-DG hybrid system. It is clear from the algorithm that initially load is to be supplied by wind power plus battery power and if both powers are not sufficient than it takes a decision to start DG. Before starting DG, RL_1 and RL_2 are to be OFF and simultaneously RL_3 and RL_4 are to be in ON condition, after a delay RL_5 is to be in ON state and provides a signal to the DG start circuit to start the DG. At the same time, an auxiliary charger circuit starts to the charge battery with the excess power available with DG after supplying the load.

Figure 4.23 shows the developed Matlab/Simulink model of proposed stand-alone wind-battery-DG hybrid system. Figure 4.24 shows the wind speed profile indicating the wind speed input to stand-alone wind-battery-diesel generator hybrid system. In which wind speed variations are taken as 10 m/sec in the duration of 0 sec - 1 sec, 6 m/sec in the duration of 1 sec - 2 sec, 8 m/sec till 3 sec and from 3 sec – 4.8 sec (3 pm to 00 am) with no wind speed.

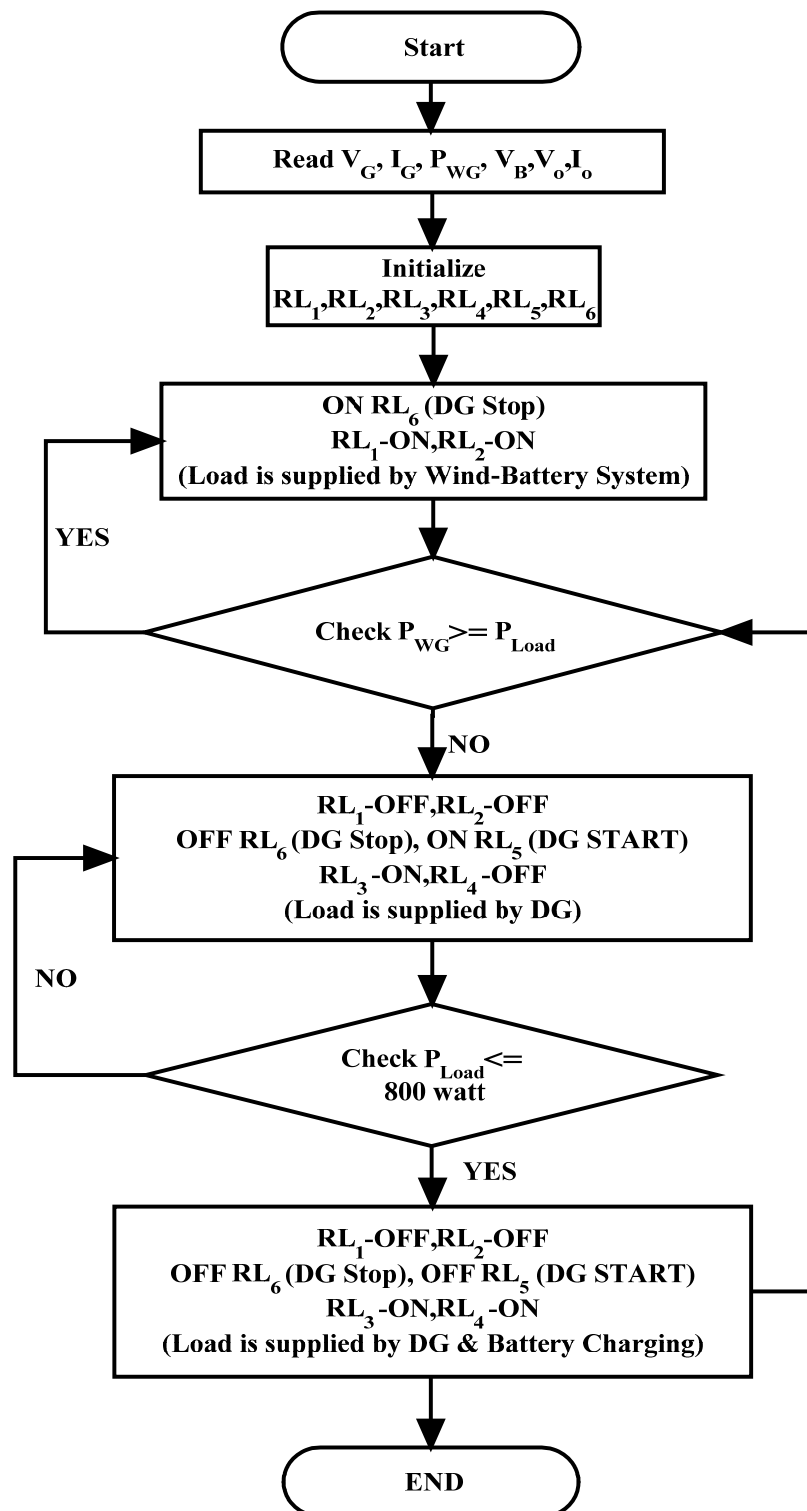


Figure 4.22 Algorithm of the HSC for stand-alone wind-battery-diesel generator hybrid system

Figure 4.25 (a) shows the test load profile pattern for a summer day for analyses purpose, which follows the similar pattern as shown in Figure 2.6.

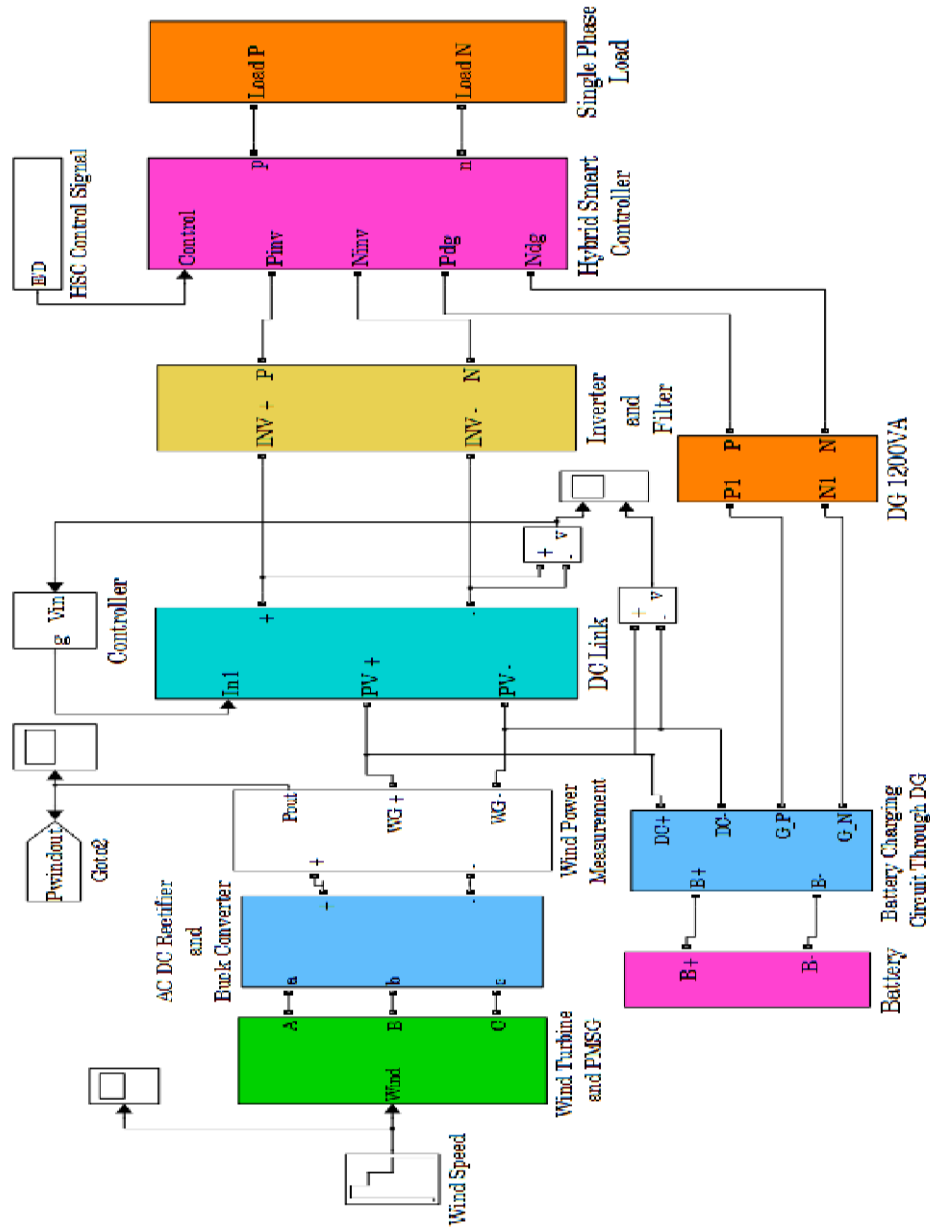


Figure 4.23 Matlab/Simulink model of proposed stand-alone wind-battery-diesel generator hybrid system

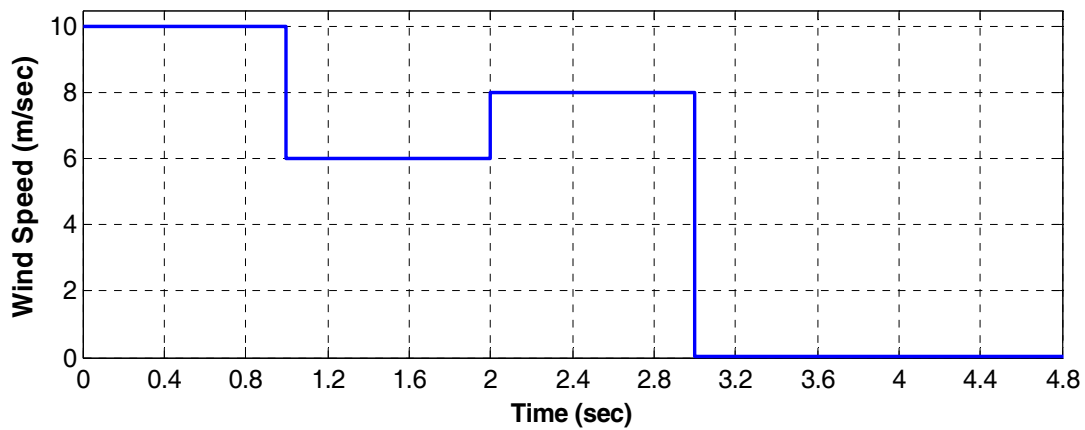
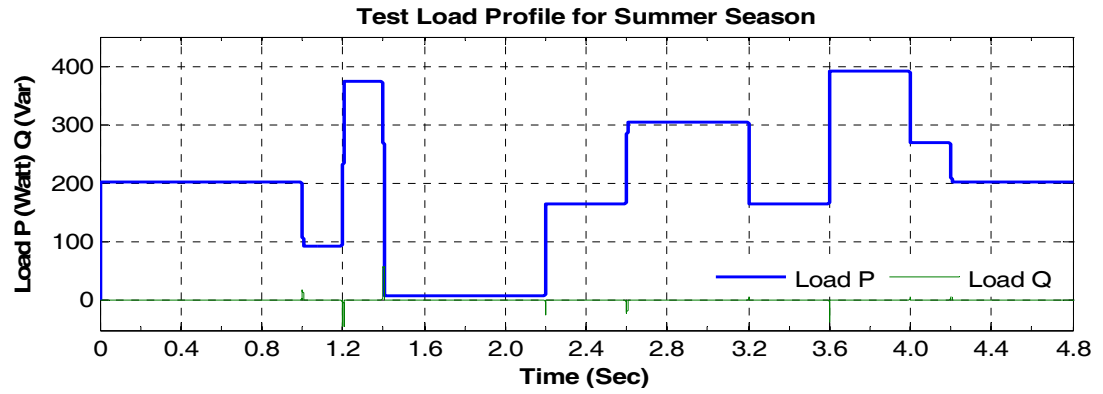
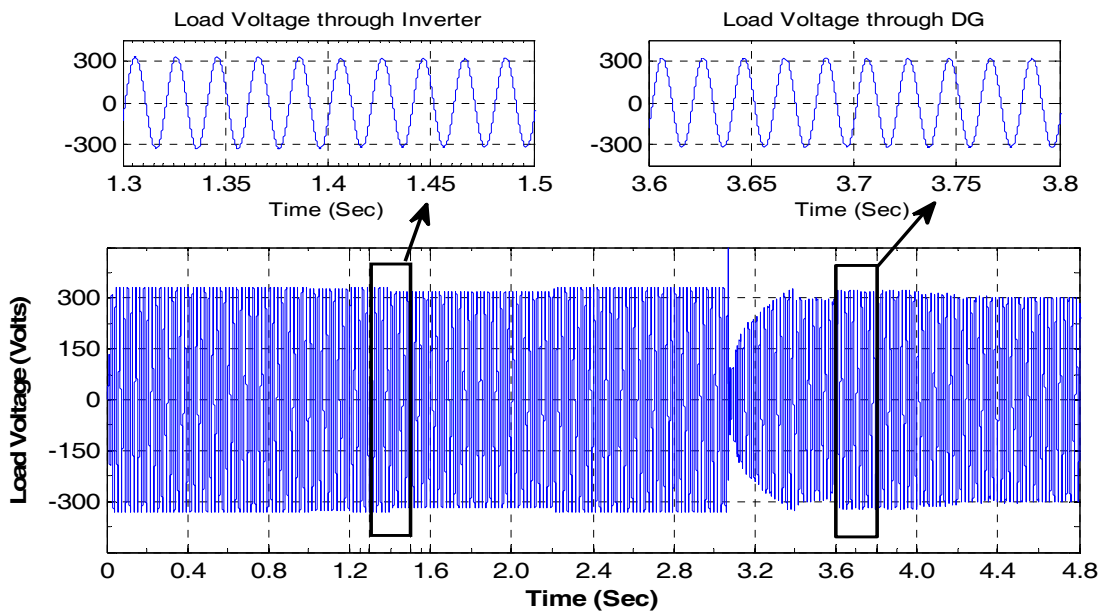


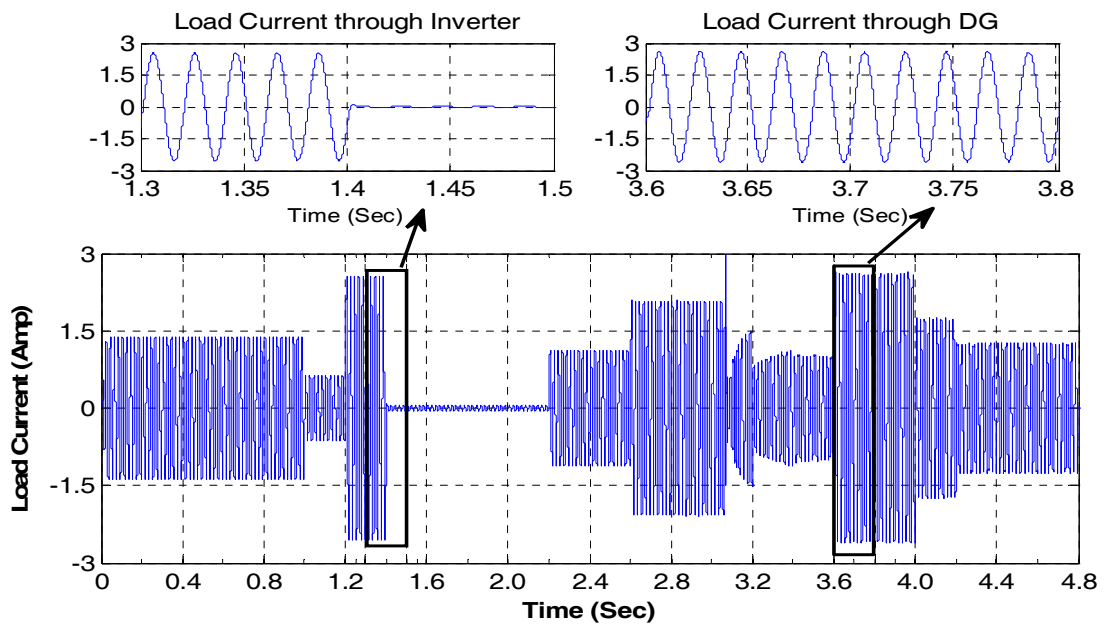
Figure 4.24 Wind speed profile



(a) Typical load variation



(b) Variation of load voltage



(c) Variation of load current

Figure 4.25 Load profile of stand-alone wind-battery-diesel generator hybrid system

Further the output load voltage and load current of wind-battery-diesel generator hybrid system are being shown in Figures 4.25 (b) and (c) respectively. It is observed that, the load is supplied by wind-battery system in the duration of 0 sec to 3.0 sec and after 3.0 sec load is supplied by DG. During time 3.1 sec to 3.3 sec the variations in voltage waveform indicate the starting and establishment period of DG. Corresponding variations are observed in the inverter output voltage and current of stand-alone wind-battery-diesel generator hybrid system as shown in Figure 4.26. An inverter current becomes zero at time 3.1 sec as shown in Figure 4.26 (b), whereas at the same time inverter voltage is equal to open circuit voltage as shown in Figure 4.26 (a).

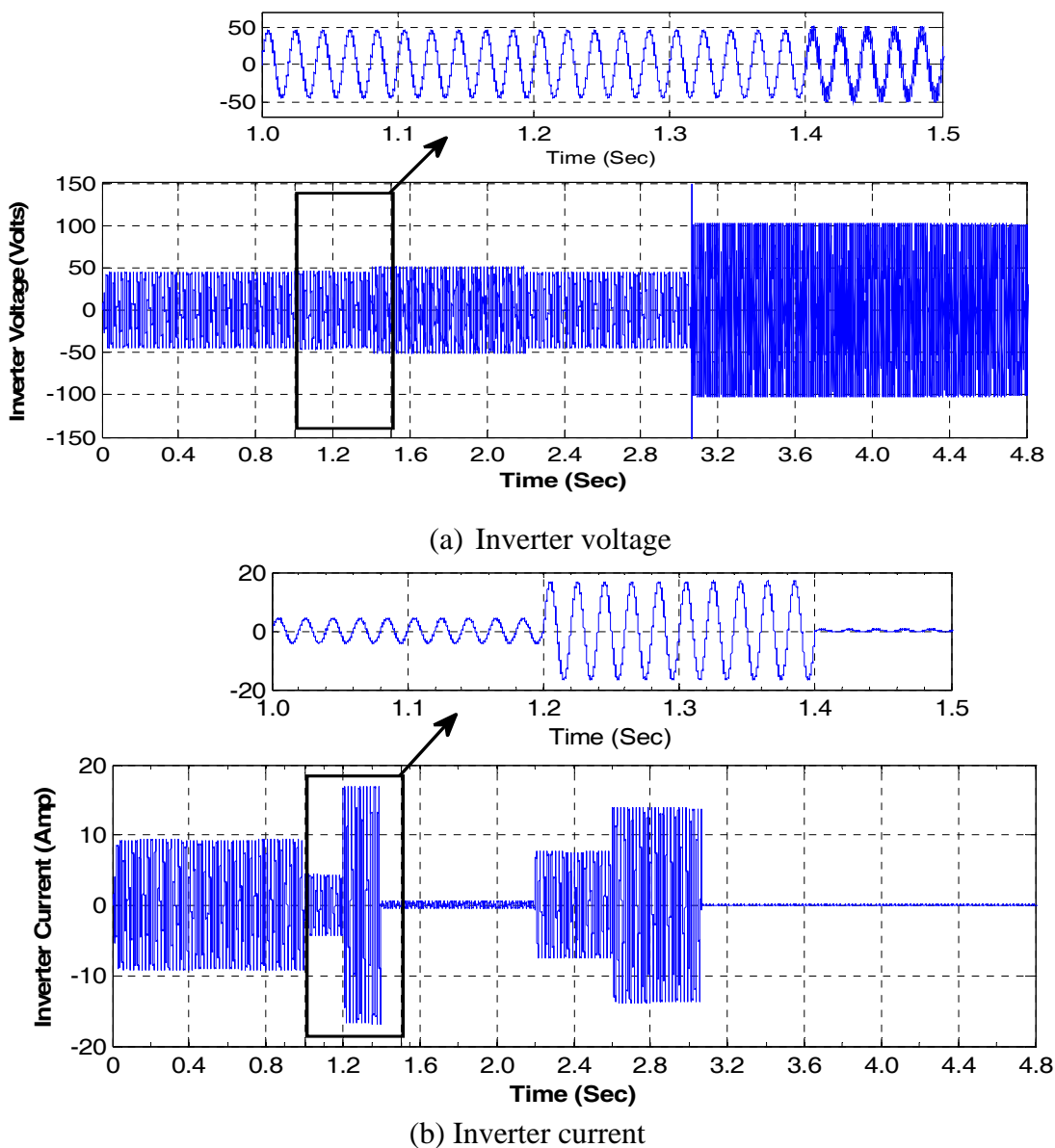
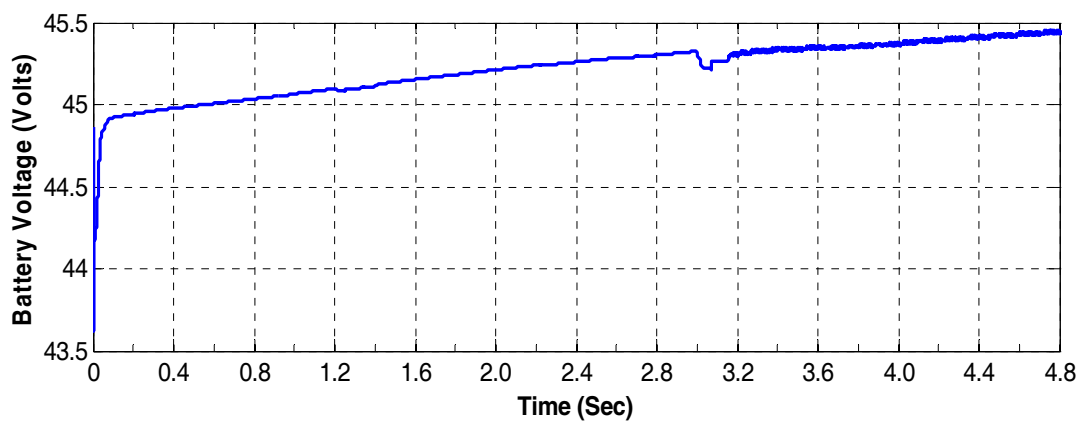
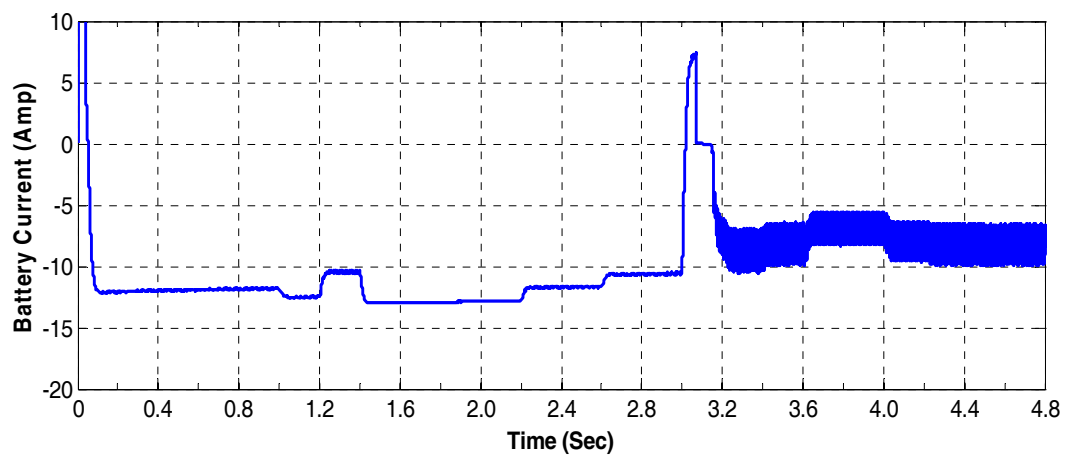


Figure 4.26 Inverter output of stand-alone wind-battery-diesel generator hybrid system

The battery output voltage and current of stand-alone wind-battery-diesel generator hybrid system are shown in Figure 4.27(a) and Figure 4.27(b) respectively.



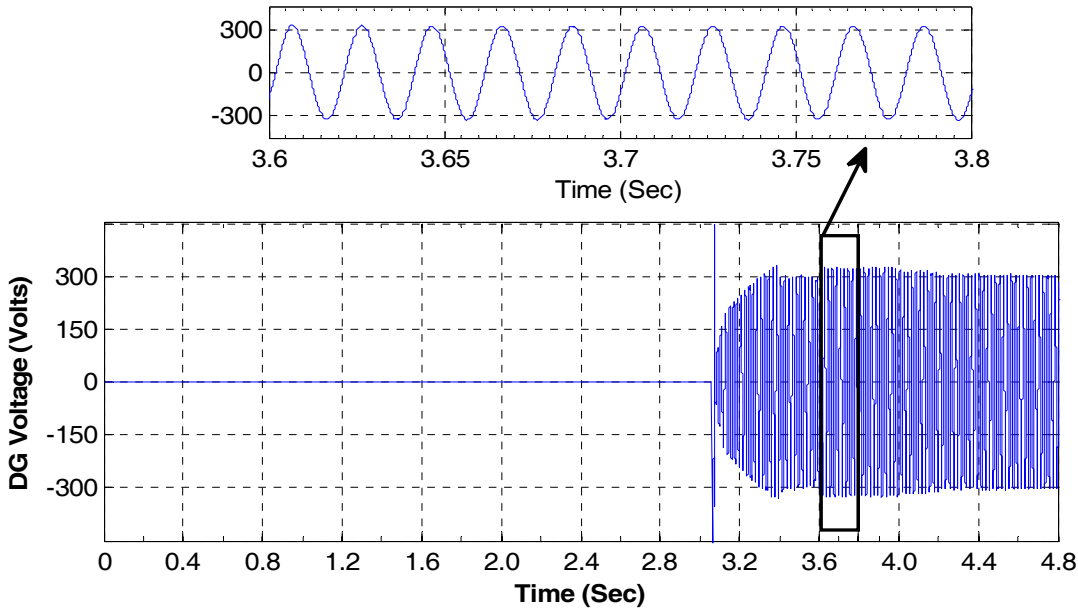
(a) Battery voltage



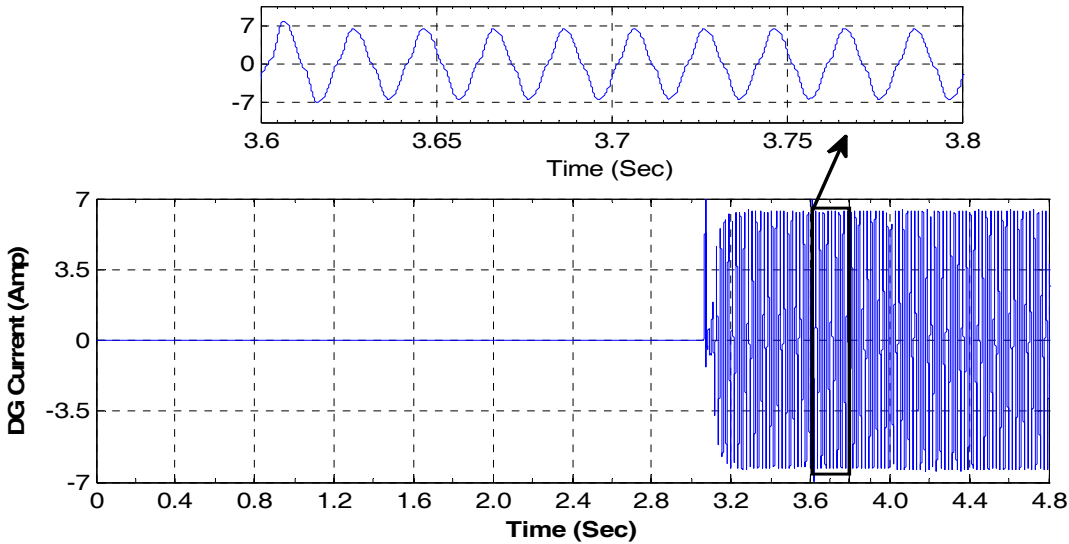
(b) Battery current

Figure 4.27 Battery output of stand-alone wind-battery-diesel generator hybrid system

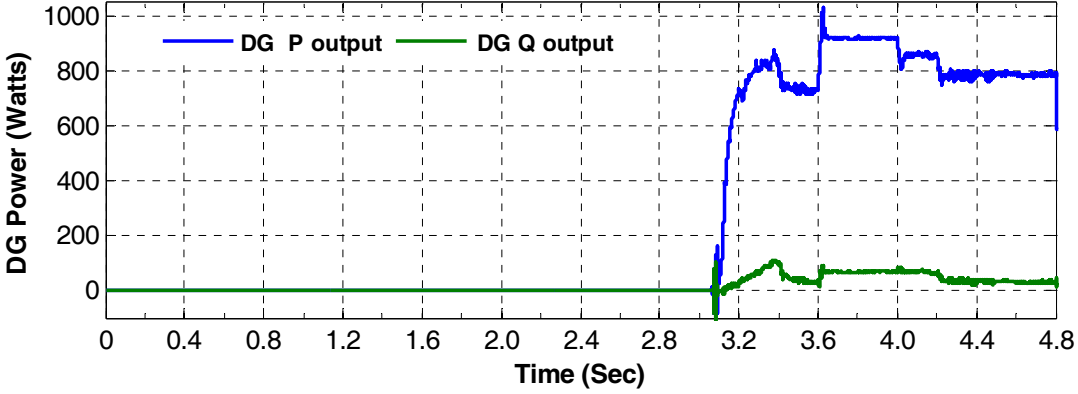
In this simulation, initially it assumed that battery bank is charged up to 25%, now the battery bank is to be charged through wind or DG up to 80% of its rated capacity than it starts to supply the load. When the battery bank is supplying the load in the absence of wind, DG starts again if the battery discharges and reaches 30% of its capacity, this leads to an increase the life cycle of the battery bank. At 3.0 sec, as shown in Figure 4.24 wind speed is zero, therefore the load is to be supplied by the battery bank as shown in Figure 4.27 (b). However, at this instant battery charge level is less than 30%, so HSC takes care to start the DG system as shown in Figure 4.28. Corresponding variations in battery charging current are shown in Figure 4.27 (b).



(a) DG voltage



(b) DG current



(c) DG power

Figure 4.28 DG output of stand-alone wind-battery-diesel generator hybrid system

DG output of stand-alone wind-battery-diesel generator hybrid system is shown in Figure 4.28, where Figure 4.28 (a) represents the DG voltage, Figure 4.28 (b) represents the DG current and Figure 4.28 (c) represents the DG power.

From Figure 4.28 (c), it is observed that DG power that consists both active and reactive powers which are utilized when wind power is not available to supply the load and to charge the battery bank during its running period through auxiliary charger. As discussed in previous section, the charging current of battery bank through DG is limited to maximum of 10 A as the maximum load demand is 400 W and DG power is 1200 VA. Corresponding charging of battery bank is shown in Figure 4.27 (b) in the time duration of 3.2 sec to 4.8 sec. However, at 3.1 sec, abnormal variations in battery voltage and current are observed as shown in Figure 4.27. This variation is due to the switching operation of relays and DG (*i.e.* OFF to ON) and it takes around 0.2 - 0.3 sec in this process.

From the simulation results it is cleared that, when wind power is available, it is sufficient to supply the typical load demand. As wind is not available after 3.0 sec of simulation than the load supply is shifted to DG system. As discussed in previous chapter that wind availability is uncertain, so it is difficult to obtain continuous wind profile for whole time to meet cut-in speed, which yields uncertainty of wind power availability. Hence DG operation is to be increased; however frequent operation of DG system is to be reduced by the use of auxiliary charger, which increases the use of battery bank-inverter system to supply the load in the absence of wind power. Hence, stand-alone wind-battery-diesel hybrid system can also not be recommended due to more diesel consumption, which is not viable economically as well as environment concern; however it provides a better solution for those areas which possess a good wind speed profile throughout the year.

4.5 DESIGN AND SIMULATION OF STAND-ALONE SOLAR-WIND-BATTERY-DIESEL GENERATOR HYBRID SYSTEM

As discussed in previous sections, a stand-alone solar-wind-battery hybrid system is capable to supply the load if continuous solar and wind power are available in rainy and winter season. In summer season, however the same system may be capable to supply the load if the load profile is as per Figure 2.6(a). Likewise, in stand-alone solar/wind-battery-diesel generator hybrid system, as solar/wind profile is not available for whole day; the load demand is to be supplied by the DG in absence of solar/wind power. This results in overall increased operating cost of the system. Hence, for supplying the varying load demand, another configuration of hybrid system is designed, which includes solar and wind power as renewable source, battery as storage device and a diesel generator as backup source. A typical block diagram of stand-alone solar-wind-battery-diesel generator hybrid system is shown in Figure 4.29.

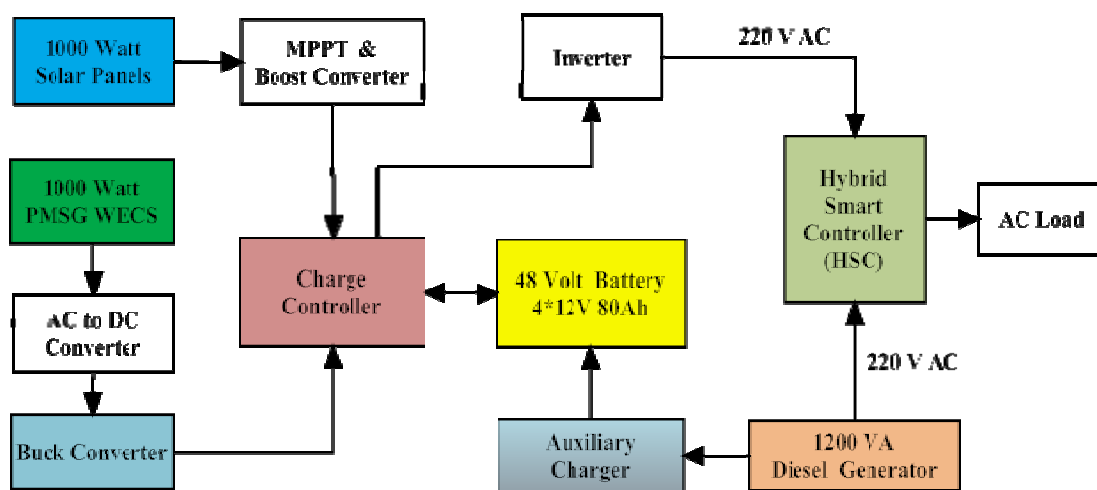


Figure 4.29 Block diagram of proposed stand-alone solar-wind-battery-diesel generator hybrid system

Figure 4.30 shows the proposed schematic connection diagram with proper connection of all the components such as solar PV with a boost converter and MPPT, wind power system with buck converter, DC link, battery bank, a VSI inverter with filter and step-up transformer, a diesel generator, and load sub system etc. As discussed in previous section, a hybrid smart controller (HSC) and auxiliary charger are introduced to control the diesel generator operation with solar PV system and wind energy system to supply the load without interruption and to charge the battery bank with excess DG power.

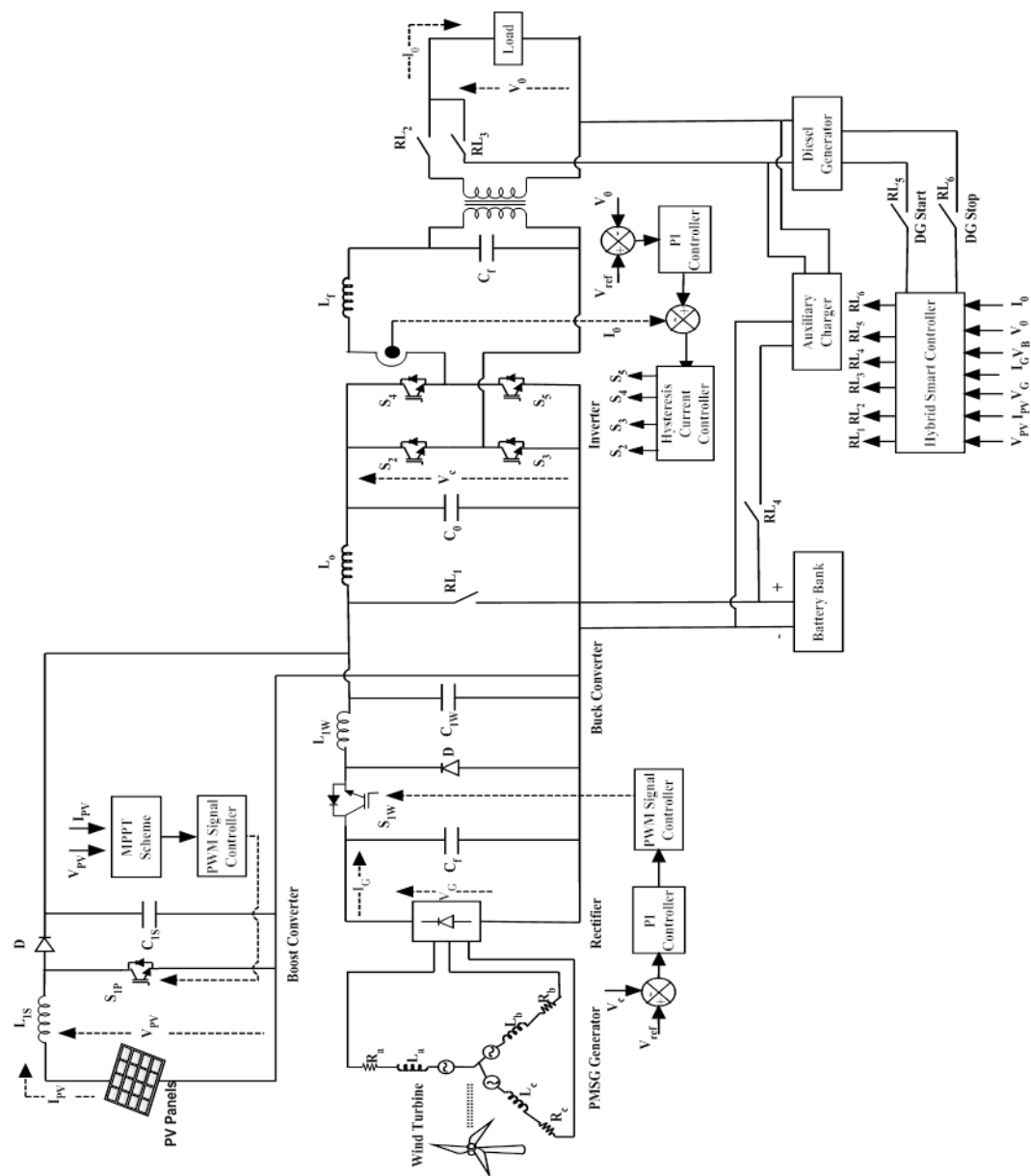


Figure 4.30 Schematic diagram of proposed stand-alone solar-wind-battery-diesel generator hybrid system

The working of the solar PV system with wind energy conversion system as explained in previous section, introduces some more modifications at load side and battery side, such as four relays *i.e.* RL_1 and RL_4 in battery side, and RL_2 and RL_3 at load side as shown in Figure 4.30 for optimum utility of battery and DG. Two more relays RL_5 and RL_6 are also introduced for DG start and stop circuit, to start and stop the diesel generator. Figure 4.31 shows the algorithm of the HSC for stand-alone solar-wind-battery- diesel generator hybrid system.

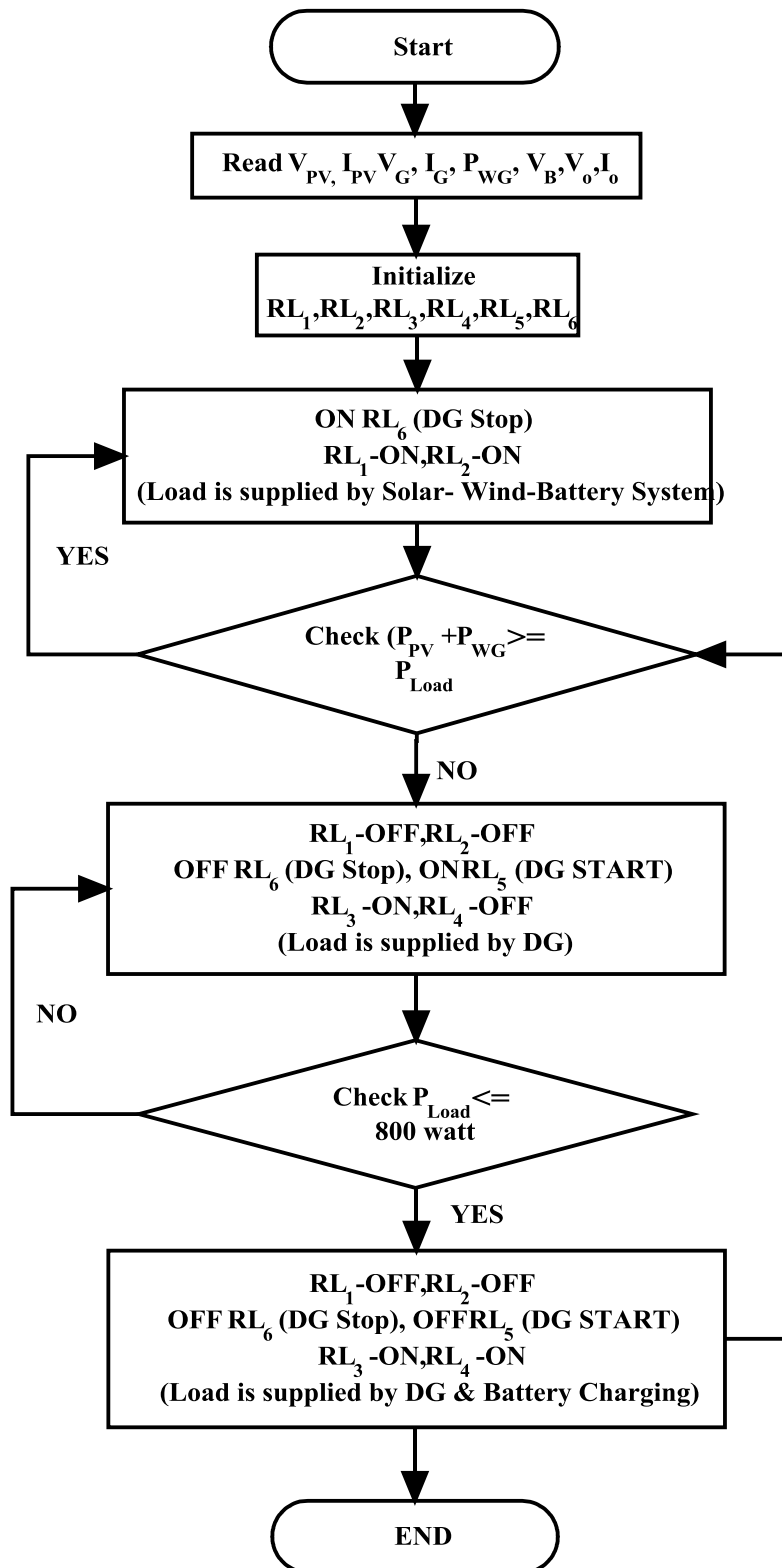


Figure 4.31 Algorithm of the HSC for stand-alone solar-wind-battery-diesel generator hybrid system

Figure 4.32 shows the developed Matlab/Simulink model of proposed stand-alone solar-wind-battery-diesel generator hybrid system.

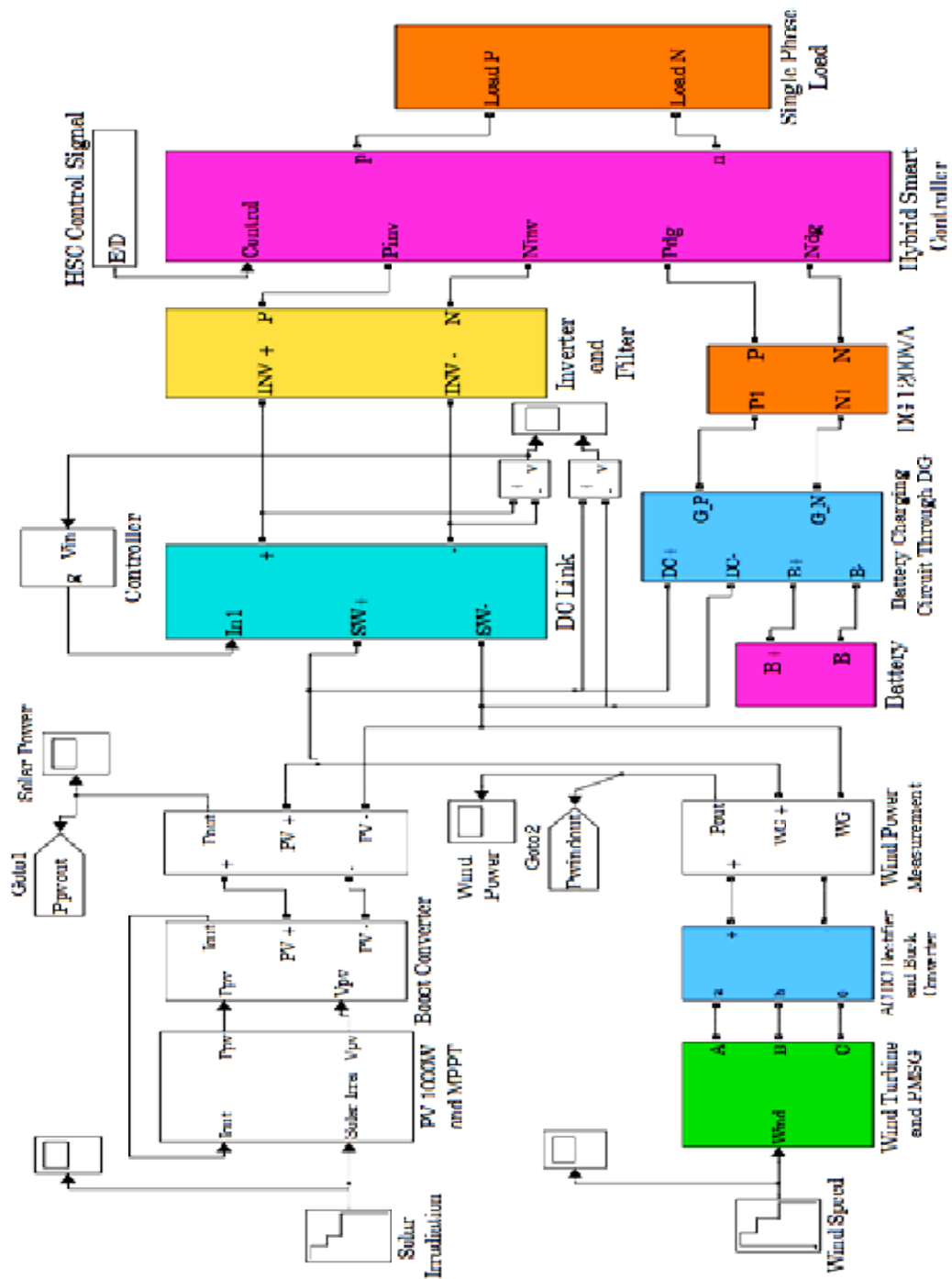
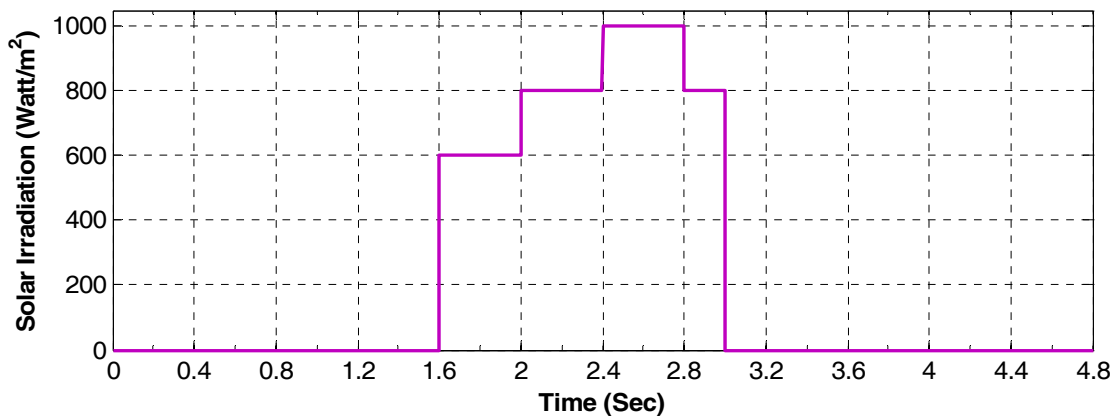


Figure 4.32 Matlab/Simulink model of proposed stand-alone solar-wind-battery-diesel generator hybrid system

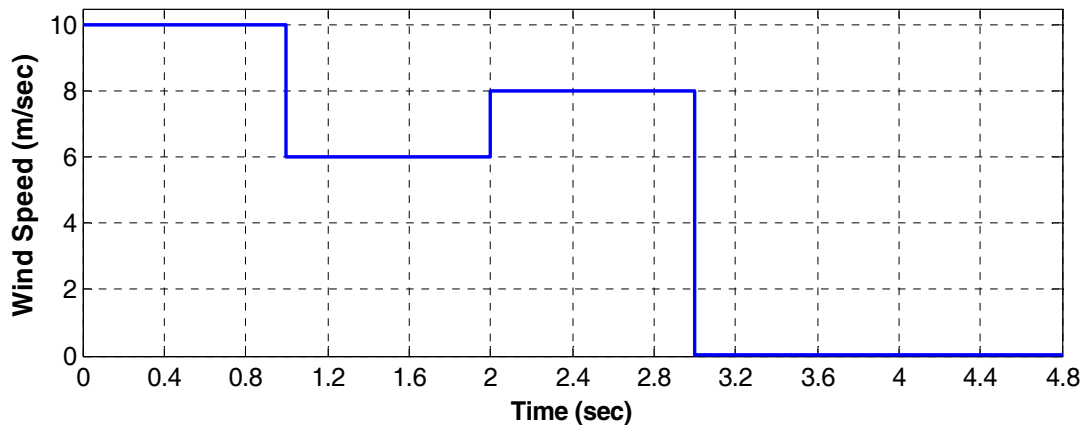
Initially, RL_1 and RL_2 are kept in ON condition *i.e.* load is connected to solar-wind-battery system through a inverter. At the same time, HSC is measuring the available power from solar plus wind and battery and compares it with power requirement from load side. It is clear from the algorithm that initially load is to be supplied by solar, wind plus battery power and if both powers are not sufficient than it takes a decision

to start DG. Before starting DG, RL₁ and RL₂ are to be OFF and simultaneously RL₃ and RL₄ are to be in ON condition, after a delay RL₅ is to be in ON state and provides a signal to the DG start circuit to start the DG. At the same time, auxiliary charger circuit starts to charge battery with the excess power available with DG after supplying the load.

Figures 4.33(a-b) shows the solar irradiation and wind speed profile data of a typical summer day, which is being taken into the account for the simulation purpose.



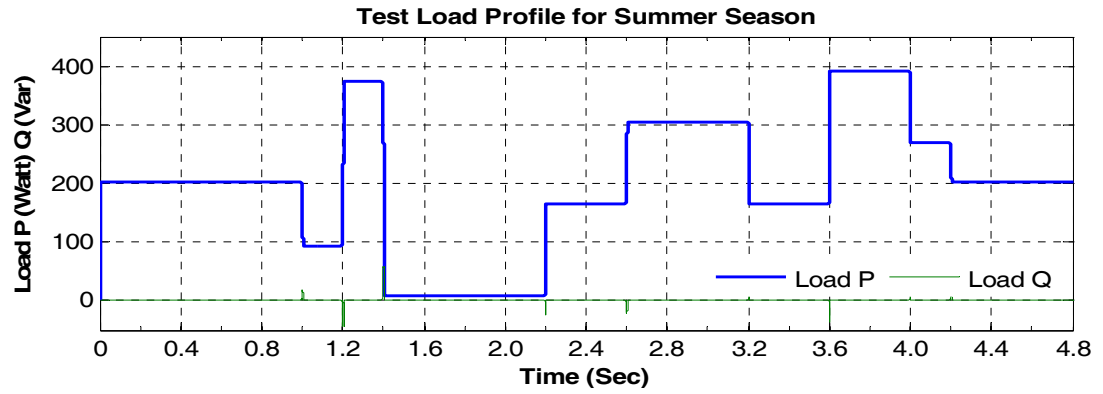
(a)



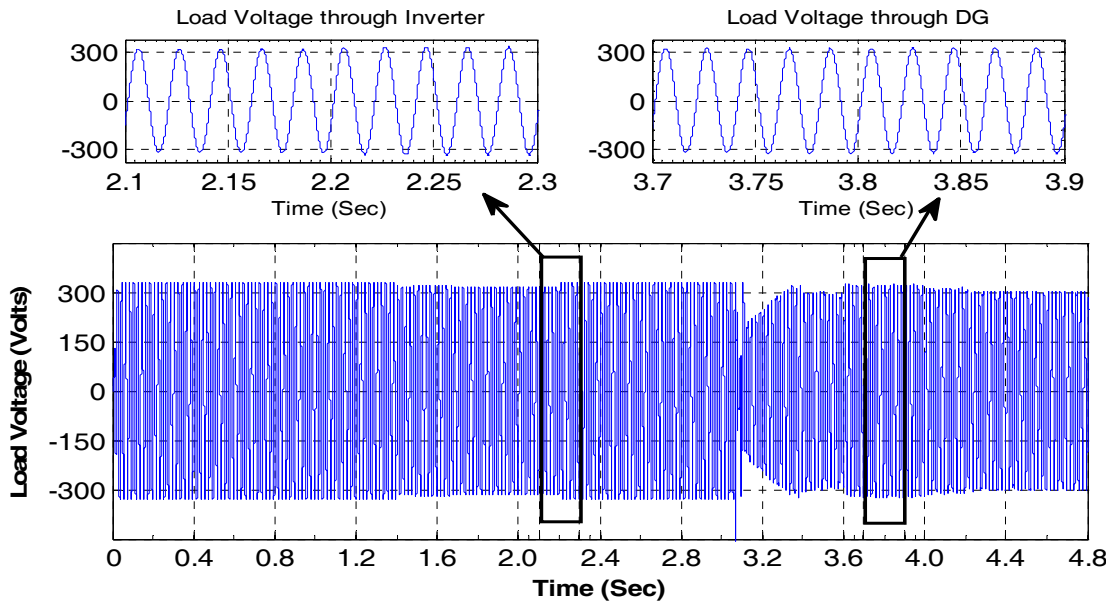
(b)

Figure 4.33 (a) Solar irradiation profile, (b) Wind speed profile

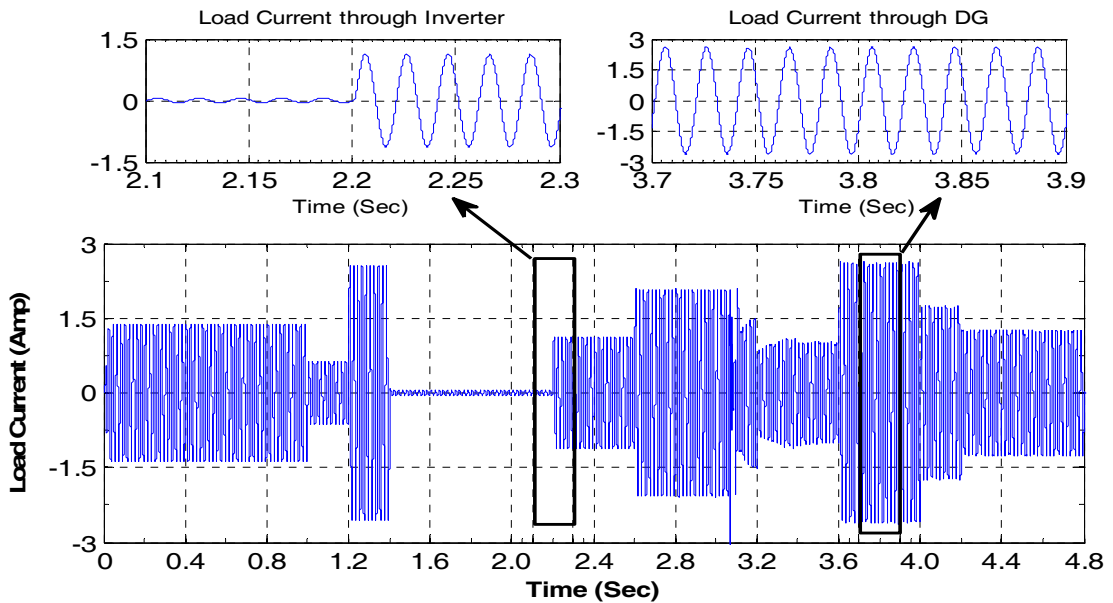
At time duration 0 sec - 1.6 sec and 3.0 sec - 4.8 sec the solar irradiation are 0 watt/m², however during 1.6 sec - 2.0 sec the solar irradiation is 600 watt/m² as shown in Figure 4.33 (a). During 2.0 sec - 2.4 sec the solar irradiation is 800 watt/m² after that it increases up to 1000 watt/m² till 2.8 sec and after that it reduces in sub sequential manner to 0 watt/m² at 3.0 sec.



(a) Typical load variation



(b) Variation of load voltage



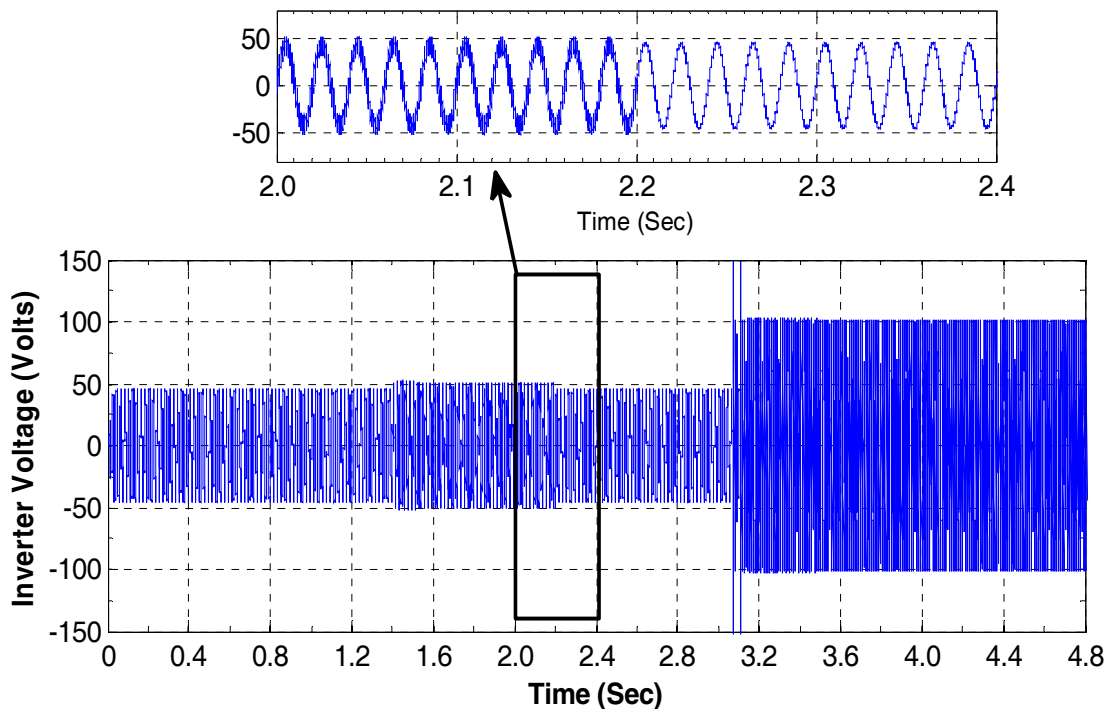
(c) Variation of load current

Figure 4.34 Load profile of stand-alone solar-wind-battery-diesel generator hybrid system

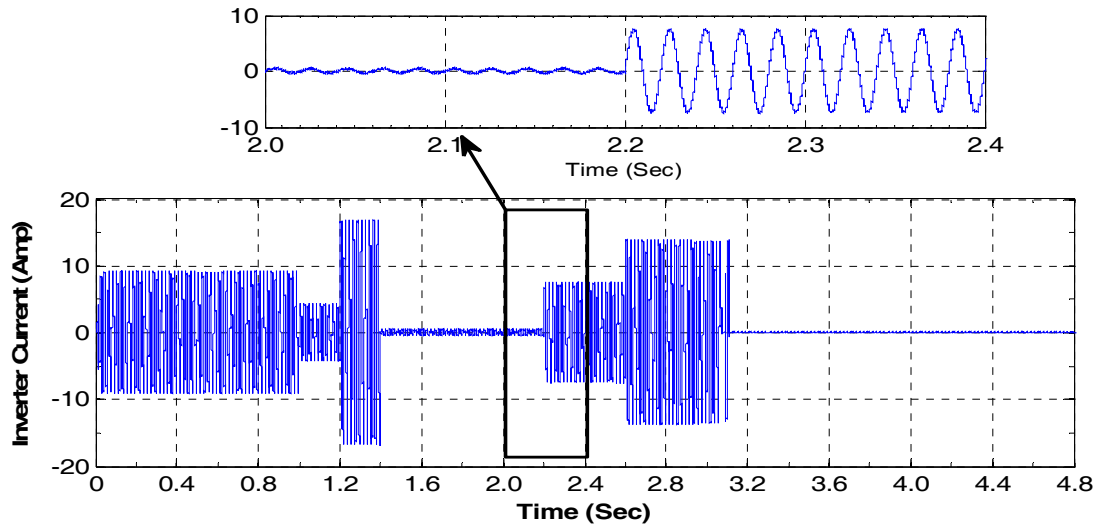
In wind speed profile, wind speed variations is taken as 10 m/sec in the duration of 0 sec - 1 sec, 6 m/sec in the duration of 1 sec - 2 sec, 8 m/sec till 3 sec and then it reduces to zero from 3 sec – 4.8 sec as shown in Figure 4.33 (b).

A typical summer load profile, as shown in Figure 4.34 (a), is considered for simulation purpose. Here, system is simulated for a time period of 4.8 sec. Figures 4.34 (b) and (c) show the variation of load voltage and load current respectively according to the load variations. After 3.0 sec, as shown in Figure 4.34 solar and wind power both are not available the load is supplied by the battery bank till 3.1 sec and after that it is to be supplied by DG as the level of stored energy in the battery bank is less than 30%.

As shown in Figure 4.34 (b), at the time duration 3.1 sec to 3.3 sec, a variation in voltage waveform indicates the starting and establishment period of DG. Corresponding variations are observed in the inverter output of stand-alone solar-wind-battery-diesel generator hybrid system as shown in Figure 4.35. The inverter current becomes zero at time 3.1 sec as shown in Figure 4.35 (b), whereas at same time inverter voltage is equal to open circuit voltage as shown in Figure 4.35 (a).



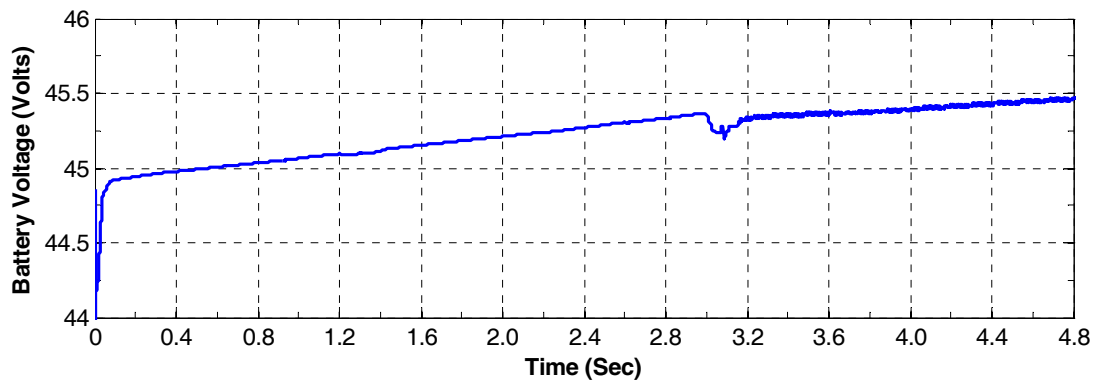
(a) Inverter voltage



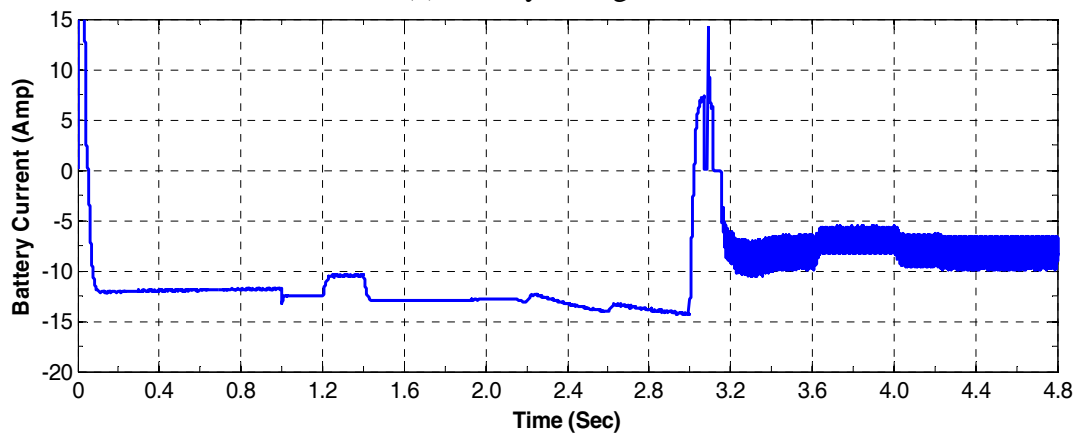
(b) Inverter current

Figure 4.35 Inverter output of stand-alone solar-wind-battery-diesel generator hybrid system

The battery output voltage and current of stand-alone solar-wind-battery-diesel generator hybrid system are shown in Figure 4.36(a) and Figure 4.36(b) respectively.



(a) Battery voltage



(b) Battery current

Figure 4.36 Battery output of stand-alone solar-wind-battery-diesel generator hybrid system

As discussed in previous section, in this simulation, initially it is assumed that battery bank is charged up to 25%, now the battery bank is to be charged through solar/wind or DG up to 80% of its rated capacity than it starts to supply the load. When the battery bank is supplying the load in the absence of solar/wind, DG starts again if the battery discharges and reaches 30% of its capacity. This leads to increase the life cycle of the battery bank. At 3.0 sec, as shown in Figure 4.33 solar irradiation and wind speed are zero, therefore the load is to be shifted to the battery bank as shown in Figure 4.36 (b). However, at this instant battery charge level is less than 30%, so HSC takes care to start the DG system as shown in Figure 4.37. Corresponding variations in battery charging current are shown in Figure 4.36 (b).

DG output of stand-alone solar-wind-battery-diesel generator hybrid system is shown in Figure 4.37, where Figure 4.37 (a) represents the DG voltage, Figure 4.37 (b) represents the DG current and Figure 4.37 (c) represents the DG power.

From Figure 4.37 (c), it is observed that DG power that consists both active and reactive powers which are utilized when solar and wind power are not available to supply the load and to charge the battery bank during its running period through auxiliary charger. As discussed in previous section, the charging current of battery bank through DG is limited to maximum of 10 A as the maximum load demand is 400 W and DG power is 1200 VA. Corresponding charging of battery bank is shown in Figure 4.36 (b) in the time duration of 3.2 sec to 4.8 sec. However, at 3.1 sec, as shown in Figure 4.27, abnormal variations in battery voltage and current are observed. This variation is due to the switching operation of relays and DG (*i.e.* OFF to ON) and it takes around 0.2-0.3 sec in this process.

From the simulation results, it is clear that, when solar and wind powers are available, it is sufficient to supply the typical load demand. Since solar and wind powers are not available after 3 sec, as shown in Figure 4.33, than the load supply is shifted to DG system. As discussed in previous chapter that wind availability is uncertain so it is difficult to obtain continuous wind profile for whole time to meet cut-in speed, which yields uncertainty of wind power availability. However, solar power availability from 1.6 sec to 3 sec, increases the battery charging for this duration. Hence DG operation

is to be reduced as compared to stand-alone solar-battery-diesel and stand-alone wind-battery-diesel hybrid system.

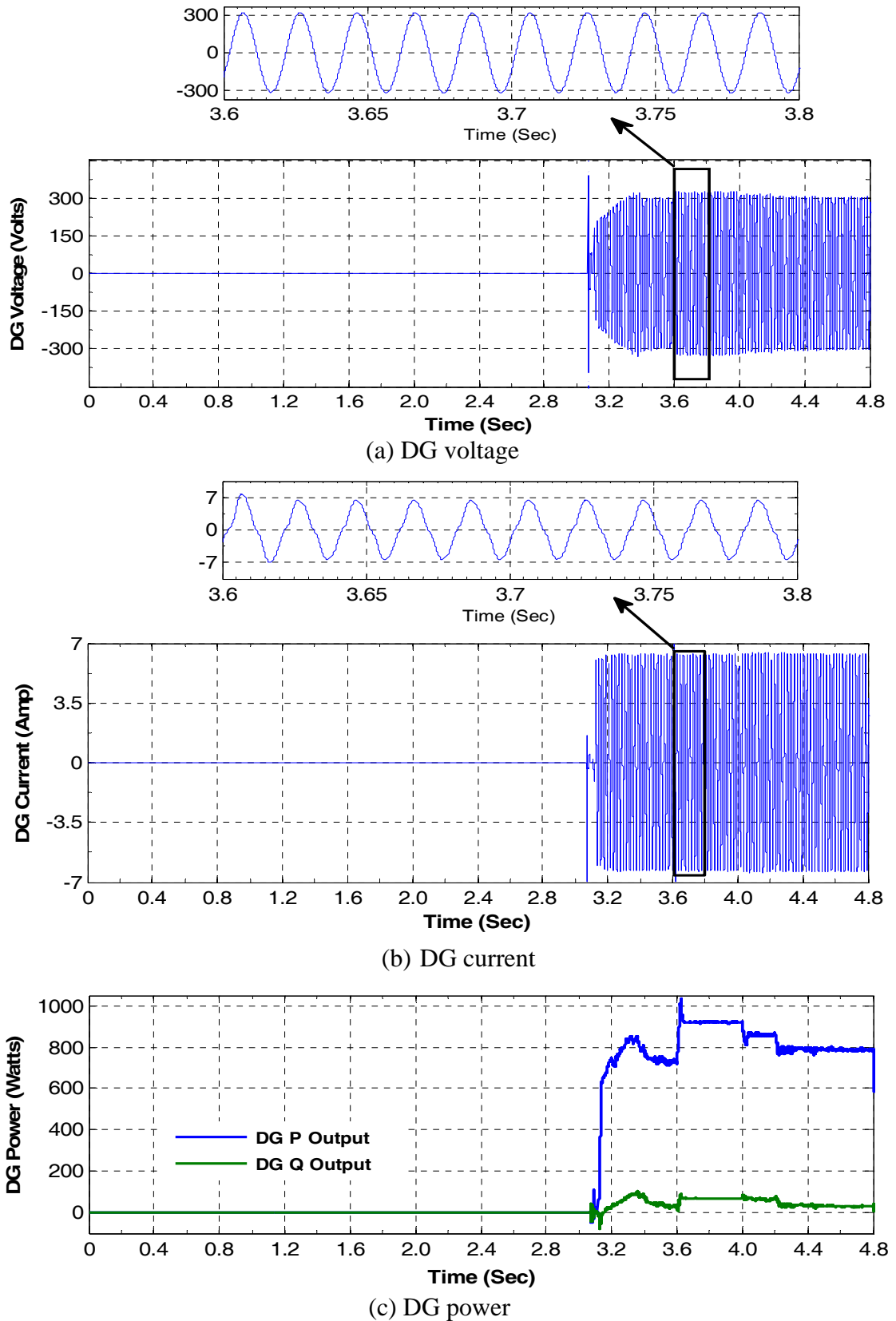


Figure 4.37 DG output of stand-alone solar-wind-battery-diesel generator hybrid system

Frequent operation of DG system is also to be reduced by the use of auxiliary charger, which increases the use of battery bank-inverter system to supply the load in the absence of solar and wind power. Hence, less consumption of diesel in DG operation *i.e.* less emission of CO₂ provides low operating cost with better running condition.

Hence, stand-alone solar-wind-battery-diesel hybrid system is recommended for operation at rural or remote area as economically as well as environment concern. However, it provides a better solution for those areas which possess a good solar irradiation and wind speed profile throughout the year.

4.6 COMPARATIVE ANALYSIS OF HYBRID SYSTEMS

Table 4.1 shows the comparative analysis of four types of stand-alone hybrid systems as discussed in previous sections. On the basis of the analysis, it is observed that the stand-alone solar-wind-battery hybrid system has lowest operating cost. However, stand-alone solar-wind-battery-diesel generator hybrid system is more reliable than any other hybrid system with comparatively little higher installation and operating cost.

Table 4.1 Comparative analysis of stand-alone hybrid systems

Particular	Solar-Wind-Battery-Hybrid System	Solar-Battery-Diesel Generator Hybrid System	Wind-Battery-Diesel Generator Hybrid System	Solar-Wind-Battery-Diesel Generator Hybrid System
Primary Source	Solar & Wind	Only Solar	Only Wind	Solar & Wind
Secondary Source	Battery	Battery	Battery	Battery
Backup Source	No	Diesel Generator	Diesel Generator	Diesel Generator
Auxiliary Charger	No	Yes	Yes	Yes
CO ₂ Emission	No	Yes	Yes	Yes (Less as compared to previous)
Controller Design	Simple	Complicated	Complicated	Complicated
Operating Cost	Very Less	More	More	Less
Reliability	Very Low	Low	Low	High

4.7 CONCLUSIONS

In this chapter, Matlab/Simulink models of various hybrid systems configuration like solar-wind-battery hybrid system, solar-battery-diesel generator hybrid system, wind-battery-diesel generator hybrid system and solar-wind-battery-diesel generator hybrid system have been developed and simulation results are obtained which discussed for typical solar, wind and load profile.

Further, power sharing curves of solar-wind-battery hybrid system for a typical day of all three seasons have been discussed, which show the available power from solar and wind to fulfill the load requirement. A comparative analysis of these power sharing curves for all three seasons has been carried out. On the basis of comparative analysis, it is concluded that only solar or wind power is not capable to fulfill the load requirement as solar or wind power is not available continuously throughout the year. However to meet the load requirements continuously, a diesel generator may be incorporated in the hybrid system.

In a diesel generator based hybrid systems like solar-battery-diesel generator hybrid system, wind-battery-diesel generator hybrid system and solar-wind-battery-diesel generator hybrid system, a new concept of auxiliary charger has been introduced. An auxiliary charger charges the battery bank when the diesel generator is ON condition in the absence of solar or/and wind power while supplying the load. When the battery bank is fully charged, the load is supplied by battery bank till the battery bank reaches 30% of its capacity, after that it is to be shifted to a diesel generator. This concept reduces the diesel generator running time; hence the battery life cycle and the diesel generator efficiency are increased.

So, on the basis of this analysis it is recommended that stand-alone solar-wind-battery-diesel generator hybrid system is optimally suitable for fulfilling the typical load demand of a remote location by minimizing the use of diesel generator power and maximize the use of solar and wind power.

Hardware Implementation of Proposed Stand-alone Hybrid System

T HIS chapter details out the hardware prototype of solar-wind-battery-diesel generator hybrid system. Various hardware results are compared with simulated results of proposed system. On the basis of monthly solar irradiation profile, wind speed profile and typical load profile (in the Kukas area) required DG power is calculated for different contribution level of solar and wind power for summer, rainy and winter seasons.

CHAPTER 5

HARDWARE IMPLEMENTATION OF PROPOSED STAND-ALONE HYBRID SYSTEM

5.1 GENERAL

Stand-alone hybrid system configurations with solar PV system, WECS, a battery and the diesel generator are described in previous chapter. A stand-alone solar-wind-battery hybrid system is capable to supply load power if continuous solar and wind power are available in rainy and winter seasons. In summer season, however it may be capable to supply the load if there is to be no change occurs in the load profile as shown in Figure 2.6. However, in stand-alone solar-battery-diesel hybrid system, whenever solar power is not available the demand is to be supplied by the DG that results in overall increased operating cost of the system. Similarly, stand-alone wind-battery-diesel hybrid system is also not suitable due to uncertain of wind throughout the day/month/year. Therefore, to meet the load demand economically with high reliability and less pollution, a stand-alone solar-wind-battery-diesel generator hybrid system is proposed for rural or remote area electrification. In this chapter, the hardware of this configuration is developed and demonstrated the operation of stand-alone solar-wind-battery-diesel generator hybrid system.

5.2 HARDWARE COMPONENTS FOR STAND-ALONE SOLAR-WIND-BATTERY-DIESEL GENERATOR HYBRID SYSTEM

A hardware of stand-alone solar-wind-battery-diesel generator hybrid system is developed at Kukas, Jaipur, India, which consists of following major components:

- (a) 1.0 kW Solar PV Array
- (b) Solar MPPT Controller
- (c) 1.0 kW Wind Energy Conversion System (WECS)
- (d) 1.2 kVA Diesel Generator
- (e) 48 V, 80 Ah Battery Bank
- (f) An inverter
- (g) Auxiliary Charger
- (h) Hybrid Smart Controller (HSC)
- (i) Data Logger and Sensor Circuit

5.2.1 Hardware Configuration of 1.0 kW Solar PV Array

For realizing such system, a 1.0 kW solar PV array system is considered which has eight solar panels manufactured by REIL, India of 125W each, which has been considered for installation. All the eight solar panels are installed in Kukas (in series/parallel combination as discussed in earlier Figure 3.8) as shown in Figure 5.1.



Figure 5.1 Actual installation setup of 1.0 kW solar PV array, at Kukas, Jaipur

5.2.2 Solar MPPT Controller

The hardware configuration of solar MPPT controller has been shown in Figure 5.2.

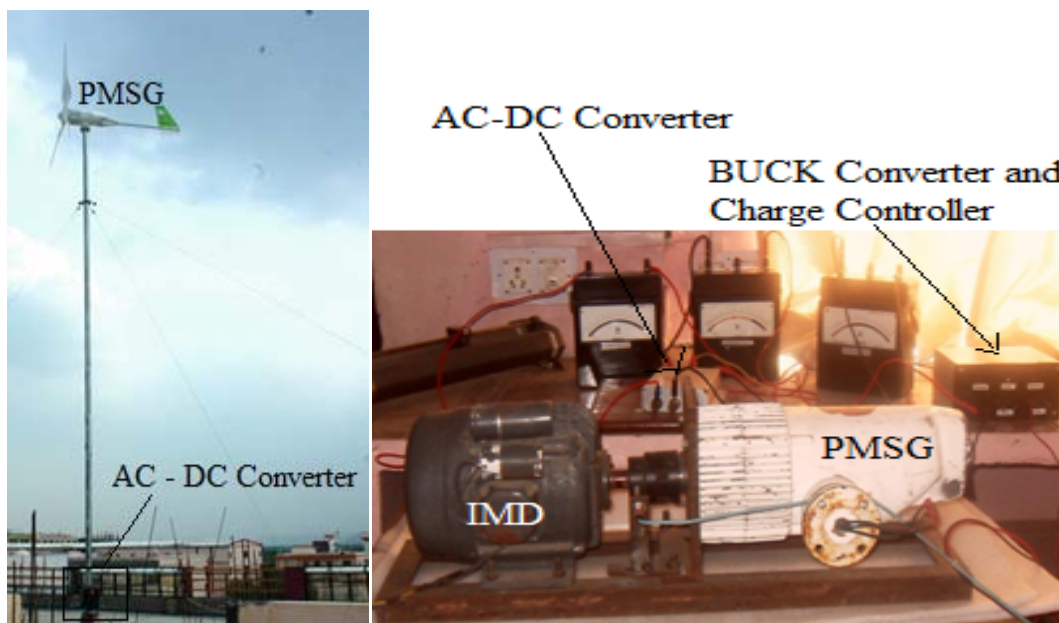


Figure 5.2 Hardware configuration of solar MPPT controller

The DC-DC converter is connected with the solar PV array to regulate the operating point through a MPPT controller. The output power, controlled by MPPT of PV panel is varied due to change in solar irradiation, temperature, and load variations.

5.2.3 Hardware Configuration of 1.0 kW Wind Energy Conversion System

For realizing a 1.0 kW wind energy conversion system (WECS), a wind turbine of 1.0 kW, blade size of 1.25 m, with 3.0 m pole structure, manufactured by Monad Electronics Ltd. Jaipur has been installed at 11m height from ground at Kukas, Jaipur as shown in Figure 5.3 (a), with an AC-DC converter and a buck converter and charge controller. An equivalent prototype of this installation is also developed for experimental purposes as shown in Figure 5.3 (b).



(a)

(b)

Figure 5.3 (a) Actual installation setup of 1.0 kW wind generator at 11 m height

(b) Real prototype model of 1.0 kW wind energy conversion system (WECS) at Kukas, Jaipur

5.2.4 Hardware Configuration of 1.2 KVA Diesel Generator

For realizing a 1.2 kVA diesel generator, a diesel generator of 1.2 kVA with its start and stop circuit has been installed at Kukas, Jaipur as shown in Figure 5.4.



Figure 5.4 Real installation of 1.2 kVA diesel generator at Kukas, Jaipur

5.2.5 Battery Bank

For energy storage, a battery bank consisting of four 12V batteries of 80 AH capacity are connected in series to make a 48 V, 80Ah battery bank has been installed at Kukas, Jaipur as shown in Figure 5.5.

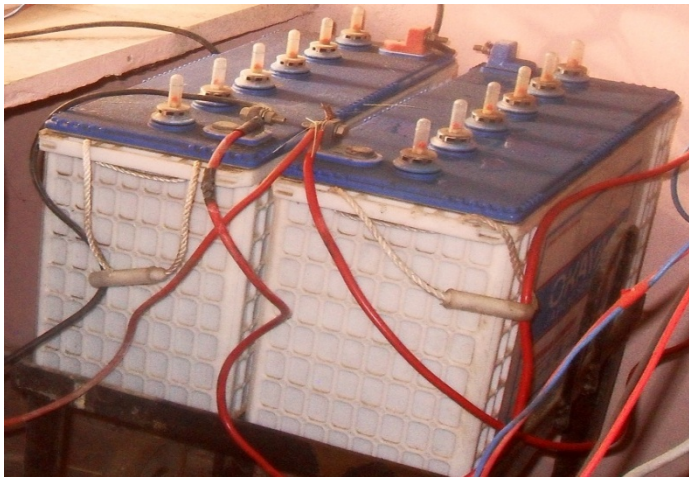


Figure 5.5 Real installation of battery bank at Kukas, Jaipur

5.2.6 Hardware Configuration of Hybrid Smart Controller (HSC)

As discussed in chapter 4, a hybrid smart controller (HSC) is introduced in the stand-alone solar-wind-battery-diesel generator hybrid system, for coordination of all relays

and proper working of the system. The major function of HSC is to supply the load through renewable power or DG power. The hardware configuration of HSC is shown in Figure 5.6.

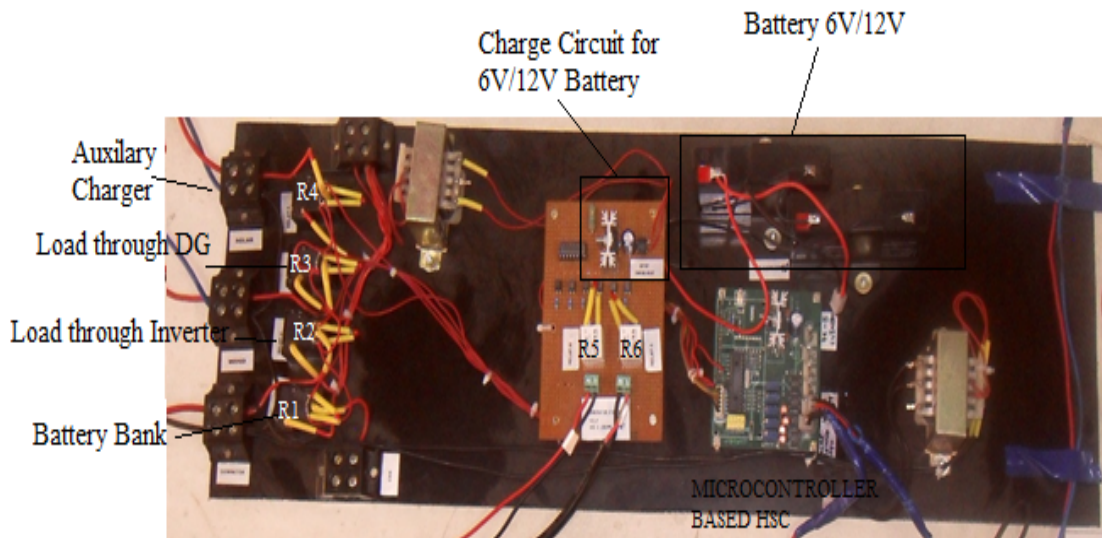


Figure 5.6 Hardware configuration of hybrid smart controller (HSC)

5.2.7 Hardware Configuration of Data Logger and Sensor Circuit

A 16-channel data logger (Monad Electronics Ltd. make) is used to record various data of the stand-alone solar-wind-battery-diesel generator hybrid system. For this purpose, various sensor circuits are used. The installation of data logger and its sensor circuits are shown in Figure 5.7 and Figure 5.8 respectively. The some outputs of sensor circuits are also fed to HSC for controlling purpose.



Figure 5.7 Installation of Data Logger

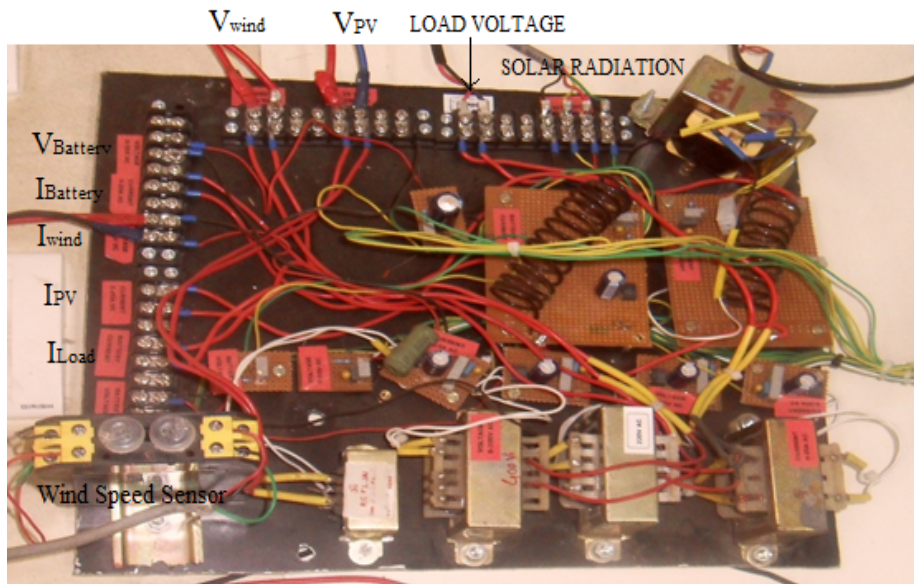


Figure 5.8 Installation of sensor circuits

A data logger is designed to record the data of proposed system. The data logger records the following signals data with help of sensor circuits:

- (a) Solar irradiation, (b) Wind speed, (c) Solar PV system voltage, (d) Solar PV system current, (e) Wind system voltage, (f) Wind system current, (g) Load voltage, (h) Load current, (i) Battery voltage, and (j) Battery current.

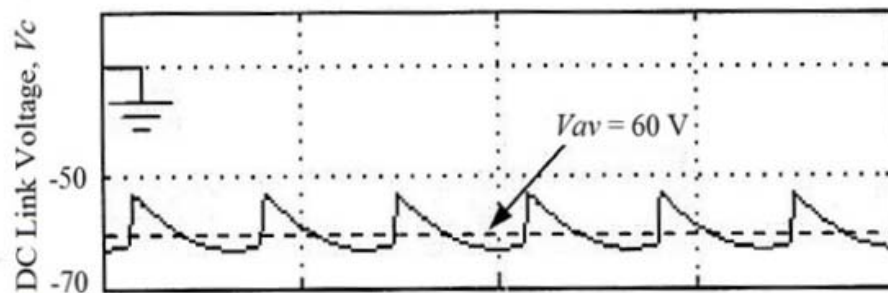
Figure 5.9 shows the overall view of the installed stand-alone solar-wind-battery-diesel generator hybrid system.



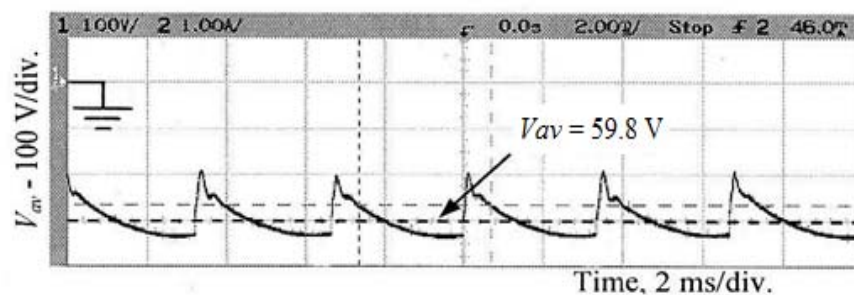
Figure 5.9 Overall view of stand-alone solar-wind-battery-diesel generator hybrid system

5.3 RESULTS AND DISCUSSION

This section deals with test results obtained on installed stand-alone solar-wind-battery-diesel generator hybrid system. Figures 5.10 (a-b) show the DC link voltage for proposed system obtained from simulation as well as experimental prototype respectively. From Figure 5.10(a) and Figure 5.10(b), it is observed that DC link average voltage obtained from simulation results is 60 V while it is 59.8 V in the experimental results. The nature of the DC Link voltage is almost similar as shown in Figure 5.10.



(a) Simulated



(b) Experimental

Figure 5.10 DC Link Voltages

Further Figure 5.11 shows the simulated and experimental results of load voltage and load current, due to solar PV system in the proposed stand-alone solar-wind-battery-diesel generator hybrid system. From Figure 5.11(a) and Figure 5.11(b), it is observed that the rms value of load voltage in simulation and experimental results is 230 V and 233.8 V respectively. Similarly, the rms value of load current is 2.608 A and 2.618 A in simulation and experimental results respectively. The nature of the load voltage and load current are also similar as shown in Figure 5.11(a) and Figure 5.11(b).

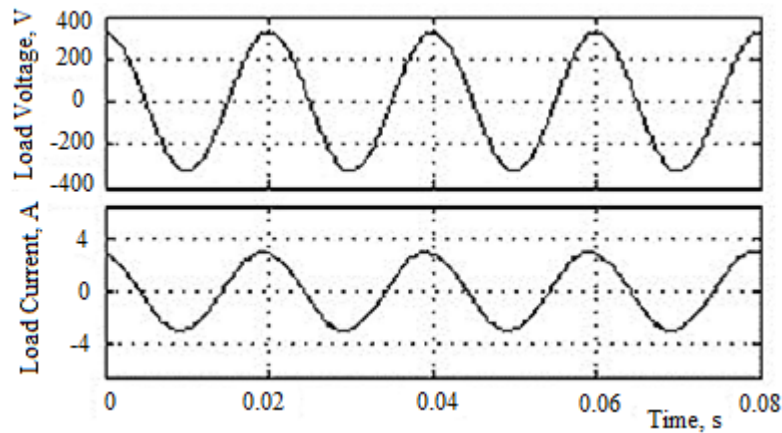
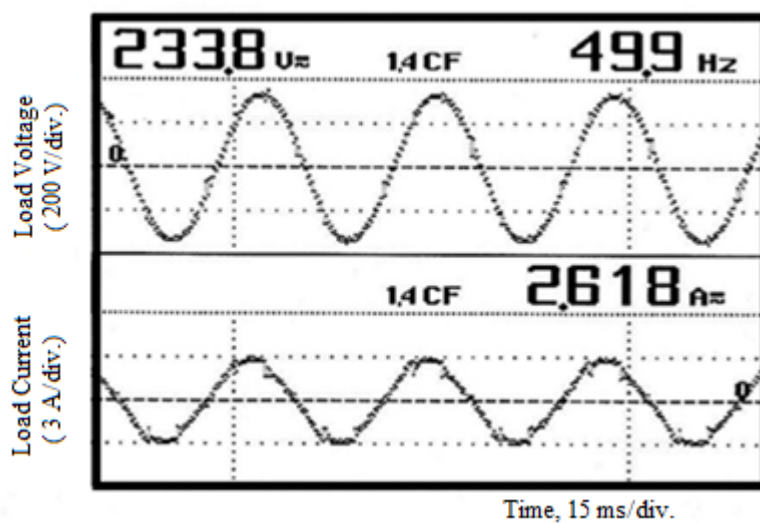
(a) Simulated ($V_{\text{rms}}=230$ volt, $I_{\text{rms}}=2.608$ Amp)(b) Experimental ($V_{\text{rms}}=233.8$ volt, $I_{\text{rms}}=2.618$ Amp)

Figure 5.11 Load voltage and current with solar PV system of proposed hybrid system

Figure 5.12 shows the simulated and experimental results of load voltage and load current, due to wind energy conversion (WECS) system in the proposed stand-alone solar-wind-battery-diesel generator hybrid system. From the Figure 5.12(a) and Figure 5.12(b), it is clear that the rms value of load voltage is 230 volts in simulation results while it is 236.1 volts in experimental results. Similarly, the rms value of load current is 0.652 A and 0.707 A in simulation and experimental results respectively. The nature of the load voltage and load current are also similar as shown in Figure 5.12(a) and Figure 5.12(b).

On the basis of monthly average typical load profile, average solar irradiation profile, and average wind speed profile, as shown in Figure 2.6, 2.8 and 2.10 respectively of Kukas area diesel power requirement is calculated for different contribution level of solar and wind power.

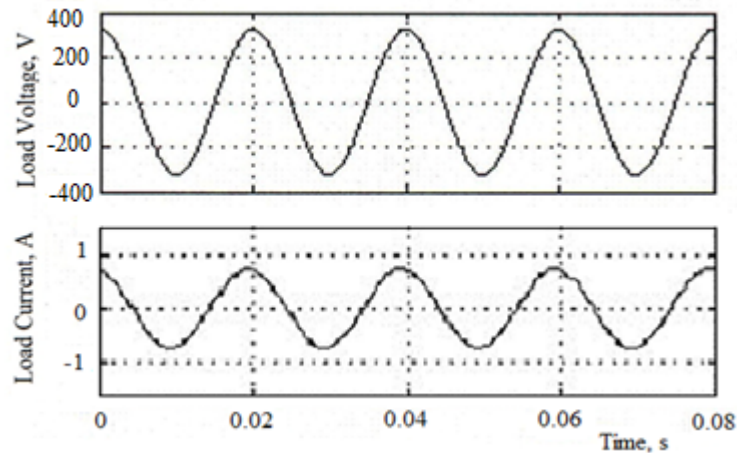
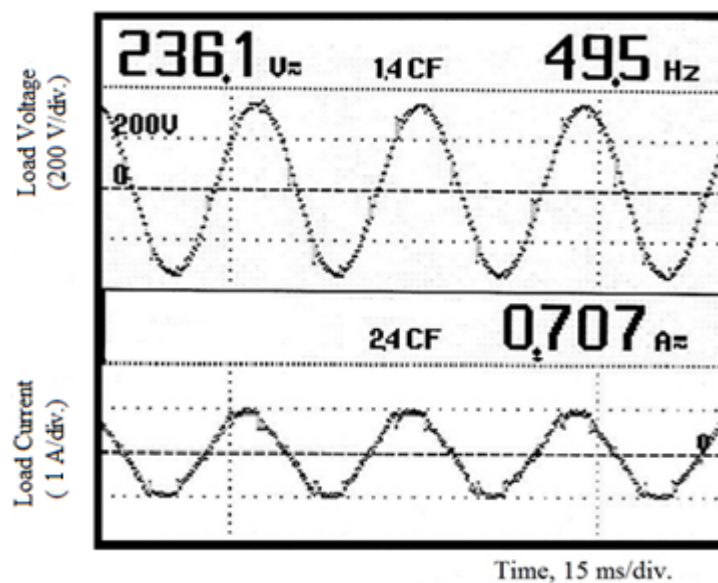
(a) Simulated ($V_{\text{rms}}=230$ volt, $I_{\text{rms}}=0.652$ Amp)(b) Experimental ($V_{\text{rms}}=236.1$ volt, $I_{\text{rms}}=0.707$ Amp)

Figure 5.12 Load Voltage and Load Current for PMSG of proposed hybrid system

Table 5.1 to Table 5.4 show the diesel power requirement with solar and wind power contribution in summer season. Table 5.5 to Table 5.8 show the diesel power requirement with solar and wind power contribution in rainy season. Similarly, Table 5.9 to Table 5.12 show the diesel power requirement with solar and wind power contribution, in winter season.

It is clear from Tables 5.1 to 5.12; positive values show the shortage of energy from the renewable sources *i.e.* DG operation is required. First priority is to be given to battery over DG; however battery is able to provide one day autonomy if it is charged with 3072 watt-hr capacity on previous day.

Table 5.1 Diesel power requirement (in watt-hr) with average solar and wind power contribution in the **Month of March**

Average Solar Power Available : 6300 watt-hr Average Wind Power Available : 3658 watt-hr Load Requirement : 4607 watt-hr												
		Solar Power Contribution										
		0%	10%	20%	30%	40%	50%	60%	70%	80%	90%	100%
Wind Power Contribution	0%	4607	3977	3347	2717	2087	1457	827	197	-433	-1063	-1693
	10%	4241.2	3611.2	2981.2	2351.2	1721.2	1091.2	461.2	-168.8	-798.8	-1428.8	-2058.8
	20%	3875.4	3245.4	2615.4	1985.4	1355.4	725.4	95.4	-534.6	-1164.6	-1794.6	-2424.6
	30%	3509.6	2879.6	2249.6	1619.6	989.6	359.6	-270.4	-900.4	-1530.4	-2160.4	-2790.4
	40%	3143.8	2513.8	1883.8	1253.8	623.8	-6.2	-636.2	-1266.2	-1896.2	-2526.2	-3156.2
	50%	2778	2148	1518	888	258	-372	-1367.8	-1632	-2262	-2892	-3522
	60%	2412.2	1782.2	1152.2	522.2	-107.8	-737.8	-1367.8	-1997.8	-2627.8	-3257.8	-3887.8
	70%	2046.4	1416.4	786.4	156.4	-473.6	-1103.6	-1733.6	-2363.6	-2993.6	-3623.6	-4253.6
	80%	1680.6	1050.6	420.6	-209.4	-839.4	-1469.4	-2099.4	-2729.4	-3359.4	-3989.4	-4619.4
	90%	1314.8	684.8	54.8	-575.2	-1205.2	-1835.2	-2465.2	-3095.2	-3725.2	-4355.2	-4985.2
100%	949	319	-311	-941	-1571	-2201	-2831	-3461	-4091	-4721	-5351	

Table 5.2 Diesel power requirement (in watt-hr) with average solar and wind power contribution in the **Month of April**

Average Solar Power Available : 6525 watt-hr Average Wind Power Available : 3270 watt-hr Load Requirement : 4607 watt-hr												
		Solar Power Contribution										
		0%	10%	20%	30%	40%	50%	60%	70%	80%	90%	100%
Wind Power Contribution	0%	4607	3954.5	3302	2649.5	1997	1344.5	692	39.5	-613	-1265.5	-1918
	10%	4280	3627.5	2975	2322.5	1670	1017.5	365	-287.5	-940	-1592.5	-2245
	20%	3953	3300.5	2648	1995.5	1343	690.5	38	-614.5	-1267	-1919.5	-2572
	30%	3626	2973.5	2321	1668.5	1016	363.5	-289	-941.5	-1594	-2246.5	-2899
	40%	3299	2646.5	1994	1341.5	689	36.5	-616	-1268.5	-1921	-2573.5	-3226
	50%	2972	2319.5	1667	1014.5	362	-290.5	-1270	-1595.5	-2248	-2900.5	-3553
	60%	2645	1992.5	1340	687.5	35	-617.5	-1270	-1922.5	-2575	-3227.5	-3880
	70%	2318	1665.5	1013	360.5	-292	-944.5	-1597	-2249.5	-2902	-3554.5	-4207
	80%	1991	1338.5	686	33.5	-619	-1271.5	-1924	-2576.5	-3229	-3881.5	-4534
	90%	1664	1011.5	359	-293.5	-946	-1598.5	-2251	-2903.5	-3556	-4208.5	-4861
100%	1337	684.5	32	-620.5	-1273	-1925.5	-2578	-3230.5	-3883	-4535.5	-5188	

Table 5.3 Diesel power requirement (in watt-hr) with average solar and wind power contribution in the Month of May

Average Solar Power Available : 6525 watt-hr Average Wind Power Available : 3658 watt-hr Load Requirement : 4607 watt-hr												
		Solar Power Contribution										
		0%	10%	20%	30%	40%	50%	60%	70%	80%	90%	100%
Wind Power Contribution	0%	4607	3954.5	3302	2649.5	1997	1344.5	692	39.5	-613	-1265.5	-1918
	10%	4241.2	3588.7	2936.2	2283.7	1631.2	978.7	326.2	-326.3	-978.8	-1631.3	-2283.8
	20%	3875.4	3222.9	2570.4	1917.9	1265.4	612.9	-39.6	-692.1	-1344.6	-1997.1	-2649.6
	30%	3509.6	2857.1	2204.6	1552.1	899.6	247.1	-405.4	-1057.9	-1710.4	-2362.9	-3015.4
	40%	3143.8	2491.3	1838.8	1186.3	533.8	-118.7	-771.2	-1423.7	-2076.2	-2728.7	-3381.2
	50%	2778	2125.5	1473	820.5	168	-484.5	-1502.8	-1789.5	-2442	-3094.5	-3747
	60%	2412.2	1759.7	1107.2	454.7	-197.8	-850.3	-1502.8	-2155.3	-2807.8	-3460.3	-4112.8
	70%	2046.4	1393.9	741.4	88.9	-563.6	-1216.1	-1868.6	-2521.1	-3173.6	-3826.1	-4478.6
	80%	1680.6	1028.1	375.6	-276.9	-929.4	-1581.9	-2234.4	-2886.9	-3539.4	-4191.9	-4844.4
	90%	1314.8	662.3	9.8	-642.7	-1295.2	-1947.7	-2600.2	-3252.7	-3905.2	-4557.7	-5210.2
	100%	949	296.5	-356	-1008.5	-1661	-2313.5	-2966	-3618.5	-4271	-4923.5	-5576

Table 5.4 Diesel power requirement (in watt-hr) with average solar and wind power contribution in the Month of June

Average Solar Power Available : 6615 watt-hr Average Wind Power Available : 4014 watt-hr Load Requirement : 4607 watt-hr												
		Solar Power Contribution										
		0%	10%	20%	30%	40%	50%	60%	70%	80%	90%	100%
Wind Power Contribution	0%	4607	3945.5	3284	2622.5	1961	1299.5	638	-23.5	-685	-1346.5	-2008
	10%	4205.6	3544.1	2882.6	2221.1	1559.6	898.1	236.6	-424.9	-1086.4	-1747.9	-2409.4
	20%	3804.2	3142.7	2481.2	1819.7	1158.2	496.7	-164.8	-826.3	-1487.8	-2149.3	-2810.8
	30%	3402.8	2741.3	2079.8	1418.3	756.8	95.3	-566.2	-1227.7	-1889.2	-2550.7	-3212.2
	40%	3001.4	2339.9	1678.4	1016.9	355.4	-306.1	-967.6	-1629.1	-2290.6	-2952.1	-3613.6
	50%	2600	1938.5	1277	615.5	-46	-707.5	-1770.4	-2030.5	-2692	-3353.5	-4015
	60%	2198.6	1537.1	875.6	214.1	-447.4	-1108.9	-1770.4	-2431.9	-3093.4	-3754.9	-4416.4
	70%	1797.2	1135.7	474.2	-187.3	-848.8	-1510.3	-2171.8	-2833.3	-3494.8	-4156.3	-4817.8
	80%	1395.8	734.3	72.8	-588.7	-1250.2	-1911.7	-2573.2	-3234.7	-3896.2	-4557.7	-5219.2
	90%	994.4	332.9	-328.6	-990.1	-1651.6	-2313.1	-2974.6	-3636.1	-4297.6	-4959.1	-5620.6
	100%	593	-68.5	-730	-1391.5	-2053	-2714.5	-3376	-4037.5	-4699	-5360.5	-6022

Table 5.5 Diesel power requirement (in watt-hr) with average solar and wind power contribution in the Month of July

Average Solar Power Available : 4230 watt-hr Average Wind Power Available : 3270 watt-hr Load Requirement : 3532 watt-hr												
		Solar Power Contribution										
		0%	10%	20%	30%	40%	50%	60%	70%	80%	90%	100%
Wind Power Contribution	0%	3532	3109	2686	2263	1840	1417	994	571	148	-275	-698
	10%	3205	2782	2359	1936	1513	1090	667	244	-179	-602	-1025
	20%	2878	2455	2032	1609	1186	763	340	-83	-506	-929	-1352
	30%	2551	2128	1705	1282	859	436	13	-410	-833	-1256	-1679
	40%	2224	1801	1378	955	532	109	-314	-737	-1160	-1583	-2006
	50%	1897	1474	1051	628	205	-218	-968	-1064	-1487	-1910	-2333
	60%	1570	1147	724	301	-122	-545	-968	-1391	-1814	-2237	-2660
	70%	1243	820	397	-26	-449	-872	-1295	-1718	-2141	-2564	-2987
	80%	916	493	70	-353	-776	-1199	-1622	-2045	-2468	-2891	-3314
	90%	589	166	-257	-680	-1103	-1526	-1949	-2372	-2795	-3218	-3641
100%	262	-161	-584	-1007	-1430	-1853	-2276	-2699	-3122	-3545	-3968	

Table 5.6 Diesel power requirement (in watt-hr) with average solar and wind power contribution in the Month of August

Average Solar Power Available : 4095 watt-hr Average Wind Power Available : 2430 watt-hr Load Requirement : 3532 watt-hr												
		Solar Power Contribution										
		0%	10%	20%	30%	40%	50%	60%	70%	80%	90%	100%
Wind Power Contribution	0%	3532	3122.5	2713	2303.5	1894	1484.5	1075	665.5	256	-153.5	-563
	10%	3289	2879.5	2470	2060.5	1651	1241.5	832	422.5	13	-396.5	-806
	20%	3046	2636.5	2227	1817.5	1408	998.5	589	179.5	-230	-639.5	-1049
	30%	2803	2393.5	1984	1574.5	1165	755.5	346	-63.5	-473	-882.5	-1292
	40%	2560	2150.5	1741	1331.5	922	512.5	103	-306.5	-716	-1125.5	-1535
	50%	2317	1907.5	1498	1088.5	679	269.5	-383	-549.5	-959	-1368.5	-1778
	60%	2074	1664.5	1255	845.5	436	26.5	-383	-792.5	-1202	-1611.5	-2021
	70%	1831	1421.5	1012	602.5	193	-216.5	-626	-1035.5	-1445	-1854.5	-2264
	80%	1588	1178.5	769	359.5	-50	-459.5	-869	-1278.5	-1688	-2097.5	-2507
	90%	1345	935.5	526	116.5	-293	-702.5	-1112	-1521.5	-1931	-2340.5	-2750
100%	1102	692.5	283	-126.5	-536	-945.5	-1355	-1764.5	-2174	-2583.5	-2993	

Table 5.7 Diesel power requirement (in watt-hr) with average solar and wind power contribution in the Month of September

Average Solar Power Available : 3695 watt-hr Average Wind Power Available : 2280 watt-hr Load Requirement : 3532 watt-hr												
		Solar Power Contribution										
		0%	10%	20%	30%	40%	50%	60%	70%	80%	90%	100%
Wind Power Contribution	0%	3532	3162.5	2793	2423.5	2054	1684.5	1315	945.5	576	206.5	-163
	10%	3304	2934.5	2565	2195.5	1826	1456.5	1087	717.5	348	-21.5	-391
	20%	3076	2706.5	2337	1967.5	1598	1228.5	859	489.5	120	-249.5	-619
	30%	2848	2478.5	2109	1739.5	1370	1000.5	631	261.5	-108	-477.5	-847
	40%	2620	2250.5	1881	1511.5	1142	772.5	403	33.5	-336	-705.5	-1075
	50%	2392	2022.5	1653	1283.5	914	544.5	-53	-194.5	-564	-933.5	-1303
	60%	2164	1794.5	1425	1055.5	686	316.5	-53	-422.5	-792	-1161.5	-1531
	70%	1936	1566.5	1197	827.5	458	88.5	-281	-650.5	-1020	-1389.5	-1759
	80%	1708	1338.5	969	599.5	230	-139.5	-509	-878.5	-1248	-1617.5	-1987
	90%	1480	1110.5	741	371.5	2	-367.5	-737	-1106.5	-1476	-1845.5	-2215
	100%	1252	882.5	513	143.5	-226	-595.5	-965	-1334.5	-1704	-2073.5	-2443

Table 5.8 Diesel power requirement (in watt-hr) with average solar and wind power contribution in the Month of October

Average Solar Power Available : 3425 watt-hr Average Wind Power Available : 980 watt-hr Load Requirement : 3532 watt-hr												
		Solar Power Contribution										
		0%	10%	20%	30%	40%	50%	60%	70%	80%	90%	100%
Wind Power Contribution	0%	3532	3189.5	2847	2504.5	2162	1819.5	1477	1134.5	792	449.5	107
	10%	3434	3091.5	2749	2406.5	2064	1721.5	1379	1036.5	694	351.5	9
	20%	3336	2993.5	2651	2308.5	1966	1623.5	1281	938.5	596	253.5	-89
	30%	3238	2895.5	2553	2210.5	1868	1525.5	1183	840.5	498	155.5	-187
	40%	3140	2797.5	2455	2112.5	1770	1427.5	1085	742.5	400	57.5	-285
	50%	3042	2699.5	2357	2014.5	1672	1329.5	889	644.5	302	-40.5	-383
	60%	2944	2601.5	2259	1916.5	1574	1231.5	889	546.5	204	-138.5	-481
	70%	2846	2503.5	2161	1818.5	1476	1133.5	791	448.5	106	-236.5	-579
	80%	2748	2405.5	2063	1720.5	1378	1035.5	693	350.5	8	-334.5	-677
	90%	2650	2307.5	1965	1622.5	1280	937.5	595	252.5	-90	-432.5	-775
	100%	2552	2209.5	1867	1524.5	1182	839.5	497	154.5	-188	-530.5	-873

Table 5.9 Diesel power requirement (in watt-hr) with average solar and wind power contribution in the **Month of November**

Average Solar Power Available : 3442 watt-hr Average Wind Power Available : 2430 watt-hr Load Requirement : 1999 watt-hr												
		Solar Power Contribution										
		0%	10%	20%	30%	40%	50%	60%	70%	80%	90%	100%
Wind Power Contribution	0%	1999	1654.8	1310.6	966.4	622.2	278	-66.2	-410.4	-754.6	-1098.8	-1443
	10%	1756	1411.8	1067.6	723.4	379.2	35	-309.2	-653.4	-997.6	-1341.8	-1686
	20%	1513	1168.8	824.6	480.4	136.2	-208	-552.2	-896.4	-1240.6	-1584.8	-1929
	30%	1270	925.8	581.6	237.4	-106.8	-451	-795.2	-1139.4	-1483.6	-1827.8	-2172
	40%	1027	682.8	338.6	-5.6	-349.8	-694	-1038.2	-1382.4	-1726.6	-2070.8	-2415
	50%	784	439.8	95.6	-248.6	-592.8	-937	-1524.2	-1625.4	-1969.6	-2313.8	-2658
	60%	541	196.8	-147.4	-491.6	-835.8	-1180	-1524.2	-1868.4	-2212.6	-2556.8	-2901
	70%	298	-46.2	-390.4	-734.6	-1078.8	-1423	-1767.2	-2111.4	-2455.6	-2799.8	-3144
	80%	55	-289.2	-633.4	-977.6	-1321.8	-1666	-2010.2	-2354.4	-2698.6	-3042.8	-3387
	90%	-188	-532.2	-876.4	-1220.6	-1564.8	-1909	-2253.2	-2597.4	-2941.6	-3285.8	-3630
100%	-431	-775.2	-1119.4	-1463.6	-1807.8	-2152	-2496.2	-2840.4	-3184.6	-3528.8	-3873	

Table 5.10 Diesel power requirement (in watt-hr) with average solar and wind power contribution in the **Month of December**

Average Solar Power Available : 3082 watt-hr Average Wind Power Available : 2430 watt-hr Load Requirement : 1999 watt-hr												
		Solar Power Contribution										
		0%	10%	20%	30%	40%	50%	60%	70%	80%	90%	100%
Wind Power Contribution	0%	1999	1690.8	1382.6	1074.4	766.2	458	149.8	-158.4	-466.6	-774.8	-1083
	10%	1756	1447.8	1139.6	831.4	523.2	215	-93.2	-401.4	-709.6	-1017.8	-1326
	20%	1513	1204.8	896.6	588.4	280.2	-28	-336.2	-644.4	-952.6	-1260.8	-1569
	30%	1270	961.8	653.6	345.4	37.2	-271	-579.2	-887.4	-1195.6	-1503.8	-1812
	40%	1027	718.8	410.6	102.4	-205.8	-514	-822.2	-1130.4	-1438.6	-1746.8	-2055
	50%	784	475.8	167.6	-140.6	-448.8	-757	-1308.2	-1373.4	-1681.6	-1989.8	-2298
	60%	541	232.8	-75.4	-383.6	-691.8	-1000	-1308.2	-1616.4	-1924.6	-2232.8	-2541
	70%	298	-10.2	-318.4	-626.6	-934.8	-1243	-1551.2	-1859.4	-2167.6	-2475.8	-2784
	80%	55	-253.2	-561.4	-869.6	-1177.8	-1486	-1794.2	-2102.4	-2410.6	-2718.8	-3027
	90%	-188	-496.2	-804.4	-1112.6	-1420.8	-1729	-2037.2	-2345.4	-2653.6	-2961.8	-3270
100%	-431	-739.2	-1047.4	-1355.6	-1663.8	-1972	-2280.2	-2588.4	-2896.6	-3204.8	-3513	

Table 5.11 Diesel power requirement (in watt-hr) with average solar and wind power contribution in the Month of January

Average Solar Power Available : 3082 watt-hr Average Wind Power Available : 1580 watt-hr Load Requirement : 1999 watt-hr												
		Solar Power Contribution										
		0%	10%	20%	30%	40%	50%	60%	70%	80%	90%	100%
Wind Power Contribution	0%	1999	1690.8	1382.6	1074.4	766.2	458	149.8	-158.4	-466.6	-774.8	-1083
	10%	1841	1532.8	1224.6	916.4	608.2	300	-8.2	-316.4	-624.6	-932.8	-1241
	20%	1683	1374.8	1066.6	758.4	450.2	142	-166.2	-474.4	-782.6	-1090.8	-1399
	30%	1525	1216.8	908.6	600.4	292.2	-16	-324.2	-632.4	-940.6	-1248.8	-1557
	40%	1367	1058.8	750.6	442.4	134.2	-174	-482.2	-790.4	-1098.6	-1406.8	-1715
	50%	1209	900.8	592.6	284.4	-23.8	-332	-798.2	-948.4	-1256.6	-1564.8	-1873
	60%	1051	742.8	434.6	126.4	-181.8	-490	-798.2	-1106.4	-1414.6	-1722.8	-2031
	70%	893	584.8	276.6	-31.6	-339.8	-648	-956.2	-1264.4	-1572.6	-1880.8	-2189
	80%	735	426.8	118.6	-189.6	-497.8	-806	-1114.2	-1422.4	-1730.6	-2038.8	-2347
	90%	577	268.8	-39.4	-347.6	-655.8	-964	-1272.2	-1580.4	-1888.6	-2196.8	-2505
	100%	419	110.8	-197.4	-505.6	-813.8	-1122	-1430.2	-1738.4	-2046.6	-2354.8	-2663

Table 5.12 Diesel power requirement (in watt-hr) with average solar and wind power contribution in the Month of February

Average Solar Power Available : 3442 watt-hr Average Wind Power Available : 2430 watt-hr Load Requirement : 1999 watt-hr												
		Solar Power Contribution										
		0%	10%	20%	30%	40%	50%	60%	70%	80%	90%	100%
Wind Power Contribution	0%	1999	1654.8	1310.6	966.4	622.2	278	-66.2	-410.4	-754.6	-1098.8	-1443
	10%	1756	1411.8	1067.6	723.4	379.2	35	-309.2	-653.4	-997.6	-1341.8	-1686
	20%	1513	1168.8	824.6	480.4	136.2	-208	-552.2	-896.4	-1240.6	-1584.8	-1929
	30%	1270	925.8	581.6	237.4	-106.8	-451	-795.2	-1139.4	-1483.6	-1827.8	-2172
	40%	1027	682.8	338.6	-5.6	-349.8	-694	-1038.2	-1382.4	-1726.6	-2070.8	-2415
	50%	784	439.8	95.6	-248.6	-592.8	-937	-1524.2	-1625.4	-1969.6	-2313.8	-2658
	60%	541	196.8	-147.4	-491.6	-835.8	-1180	-1524.2	-1868.4	-2212.6	-2556.8	-2901
	70%	298	-46.2	-390.4	-734.6	-1078.8	-1423	-1767.2	-2111.4	-2455.6	-2799.8	-3144
	80%	55	-289.2	-633.4	-977.6	-1321.8	-1666	-2010.2	-2354.4	-2698.6	-3042.8	-3387
	90%	-188	-532.2	-876.4	-1220.6	-1564.8	-1909	-2253.2	-2597.4	-2941.6	-3285.8	-3630
	100%	-431	-775.2	-1119.4	-1463.6	-1807.8	-2152	-2496.2	-2840.4	-3184.6	-3528.8	-3873

In Tables 5.1 to 5.12, autonomy day is represented by pink color cells. However, this is to be possible only in those cases where solar and wind contribution is more than 70% in summer season, 90% in rainy season and 90% in winter season which is not possible continuously for every day.

Similarly, available extra power for charging the battery bank after supplying the load is shown in Tables 5.1 to 5.12 with blue color cells. However, this is to be possible only those cases when solar and wind contribution is more than 40% in summer season, 50% in rainy season and 50% in winter season.

It is clear from Tables 5.1 to 5.12 that average load requirement is less in rainy and winter seasons as compared to summer season *i.e.* 76.7% and 43.4% *w.r.t.* summer season respectively. However, solar and wind powers are also less available as compared to summer season. Hence, DG operation is highly depends on the average load requirement of the day and contribution of solar and wind power. It is observed from Tables 5.1 to 5.12 that as contribution of solar and wind powers are increased, corresponding DG requirement is decreased.

It is also clear from the Tables 5.1 to 5.12 that the diesel requirement is less, when contribution of wind power is zero as compared to the condition when solar contribution is zero at Kukas area. This is due the reason that the wind speed profile at Kukas area is poor as compared to solar irradiation profile. Therefore, a combination of solar, wind and DG power is proposed in Kukas area to fulfill the load demand with less consumption of diesel.

5.4 CONCLUSIONS

In this chapter, hardware prototype of solar-wind-battery-diesel generator hybrid system has been presented. Various hardware results are compared with simulated results of proposed system.

On the basis of monthly solar irradiation profile, wind speed profile and typical load profile (in the Kukas area)required DG power is calculated for different contribution level of solar and wind power for summer, rainy and winter seasons.

Hence, on the basis of this analysis it is recommended that, stand-alone solar-wind-battery-diesel generator hybrid system is optimally suitable for fulfilling the typical load demand of a remote location by minimizing the use of diesel generator power and maximizing the use of solar and wind power.

Chapter 6

Main Conclusions and Suggestions for Further Work

T HIS chapter summarizes the thesis by outlining the major contributions and findings from the research. It further proposes some future works that can be done to improve incorporations of Hybrid Energy Systems in rural areas.

CHAPTER 6

MAIN CONCLUSIONS AND SUGGESTIONS FOR FURTHER WORK

6.1 GENERAL

Hybrid Energy Systems (HESs) are emerging as the most popular and effective solution for energy issues encountered in many parts of the world. HES can be installed either as grid connected systems or stand-alone systems depending upon the requirements. Stand-alone HESs which include renewable energy sources serve as reliable and clean sources of energy and have huge scope, especially in areas that are isolated and not connected to the utility grid. The prospect of supplying electrical energy to an off-grid rural village using suitably designed stand-alone hybrid system has been investigated in this thesis. The site selected for this study is Kukas, which is a village near Jaipur, Rajasthan, India. A stand-alone HES with solar PV system, wind power system, a battery storage and a diesel generator has been proposed to cater the electrical energy requirements of the village.

6.2 MAIN CONCLUSIONS

Initially, the mathematical model of each component of HESs is developed for clear understanding of their characteristics. The seasonal load profile (i.e. summer, rainy and winter seasons) of the selected area has been investigated. The solar irradiation data, wind speed data and other associated data required for system analysis have been recorded for all the months considering seasonal variations in the year 2014. The initial investment required in HESs for a rural setup with a low energy demand may be comparatively higher especially when components like a diesel generator and a battery bank are involved.

To examine the behavior of the system under varying load demand, simulation model of various HES and their components have been developed in MATLAB/Simulink platform. Performance of the each HES is investigated for a typical day of each season, for the given load profile, solar radiation data, wind speed data and other

relevant input data to the model. The power shared by each source and the battery with respect to time has also been investigated.

From the obtained results, it is concluded that use of solar PV as a stand-alone system to supply the load is not a practical and economical system. Higher capacities of PV array and battery bank are required to meet the varying load demand due to low solar irradiation profile in rainy and winter seasons. It is also observed that stand-alone wind system is also not a good choice because of unavailability of continuous wind throughout the year. Therefore, a higher capacity of a wind turbine and a battery bank is required to meet the load demand. Stand-alone diesel generator system, solar-battery-diesel generator hybrid system and wind-battery-diesel generator hybrid system need to run the diesel generator for more time in a day. Hence, large quantity of diesel fuel is required with more maintenance and high operating cost as well as more CO₂ is produced which pollutes the environment. However, the use of a solar PV system and/or a wind energy system with a diesel generator reduces the above problems at an acceptable level. Another main advantage of the diesel generator in stand-alone solar-wind system is to provide back up to ensure continuous power supply.

Using the same model, the response of the system for sudden load increase or decrease has been obtained by simulating the varying load conditions for four different cases such as solar-wind-battery hybrid system, solar-battery-diesel generator hybrid system, wind-battery-diesel generator hybrid system and solar-wind-battery-diesel generator hybrid system. From the performance analysis, it is concluded that the proposed stand-alone solar-wind-battery-diesel generator hybrid system is successful in meeting the load requirements of the village throughout the year and handles the variations in load profile as well as transient load conditions effectively.

Hence, the proposed work has demonstrated successfully, the suitability and effectiveness of the solar-wind-battery-diesel generator based stand-alone hybrid system for Kukas village, and has established that the proposed hybrid system is indeed a clean, reliable and economical solution for supplying energy to such off-grid villages.

6.3 SUGGESTIONS FOR FURTHER WORK

This thesis offers scope for further studies which enhances the feasibility and applicability of the hybrid energy systems. Some of the areas where there is potential for conducting further study have been as follows:

A prototype model of the present work can successfully be implemented for catering the energy needs of the Institute. For institutes, the hybrid energy system could be developed as grid connected in place of stand-alone systems, which would further reduce the operating cost of the system.

The present system can be augmented using other renewable sources of energy such as fuel cell, small hydro, bio-mass gasifier etc. depending on the features of the site, which would further increase the capacity of the system and improve its reliability.

For the optimal sizing and operation of the HES, a dedicated program can be developed using any heuristic optimization technique, considering the hourly load profile of the site along with all the constraints of the sources and the suitable power dispatch strategy.

References

REFERENCES

- [1] Kamil. Kaygusuz, "Energy for sustainable development: Key issues and challenges," *Energy Sources, Part B: Economics, Planning, and Policy* 2.1,73-83, 2007.
- [2] I. Yüksel, "Development of hydropower: a case study in developing countries," *Energy Sources, Part B* 2, no. 2,113-121, 2007.
- [3] M. R. Patel, "Wind and solar power systems," CRC Press, 1999, New York.
- [4] F. Jurado and J. Saenz, "Possibilities for biomass-based power plant and wind system integration," *Energy*, vol. 27, no. 10, pp. 955-966, 2002.
- [5] G. C. Bakos, "Feasibility study of a hybrid wind/hydro power-system for low-cost electricity production," *Appl Energy*, no. 72, pp. 599-608, 2002.
- [6] H. Khatib, "Renewable energy in developing countries," *Renewable Energy Conference*, Publication no. 385, @ IEE, pp 1-6, Nov. 1993.
- [7] Gary L. Johnson, "Wind energy system," Phi, 2001.
- [8] T J Hammons, "Renewable energy," In-Tech, 2009.
- [9] Baldev Raj Nayar, "Globalization and India's Economic Integration," Georgetown University Press, 2014.
- [10] MNRE (Ministry of New and Renewable Energy), "Strategic Plan for New and Renewable energy sector for the period of 2011-2017," Government of India, New Delhi, 2013. <http://www.mnre.gov.in/information/policies-2/>.
- [11] Ministry of Statistics and Programme Implementation, "Energy statistics 2013 (twentieth issue),"Government of India, New Delhi, 2014. http://mospi.nic.in/mospi.new upload/energy_statistics_2013.pdf.
- [12] Ministry of Power Central Electricity Authority, "Executive summary power sector September 2015," Government of India, New Delhi,2015. <http://www.cea.nic.in/reports/monthly/ executive summary/sept15.pdf>.
- [13] Pandey, Shreemat, et al. , "Determinants of success for promoting solar energy in Rajasthan, India," *Renewable and Sustainable Energy Reviews*, vol.16, no. 6, pp: 3593-3598, 2012.
- [14] Ahmed-Mahmoud, Ashraf, "Power conditioning unit for small scale hybrid PV-wind generation system," Ph.D. dissertation, Durham University, 2011.

- [15] Mahmoud Salah Ismail Abdel-Qader, "Simulation of a hybrid power system consisting of wind turbine, PV, storage battery and diesel generator with compensation network: design, optimization and economical evaluation," An-Najah National University, Palestine, 2008.
- [16] H. G. Beyer and C. Langer, "A method for the identification of configurations of PV /wind hybrid systems for the reliable supply of small loads," *Solar Energy*, vol. 57, no. 5, pp. 381-391, 1996.
- [17] B. Wichert, "PV–diesel hybrid energy systems for remote area power generation—A review of current practices and future developments," *Renew Sustain Energy Rev*, vol. 1, no. 3, pp. 209-228, 1997.
- [18] W. D. Kellogg, M. H. Nehrir, G. Venkataramanan and V. Gerez, "Generation unit sizing and cost analysis for stand-alone wind photovoltaic and hybrid wind/PV systems," *IEEE Trans. on Energy Conversion*, vol. 13, no. 1, pp. 70-75, 1998.
- [19] R. Chedid, H. Akiki H and S. Rahman, "A decision support technique for the design of hybrid solar–wind power systems," *IEEE Trans. on Energy Conversion*, vol. 13, no. 1, pp. 76-83, 1998.
- [20] A.G. Bhave, "Hybrid solar–wind domestic power generating system - A case study," *Science Direct Journal on Renewable Energy*, vol. 17, no. 3, pp.355-358, 1999.
- [21] S. H. El-Hefnawi, "Photovoltaic diesel–generator hybrid power system sizing," *Science Direct Journal on Renewable Energy*, vol. 13, no. 1, pp. 33-40, 1998.
- [22] M. A. Elhadidy and S. M. Shaahid, "Optimal sizing of battery storage for hybrid power systems," *Science Direct Journal on Renewable Energy*, vol. 18, no. 1, pp. 77-86, 1999.
- [23] E.S. Abdin, A.M. Osheiba and M.M. Khater, "Modeling and optimal controllers design for a stand-alone photovoltaic-diesel generating unit," *IEEE Trans. on Energy Conversion*, vol. 14, no. 3, pp.560 – 565, Sept. 1999.
- [24] S. H. Karaki, R. B. Chedid and R. Ramadan, "Probabilistic production costing of diesel–wind energy conversion systems," *IEEE Trans. on Energy Conversion*, vol. 15, no. 3, pp.284 – 289, 2000.
- [25] F. Jurado, J. R. Saenz, "Neuro-fuzzy control for autonomous wind–diesel systems using biomass," *Science Direct Journal on Renewable Energy*, vol. 27, no. 1, pp.39 – 56, 2002.

- [26] Swati Negi and Lini Methew, "Hybrid renewable energy system: a review," *International Journal of Electronic and Electrical Engineering*, vol. 7, no. 5, pp.535-542, 2014.
- [27] A.N. Celik, "Techno-economic analysis of autonomous PV-Wind hybrid energy systems using different sizing methods," *Energy Conversion and Management*, vol. 44, no. 12, pp. 1951-1968, 2003.
- [28] A. Bin, Y. Hongxing, S. Hui and L. Xianbo, "Computer Aided Design for PV/Wind Hybrid system," in *Proc. of 3rd World Conference on Photovoltaic Energy Conversion*, vol. 3, pp. 2411- 2414, 2003.
- [29] B. Ai, H. Yang, H. Shen and X. Liao, "Computer-aided design of PV/wind hybrid system," *Science Direct Journal on Renewable Energy*, vol. 28, no. 10, pp.1491 – 1512, 2003.
- [30] F. Valenciaga, P. F. Puleston and P. E. Battaiotto, "Power control of solar/wind generation system without wind measurement: a passive/sliding mode approach," *IEEE Trans. on Energy Conversion*, vol. 18, no. 4, pp.501–507, 2003.
- [31] F. Jurado and J. R. Saenz, "An adaptive control scheme for biomass-based diesel–wind system," *Science Direct Journal on Renewable Energy*, vol. 28, no. 1, pp.45 – 57, 2003.
- [32] S. M. Shaahid and M. A. Elhadidy, "Opportunities for utilization of stand-alone hybrid power systems in hot climates," *Science Direct Journal on Renewable Energy*, vol. 28, no. 11, pp.1741 – 1753, 2003.
- [33] J. Eto, V. Budhraj, C. Martinez, J. Dyer and M. Kondragunta, "Research, development, and demonstration needs for large-scale, reliability-enhancing, integration of distributed energy resources," *33rd Annual Hawaii International Conference*, pp.7, 4 - 7 Jan. 2000.
- [34] R. Karki and R. Billinton, "Reliability/cost implications of PV and wind energy utilization in small isolated power systems," *IEEE Trans. on Energy Conversion*, vol. 16, no. 4, pp. 368-373, 2001.
- [35] H. X. Yang, L. Lu and J. Burnett, "Weather data and probability analysis of hybrid photovoltaic–wind power generation systems in Hong Kong," *Science Direct Journal on Renewable Energy*, vol. 28, no. 11, pp.1813–24, 2003.

- [36] M. Muselli, G. Notton, P. Poggi and A. Louche, "PV-hybrid power systems sizing incorporating battery storage: An analysis via simulation calculations," *Science Direct Journal on Renewable Energy*, vol. 20, no. 1, pp-1-7, 2000.
- [37] M. H. Rashid, "Power electronics handbook," Elsevier, 2011, U.K.
- [38] Wu, B., Lang, Y., Zargari, N. and S. Kouro, "Power conversion and control of wind energy systems," Wiley, 2011.
- [39] S. Heier, "Grid integration of wind energy conversion systems," Wiley, 2006.
- [40] S. J. Chiang, K. T. Chang and C. Y. Yen, "Residential Photovoltaic Energy Storage System," *IEEE Trans. on Industrial Electronics*, vol. 45, no. 3, pp 385-394, Jun. 1998.
- [41] GB. Shrestha and L. Goel, "A study on optimal sizing of stand-alone photovoltaic stations," *IEEE Trans. on Energy Conversion*, vol. 13, no. 4, pp373-378, 1998.
- [42] J. A. Gow and C. D. Manning, "Development of a photovoltaic array model for use in power-electronics simulation studies," *IEE Proc. Elect. Power Appl.*, vol. 146, no. 2, pp. 193-200, 1999.
- [43] M. A. S. Masoum, S. M. M. Badejani, and E. F. Fuchs, "Microprocessor-controlled new class of optimal battery chargers for photovoltaic applications," *IEEE Trans. on Energy Conversion*, vol. 19, no. 3, pp.599 – 606, Sep. 2004.
- [44] J. T. Bialasiewicz, "Renewable energy systems with photovoltaic power generators: operation and modeling," *IEEE Trans. on Industrial Electronics*, vol. 55, no. 7, pp 2752-2758, Jul. 2008.
- [45] S. M. Shaahid and M. A. Elhadidy, "Prospects of autonomous/stand-alone hybrid power systems in commercial applications in hot regions," *Science Direct Journal on Renewable Energy*, vol. 29, no. 2, pp.165 – 177, 2004.
- [46] M. Purk, B. T. Kim and I. K. Yu, "Novel Simulation Method for PV Power Generation Systems Using Real Weather Conditions," 0-7803-7090-2/01@ *IEEE*, pp 526-530, 2001.
- [47] K. Ogawa and F. Aratani, "Present status of research and development of PV technology in Japan," in *Proc.of Twenty-Ninth IEEE PSC*, pp. 3-7, 19-24 May 2002.
- [48] E. V. R. Sastry, "The photovoltaic program in India," 0-7803-7471-1/02@ *IEEE*, pp 28-31, 2002.

- [49] A. H. Abdullah, A. A. Ghoneim, and A.Y. Hasan, "Assessment of grid-connected photovoltaic systems in the Kuwaiti climate," *Science Direct Journal on Renewable Energy*, vol. 26, no. 2, pp-189-99, 2002.
- [50] Dr. A. Moussi, A. Saadi, A. Betka and G.M. Asher, "Photovoltaic pumping systems technologies trends," *Laboratoire de Recherche en Hydraulique Souterraine et de Surface Larhyss Journal*, ISSN 1112-3680, no. 02,2003, pp 127-150.
- [51] P. Valera and A. Esteban, "Solar energy: Comparative analysis of solar technologies for electricity production," *3rd World Conference on Photovoltaic Energy Conversion*, TP-CP-24, pp 2482-2485, May 2003.
- [52] M. M. H. Bhuiyan, and M. A. Asgar, "Sizing of a stand-alone photovoltaic power system at Dhaka," *Science Direct Journal on Renewable Energy*, vol. 28, no. 6, pp 929–938, 2003.
- [53] P. P. Barker and J. M. Bing, "Advances in solar photovoltaic technology: An applications perspective," *IEEE Power Engineering Society Summer meeting*, pp 1-6, Jun. 2004.
- [54] I. Abouzahr and R. Ramakumar, "Loss of power supply probability of stand-alone photovoltaic systems: a closed form solution approach," *IEEE Trans. on Energy Conversion*, vol. 6, no. 1, pp1-11, 1991.
- [55] K. Heidler, Alexandra Raicu and H. R. Wilson, "A new approach for the performance evaluation of solar cells under realistic reporting conditions," *0160-8371/90/0000-1017, IEEE*, pp 1017-1022, 1990.
- [56] MKC Marwali, SM. Shahidehpour and M. Daneshdoost, "Probabilistic production costing for photovoltaic-utility systems with battery storage," *IEEE Trans. on Energy Conversion*, vol. 112, no. 2, pp175–180, 1997.
- [57] H. A. V. Linde and A. A. M. Sayigh, "The economics of a solar/diesel hybrid—a case study," *Renewable Energy: World Renewable Energy Congress*, June 1996 at Colorado USA, p. 884–886, 1996.
- [58] Sachin Jain and Vivek Agarwal, "An integrated hybrid power supply for distributed generation applications fed by nonconventional energy sources," *IEEE Trans. on Energy Conversion*, vol. 23, no. 2, pp.622-631 June 2008.
- [59] M. Kolhe, S. Kolhe and J. C. Joshi, "Economic viability of stand- alone solar photovoltaic system in comparison with diesel-powered system for India," *Energy Economics incorporating Journal of Energy Finance & Development*, vol. 24, no.2, pp. 155-165, Mar. 2002.

- [60] G. Notton, M. Muselli, and A. Louche, "Autonomous hybrid photovoltaic power plant using a back-up generator: a case study in a Mediterranean Island," *Science Direct Journal on Renewable Energy*, vol. 7, issue 4, pp- 371–391, 1996.
- [61] A. D. Bagul, Z. M. Salameh and B. Borowy, "Sizing of stand-alone hybrid wind–photovoltaic system using a three-event probability density approximation," *Solar Energy*, vol. 5, no. 4, pp. 323-335, 1996.
- [62] D. P. Papadopoulos and J. C. Dermentzoglou, "Economic viability analysis of planned WEC system installations for electrical power production," *Science Direct Journal on Renewable Energy*, vol. 25, no. 2, pp. 199-217, 2002.
- [63] Nfaoui H, Buret J, Sayigh AMM and Dunn PD, "Modeling of a wind/diesel system with battery storage for Tangier Morocco," *Science Direct Journal on Renewable Energy*, vol. 4, no. 2, pp. 155-167, 1994.
- [64] G. N. Kariniotakis, G. S. Stavrakakis and E. F. Nogaret, "Wind power forecasting using advanced neural networks models," *IEEE Trans. on Energy Conversion*, vol. 11, no. 4, pp-762-767, 1996.
- [65] Al. Ashwal AM and I. S. Moghram, "Proportion assessment of combined PV–wind generating systems," *Science Direct Journal on Renewable Energy*, vol. 10, no. 1, pp.43–51, 1997.
- [66] C. Protopopoulou, B. J. Brinkworth and R. H. Marshall, "Sizing and techno-economical optimization for hybrid solar photovoltaic/wind power systems with battery storage," *Int J Energy Res*, vol. 21, pp. 465-479, 1997.
- [67] T. S. Bhatti, Al-ademi AAF and N. K. Bansal, "Load–frequency control of isolated wind–diesel–micro hydro hybrid power systems," *Energy*, vol. 22, no. 5, pp. 461-470, 1997.
- [68] A. E. Feijoo, J. Cidras and J. L. G. Dornelas, "Wind speed simulation in wind farms for steady-state security assessment of electrical power systems," *IEEE Trans. on Energy Conversion*, vol. 14, no. 4, pp.1582-1588, 1999.
- [69] Z.M. Salameh and I. Safari, "The effect of the windmill's parameters on the capacity factor," *IEEE Trans. on Energy Conversion*, vol. 10, no. 4, pp. 747-751, 1995.
- [70] S. Roy, "Optimal planning of wind energy conversion systems over an energy scenario," *IEEE Trans. on Energy Conversion*, vol. 12, no. 3, pp. 248-254, 1996.

- [71] R. B. Chedid, S. H. Karaki and E. C. Chamali, "Adaptive fuzzy control for wind–diesel weak power system," *IEEE Trans. on Energy Conversion*, vol. 15, no. 1, pp.71-78, 2000.
- [72] P. Delarue, A. Bouscayrol, A. Tounzi, X. Guillaud and G. Lancigu, "Modeling, control and simulation of an overall wind energy conversion system," *Science Direct Journal on Renewable Energy*, vol. 28, no. 8, pp. 1169-1185, 2003.
- [73] Neha Adhikari, Bhim Singh and A. L. Vyas, "Design of a stand-alone wind energy conversion system using sensor less MPPT approach," *Proc. of 3rd IEEE International Conference on Sustainable Energy Technologies (ICSET'12), Nepal*, pp.409-414, Sept. 2012.
- [74] A. N. Celik, "A simplified model for estimating the monthly performance of autonomous wind energy systems with battery storage," *Science Direct Journal on Renewable Energy*, vol. 28, no. 4, pp. 561-572, 2003.
- [75] M. A. Elhadid, "Performance evaluation of hybrid power systems," *Science Direct Journal on Renewable Energy*, vol. 26, no. 33, pp. 401-413, 2002.
- [76] I. Abouzahr and R. Ramakumar, "Loss of power supply probability of stand-alone wind electric conversion systems: A closed form solution approach," *IEEE Trans. on Energy Conversion* vol. 5, no. 3, pp. 445–452, 1990.
- [77] R. Karki and R. Billinton, "Cost-effective wind energy utilization for reliable power supply," *IEEE Trans. on Energy Conversion*, vol. 19, no. 2, pp. 435-440, 2004.
- [78] F. Giraud and M. Z. Salameh, "Steady-state performance of a grid-connected rooftop hybrid wind–photovoltaic power system with battery storage," *IEEE Trans. on Energy Conversion*, vol. 16, no. 1, pp. 1-7, 2001.
- [79] J. G. McGowan, J. F. Manwell, C. Avelar and C. L. Warner, "Hybrid wind/PV/diesel hybrid power systems modeling and South American applications," *Renewable Energy: World Renewable Energy Congress*, June 1996 at Colorado USA, pp. 836–47, 1996.
- [80] M. H. Nehrir, B. J. LaMeres, G. Venkataramanan, V. Gerez and L. A. Alvarado, "An approach to evaluate the general performance of stand-alone wind/photovoltaic generating systems," *IEEE Trans. on Energy Conversion*, vol. 15, no. 4, pp. 433-439, 2000.

- [81] A. N. Celik, "Optimization and techno-economic analysis of autonomous photovoltaic–wind hybrid energy systems in comparison to single photovoltaic and wind systems," *Energy Conversion Manage*, vol. 43, no. 18, pp. 2453-2468, 2002.
- [82] N. Jenkins, "Photovoltaic systems for small-scale remote power supplies," in *Proc. IEEE Conf. on Power Engineering*, vol. 9, no. 2, pp.89 – 96, Apr. 1995.
- [83] S. Li, D. C. Wunsch, E. O'Hair and M. G. Giesselmann, "Comparative analysis of regression and artificial neural network models for wind turbine power curve estimation," *Journal Solar Energy Eng*, no. 123, pp. 327-332, 2001.
- [84] Mohammed H and C. O. Nwankpa, "Stochastic analysis and simulation of grid-connected wind energy conversion system," *IEEE Trans. on Energy Conversion*, vol. 15, no. 1, pp. 85-90, 2000.
- [85] R. Yokoyama, K. Ito and Y. Yuasa, "Multi-objective optimal unit sizing of hybrid power generation systems utilizing photovoltaic and wind energy," *Journal of Solar Energy Engg.*, vol.116, pp-167-173, 1994.
- [86] M. T. Samarakou, M. Grigoriado and C. Caroubalos, "Comparison results of two optimization techniques for a combined wind and solar power plant," *Int J Energy Res*, no. 12, pp. 293-297, 1988.
- [87] A. N. Celik, "The system performance of autonomous photovoltaic–wind hybrid energy systems using synthetically generated weather data," *Science Direct Journal on Renewable Energy*, vol. 27, no. 1, pp. 107-121, 2002.
- [88] R. Chedid and S. Rahman, "Unit sizing and control of hybrid wind–Solar power systems," *IEEE Trans. on Energy Conversion*, vol. 12, no. 1, pp. 79-85, 1997.
- [89] Richards, Bryce S., and Avi Shalav. "Photovoltaic Devices," 2007.
- [90] M. G. Villava, J. R. Gazoli and E. F. Ruppert, "Modelling and circuit based simulation of photovoltaic arrays," *Brazilian Journal of Power Electronics*, vol. 14, no. 1, pp.35-45, 2009.
- [91] M. Hamdaoui, A. Rabhi, A. E. Hajjaji, M. Rahmoun and M. Azizi, "Monitoring and control of the performances for photovoltaic systems," *International Renewable Energy Congress*, pp 69-71, Nov. 2009.

- [92] M. Azab, "Improved circuit model of photovoltaic array," *International Journal of Electrical Power and Energy System Engineering*, pp 185-188, Mar. 2009.
- [93] Kashif Ishaque, Zainal Salam, Hamed Taheri and Syafaruddin, "Modeling and simulation of photovoltaic (PV) system during partial shading based on a two-diode model," *Science Direct Journal on Simulation Modelling Practice and Theory*, pp 1613-1626, 2011.
- [94] C. Carrero, J. Amador, and S. Arnaltes., "A single procedure for helping PV designers to select silicon PV module and evaluate the loss resistances," *Renewable Energy*, vol. 32, no. 7, pp.511 – 518, 2007.
- [95] J. C. Wiles and D. L. King, "Blocking diodes and fuses in low-voltage PV systems," in *Proc. 26th IEEE Photovoltaic Spec. Conf.*, Sep. 29– Oct. 3, pp. 1105–1108, 1997.
- [96] Silvestre, S., A. Boronat, and A. Chouder, "Study of bypass diodes configuration on PV modules," *Applied Energy*, vol. 86, no .9, pp. 1632-1640, 2009.
- [97] Xiao, Weidong, William G. Dunford, and Antoine Capel, "A novel modeling method for photovoltaic cells," *In Power Electronics Specialists Conference, 2004. PESC 04. 2004 IEEE 35th Annual*, vol. 3, pp. 1950-1956. IEEE, 2004.
- [98] J. A. Gow & C. D. Manning, "Photovoltaic converter system suitable for use in small scale stand-alone or grid connected applications," *IEE Proc. Electr. Power Appl.*, vol. 147, no. 6, pp 535-543, Nov. 2000.
- [99] Y.M. Chen and Y.C. Liu., "Development of multi-port converters for hybrid wind photovoltaic power system," *IEEE Proc. on Electrical and Electronic Technology*, vol. 2, pp.804 – 808, Aug. 19-22, 2001.
- [100] Z. M. Salameh, F. Dagher and W. A. Lynch, "Step-down maximum power point tracker for photovoltaic systems," *Solar Energy*, vol. 46, no. 5, pp. 279-282, 1991.
- [101] C.W Tan, T.C Green and C.A Hernandez, "An improved maximum power point tracking algorithm with current mode control for photovoltaic application," in *Proc. IEEE ICPEDS 1991*, Nov.28-Dec.1.1991.
- [102] M. A. S. Masoum, H. Dehbonei and E. F. Fuchs, "Theoretical and experimental analysis of photovoltaic systems with voltage and current-based maximum power-point tracking," *IEEE Trans. Energy Conversion.*, vol. 17, no. 4, pp. 514–522, Dec. 2002.

- [103] M. Veerachary, T. Senjyu and K. Uezato, "Neural-network-based maximum-power-point tracking of coupled inductor inter leaved-boost-converter-supplied PV system using fuzzy controller," *IEEE Trans. Ind. Electron*, vol. 50, no. 4, pp.749–758, Dec. 2003.
- [104] T. Noguchi, and H. Matsumoto "Maximum-power-point tracking method of photovoltaic using only single current sensor," *EPE 200 –Toulouse*, ISBN: 90-75815-07-7, 2003.
- [105] Y. Jung, So. Junghun , Yu. Gwonjong, and J. Choi, "Improved Perturbation and Observation Method (IP&O) of MPPT control for photovoltaic power systems," 0-7803-8707-4/05/\$20.00 ©2005 IEEE, 2005, pp1788-1791.
- [106] W. Xiao, N. Ozog and W. G. Dunford, "Topology study of photovoltaic interface for maximum power point tracking," *IEEE Trans. on Industrial Electronics*, vol. 54, no. 3, pp.532-537, Jun. 2007.
- [107] M. S. Aït Cheikh, C. Larbes, G. F. T. Kebir and A. Zerguerras, "Maximum power point tracking using a fuzzy logic control scheme," *Revue des Energies Renouvelables*, vol. 10 no. 3, pp 387 – 395, 2007.
- [108] T. Esram and P. L. Chapman, "Comparison of photovoltaic array maximum power point tracking techniques," *IEEE Trans. on Energy Conversion*, vol. 22, no. 2, pp-439-448, Jun. 2007.
- [109] B. Amrouche¹, M. Belhamell and A. Guessoum, "Artificial intelligence based P&O MPPT method for photovoltaic systems," *Revue des Energies Renouvelables ICRESD-07 Tlemcen*, pp 11 – 16, 2007.
- [110] A. Daoud, and A. Midoun, "Single sensor based photovoltaic maximum power point tracking technique for solar water pumping system electrical power quality and utilization," *Journal*, vol. 14, no. 2, pp 69-72, 2008.
- [111] T. C. Yu and Y. C. Lin, "A study on maximum power point tracking algorithms for photovoltaic systems," *Lunghwa University of Science and Technology*, pp 27-37, 2010.
- [112] H. N. Zainudin and S. Mekhilef, "Comparison study of maximum power point tracker techniques for PV systems," *14th International Middle East Power Systems Conference (MEPCON'10)*, Cairo University, Egypt, Paper ID 278, pp-750-755, Dec. 19-21, 2010.

- [113] A. J. Mahdi, W.H. Tang and Q.H. Wu, "Improvement of a MPPT algorithm for PV systems and its experimental validation," *International Conference on Renewable Energies, Environment and Power Quality (ICREPQ, 10), Granada (Spain)*, Mar. 23-25, 2010.
- [114] M. Calavia¹, J.M. Perié, J. F. Sanz and J. Sallán, "Comparison of MPPT strategies for solar modules," *International Conference on Renewable Energies, Environment and Power Quality (ICREPQ,10),Granada(Spain)*, Mar. 23-25, 2010.
- [115] S. L. Brunton, C. W. Rowley, S. R. Kulkarni and C. Clarkson, "Maximum power point tracking for photovoltaic optimization using ripple-based extremum seeking control," *IEEE Trans. on Power Electronics*, vol. 25, no. 10, pp 2531-1540, Oct. 2010.
- [116] Subiyanto, A. Mohamed and H. Shareef, "Hopfield neural network optimized fuzzy logic controller for maximum power point tracking in a photovoltaic system," *Hindawi Publishing Corporation International Journal of Photo energy* Volume 2012, Article ID 798361, 13 pages doi:10.1155/2012/798361.
- [117] Neha Adhikari, Bhim Singh and A.L. Vyas, "Design and Control of Small Power Standalone Solar PV Energy System," *Asian Power Electronics Journal*, vol. 6, no.1, pp. 17-24, October 2012.
- [118] Mattavelli, P., L. Rossetto, G. Spiazzi, and P. Tenti, "General-purpose sliding-mode controller for DC/DC converter applications," In *Power Electronics Specialists Conference, 1993. PESC'93 Record., 24th Annual IEEE*, pp. 609-615, IEEE, 1993.
- [119] M. K. Kazimierczuk, "Synthesis of phase-modulated dc/ac inverters and dc/dc converters," *Proc. Inst. Elect. Eng. B*, vol. 139, pp. 387-394, Jul.1992.
- [120] P. Mattavelli, L. Rossetto and G. Spiazzi, "General purpose sliding mode controller for dc-dc converter applications," in *Proc. Power Electronic Specialist Conf. (PESC'93)*, pp. 609-615.
- [121] R. Cáceres and I. Barbi, "A Boost DC-AC converter: operation, analysis, control and experimentation," in *Proc. IEEE IECON'95 Conf.*, Orlando, FL, pp. 546-551, Nov. 5-11, 1995.

- [122] M. Jain, M. Daniele and P. K. Jain, "A bidirectional DC-DC converter topology for low power applications," *IEEE Trans on Power Electronics*, vol. 15, no. 4, Jul. 2000.
- [123] M. A. S. Masou and S. M. Mousavi, "Analysis of photovoltaic system with DC/DC converters using PWM and sliding controllers," *International Journal of Renewable Energy Engineering*, vol. 4, no. 1, Apr. 2002.
- [124] B. Singh and M. Agrawal, "Analysis and design of single-phase power factor corrected AC-DC Cuk converter with high-frequency isolation," *Int. J. Energy Technology and Policy*, vol. 4, no. 1/2, 2006.
- [125] Suvarun Dalapati and Chandan Chakraborty, "A direct pwm technique for a single-phase full-bridge inverter through controlled capacitor charging," *IEEE Trans. on Industrial Electronics*, vol. 55, no. 8, pp.2912 – 2922, Aug. 2008.
- [126] Z. Miao, W. Feng and Y. J. Hua, "Novel cuk circuit and its application in photovoltaic system," in *proc. of Third International Conference on Power Electronics systems and Applications*, vol. 1, pp.15-21, May 2009.
- [127] Y. H. Kim and H. D. Ha, "Design of interface circuit with electrical battery models," *IEEE Trans. on Industrial Electronics*, vol.44, no.1, pp. 81-86, Feb. 1997.
- [128] H. L. Chan and D. Sutanto, "A New topology for battery energy storage system," in *Proc of IEEE International Conf on Energy Management and Power Delivery*, vol. 1, pp. 253-258, 1998.
- [129] Massimo Ceraola, "New Dynamic models of lead-acid batteries," *IEEE Trans. on Power System*, vol. 15, no. 4, pp. 1184-1190, Nov 2000.
- [130] R. O. Cáceres and I. Barbi, "Sliding mode controller for the Boost inverter," in *Proc. IEEE CIEP'96*, Cuernavaca, Mexico, pp. 247–252, Oct. 14–17, 1996.
- [131] N. Vázquez, J. Álvarez, C. Aguilar and J. Arau, "Some critical aspects in sliding mode control design for the Boost inverter," in *Proc. IEEE CIEP'98 Conf.*, Morelia, Mexico, pp. 76–81, Oct. 12–15, 1998.
- [132] R. O. Cáceres and I. Barbi, "A Boost DC-AC converter: analysis, design and experimentation," *IEEE Trans. on Power Electronics.*, vol. 14, no. 1, pp. 134–141, Jan. 1999.
- [133] T. F. Wu, C. H. Chang and Y. H. Chen, "A fuzzy-logic controlled single-stage converter for PV-powered lighting system applications," *IEEE Trans. on Industrial Electronics*, vol. 47, no. 2, pp.287 – 296, Apr. 2000.

- [134] Gerardo Vázquez, Pedro Rodriguez and *etal*, “Adaptive hysteresis band current control for transformer less single-phase PV inverters,” in *proc. of International Conference on Industrial Electronics IECON 2009*, vol., pp.173-177, Nov. 2009.
- [135] G. S. Ilango, P. S. Rao, A. Karthikeyan and C. Nagamani, “Single-stage sine-wave inverter for an autonomous operation of solar photovoltaic energy conversion system,” *Science Direct Journal on Renewable Energy*, vol. 35, pp. 275-282, May 2010.
- [136] B. Singh and S. Singh, “Single-phase power factor controller topologies for permanent magnet brushless DC motor drives,” *IET Power Electronics*, vol. 3, issue 2, pp. 147 – 175, 2010.
- [137] Singh, Bhim, Brij N. Singh, Ambrish Chandra, Kamal Al-Haddad, Ashish Pandey, and Dwarka P. Kothari, “A review of single-phase improved power quality AC-DC converters,” , *IEEE Trans. on Industrial Electronics*, vol.50, no. 5 ,pp. 962-981,2003.
- [138] C. Krause, “Analysis of electric machinery,” Willey, 2002.
- [139] Manwell, James F., Jon G. McGowan, and Anthony L. Rogers, “Wind energy explained: theory, design and application,” John Wiley & Sons, 2010.
- [140] Chen, Zhe, Josep M. Guerrero, and Frede Blaabjerg, “A review of the state of the art of power electronics for wind turbines,” *IEEE Trans. on Power Electronics*, vol. 24, no. 8, pp.1859-1875, 2009.
- [141] Nfah, E. M., J. M. Ngundam, and R. Tchinda, “Modelling of solar/diesel/battery hybrid power systems for far-north Cameroon,” *Science Direct Journal on Renewable Energy*, vol.32, no. 5, pp. 832-844,2007.
- [142] Rashed, Mohamed, A. Elmitwally, and Sahar Kaddah, “New control approach for a PV-diesel autonomous power system,” *Science Direct Journal on Electric Power Systems Research*, vol. 78, no. 6, pp. 949-956,2008.
- [143] MATLAB Simulink Sim Power System Toolbox in.mathworks.com.
- [144] Jincy Philip, Chinmay Jain, Krishan Kant, Bhim Singh, Sukumar Mishra, Ambrish Chandra, Kamal Al-Haddad, “Control and Implementation of a Standalone Solar Photovoltaic Hybrid System”, *IEEE Trans. on Industrial Applications*, vol.52, no. 4 ,pp. 3472-3479,2016.

-
- [145] Sk. A. Shezan; A. Z. M. Salahuddin; M. Farzana; A. Hossain, “Techno-economic analysis of a hybrid PV-wind-diesel energy system for sustainable development at coastal areas in Bangladesh, in proc. of *International Conference on Development in the in Renewable Energy Technology ICDRET*, pp.1-6,2016.
- [146] Lee Wai Chong, Yee Wan Wong et al.,“Hybrid energy storage systems and control strategies for stand-alone renewable energy power systems”, *Science Direct Journal on Renewable and Sustainable Energy Reviews*, vol. 66, pp.174-189,2016.
- [147] Ankit Bhatt, M.P. Sharma, R.P. Saini, “Feasibility and sensitivity analysis of an off-grid micro hydro–photovoltaic–biomass and biogas–diesel–battery hybrid energy system for a remote area in Uttarakhand state, India”, *Science Direct Journal on Renewable and Sustainable Energy Reviews*, vol. 61, pp.53-69,2016.

Appendix

APPENDIX- 1

Table A 1.1 Different parameters of 125 watt solar panel (Make: REIL, India)

Parameter	Value
Short Circuit Current (I_{sc})	7.759 A
Open Circuit Voltage (V_{oc})	22.73 V
Number of Parallel Cells (N_p)	1
Number of series Cells (N_s)	36
Reference Temperature (T_{ref})	298 Kelvin
Boltzmann's Constant (K)	1.381×10^{-23} J/K
Ideality Factor (n)	1.3
Electron Charge (q)	1.602×10^{-19} C
Short Circuit Temperature Coefficient (K_i)	0.003
Maximum Power (P_{max})	128.53 W
Voltage at P_{max}	18.32 V
Current at P_{max}	7.016 A

Table A 1.2 Different parameters of DC-DC boost converter

Parameter	Calculated	Selected
Input Voltage (V_{PV})	16-36 V	
Output Voltage (V_{out})	53 V	
Duty Cycle (D)	0.32-0.698	
Ripple of output Current (ΔI_0)	5%	
Switching frequency (F_{sw})	50 kHz	
Ripple of output Voltage (ΔV)	10%	
Inductance (L_{1S})	2.24 mH	2.5 mH
Capacitance (C_{1S})	1792 μ F	2200 μ F

Table A 1.3 Parameters of 1kW Wind Turbine and PMSG

Parameter	Value
Rated Mechanical power (P_m)	1000 W
Wind Speed for the rated power (V_w)	10 m/s
Density of air (ρ_a)	1.2kg/m ³
Radius of the blade for the rated power (R)	1.15m
Area swept by the rotor blades (A_w), πR^2	4.16m ²
Stator Resistance (R_s)	2.875 Ω
d-axis Inductance (L_d)	0.0085H
q-axis Inductance (L_q)	0.0085H
Permanent Magnet Flux Density (λ_0)	0.175Weber
Pole Pairs (N_{pp})	4
Moment of Inertia (J)	0.0008Kgm ²

Table 3.5 Parameters of DC-DC buck converter

Parameter	Calculated	Selected
Input Voltage (V_{wg})	80V	
Output Voltage (V_{out})	53V	
On Voltage (V_{on})	27 V	
Current Ripple Factor (r)	0.4	
Minimum & Maximum Power	50 W & 1000W	
Minimum & Maximum Load Current (I_0)	0.9 A & 18.1 A	
Minimum & Maximum Peak Current (ΔI)	0.36 A & 7.24 A	
Duty Cycle (D)	0.6875	
Switching frequency (F_{si})	30 kHz	
Inductance (L_{1w})	1.72 mH	1.75 mH
Capacitance (C_{1w})	151 μ F	150 μ F

Publications from the Work

PUBLICATION FROM THESIS

Following papers have been published, and communicated out of this thesis:

Published Papers:

- (1) R. A. Gupta, Bhim Singh and Bharat Bhushan Jain, “Wind Energy Conversion System using PMSG,” in *Proc. IEEE International Conference on Recent Developments in Control, Automation and Power Engineering (RDCAPE), Amity University, Noida, India*, pp. 199-203 CFP15RDC-ART 978-1-4799-7247-0, 12-13 Mar.,2015
- (2) R. A. Gupta, Bhim Singh and Bharat Bhushan Jain, “Solar Wind & Diesel Hybrid Energy System: A Review”, in *Proc. Springer International Conference on Recent Cognizance in Wireless Communication & Image Processing, Jaipur, India*, Jan-16-17, 2015,paper id 365.
- (3) R. A. Gupta, Bhim Singh and Bharat Bhushan Jain,, “Interconnection of Microgrid with Electric Power System”, in *Proc. International Conference on “Advance Research & Innovation in Engineering & Technology(ICARIET’15), Jaipur, India*, pp. 306-310, 2015.
- (4) R. A. Gupta, Bhim Singh and Bharat Bhushan Jain, “Solar-Wind Hybrid Energy System: Theory & Approaches”, in *Proc. International Conference on “Advance Research & Innovation in Engineering & Technology (ICARIET’15), Jaipur, India*,3-4 Mar,2015, pp. 5-36

Communicated Papers:

- (5) R. A. Gupta, Bhim Singh and Bharat Bhushan Jain, “Investigation and installation of 1 KW battery storage solar energy system with MPPT technique” *under review in Energy Policies, Elsevier.*
- (6) R. A. Gupta, Bhim Singh and Bharat Bhushan Jain, “Modeling, control, and simulation of battery storage solar/PV and wind energy hybrid energy system for standalone rural electrification in Kukas, India, under review in *Electric Power and Energy System, Elsevier.*

